AD_____

Award Number: DAMD17-00-1-0346

TITLE: Transforming Growth Factor Beta Regulation of Tumor Progression in Metastatic Cancer

PRINCIPAL INVESTIGATOR: Merry Jo Oursler, Ph.D.

CONTRACTING ORGANIZATION: The University of Minnesota
Minneapolis, Minnesota 55455-2070

REPORT DATE: June 2004

TYPE OF REPORT: Final

PREPARED FOR: U.S. Army Medical Research and Materiel Command
Fort Detrick, Maryland 21702-5012

REPORT DOCUMENTATION PAGE

Form Approved
OMB No. 074-0188

1. AGENCY USE ONLY (Leave blank)	2. REPORT DATE	3. REPORT TYPE AND DATES COVERED
	June 2004	Final (1 Jun 2000 - 31 May 2004)

4. TITLE AND SUBTITLE
Transforming Growth Factor Beta Regulation of Tumor Progression in Metastatic Cancer

5. FUNDING NUMBERS
DAMD17-00-1-0346

6. AUTHOR(S)
Merry Jo Oursler, Ph.D.

7. PERFORMING ORGANIZATION NAME(S) AND ADDRESS(ES)
The University of Minnesota
Minneapolis, Minnesota 55455-2070

E-Mail: moursler@d.umn.edu

8. PERFORMING ORGANIZATION REPORT NUMBER

9. SPONSORING / MONITORING AGENCY NAME(S) AND ADDRESS(ES)
U.S. Army Medical Research and Materiel Command
Fort Detrick, Maryland 21702-5012

11. SUPPLEMENTARY NOTES
Original contains color plates: All DTIC reproductions will be in black and white.

12a. DISTRIBUTION / AVAILABILITY STATEMENT
Approved for Public Release; Distribution Unlimited

12b. DISTRIBUTION CODE

13. ABSTRACT (Maximum 200 Words)
During the metastatic tumor development, osteoclasts differentiate in the presence of high transforming growth factor beta (TGF-β) concentrations. We hypothesize that TGF-β is a survival factor for TGF-β-induced osteoclasts. We tested our hypothesis by: (1)Determining the effects of TGF-β on tumor development in bone in vivo and (2) Determining the role of TGF-β signal transduction in TGF-β influences on mouse osteoclasts-like cell survival. We have compared mice with cardiac verses direct bone deposition of tumor cells expressing either the constitutively active or the dominant interfering TGF-β receptors. Cardiac injected mice containing the constitutively active receptor had a significantly lower rate of osteolytic lesion development compared to either the parental cells or the dominant interfering receptor cells. In contrast, there were no differences in parameters of osteolysis between the cell types with direct bone injection. We conclude that the rate of metastasis in impacted by TGF-β yet the rate of osteolysis is independent of TGF-β effects on tumor cells. In studies for objective 2, we examined the PI3K/AKT and MEK/ERK signaling pathways and have found evidence that they are important in osteoclast survival. We have pursued the impacts of TGF-β on these pathways. We report here on these studies.

14. SUBJECT TERMS
Breast cancer

15. NUMBER OF PAGES
138

16. PRICE CODE

17. SECURITY CLASSIFICATION OF REPORT	18. SECURITY CLASSIFICATION OF THIS PAGE	19. SECURITY CLASSIFICATION OF ABSTRACT	20. LIMITATION OF ABSTRACT
Unclassified	Unclassified	Unclassified	Unlimited

Table of Contents

INTRODUCTION

The purpose of this research is to determine the roles of transforming growth factor beta (TGF-ß) in metastatic tumor progression. The approach to this issue, both *in vivo* and *in vitro* studies were planned. *In vivo* studies used MDA MB 231 breast cancer cell lines that express either the dominant interfering or constitutively active TGF-ß receptors that were (1) directly injected into the marrow cavity of nude mice and (2) injected into the left ventrical of nude mice. Direct injection looks at interactions within the bone compartment only whereas cardiac injection looks at survival in circulation, targeting to bone, and interactions within the bone itself. The *in vitro* studies focused on the signaling pathway utilized by osteoclasts that differentiate in the presence of TGF-ß (when TGF-ß is a survival factor) and cells differentiated without TGF-ß exposure (when addition of TGF-ß to the mature cells causes apoptosis). These studies are also progressing, as detailed below

BODY: NONE OF THESE DATA HAVE BEEN PUBLISHED, SO SHOULD BE PROTECTED (PAGES 4-12)

This report is detailed with specific reference to the Statement of Work.

Objective 1: Determine the effects of TGF-ß on tumor development in bone *in vivo*.

Task 1. Cardiac injections and antibody treatment: month 1 to month 16

As noted in our progress report the first year, antibodies were rapidly degraded when injected, so we altered our experiment by stably expressing either dominant negative or constitutively active TGF-ß receptors in the MDA MB 231 cells prior to injection. The cardiac injection has been completed and the bones have been harvested. Thus we have completed this task.

Task 2: analysis of above: month 16 to month 30

We performed analysis of X-rays of the injected animals to determine the incidence and areas of osteolysis. As can be seen from the table below, the metastatic subclone was significantly more osteolytic than the parental MDA MB 231 cells. When the constitutively active (CA) TGF-ß receptor construct was expressed in this subclone, there was a significant reduction in the number of osteolytic lesions per animal and the size of the lesions. In contrast, the subclone cells expressing the dominant negative (dn) receptor construct exhibited less of a reduction in osteolytic lesions and size, although this was still a significant reduction over the metastatic subclone.

All of the bones from these animals have been imbedded, sectioned, stained, and analyzed by histomorphometry. The bones from all types of animals had little trabecular bone and no evidence of alterations in osteoclast numbers, so we are unable to draw conclusions from the histomorphometry that extend the observations from X-ray analysis.

CELLS INJECTED	# OSTEOLYTIC LESIONS PER ANIMAL ± SEM	AREA/OSTEOLYTIC LESION (μM) ± SEM
parental MDA MB 231	0.25 ± 0.25	0.85 ± 0.85
metastatic subclone	8.67 ± 0.80*	6.44 ± 0.79*
sublclone expressing CA receptor	1.25 ± 0.17**	0.56 ± 0.19**
subclone expression dn receptor	6.50 ± 0.33**; §	3.48 ± 0.83**;§

*p<0.05 compared to parental cell line
**p<0.05 compared to metastatic subclone
§p<0.05 compared to metastatic subclone expressing the CA receptor.

Task 3: Cardiac injections and LAP treatment : month 13 to month 24

Similar to the Task 1 difficulties, we have discovered that the LAP protein is rapidly degraded *in vivo* and we substituted the alternate approach as outlined in Task 1.

Task 4: analysis of above: month 24 to month 36

See Task 2 above.

Task 5: Bone injections and antibody treatment: month 1 to month 19

As noted in Task 1, antibodies were rapidly degraded *in vivo*. For this reason, we have generated the cells for both cardiac and bone injection as outlined above. We reported the first year that we had completed this task as the bones had been injected and harvested. Upon analysis, we discovered that there was extensive osteolysis in all samples, irrespective of the cell type injected. We conjectured that this was due to accelerated osteolysis and have repeated this protocol with a new series of animals and harvested the bones at an earlier time point to attempt to rectify this problem. This second series of injections has been completed and the bones have been harvested and processed.

Task 6: analysis of above: month 19 to month 32

As noted above, the first series of animals had extensive osteolysis in all animals. We therefore have repeated the experiment and have sectioned and stained these bones. Histomorphometric analysis has revealed no difference in the rates of bone resorption or the number of osteoclasts with the type of tumor injected. We conclude from the combined data from both methods of tumor cell introduction that TGF-ß activation impacts the rate at which tumor cells arrive and establish in bone but has no dramatic influence on the rate of tumor development once it is established in the bone environment.

Task 7: Bone injections and LAP treatment: month 15 to month 30

As with the antibodies, the LAP protein was rapidly degraded and we have used the cell lines as detailed in Task 5.

Task 8: analysis of above: month 30 to month 36

See Task 6 above.

Objective 2: Determine the role of TGF-ß signal transduction in TGF-ß influences on mouse osteoclast-like cell survival

Task 9: receptor construct studies: month 1 to month 18

We have been unable to generate mature osteoclasts expressing the constitutively active receptor as they all apoptose. We conjecture that this is due to activation of TGF-ß-mediated apoptosis. The dominant interfering receptor construct has proven to be difficult to insert into the adenoviral system. With time running out on this project, we instead focused on the role of the TGF-ß-SMAD signaling pathway in osteoclast responses to TGF-ß. We were unable to find evidence of phosphorylation of either SMAD 2 or SMAD 3 following TGF-ß treatment. We conclude that this pathway is unlikely to be involved in TGF-ß induction of osteoclast apoptosis.

Task 10: pathway studies

interactions (month 13 to month 18) and phosphorylations (month 18 to month 36):
Since we have been unable to detect consistent changes in SMAD protein phosphorylation with TGF-ß treatment during differentiation, we have focused this section of the project on other possible signaling pathways involved in the differences between naïve and TGF-ß-induced osteoclasts. Please see below for our interesting results.

We have examined both TGF-ß-induced and un-induced (naïve) osteoclasts for evidence of an involvement of either apoptotic or survival signaling during culture.

I. Examination of naïve osteoclast survival without TGF-ß treatment

A. Survival studies have been published, as have the studies reported that the AKT/NFkB and MEK/ERK pathways are important in osteoclast survival (1).

B. Studies of survival pathway activation:

Since our data document that many osteoclasts survive for relatively long periods of time in culture, we have explored the impact of this on osteoclast gene expression. We have used apoptosis gene-specific gene arrays to examine a spectrum of Bcl-2 family member genes whose proteins products impact survival (Superarray). Mature osteoclasts were purified and either harvested or returned to culture for 30 minutes prior to harvest. RNA was isolated from the harvested cells and subjected to analysis. As shown in the graphs to the right, most survival promoting genes were downregulated with culture. However, mcl-1 was upregulated while all other Bcl-2 family members were down-regulated. We are currently

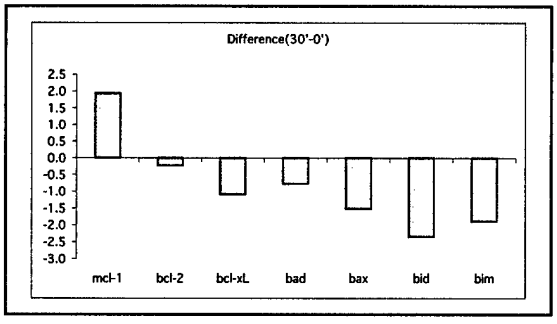

carrying out experiments to confirm these changes using log phase reverse transcriptase polymerase chain reaction studies. If we confirm up-regulation, we will next examine whether we can detect changes in protein expression

II. TGF-ß influences on naïve osteoclast survival: Now that we have evidence of the importance of both the MEK/ERK and AKT/NFκB pathway in osteoclast survival (1), we are examining the impact of TGF-ß treatment on these pathways.

A. TGF-ß causes degradation of survival-promoting proteins. We have examined mature osteoclast cultures for the impact of TGF-ß on survival-promoting protein levels. As documented here, there is rapid degradation of AKT, ERK 1/2, and MEK, but not actin following TGF-ß treatment. We have examined the p38 MAPK/JNK/ AP-1 pro-apoptotic pathway been unable to detect activation of the p38 MAPK, JNK, or AP-1 following TGF-ß treatment (data not shown). Taken together, these data support that targeted degradation of survival promoting proteins is a likely mechanism by which TGF-ß induces osteoclast apoptosis. We pursued the mechanisms of this degradation by examining whether it is caspase or proteasome mediated. Our studies blocking proteasomes have shown that this reduces osteoclast apoptosis, suggesting that this may the mechanism by which apoptosis is driven.

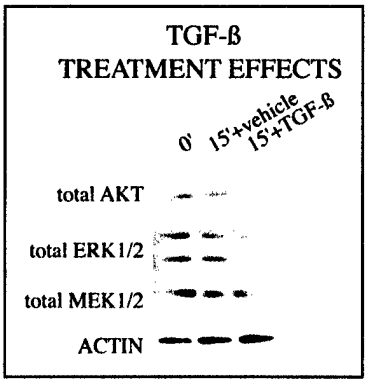

B. TGF-ß induces TIEG gene expression. TGF-ß Inducible Early Gene has been implicated in apoptosis of a number of cell types (2-6). We have therefore examined the impact of TGF-ß on TIEG expression in osteoclasts using Real Time Polymerase Chain Reaction. As shown to the right, 60 minutes of 2 ng/ml TGF-ß treatment resulted in a significant increase in TIEG expression (data are the mean ± SD of 2 replicates). This supports that the mechanisms by which TGF-ß induces osteoclast apoptosis may involve TIEG expression.

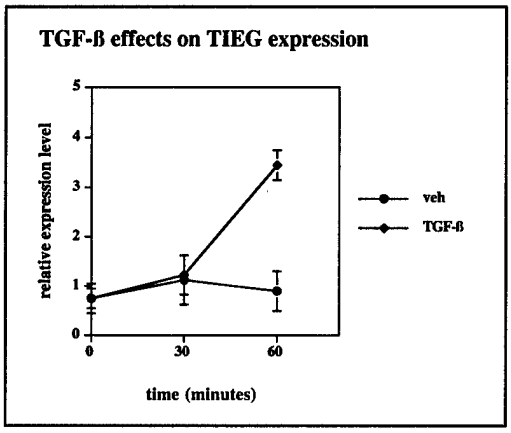

C. Osteoclasts from TIEG knockout mice survive longer in culture. We have examined osteoclast precursors for their ability to survive stromal cell removal. Marrow cells from TIEG knockout and wildtype mice were cultured with ST2 stromal cells until osteoclasts develop (13 days) (1). Once mature, osteoclasts were purified by enzymatic removal of stromal cells and culture continued for the indicated times. Cells were fixed and processed as described (1). As documented in the figure to the right, osteoclasts lacking TIEG gene (-/-) survive better than osteoclasts from wildtype (+/+) osteoclasts. These data support that TIEG is pro-apoptotic in osteoclasts

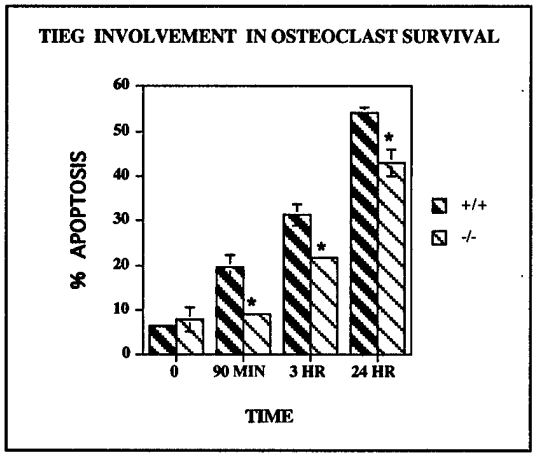

III. Examination of survival of osteoclasts that differentiate in the presence of TGF-ß.

A. PTEN expression is repressed when osteoclasts differentiate in the presence of TGF-ß. As outlined in last year's progress report, we have evidence that the MEK/ERK and AKT/NFκB pathways are important in survival of TGF-ß-induced osteoclasts as well as naïve osteoclasts. We have published that the AKT/NFκB and MEK/ERK pathways are coordinately regulated by PI3K in naïve osteoclasts (1). Since PTEN is regulated by TGF-ß, we have examined PTEN levels in naïve and TGF-ß-induced osteoclasts. Osteoclasts were differentiated in the absence (naïve) or presence of $2x10^{-4}$ ng/ml TGF-ß. Interestingly, mature TGF-ß-induced osteoclasts have lower levels of PTEN than naïve osteoclasts. PTEN acts as a repressor of PI3K/Akt/NFκB pathway. Since we have found that NFκB is involved in PI3K-mediated naïve osteoclast survival, we have examined TGF-ß-induced osteoclasts for the level of NFκB activation.

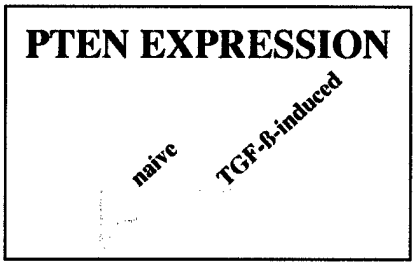

B. NFκB activation is higher in TGF-ß induced osteoclasts compared to osteoclasts that differentiate in the absence of TGF-ß. Osteoclasts were differentiated in the absence (naïve) or presence of $2x10^{-4}$ ng/ml TGF-ß. Nuclear extracts were analyzed for the presence of active NFκB by electromobility shift assay as we have reported (1). On the basis of antibody supershifts, the lower two bands are active NFκB complexed with labeled oligo of the NFκB binding sequence (1). These data document that differentiation in the presence of TGF-ß results in a marked increase in active NFκB. Since PTEN represses PI3K, the lower levels of PTEN and higher levels of NFκB activation in TGF-ß-induced osteoclasts are consistent with increased activation of the PI3K/AKT/NFκB pathway in TGF-ß-induced osteoclasts. These data support that signals from PI3K may be important components of osteoclast survival and that these survival signals include NFκB activation and may hinge on PTEN regulation.

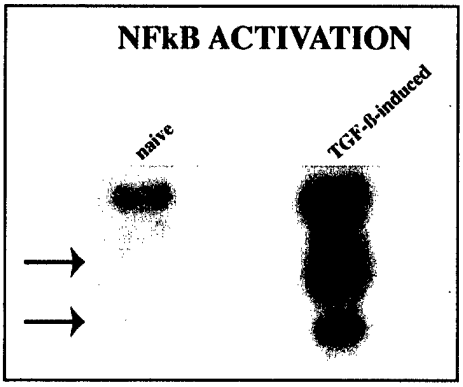

C. TGF-ß-induced osteoclasts maintain survival protein expression when cultured with TGF-ß but survival proteins are rapidly lost when TGF-ß in withdrawn. As reported previously, continued osteoclast culture with TGF-ß promotes osteoclast survival whilst culture of TGF-ß-induced osteoclasts without TGF-ß results in rapid apoptosis. We have examined expression of survival-promoting proteins in TGF-ß-induced osteoclasts and the impact of culture with and without TGF-ß on protein expression (time is in minutes). Interestingly, examination of the amount of total AKT (tAKT) and total MEK (tMEK) protein expression reveals that there is a rapid significant decrease in both survival-promoting proteins in the cells withdrawn from TGF-ß (-) compared with TGF-ß-maintained cells (+). These data raise the possibility that the withdrawal of TGF-ß activates a targeted degradation of survival promoting signaling molecules to drive osteoclast apoptosis.

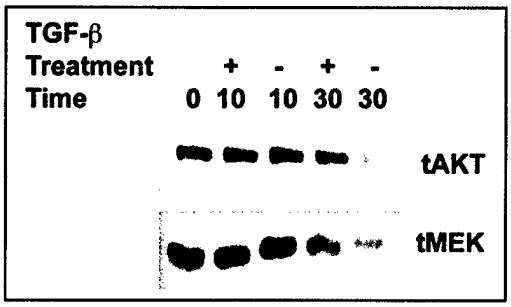

D. Evidence of a role of the proteasome in apoptosis: To examine the role of the AKT and MEK pathways as well as the proteasome in osteoclast survival, naïve and TGF-ß-induced osteoclasts were purified and either fixed or cultured with vehicle (DMSO) or chemical inhibitors of these cellular components in the absence or presence of TGF-ß. As can be seen on the graph on the next page, the responses were complex. The AKT and MEK pathways appears to be important in survival of TGF-ß-induced and maintained and naïve osteoclasts that are cultured without TGF-ß. Interestingly, the TGF-ß-maintained osteoclasts were all apoptotic when the proteasome

was blocked and the naïve cells treated with TGF-ß also exhibited increased apoptosis. We are currently completing western blot studies to determine the protein targets that are degraded in the proteasome to complete this project.

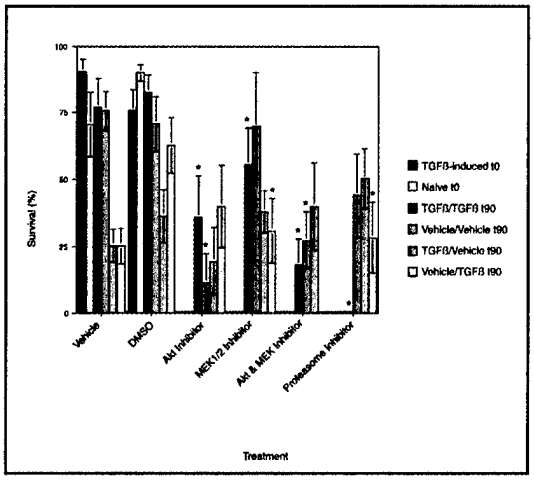

KEY RESEARCH ACCOMPLISHMENTS:

Have evidence of significant disruption of metastasis by over-expression of the constitutively active TGF-ß receptor in metastatic breast cancer cells.

Osteoclast survival is due to activation of survival pathways and may involve increased mcl-1 expression.

Osteoclast apoptosis may be due to repression of survival signaling by targeted degradation in naïve osteoclasts treated with TGF-ß and TGF-ß removal from TGF-ß-induced osteoclasts.

TGF-ß induces pro-apoptotic TIEG gene expression in naïve osteoclasts.

The PI3K/AKT/NFκB and MEK pathways are implicated in survival of TGF-ß-induced osteoclasts.

REPORTABLE OUTCOMES

2 abstracts to the 2001 American Society for Bone and Mineral Research annual meeting.

2 abstracts at the 2002 American Society for Bone and Mineral Research annual meeting.

3 abstracts to the 2003 American Society for Bone and Mineral Research annual meeting.

3 abstracts to the 2004 American Society for Bone and Mineral Research annual meeting.

2 abstracts to the 2003 American Society for Cell Biology annual meeting.

1 abstract at the 2002 ERA of Hope Department of Defense Breast Cancer Research meeting.

11 published papers and 2 published book chapters.

Shaw, A. and Oursler, M.J. (2000). Paracrine regulation of osteoclast activity in metastatic breast cancer. Cancer Research Alert 1:124-127.

Winding, B., Misander, H., Sveigaard, C., Therkildsen, B., Jakobsen, M., Overgaard, T., Oursler, M.J., Foged, N.K. (2000). Human breast cancer cell-induced angiogenesis, recruitment, and activation of osteoclasts in bone. J Cancer Research and Clinical Oncology 126:631-640.

Pascoe, D. and Oursler, M.J. (2001). The Src signaling pathway is regulates osteoclast lysosomal enzyme secretion and is rapidly modulated by estrogen. J. Bone and Min. Research. 16:1028-1036.

Gingery, A., Oursler, M.J. (2002). The Roles of TGF-beta in Metastatic Cancer Progression in Bone. Recent Research Developments in Cancer. 4:13-24.

Sanyal, A., Oursler, M.J., Clemens, V.C., Fukumoto, T., Fitzsimmons J.S., O'Driscoll, S.W. (2002). Temporal Expression Patterns Of BMP Receptors And Collagen II (B) During Periosteal Chondrogenesis. J. Orthopedic Res. 20:58-65.

Mizuta, H., Sanyal, A., Fukumoto, T., Fitzsimmons, J.S., Matsui, N., Bolander, M.E., Oursler, M.J., O'Driscoll, S.W. .J. (2002). The Spatiotemporal Expression of TGF-ß1 and its Receptors during Periosteal Chondrogenesis *In Vitro*. J. Orthopedic Res. 20:562-574.

Giulivi, C. and Oursler, M.J. Role of Mitochondrial Oxygen and Nitrogen Reactive Species in Signaling. (Invited Review). (2002). In Signal Transduction by Reactive Oxygen and Nitrogen Species: Pathways and Chemical Principles. M. Torres, J. Fukuto, and H. J. Forman, eds. Kluwer Press, New York.

Gingery, A., Bradley. E., Shaw A., and Oursler, M.J. (2003). Phosphatidylinositol 3-kinase Coordinately Activates the MEK/ERK and AKT/NFκB pathways to Maintain Osteoclast Survival. J. Cellular Biochem. 89:165-179.

Oursler, MJ. (2003). Direct and indirect effects of estrogen on osteoclasts. J. Musculoskeletal and Neuronal Interactions. 3:363-366.

Gorny, G., Shaw, A.K. Oursler, MJ. (2004). IL-6, LIF, and TNF-α Regulation of GM-CSF Inhibition of Osteoclastogenesis *in vitro*. Experimental Cell Research. 294:149-158.

Karst, M., Gorny, G., Galvin, R.J., and Oursler, M.J. (2004) The Roles of Stromal Cell RANKL, OPG, and M-CSF Expression in Biphasic TGF-ß Regulation of Osteoclast Differentiation. J. Cell. Physiology. 200:99-106.

IN PRESS

Oursler, MJ. Osteolytic Enzymes of Osteoclasts in Springer-Verlag

Bradley. E. and Oursler, M.J. Mitogen Activated Protein Kinase Regulation of Osteolytic Bone Loss in Breast Cancer Metastases. Recent Research Developments in Cancer

1 manuscript submitted to the American Journal of Physiology.

Oursler, M.J., Bradley, E.W., Elfering, S.L., and Giulivi, C. Native, Not Nitrated, Cytochrome *c* and Mitochondrial-derived Hydrogen Peroxide Drive Osteoclast Apoptosis

1 manuscript submitted to the Molecular and Cellular Biology.

Subramaniam, M., Gorny, G., Monroe, D.G., Johnsen, S.A., Rickard, D.J., van Deursen, M.A., Oursler, M.J., and Spelsberg, T.C. TIEG1 Null Mouse-Derived Osteoblasts Are Defective in Mineralization And In Support of Osteoclast Differentiation *in vitro*.

2 manuscripts in preparation.

Funding obtained: TGF Beta Regulation of Osteoclast Apoptosis. National Institutes of Health. PI: Merry Jo Oursler. August 1, 2003- June 1, 2008.

List of Personnel supported by this funding

Anne Gingery
Misty Eliason
Elizabeth Bradley
Genevieve Gorny
David Pascoe
Mary Karst
Aubie Shaw
Dana Fleming

CONCLUSIONS:

We made excellent progress on dissecting the roles of TGF-ß in tumor-driven osteolysis. We have successfully carried out both cardiac and bone injections of parental cells and cells expressing either a dominant interfering or a constitutively active TGF-ß receptor construct. Our data from the cardiac injection model suggest that expression of a constitutively active form the TGF-ß receptor greatly reduces osteolytic lesions. Comparing these data with the direct bone injection model determined that expression impacted getting to bone but not activity of the tumor in bone. *In vitro* studies have not implicated TGF-ß-SMAD signaling in osteoclast survival and apoptosis decisions. But we have evidence that a newly discovered pro-apoptotic transcription factor, TIEG, is involved in TGF-ß-induced apoptosis. One of the known targets for TIEG is repression of SMAD 7. We are continuing to pursue this avenue in our current NIH-funded project. Our data show that osteoclast survival appears to require activation of both MEK/ERK and AKT/NFκB pathways in both naïve osteoclasts (osteoclasts differentiated in the absence of TGF-ß) and TGF-ß-induced osteoclasts. TGF-ß withdrawal from TGF-ß-induced osteoclasts may cause disruption of the AKT/NFκB pathway by targeted degradation of AKT via proteasome-mediated degradation.

REFERENCES

1. Gingery A, Bradley E, Shaw A, Oursler MJ 2003 Phosphatidylinositol 3-kinase coordinately activates the MEK/ERK and AKT/NFkappaB pathways to maintain osteoclast survival. J Cell Biochem 89(1):165-79.
2. Ribeiro A, Bronk SF, Roberts PJ, Urrutia R, Gores GJ 1999 The transforming growth factor beta(1)-inducible transcription factor TIEG1, mediates apoptosis through oxidative stress. Hepatology 30(6):1490-7.
3. Chalaux E, Lopez-Rovira T, Rosa JL, Pons G, Boxer LM, Bartrons R, Ventura F 1999 A zinc-finger transcription factor induced by TGF-beta promotes apoptotic cell death in epithelial Mv1Lu cells. FEBS Lett 457(3):478-82.
4. Tachibana I, Imoto M, Adjei PN, Gores GJ, Subramaniam M, Spelsberg TC, Urrutia R 1997 Overexpression of the TGFbeta-regulated zinc finger encoding gene, TIEG, induces apoptosis in pancreatic epithelial cells. J Clin Invest 99(10):2365-74.

5. Subramaniam M, Hefferan TE, Tau K, Peus D, Pittelkow M, Jalal S, Riggs BL, Roche P, Spelsberg TC 1998 Tissue, cell type, and breast cancer stage-specific expression of a TGF-beta inducible early transcription factor gene. J Cell Biochem 68(2):226-36.
6. Tau KR, Hefferan TE, Waters KM, Robinson JA, Subramaniam M, Riggs BL, Spelsberg TC 1998 Estrogen regulation of a transforming growth factor-beta inducible early gene that inhibits deoxyribonucleic acid synthesis in human osteoblasts. Endocrinology 139(3):1346-53.

Appendices
Merry Jo Oursler

Shaw, A. and Oursler, M.J. (2000). Paracrine regulation of osteoclast activity in metastatic breast cancer. Cancer Research Alert 1:124-127.

Winding, B., Misander, H., Sveigaard, C., Therkildsen, B., Jakobsen, M., Overgaard, T., Oursler, M.J., Foged, N.K. (2000). Human breast cancer cells induce angiogenesis, recruitment, and activation of osteoclasts in osteolytic metastasis. J. Cancer Res Clin Oncol 126:631-640

Pascoe, D. and Oursler, M.J. (2001). The Src signaling pathway regulates osteoclast lysosomal enzyme secretion and is rapidly modulated by estrogen. J. Bone Miner Res 16:1028-1036.

Sanyal, A., Oursler, M.J., Clemens, V.R., Fukumoto, T., Fitzsimmons J.S., O'Driscoll, S.W. (2002). Temporal expression patterns of BMP receptors and collagen II (B) during periosteal chondrogenesis. J Orthop Res 20:58-65.

Mizuta, H., Sanyal, A., Fukumoto, T., Fitzsimmons, J.S., Matsui, N., Bolander, M.E., Oursler, M.J., O'Driscoll, S.W. (2002). The spatiotemporal expression of TGF-ß1 and its receptors during periosteal chondrogenesis *in vitro*. J Orthop Res 20:562-574.

Giulivi, C. and Oursler, M.J. Role of mitochondrial oxygen and nitrogen reactive species in signaling. (Invited Review). (2002). In Signal Transduction by Reactive Oxygen and Nitrogen Species: Pathways and Chemical Principles. M. Torres, J. Fukuto, and H.J. Forman, eds. Kluwer Press, New York.

Gingery, A., Bradley. E., Shaw A., and Oursler, M.J. (2003). Phosphatidylinositol 3-kinase coordinately activates the MEK/ERK and AKT/NFKκB pathways to maintain osteoclast survival. J Cell Biochem 89:165-179.

Oursler, M.J. (2003). Direct and indirect effects of estrogen on osteoclasts. J Musculoskel Neuron Interact 3:363-366.

Gorny, G., Shaw, A.K., Oursler, M.J. (2004). IL-6,LIF, and TNF-α regulation of GM-CSF inhibition of osteoclastogenesis *in vitro*. Exp Cell Res 294:149-158.

Karst, M., Gorny, G., Galvin, R.J., and Oursler, M.J. (2004) Roles of stromal cell RANKL, OPG, and M-CSF expression in biphasic TGF-ß regulation of osteoclast differentiation. J Cell Physiol 200:99-106.

Oursler, M.J. (In Press) Osteolytic Enzymes of Osteoclasts

and prognostic importance of pretreatment clinical characteristics in patients with advanced non-small-cell lung cancer treated with combination chemotherapy. *J Clin Oncol* 1986;4:1604-1614.
12. Takahashi T, Suzuki H, Hida T, et al. The *p53* gene is very frequently mutated in small-cell lung cancer with a distinct nucleotide substitution pattern. *Oncogene* 1991;6:1775-1778.
13. Sameshima Y, Matsuno Y, Hirohashi S, et al. Alterations of the *p53* gene are common and critical events for the maintenance of malignant phenotypes in small-cell lung carcinoma. *Oncogene* 1992;7:451-457.
14. Reichel MB, Ohgaki H, Petersen I, et al. *p53* mutations in primary human lung tumors and their metastases. *Mol Carcinog* 1994;9:105-109.
15. Mitsudomi T, Oyama T, Kusano T, et al. Mutations of the *p53* gene as a predictor of poor prognosis in patients with non-small-cell lung cancer. *J Natl Cancer Inst* 1993;85:2018-2023.
16. Greenblatt MS, Bennett WP, Hollstein M, et al. Mutations in the *p53* tumor suppressor gene: Clues to cancer etiology and molecular pathogenesis. *Cancer Res* 1994;54:4855-4878.
17. D'Amico D, Carbone D, Mitsudomi T, et al. High frequency of somatically acquired *p53* mutations in small-cell lung cancer cell lines and tumors. *Oncogene* 1992;7:339-346.
18. Kure EH, Ryberg D, Hewer A, et al. *p53* mutations in lung tumors: Relationship to gender and lung DNA adduct levels. *Carcinogenesis* 1996;17:2201-2205.
19. Tammemagi MC, McLaughlin JR, Bull SB. Meta-analyses of *p53* tumor suppressor gene alterations and clinicopathological features in resected lung cancers. *Cancer Epidemiol Biomarkers Prev* 1999;8:625-634.
20. Tseng JE, Rodriguez M, Ro J, et al. Gender differences in *p53* mutational status in small cell lung cancer. *Cancer Res* 1999;59:5666-5670.
21. Denissenko MF, Pao A, Tang M, et al. Preferential formation of benzo[a]pyrene adducts at lung cancer mutational hotspots in *p53*. *Science* 1996;274:430-432.
22. Eckert KA, Ingle CA, Drinkwater NR. N-ethyl-N-nitrosourea induces A:T to C:G transversion mutations as well as transition mutations in SOS-induced *Escherichia coli*. *Carcinogenesis* 1989;10:2261-2267.
23. Eisenstadt E, Warren AJ, Porter J, et al. Carcinogenic epoxides of benzo[a]pyrene and cyclopenta[cd]pyrene induce base substitutions via specific transversions. *Proc Natl Acad Sci U S A* 1982;79:1945-1949.
24. Ruggeri B, DiRado M, Zhang SY, et al. Benzo[a]-pyrene-induced murine skin tumors exhibit frequent and characteristic G to T mutations in the *p53* gene. *Proc Natl Acad Sci U S A* 1993;90:1013-1017.

Paracrine Regulation of Osteoclast Activity in Metastatic Breast Cancer

By A. Shaw and M. J. Oursler, PhD

BONE IS THE MOST COMMON SITE OF BREAST CANCER metastasis. Breast tumors in the bone marrow cavity recruit osteoclasts to degrade bone, forming localized areas where bone is considerably weakened. Metastatic breast cancer-induced bone loss is termed osteolysis. Osteolysis leads to hypercalcemia and bone fractures, resulting in considerable pain for patients with metastatic breast cancer. Elevated bone resorption by osteoclasts is responsible for tumor-induced osteolysis. The mechanism of the increase in osteoclast activity that causes osteolysis is believed to involve soluble growth factors secreted by the tumor. Recently, the importance of these paracrine influences on osteoclast activity have been recognized, and it is the purpose of this review to discuss the results of investigations into the mechanism of tumor-derived growth factor actions on osteoclasts.

Introduction

Paracrine factors are implicated as mediators of bone loss associated with tumor osteolysis in patients with metastatic breast cancer. Osteolytic lesions result from an increase in osteoclast bone resorption activity at sites adjacent to a tumor in the marrow cavity.[1] Bone loss during tumor osteolysis may result from any of the following mechanisms: 1) increased formation of osteoclasts; 2) increased resorption activity by mature osteoclasts; or 3) increased survival of mature osteoclasts.

Osteolytic bone loss may result from increased formation of mature osteoclasts from osteoclast precursors. Mature osteoclasts form by differentiation from hematopoietic stem cells found in the marrow activity. This process requires direct cell-cell contact between osteoclast precursors and marrow stromal cells. Later stages in osteoclast differentiation include fusion of mononuclear osteoclast precursors to form multinucleated cells, and activation of multinucleated osteoclasts to induce adhesion to bone and secretion of bone-degrading enzymes.[2]

Osteolytic bone loss may result from an increase in the resorption activity of each individual osteoclast. Bone resorption activity is related to the ability of an osteoclast to adhere to bone, secrete bone-degrading lysosomal enzymes, and migrate to form more and/or larger resorption

pits on bone slices. A mature osteoclast may be activated by a number of stimuli. Upon activation, an osteoclast will adhere to bone, forming a tight-sealing zone around the periphery of the bone resorption compartment, which is analogous to a secondary lysosome. Bone-degrading proteases are secreted into this compartment by fusion of lysosomal vesicles with the plasma membrane adjacent to the bone surface. Fusion of these vesicles increases the amount of membrane at this interface and this portion of the plasma membrane becomes highly convoluted, forming a structure called the ruffled border of the osteoclast.

The bone resorption compartment becomes acidified by the action of numerous proton pumps on the ruffled border. The combined action of acid and proteases degrades the bone surface enclosed by the sealing zone. An active osteoclast may detach, migrate, and reattach at another site to form multiple resorption pits. The important role that soluble growth factors play in activation of osteoclasts in metastatic breast cancer was first alluded to by a study that examined the conditioned medium of an osteolytic breast cancer cell line, MDA MB 231.[3]

This study revealed that 231 cell conditioned medium was capable of increasing the activity of mature osteoclasts, suggesting that the medium contained soluble factors that could act on osteoclasts. Analysis of the 231 cell conditioned medium revealed that it contained many growth factors that have been implicated as regulators of osteoclast activity. This conditioned medium was fractionated over a sizing column and used to treat osteoclasts. Some fractions stimulated, while some fractions inhibited osteoclast activity. This observation suggests that stimulatory factors overcome the actions of inhibitory factors to increase osteoclast activity. Paracrine stimulation of osteoclast activity may be a primary mechanism by which metastatic breast tumors are able to degrade bone.

Osteolytic bone loss may result from increased survival of mature osteoclasts. It is believed that mature osteoclasts are removed from the bone surface by a signal to undergo apoptosis. Soluble factors secreted by tumors may delay the apoptotic signal, allowing osteoclasts to continue with their bone resorption program for a longer period of time. Below, several paracrine factors that may be important in the development of osteolytic lesions are discussed.

OPG/RANKL/RANK

Osteoprotegerin (OPG) is a recently discovered protein that plays an important role in osteoclast formation. OPG is a soluble factor secreted by bone marrow stromal cells and osteoblasts. OPG functions as an inhibitor of osteoclast formation. OPG interferes with a critical interaction between the osteoclast precursor receptor-activator of NFkB (RANK) and its cognate ligand (RANKL). RANK is present on the plasma membrane of osteoclast precursors and mature osteoclasts, while RANKL is expressed on the plasma membrane of stromal cells. In addition, the interaction between RANKL and RANK gives rise to signaling events that inhibit apoptosis in mature osteoclasts. In this way, OPG reduces overall osteoclast numbers by blocking osteoclast formation and stimulating apoptosis of mature osteoclasts. Conversely, increased levels of RANKL are correlated with increased osteoclast numbers. One might expect that osteolytic tumors would express RANKL or induce RANKL expression. However, we and others have shown that most primary breast cancers, metastatic breast cancers, and breast cancer cell lines do not express RANKL.[4] When breast cancer cells are co-cultured with bone marrow stromal cells, expression of RANKL is induced and OPG is inhibited.[5] These results indicate that another factor produced by breast cancer cells within the bone marrow cavity induces RANKL expression and inhibits OPG secretion by bone marrow stromal cells.

Macrophage-Colony Stimulating Factor

Macrophage-colony stimulating factor (M-CSF) is absolutely required for osteoclast formation. M-CSF is expressed by bone marrow stromal cells and osteoblasts. The essential role of M-CSF is evident in mutant op/op mice that express nonfunctional M-CSF. These mice show a complete lack of mature osteoclasts, a condition that is reversed by infusion of M-CSF. M-CSF stimulates proliferation of early osteoclast precursors and induces migration of actively resorbing osteoclasts. Estrogen deficiency enhances M-CSF production, which results in the overall increase in osteoclast number seen in osteoporosis. M-CSF also promotes the survival of mature osteoclasts by delaying the onset of apoptosis. M-CSF and RANKL have been shown to be essential factors for osteoclast formation in vitro.[6]

Granulocyte-Macrophage Colony Stimulating Factor

Granulocyte-macrophage colony stimulating factor (GM-CSF) has opposing effects on osteoclast formation. Effects of GM-CSF appear to depend on the differentiation state of the target cell. GM-CSF stimulates proliferation of early osteoclast precursors, but potently inhibits late stages of osteoclast differentiation. GM-CSF inhibits formation of osteoclasts from mouse bone marrow, which contains mid-stage osteoclast precursors. In an in vivo nude mouse model of osteolysis, expression of GM-CSF declined as osteolytic lesions appeared.[7] Local repression of GM-CSF to allow osteoclast formation may provide a mechanism by which an osteolytic tumor can mediate bone loss.

Tumor Necrosis Factor Alpha

Tumor necrosis factor alpha (TNF-α) is a soluble protein secreted by many bone marrow cells and is known to play a role in the development of other bone loss pathologies, including periodontitis and orthopedic implant loosening. Antibody blockade of TNF-α results in decreased osteoclast numbers and reduced pit formation activity of mature osteoclasts.[8] TNF-α is secreted in large quantities by osteolytic breast cancer cell lines and by breast tumors in bone. We have used a mouse model of breast cancer osteolysis to examine the timing of TNF-α expression as it relates to the appearance of osteolytic lesions. TNF-α expression by mouse marrow cells increases as tumor size increases and as osteolytic lesions appear in the mice. We have examined the effects of TNF-α added to osteoclast precursors during differentiation. TNF-α treatment results in increased osteoclast numbers and larger osteoclasts as compared to untreated osteoclasts. These larger TNF-α-stimulated osteoclasts secrete more bone-degrading enzymes and form more resorption pits per cell than unstimulated osteoclasts. TNF-α also appears to prolong the lifespan of mature osteoclasts by inhibiting apoptosis.[9] These results indicate that elevated TNF-α levels may play a role in metastatic breast cancer-induced osteolysis. TNF-α secreted by tumor cells and marrow cells may induce formation of larger osteoclasts that destroy bone at a rate faster than it can be replaced by osteoblasts.

Insulin-Like Growth Factors

Insulin-like growth factors (IGFs) are secreted by osteoblasts and stimulate proliferation of osteoblasts. Mature osteoclasts express type I IGF receptors and IGF stimulates resorption activity of mature osteoclasts in the presence of osteoblasts.[10] IGF induction is responsible for growth hormone and parathyroid hormone-induced osteoclast formation.[11] This suggests that IGF may contribute to osteoclast formation indirectly by inducing expression of another osteoclast-promoting growth factor. IGF is secreted by breast cancer cell lines and metastatic breast tumors in bone. IGF treatment of osteoclast precursors induces differentiation into mature osteoclasts. IGF secreted by metastatic breast tumors may contribute to elevated osteoclast activity by inducing differentiation of osteoclast precursors and stimulating resorption activity of mature osteoclasts.

Parathyroid Hormone-Related Peptide Expression

Parathyroid hormone-related peptide (PTHrP) expression is correlated with increased metastasis of breast cancer cells, which leads to increased frequency of osteolytic lesions in vivo. PTHrP is expressed by mature osteoclasts and 92% of breast tumors showing bone metastases.[12] PTHrP is the main causative agent of hypercalcemia that is associated with a variety of cancers. Hypercalcemia is mediated through an endocrine mechanism involving PTH receptor-mediated effects on kidney and bone metabolism. Paracrine actions of PTHrP are dual, with different portions of the PTHrP molecule giving rise to opposing effects. PTHrP(1-34) mediates stimulatory PTH-like actions by binding to the PTH receptor expressed on osteoblasts. These indirect effects include stimulation of osteoclast formation and increased bone resorption activity. However, PTHrP(107-139) mediates inhibitory actions of PTHrP, including direct inhibition of osteoclastic bone resorption, by an unknown PTH receptor-independent mechanism.[13] PTHrP expression appears to be permissive for formation of bone metastases, although its role in the induction of osteolysis remains unclear.

Interleukins

Interleukin-1 (IL-1) stimulates bone resorption primarily by prolonging survival of mature osteoclasts. IL-6 also stimulates bone resorption, but its mode of action is stimulation of osteoclast formation. IL-6 induces proliferation of osteoclast precursors and induces these precursors to commit to the osteoclast lineage. Infusion of IL-1 together with IL-6 in mice causes marked bone loss that results in hypercalcemia. Bone loss due to elevated levels of parathyroid hormone or 1, 25-dihydroxyvitamin D3 is due to the ability of these hormones to induce IL-6 secretion from osteoblasts.[6] Many breast tumors express IL-1 and IL-6, which makes these factors possible mediators of bone loss associated with metastatic breast cancer.

Leukemia Inhibitory Factor

Leukemia inhibitory factor (LIF) is so named because of its ability to inhibit proliferation and induce differentiation to the macrophage line of a myeloid leukemic cell line.[14] Since its discovery, a variety of systemic effects have been attributed to LIF. The overall effect of LIF on bone metabolism is to increase the rate of bone turnover by increasing both osteoblast and osteoclast activity. LIF overexpression in mice causes splenic enlargement due to the excessive proliferation of hematopoietic stem cells, the cells that give rise to osteoclasts. LIF prolongs survival of osteoclast precursors and induces the proliferation of osteoblasts. LIF expression is induced by cytokines known to induce bone loss, including TNF-α, IL-1, and IL-6.[15] LIF is expressed by 78% of primary breast tumors and stimulates the proliferation of breast cancer cell lines in vitro.[16] Expression of LIF by breast cancers in bone could potentially stimulate osteoclast activity to induce bone loss.

Transforming Growth Factor

Transforming growth factor (TGF-β) has biphasic effects on osteoclast activity. At high doses, TGF-β inhibits osteoclast formation. However, at low doses, TGF-β stimulates formation and survival of osteoclasts. We have shown that osteoclasts formed in the presence of TGF-β become TGF-β-dependent. Withdrawal of TGF-β from these TGF-β-dependent osteoclasts induces immediate apoptosis.[17] Osteoclasts formed in the environment adjacent to a TGF-β-secreting breast tumor may become TGF-β-dependent and may survive longer than osteoclasts formed in the absence of TGF-β. Enhanced survival of TGF-β-dependent osteoclasts may provide a mechanism by which breast tumors can induce osteolysis.

Summary

Breast tumors in the bone marrow cavity can induce bone loss by inducing the formation, activity, and survival of mature osteoclasts. These effects may be due to the secretion of growth factors in the area adjacent to the tumor. RANKL, M-CSF, TNF-α, IGF, IL-1, IL-6, LIF, and TGF-β can enhance formation of mature osteoclasts by exerting effects on various stages of osteoclast differentiation. RANKL, M-CSF, TNF-α, IGF, and LIF can promote osteoclast resorption activity by increasing adhesion to bone, secretion of lysosomal proteases, and migration. M-CSF, TNF-α, IL-1, and TGF-β increase the lifespan of mature osteoclasts by delaying apoptosis. Additionally, repression of factors that block osteoclast formation, such as GM-CSF, may enable tumors to recruit osteoclasts. In order to clarify the role of tumor-derived growth factors in development of osteolytic lesions, future investigations should explore the combined effects of growth factors on osteoclast activity. *(Ms. Shaw is a research assistant and Dr. Oursler is an Assistant Professor, Biology Department, University of Minnesota, Duluth.)* ❖

References

1. Clohisy DR, Palkert D, Ramnaraine MLR, et al. Human breast cancer induces osteoclast activation and increases the number of osteoclasts at sites of tumor osteolysis. *J Bone Joint Surg* 1996;14:396-402.
2. Reddy S, Roodman GD. Control of osteoclast differentiation. *Crit Rev Euk Gene Exp* 1998;8:1-17.
3. Pederson L, Winding B, Foged N, et al. Identification of breast cancer cell line-derived paracrine factors that stimulate osteoclast activity. *Cancer Res* 1999;59: 5849-5855.
4. Thomas R, Guise T, Yin J, et al. Breast cancer cells interact with osteoblasts to support osteoclast formation. *Endocrinol* 1999;140:4451-4458.
5. Chikatsu N, Takeuchi Y, Tamura Y, et al. Interactions between cancer and bone marrow cells induce osteoclast differentiation factor expression and osteoclast-like cell formation in vitro. *Biochem Biophys Res Commun* 2000;67:632-637.
6. Martin TJ, Romas E, Gillespie M. Interleukins in the control of osteoclast differentiation. *Crit Rev Euk Gene Exp* 1998;8:107-123.
7. Shaw A, Jakobsen M, Rock M, et al. *Metastatic breast cancer: Identification of factors involved in tumor progression in bone.* In: Second Joint Meeting of the American Society for Bone and Mineral Research and the International Bone and Mineral Society, San Francisco, CA; November 1998:S280.
8. Tani-Ishii N, Tsunoda A, Teranaka T, et al. Autocrine regulation of osteoclast formation and bone resorption by IL-1 alpha and TNF alpha. *J Dent Res* 1999;78: 1610-1623.
9. Shaw A, Gingery A, Maki J, et al. *TNF alpha stimulates osteoclast maturation and inhibits apoptosis of mature osteoclasts: A model for tumor osteolysis.* In: 21st Annual Meeting of the American Society for Bone and Mineral Research: St. Louis, MO; September 1999:S484.
10. Conover C. The role of insulin-like growth factors and binding proteins in bone cell biology. *Principles of Bone Biology*. Academic Press; 1996:607-618.
11. Chihara K, Sugimoto T. The action of GH/IGF-I/IGFBP in osteoblasts and osteoclasts. *Horm Res* 1997;48: 45-49.
12. Powell G, Southby J, Danks J, et al. Localization of parathyroid hormone-related protein in breast cancer metastases: Increased evidence in bone compared with other sites. *Cancer Res* 1991;51:3059-3061.
13. Rankin W, Grill V, Martin TJ. Parathyroid hormone-related protein and hypercalcemia. *Cancer* 1997;80: 1564-1571.
14. Van Beek E, Van der Wee-Pals L, Van de Ruit M, et al. Leukemia inhibitory factor inhibits osteoclastic resorption, growth, mineralization, and alkaline phosphatase activity in fetal mouse metacarpal bones in culture. *J Bone Miner Res* 1993;8:191-198.
15. Kurzrock R, Estrov Z, Wetzler M, et al. LIF: Not just a leukemia inhibitory factor. *Endocrine Rev* 1991;12: 208-217.
16. Dhingra K, Sahin A, Emami K, et al. Expression of leukemia inhibitory factor and its receptor in breast cancer: A potential autocrine and paracrine growth regulatory mechanism. *Breast Cancer Res Treat* 1998;48:165-174.
17. Gingery A, Shaw A, Holy J, et al. *TGF beta is a survival factor for TGF beta-induced osteoclasts.* In: 21st Annual Meeting of the American Society for Bone and Mineral Research: St. Louis, MO; September 1999:S300.

J Cancer Res Clin Oncol (2000) 126:631–640

ORIGINAL PAPER

Bent Winding · Henriette Misander · Christina Sveigaard
Bente Therkildsen · Maria Jakobsen · Trine Overgaard
Merry Jo Oursler · Niels Tækker Foged

Human breast cancer cells induce angiogenesis, recruitment, and activation of osteoclasts in osteolytic metastasis

Received: 25 January 2000 / Accepted: 11 April 2000

Abstract ***Purpose:*** The purpose of this study was to elucidate the potential of human breast cancer cells (BCC) to induce matrix degradation and neo-vascularization, essential for continued tumor growth, in osteolytic lesions. ***Methods:*** BCC were inoculated into the left cardiac ventricle of female athymic mice and osteolytic lesions were radiologically visualized within 4 weeks from inoculation. ***Results:*** Histomorphometric analysis of bone sections revealed a significant increase in the number and maturity of osteoclasts (OCl) lining the bone surfaces next to tumor tissue when compared to corresponding bone surfaces in healthy mice. In addition, a large number of newly formed blood vessels could be visualized by immunohistochemistry at the periphery of and within tumor tissue. When bone marrow (BM) cells were cultured in the presence of BCC the OCl formation was increased threefold. These OCl were also found to be more mature and to have greater resorptive activity. Moreover, BCC were found to stimulate proliferation, migration, and differentiation of BM-derived endothelial cells. ***Conclusions:*** Matrix destruction and neo-vascularization are accomplished by BCC arrested in the BM cavity by increasing recruitment and activity of OCl and by induction of angiogenesis within or in proximity to the tumor tissue.

Key words Bone metastasis · Neo-vascularization · Osteoclast recruitment · Osteolysis · MDA-231 cells

B. Winding (✉) · H. Misander · C. Sveigaard · B. Therkildsen
M. Jakobsen · T. Overgaard · N. T. Foged
Cancer and Bone Group, OsteoPro A/S,
Center for Clinical and Basic Research,
Ballerup Byvej 222, 2750 Ballerup, Denmark
Tel.: +45-4468-4700, ext. 214; Fax: +45-4468-4220
e-mail: bw@ccbr.dk

M. J. Oursler
Department of Biology, University of Minnesota,
211 Life Science Building, 10 University Drive, Duluth,
MN 55812-2496, USA

Introduction

Bone is one of the three most favored sites of solid tumor metastasis. In fact, 90% of the patients who die of breast carcinoma have bone metastases (Woodhouse et al. 1997). Breast cancer metastasis to bone often presents with severe symptoms due to osteolytic lesions and may cause multiple complications for the patient. These include pain, impaired mobility, hypercalcemia, pathologic fracture, spinal cord or nerve root compression, and bone marrow infiltration (Coleman 1997; Sasaki et al. 1995). Most importantly, once cancer cells become housed in the skeleton, the cancer is essentially noncurable with current treatments. Agents such as the bisphosphonates, which inhibit osteoclastic bone resorption, have proven to decrease the complications associated with bone metastases (Kanis et al. 1996; Diel et al. 1998).

Bone has been described as a storehouse for a variety of cytokines and growth factors, which provides an extremely fertile environment for breast cancer cells (Yoneda et al. 1994). However, because bone is mainly comprised of a hard, mineralized tissue, it is more resistant to destruction than other tissues. Thus, for cancer cells to grow in bone, they must be capable of causing bone destruction (Guise 1997). This is believed to be accomplished by the potential of breast cancer cells to recruit and activate osteoclasts (OCls) (Yoneda et al. 1994; Clohisy et al. 1996; Pederson et al. 1999).

So far, only a very few breast cancer cell-derived factors, which may be involved in cancer-induced osteolysis in vivo, have been identified. Yoneda and colleagues have shown that parathyroid hormone-related protein (PTHrP) might play an important role for cancer-induced osteolysis in vivo. They have found that mice inoculated with human breast cancer cells (MDA-231) receiving neutralizing anti-human PTHrP antibodies developed fewer and smaller osteolytic metastases than mice receiving nonspecific antibodies or vehicle as control (Guise et al. 1996). The presence of PTHrP at

the mRNA and protein levels in bone metastasis still remains to be demonstrated.

The generation of blood vessels (angiogenesis) is an essential step for the primary tumor and metastasis to grow (Woodhouse et al. 1997; Hanahan and Folkman 1996). Smaller tumors may receive all nutrients by diffusion, but further growth depends on an adequate blood supply, accomplished through cancer-induced angiogenesis (Fidler and Ellis 1994). Therefore, after the initial arrest and growth in the bone environment, the induction of angiogenesis becomes crucial for the continued secondary tumor growth.

The purpose of the present study was to investigate the influence of human breast cancer cells on OCl recruitment, maturation, and resorptive activity, and on endothelial cell proliferation, migration, and differentiation. We used bone sections from athymic mice with or without bone metastasis for immunochemical quantification of possible changes in OCl numbers and newly formed vessels within or in proximity to the tumor tissue as compared to normal bone marrow. Moreover, several bone marrow/breast cancer cell co-culture assays were used to highlight the relative importance of cancer-derived factors on each single step in OCl and endothelial cell activity.

Materials and methods

Animals and drugs

Four-week-old female Balb/C athymic (nude) mice were obtained from M&B, Denmark. Culture media, penicillin, and streptomycin were purchased from Life Technologies, Denmark. Rabbit anti-human pan-cytokeratin polyclonal antibodies (Code No. A-0575), control antibodies (Code No. X-0903), and EnVision+ were purchased from DAKO, Glostrup, Denmark. The rat anti-mouse CD31 antibody (MEC 13.3) and rat immunoglobulin isotype controls were purchased from PharMingen (San Diego, Calif., USA). Rat anti-mouse CD34 antibody (MEC 14.7) was a kind gift from Dr. Cecilia Garlanda (Istituto di Ricerche Farmacologiche Mario Negri, Milan, Italy). Biotinylated rabbit anti-rat antibodies, DAB, ExtrAvidin Peroxidase Staining kit, and Mitomycin C were obtained from Sigma Chemical, St. Louis, Mo., USA.

Cell lines

The parental human estrogen receptor-negative breast cancer cell line MDA-231/P was kindly supplied by Professor Nils Brünner, Finsen Laboratory, Denmark. An in vivo selected bone-seeking subclone, called MDA-231/B, of the MDA-231 cell line was generated by us and maintained as the parental cell line for six passages. The murine bone marrow-derived stromal cell line MBA-2.1 (endothelial-like cells) (Zipori et al. 1987) was kindly supplied by Professor Dov Zipori, Weizman Institute of Science, Israel.

In vivo studies

MDA-231/B cells were cultured in 175 cm^2 flasks (NUNC, Denmark) to confluence. The cells were released by trypsin/EDTA and after repeated washing in phosphate-buffered saline (PBS) resuspended in E-MEM without additives at a cell density of 10^6 cells/ml. The cancer cell suspension (0.1 ml) was slowly inoculated into the left cardiac ventricle of anesthetized 4-week-old mice. Less than 10% of animals died from the inoculation procedure. Four weeks after cancer cell inoculations animals were anesthetized and placed in prone position against a single coated HCM film (Imation Medical Imaging, Denmark), and exposed to X-rays at 30 kVp, 5 mA, for 18 s using a Biotron radiographic inspection unit (Renberg and Jensen, Denmark). Films were developed with the use of a 3 M Model XP-2000 (Imation Medical Imaging, Denmark). Osteolytic metastases (Fig. 1A) were detected in approximately 90% of the cancer-inoculated animals.

Fig. 1A–F Radiography and histology of osteolytic bone metastasis. **A** A representative radiography of a mouse with osteolytic lesions in the hind limbs (*arrows*). Human breast cancer cells (BCC) in single cell suspension had been inoculated into the left cardiac ventricle of 4-week-old female Balb/C athymic mice 4 weeks prior to the X-ray. **B** Using a rabbit polyclonal antibody raised against the human epithelial cell marker, cytokeratin, a strong and specific immunoreaction to human BCC was observed, without non-specific staining of bones or normal bone marrow (BM). **C** When a corresponding bone section was stained for tartrate-resistant acid phosphatases (TRAP; red color reaction), a rim of large TRAP+ cells (*arrows*) was found covering the bone surfaces next to the tumor tissue. **D** In contrast, at bone surfaces distant from tumor tissue, only a low number of small TRAP+ cells (*arrows*) was identified. **E** The MEC14.7 antibody, raised against mouse CD34, formed immunoreactions with endothelial cells lining smaller blood vessels near the cartilage growth plate in the BM and strong immunoreaction with small blood vessels and capillaries at the periphery and within tumor tissue (BCC). **F** At higher magnification the vessel-like structures (*red arrows*) of immunoreactive cells can clearly be seen. Replacing MEC14.7 antibodies with an isotypic control antibody as primary antibody confirmed the specificity of the immunoreactions, as no signal was observed in bone sections from healthy or metastatic mice (data not shown)

Histology

Bones were isolated from animals immediately after being killed and immersed in 4% formaldehyde and kept at 4 °C for 48 h. The bones were decalcified in 15% EDTA-solution (Tritriplex III, Merck), pH 7.4, for 3 weeks at 4 °C. The decalcification buffer was changed twice a week. Bones were subsequently dehydrated in increasing concentrations of ethanol before embedding in paraffin. Five-micrometer sections of tibias or femurs placed on Superfrost PLUS slides were air-dried overnight at 37 °C. Slides were deparaffinized in two changes of toluene and rehydrated in decreasing concentrations of ethanol for the tartrate-resistant acid phosphatases (TRAP)-staining procedure or dehydrated in two changes of 99% ethanol before immunohistochemistry (IHC). Following dehydration, endogenous peroxidase activity in tissue sections for IHC was blocked with 0.45% hydrogen peroxide in 99% ethanol.

For the demonstration of tumor cells in bone sections we used rabbit anti-human pancytokeratin antibodies (A 0575, DAKO, Denmark). Rabbit non-specific polyclonal antibodies were used in the same dilution as the primary antibody in adjacent sections to verify the specificity of the observed signals. Sections were washed in TBS and rinsed in running tap water before slides were treated with 0.05% protease (P 5147, Sigma) for 5 min at 37 °C to reveal antigenic sites. To reduce background staining, slides were incubated in a TBS blocking solution containing 0.5% (w/v) casein (C5890, Sigma) for 20 min. The blocking solution was used as diluent for primary/control antibodies, secondary antibody, and as washing solutions in between. Sections were incubated in primary or control antibodies (1:500) for 2 h at room temperature, washed, and subsequently incubated with Envision+, peroxidase, anti-rabbit assay (DAKO, Denmark) for 30 min at room temperature. Immunoreactive sites were visualized by submerging slides in DAB^+ (0.05% DAB (D 5637, Sigma) in TRIS/Imidazole buffer pH 7.6, to which 0.01% hydrogen peroxide had been added (just before

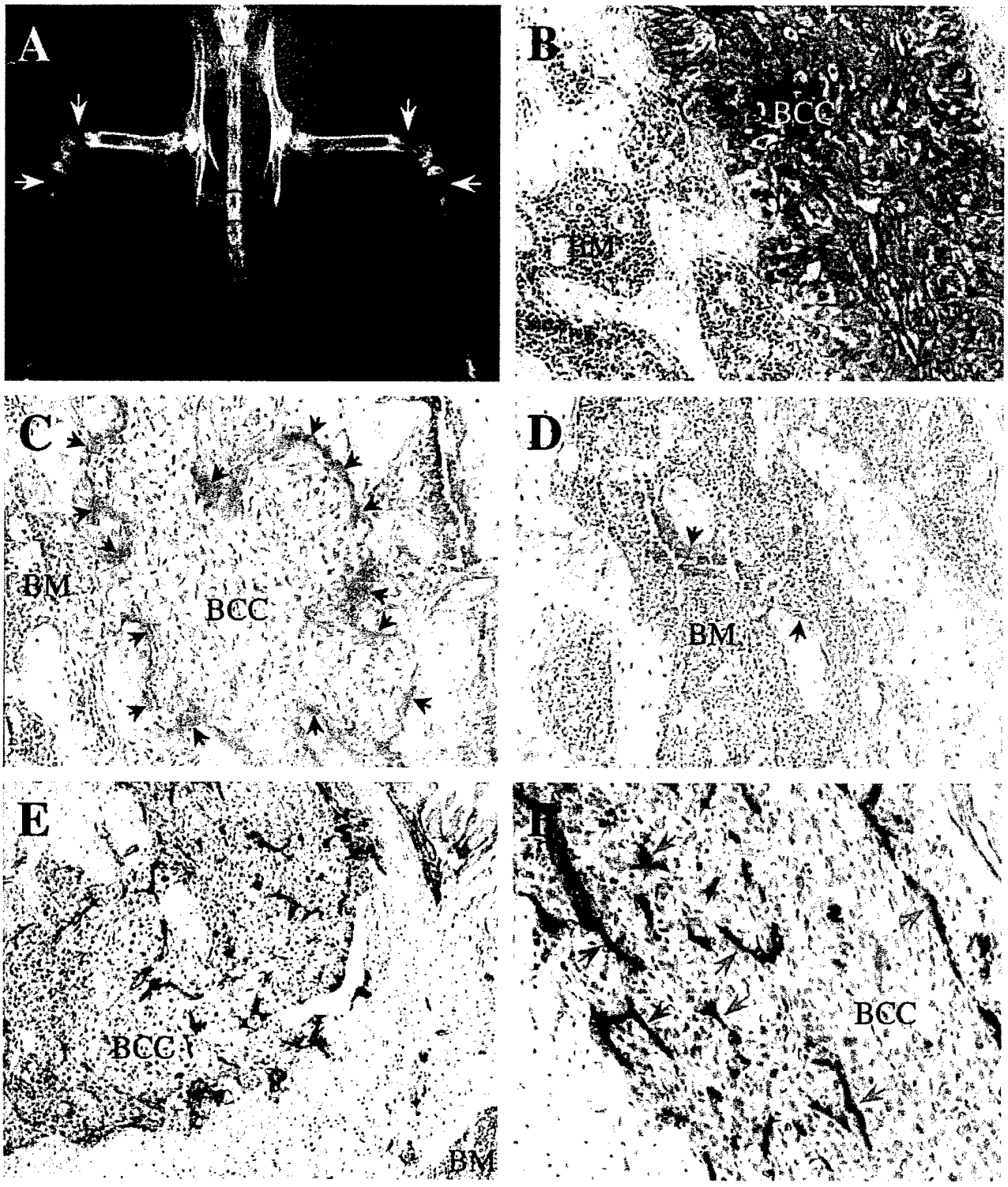

use) for 4 min. Sections were counterstained with Mayers hematoxylin, rinsed in running tap water, and finally slides were coverslipped with DPX Mountant (Fluka, Neu-Ulm, Switzerland). We did not observe any non-specific background staining on slides treated with control antibodies.

For the immunohistochemical demonstration of endothelium of blood vessels and of newly formed capillaries we used the two rat monoclonal antibodies MEC 13.3 and MEC 14.7 raised against mouse CD31 (PECAM-1) and mouse CD34, respectively. The appropriate rat immunoglobulin isotype control was used in the same dilution as primary antibodies in adjacent sections to verify the specificity of the observed signals. Sections were washed in TBS and rinsed in running tap water before slides were treated with 0.1% trypsin for 20 min at 37 °C to reveal antigenic sites. To reduce background staining, slides were incubated in a TBS blocking solution containing 0.5% (w/v) casein for 20 min. The blocking

solution was used as diluent for primary/control antibodies, secondary antibody, and ExtrAvidin, and as washing solutions in between. Sections were incubated in primary or control antibodies (1:100) for 2 h at room temperature, washed, and subsequently incubated with the secondary antibody (biotinylated rabbit anti-rat immunoglobulin, Sigma) for 30 min at room temperature. Subsequently, slides were incubated twice with ExtrAvidin for 30 min. Immunoreactive sites were visualized by submerging slides in DAB^+ for 4 min. Sections were counterstained with Mayers hematoxylin and rinsed in running tap water, and finally the slides were coverslipped with Aquamount (BDH Laboratories Supplies, UK). We did not observe any non-specific background staining on slides treated with control antibodies.

Bone histomorphometry

Serial sections (5 μm in thickness) of tibias of three mice with radiographically verified osteolytic lesions and four healthy control mice were cut longitudinally and examined using a semi-automatic system (Image-Pro Plus, Media Cybernetics, Silver Spring, Md., USA). The demonstration of TRAP-positive cells (=OCls) in bone sections was performed as previously described (Scheven et al. 1986). Histomorphometric analyses were performed 0.5–1.0 mm to the growth plate cartilage in three non-consecutive sections from each tibia at a magnification of 200. The parameters for osteoclast number and maturity included: number of osteoclasts per millimeter of bone surface (N.Oc/mm BS); osteoclast surface per bone surface (Oc.S/BS, %); osteoclast surface per osteoclast (Oc.S/Oc, μm); and number of nuclei per osteoclasts (N.Nu/Oc).

In vitro studies

Osteoclast assays

The OCl formation assay was performed as previously described (Takahashi et al. 1988). Briefly, primary bone marrow cells were harvested from tibias and femurs isolated from 5-week-old mice. The collected bone marrow cells were seeded on devitalized bovine cortical bone slices (28 mm^2) placed in 96-well plates or seeded in culture-treated 24-well plates (Falcon, Becton Dickinson) at cell densities of 5×10^5 and 1.5×10^6 cells/well, respectively. The cells were cultured in α-MEM containing 5% heat-inactivated fetal calf serum (HI-FCS) for the indicated number of days (normally 8 days) with conditioned medium (CM) being collected and replaced with fresh culture medium every second day. At the end of the culture period adherent cells were washed twice in PBS (pH 7.4), fixed in 5% glutaraldehyde–formaldehyde and stained for detection of TRAP+ cells according to the manufacturer's instructions (Sigma Chemical). The OCl escavation pits formed on the bovine cortical bone slices were stained and the area measured as previously described (Foged et al. 1996; Winding et al. 1997). The CM was analyzed for TRAP activity and CrossLaps (i.e., a carboxy-terminal telopeptide proteolytic degradation product of the α_1 chains of type I collagen) as previously described (Foged et al. 1996; Pederson et al. 1997). To study the influence of breast cancer cells on the number, maturity, activity, and survival of OCls formed in this assay, cancer cells at increasing seeding densities of proliferating (10^2–10^4 cells/well) or non-proliferating (pre-treated with 40 μg/ml Mitomycin C for 45 min) (10^3–10^5 cells/well) cells were added to the bone marrow cultures with direct cell–cell contact or separated by a membrane filter insert (pore size 0.45 μm, Falcon).

Endothelial cell assays

The influence of cancer cell-derived factors on migration, proliferation, and differentiation of bone marrow-derived endothelial cells were studied in co-cultures. For the proliferation and migration studies breast cancer cells and endothelial cells were physically separated by a membrane insert, which allowed the exchange of soluble factors but prevented direct cell–cell contact. Cancer cells were plated onto 12-well plates with increasing cell density. Cell cultures were allowed to adjust for 24 h in a culture medium containing 0.1% albumax.

In the proliferation assay, endothelial cells (10^4) were plated onto type I collagen precoated membrane inserts with a pore size of 0.45 μm and allowed to adjust for 24 h. Subsequently, inserts were transferred to 12-well plates with breast cancer cells and co-cultured for 48 h. 3-(4,5-dimethylthiazol-2-yl)-2,5-diphenyl tetrazolium bromid (MTT, Boehringer Mannheim, Germany) was added to the cell cultures for the last 3 h.

In the migration assay endothelial cells (3×10^4) were plated onto type I collagen gel-precoated membrane inserts with a pore size of 12 μm and allowed to form a monolayer on the inserts. Subsequently, the inserts were transferred to 12-well plates with breast cancer cells and co-cultured for 14 h before fixation of the endothelial cells in 5% glutaraldehyde and staining with 0.5% toluene blue in 2.5% $NaCO_3$. The number of migrating endothelial cells was measured semi-automatically by counting in hundreds randomly, but evenly distributed computer-generated counting fields for each insert.

In the microtubule formation assay MDA-231/B cells were plated onto 24-well plates at increasing seeding densities and cultured for 24 h. Cells were washed three times in serum-free media before addition of 300 μl Matrigel D-MEM (2:1) to each well. Cultures were subsequently incubated at 37 °C for 30 min, causing the Matrigel to jellify. Endothelial cells (3×10^4) were plated on top of the Matrigel and the cells were co-cultured for 48 h. Cells were fixed in 5% glutaraldehyde for 30 min and washed three times with PBS containing 50 mM glycine at 30 min intervals. The area of tubules formed in co-cultures was measured semi-automatically by counting the number of hits in 24 randomly distributed computer-generated grids for each well.

Cytokine levels

The levels of mouse-derived cytokines, i.e., interleukin-6 (IL-6), interleukin-1beta (IL-1β), and tumor necrotic factor-alpha (TNF-α), secreted into the conditioned media during cultivation of either mouse bone marrow alone or in co-culture with breast cancer cells were measured by ELISA (R&D Systems Europe, UK). The levels of human-derived cytokines were determined in conditioned media obtained from confluent MDA-231/B cell cultures. Briefly, MDA-231/B cells were plated onto 10-cm petri dishes and cultured to confluence in α-MEM containing 5% HI-FCS. Conditioned medium was harvested after culturing the cells in fresh medium for 48 h. The human cytokines, vascular endothelial growth factor (VEGF), macrophage colony stimulating factor (M-CSF), IL-6, interleukin-1alpha (IL-1α), IL-1β, and TNF-α, were measured by ELISA (R&D Systems Europe). Parathyroid hormone-related protein (PTHrP) was measured by a radioimmunoassay (Peninsula Laboratories Europe, Merseyside, UK). The background levels in conditioned media from petri dishes without cells were found to be zero for all tested cytokines.

Detection of cytokine transcripts

MDA-231 cells were cultured to confluence as described above. Total RNA was extracted by acid guanidinium thiocyanate-phenol-chloroform as previously described (Chomczynski and Sacchi 1987). Expression of M-CSF, IL-1α, IL-1β, PTHrP, TNF-α, and VEGF mRNA was examined by reverse transcriptase-polymerase chain reaction (RT-PCR) using GeneAmp Thermostable rTth kit (Perkin Elmer, USA) according to the manufacturer's recommendations. Briefly, first strand cDNA was synthesized from 250 ng total RNA with a final concentration of the downstream primer at 0.75 mM. Upstream primer and $MgCl_2$ were added to the cDNA mixture in final concentrations of 0.15 mM and 1.5 mM, respectively. PCR was performed in a Perkin Elmer 9600 PCR machine

with 1 min denaturation at 95 °C, 35 cycles of 10 s at 95 °C, and 15 s at 60 °C and a final extension step for 7 min at 60 °C.

For analysis of IL-6 mRNA expression cDNA was synthesized with the First-Strand cDNA Synthesis Kit (Pharmacia-Biotech, USA) according to the manufacturer's recommendations. In brief, 5 µg total RNA was reversibly transcribed with the supplied Not I-d(T)18 primer in a final reaction volume of 33 µl. The PCR reaction mixture contained 5 µl cDNA, 2.5 mM $MgCl_2$, 0.2 mM dATP, dCTP, dGTP, dTTP (Pharmacia-Biotech, USA), 30 pmol of each primer, 1 × PCR buffer, 2.5 U AmpliTaq Gold (Perkin Elmer, USA). The PCR was performed for 11 min at 94 °C, 40 cycles of 1 min at 94 °C, 1 min at 64 °C, and 1 min at 72 °C, and for 7 min at 72 °C as a final extension step in a Perkin-Elmer 9600 PCR machine. Control PCR was performed with MilliQ; in none of these samples were PCR products detected.

Primers used for RT-PCR were as previously reported (Brown et al. 1996); details are available on request. The oligonucleotides were obtained from DNA Technology, Denmark. The sizes of the PCR products were analyzed on a 2% wt/vol agarose gel and the specificity was confirmed either by sequencing with the 70770 Sequenase version 2.0 kit (Amersham, USA) or for VEGF by Southern blot analysis.

For the Southern blot analysis the agarose gel was pre-treated by washing: 10 min in 10 mM HCl, 2 min in MilliQ, 2 × 30 min in 0.5 M NaOH, 1.5 M NaCl, 2 min in MilliQ, and 2 × 30 min in 0.5 M Tris, 3.0 M NaCl. The products were blotted onto a nitrocellulose membrane (Schleicher and Shuell, Keene, N.H., USA) by capillary transfer o.n. using 2 × SSC. Prehybridization was performed at 58 °C in 5 × SSC, 2.5 × Denhardt's solution, 0.5% SDS, and 100 µg/ml denatured salmon sperm DNA for 1.5 h. A oligonucleotide 5′-CATCACCATGCAGATTATGCGGATCAAA CC-3′ (Brown et al. 1996), which hybridizes to all VEGF splice-variants, was labeled with γP32-ATP (Amersham Pharmacia Biotech, USA) using T4 polynucleotide kinase (Promega, Madison, Wis., USA) and purified by ProbeQuant G-50 micro column (Amersham Pharmacia Biotech, USA). Hybridization was performed at 58 °C o.n. 10 pmol labeled oligonucleotide and post-hybridization washes were: 3 × 20 min in 2 × SSC, 0.1% SDS at r.t., 2 × 20 min in 0.1 × SSC, 0.1% SDS at r.t., and 30 min in 0.1 × SSC, 0.1% SDS at 65 °C. Specifically bound oligonucleotide was visualized with a PhophorImager (Molecular Dynamics, Sunnyvale, Calif., USA).

Results

Osteolysis

Human breast cancer cells or vehicle were injected into the left cardiac ventricle of 4-week-old female athymic mice. In mice injected with cancer cells osteolytic lesions developed within 4 weeks from inoculation with a preference for the distal femurs and proximal tibias (Fig. 1A). The human origin of the tumor tissue was confirmed by species-specific immunohistochemical detection of the human epithelial cell marker, cytokeratin, in the breast cancer cells (Fig. 1B). Histomorphometric analyses of tibias and femurs showed a significant increase in the number of OCls lining bone surfaces facing nests of tumor cells as compared to bone surfaces distant from tumor cells in the same bone sample or in bones from healthy control mice (Fig. 1C, D). Furthermore, the OCls lining bone surfaces near tumor tissue were significantly larger and with a higher number of nuclei per sectioned OCl than OCls lining corresponding surfaces of long bones in healthy mice (Table 1).

Table 1 Histomorphometric analysis on bones isolated from mice with osteolytic metastases or healthy mice. The sample area was from 0.50–1.0 mm to the growth plate cartilage. *N.Oc/mm BS* number of osteoclasts per millimeter of bone surface, *Oc.S/BS*, %, osteoclast surface per bone surface, *Oc.S/Oc*, µm, osteoclast surface per osteoclast, *N.Nu/Oc*, number of nuclei per osteoclasts. Data are expressed as mean ± SEM

	Diseased mice (n = 3)	Healthy mice (n = 4)	P value
N.Oc/mm BS	14.6 ± 2.6	8.6 ± 0.7	< 0.05
Oc.S/BS, %	72 ± 9	22 ± 3	< 0.005
Oc.S/Oc, µm	52 ± 8.7	25 ± 1.1	< 0.05
N.Nu/Oc	2.5 ± 0.3	1.2 ± 0.2	< 0.05

MDA-231/B cells were also found to increase the number of OCls formed in bone marrow cultures. A nearly threefold increase in the number of TRAP + multinucleated cells was observed in both direct and indirect co-cultures of bone marrow and non-proliferating breast cancer cells when compared to bone marrow cultures alone (Fig. 2A, B). In contrast to the pure bone marrow cultures, the number of OCls remained high after day 8 in culture in bone marrow/breast cancer cell co-cultures, suggesting that breast cancer cell-derived factor(s) may prolong OCls survival. Moreover, the maturity and resorptive activity of OCls formed in bone marrow/breast cancer cell co-cultures, measured as the number of nuclei per OCls and the area of pits formed on slices of devitalized cortical bovine bone, respectively, were significantly increased when compared to control bone marrow cultures (Fig. 3A, B). Furthermore, the level of type I collagen degradation products (Cross-Laps) released into the conditioned medium in bone marrow/breast cancer cell co-cultures was significantly elevated when compared to cultures of bone marrow alone (Fig. 3B). The breast cancer cells alone were unable to degrade bone and to release collagen fragments from the bone slices (Fig. 3B). The level of TRAP activity measured in the conditioned media was increased tenfold ($P < 0.0001$, $n = 12$) in bone marrow/breast cancer cell co-cultures when compared to bone marrow cultures. Conditioned medium from breast cancer cell cultures did not contain detectable levels of TRAP activity.

Cytokines affecting formation and activity of OCls

The data from non-contact co-cultures of bone marrow and breast cancer cells strongly suggest that soluble breast cancer cell-derived factors can increase the OCl number and resorptive activity. The effect may be mediated solely by breast cancer cell-derived factors or may be due to a concurrent action of breast cancer cell and autocrine and/or paracrine bone marrow-derived factors.

As summarized in Table 2, confluent breast cancer cell layers expressed high levels of M-CSF, moderate levels of IL-6, IL-1α, and LIF, and undetectable levels of

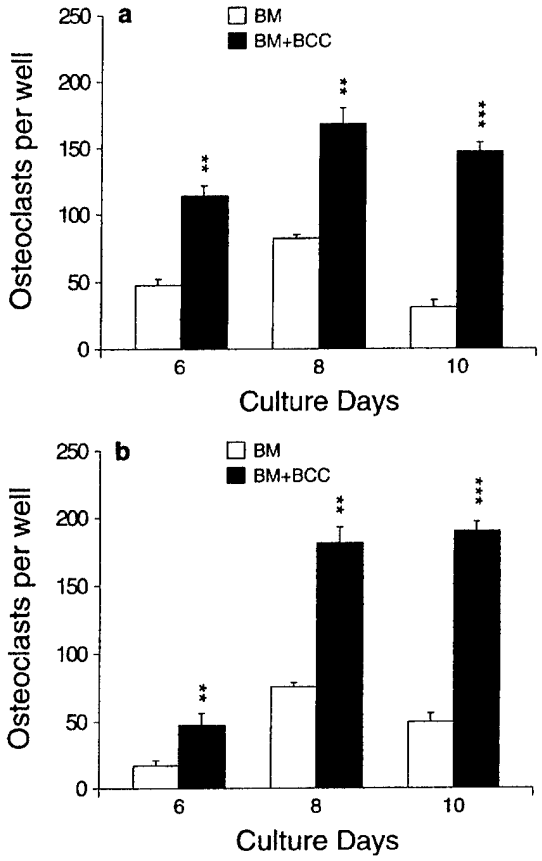

Fig. 2a, b Osteoclast recruitment in bone marrow/breast cancer co-cultures. Bone marrow cells (BM) were cultured for 6, 8 or 10 days in the absence (*white bars*) or in the presence (*gray bars*) of non-proliferating MDA-231/B breast cancer cells (BCC). Co-cultures were performed with either direct cell–cell contact (**a**) or when cells were separated by a membrane insert (**b**). At the indicated days cultures were rinsed, fixed, and stained for TRAP (*red*). TRAP+ cells with three or more nuclei were counted as mature OCls. The results are expressed as mean (+SEM) number of OCls ($n = 4$). The experiment was repeated three times with similar results. Significance levels, $^{**}P < 0.01$, $^{***}P < 0.001$

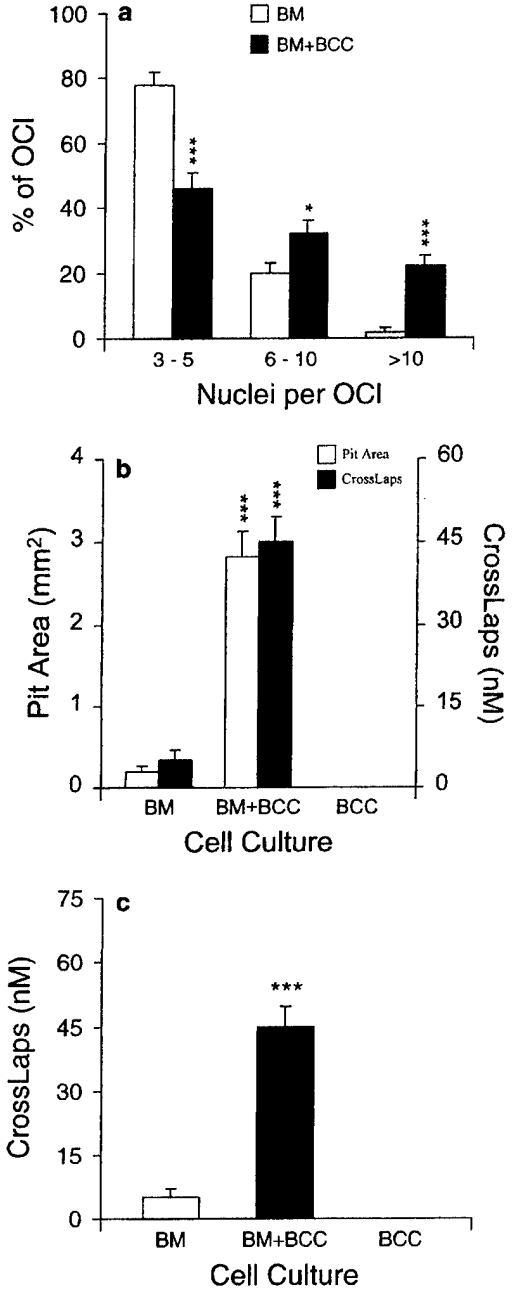

Fig. 3a–c Osteoclast maturity and resorptive activity in co-culture with breast cancer cells. **a** The osteoclast (OCl) maturity, measured as the number of nuclei per OCl, was determined in 8-day-old bone marrow cultures (BM) when cultured on plastic in the absence (*open bars*) or in the presence (*gray bars*) of 3×10^4 non-proliferating MDA-231/B breast cancer cells (BCC). **b** The resorptive activity of OCls formed in 8-day-old BM with or without BCC was measured as the plan surface area of excavation pits formed on the bovine cortical bone slices (*white bars*) or as the release of type I collagen fragments (CrossLaps) into the conditioned medium (*gray bars*). The results are expressed as mean (+SEM) nuclei per OCl, pit area, or CrossLaps concentration, respectively. The experiments were repeated three times with similar results. Significance levels, $^{*}P < 0.05$, $^{***}P < 0.001$

PTHrP, IL-1β, and TNF-α, both at mRNA and protein levels measured by RT-PCR and ELISA or RIA, respectively.

The levels of three selected mouse-derived cytokines were analyzed in CM collected every second day over 8 days from cultures of bone marrow alone and when co-cultured with breast cancer cells (Fig. 4). The secretion of bone marrow-derived IL-6 was found to be significantly increased when bone marrow was co-cultured with breast cancer cells. The secretion of mouse IL-1β in bone marrow cultures decreased during cultivation and was independent of the presence or absence of breast cancer cells. Finally, mouse TNF-α was found to be fairly constantly secreted during cultivation and just slightly affected by the presence of breast cancer cells (Fig. 4). CM harvested from cultures of breast cancer cells alone, as expected, did not contain antigenic constituents according to the ELISAs for mouse IL-6, IL-1β or TNF-α.

Table 2 Levels of human cytokines in MDA-231 cell culture. Human breast cancer cells (MDA-231) were cultured to confluence in 10-cm petri dishes. Conditioned medium was harvested after 48 h and the level of cytokines was measured by ELISA or by RIA for PTHrP (*). Cellular RNA extracts were used for determination of the expression of cytokines by reverse transcriptase-polymerase chain reaction (RT-PCR)[1]. (–) no signal, √ clear signal, *n.p.* not performed

	ELISA (pg/mg cellular protein)	RT-PCR[1]
IL-1α	13 ± 3	√
IL-1β	<3.9	(–)
IL-6	171 ± 20	√
M-CSF	7462 ± 460	√
PTHrP*	<2.0	(–)
TNF-α	<15.6	(–)
LIF	41 ± 4	n.p.
VEGF	6224 ± 120	√

Angiogenesis

Many large and small blood vessels were found in the bone marrow and within the tumor tissue (Fig. 1E, F). The vessels were visualized by immunohistochemical detection of mouse CD31 and/or CD34 positive endothelial cells with the two rat monoclonal antibodies MEC 13.3 (Vecchi et al. 1994) and MEC 14.7 (Garlanda et al. 1997), respectively. High levels of immunoreactivity for CD31 were observed in endothelial cells lining larger blood vessels in the bone marrow and moderate immunoreactivity was observed in some smaller blood vessels in both bone marrow and at the periphery of and within tumors. Immunoreactivity for CD34 was clearly restricted to small blood vessel endothelial cells. In the bone marrow and in the tumor tissue only newly formed blood vessels and capillaries appeared highly CD34 positive. The blood vessels seemed to be infiltrating the tumor tissue from the periphery.

Membrane-separated co-cultures showed that MDA-231-derived factors were able to stimulate the growth of the murine stromal endothelial cell line MBA-2.1 (Fig. 5A). Under indirect co-culture conditions, breast cancer cells also induced a 16-fold increase in the number of endothelial cells migrating through a thin layer of type I collagen ($P < 0.001$, $n = 8$) (Fig. 5B). Finally, similar conditions showed that breast cancer cells dose – dependently stimulated the differentiation of endothelial cells, since the total area of tubule-like structures formed in a three-dimensional Matrigel was increased nearly 230-fold in the presence of the highest cancer cell numbers when compared to cells cultured in the absence of cancer cells ($P < 0.001$, $n = 4$) (Fig. 5C).

Confluent breast cancer cell cultures expressed high levels of VEGF mRNA and protein (Table 2). As revealed by RT-PCR, and confirmed by Southern blotting, the two lower-molecular-weight isoforms of VEGF mRNA, $VEGF_{121}$, and $VEGF_{165}$, were expressed by the breast cancer cells, whereas the three other identified isoforms $VEGF_{145}$, $VEGF_{189}$, and $VEGF_{206}$, were not detectable (Fig. 6A, B).

Discussion

The in vivo bone metastasis model in nude mice was first described by Arguello et al. 1988, and later modified by Yoneda et al. 1994 for the study of bone metastasis of human breast cancer. One of the characteristic histological findings in sections of osteolytic tumor lesions has been the dramatic increase in the number of multinucleated OCls lining the bone surfaces near the tumor tissue. By use of the in vivo bone metastasis model, we were able to quantify the significantly increased size and maturity of OCls lining bone surfaces in the proximity of tumor cells compared to OCls lining normal bone (Table 1). Furthermore, the in vivo findings were found to be closely mimicked in the bone marrow OCl formation assay, where the number (Fig. 2), maturity (Fig. 3A), and activity (Fig. 3B) of OCls were increased in co-cultures of bone marrow and breast cancer cells as compared to bone marrow alone.

Cultures of breast cancer cells were found to secrete high levels of M-CSF (Table 2), which is an indispensable

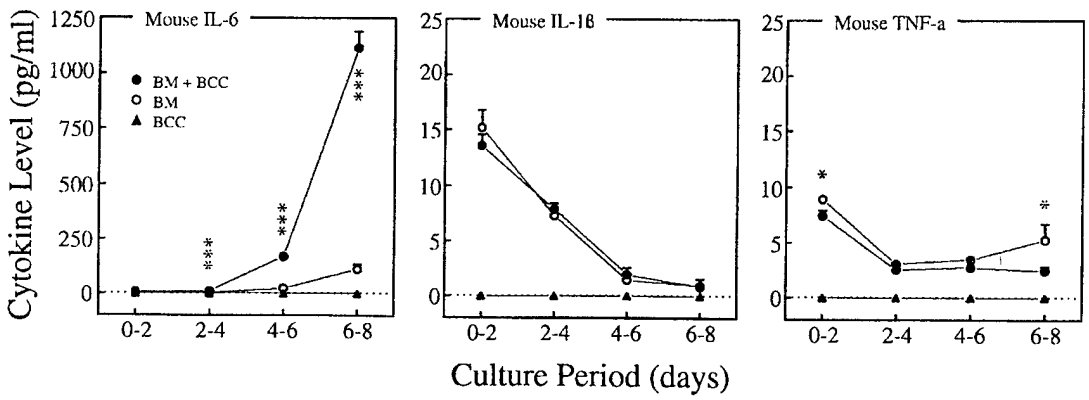

Fig. 4A–C The levels of three mouse bone marrow-derived cytokines. Interleukin-6 (IL-6) (**A**), interleukin-1 beta (IL-1β) (**B**), and tumor necrosis factor-alpha (TNF-α) (**C**), were measured in the conditioned medium harvested every second day from co-cultures or single cultures of bone marrow (BM) and breast cancer cells (BCC). Results are expressed as mean ± SEM ($n = 4$). The experiments were repeated twice with similar results. Significance levels, $*P < 0.05$, $***P < 0.001$

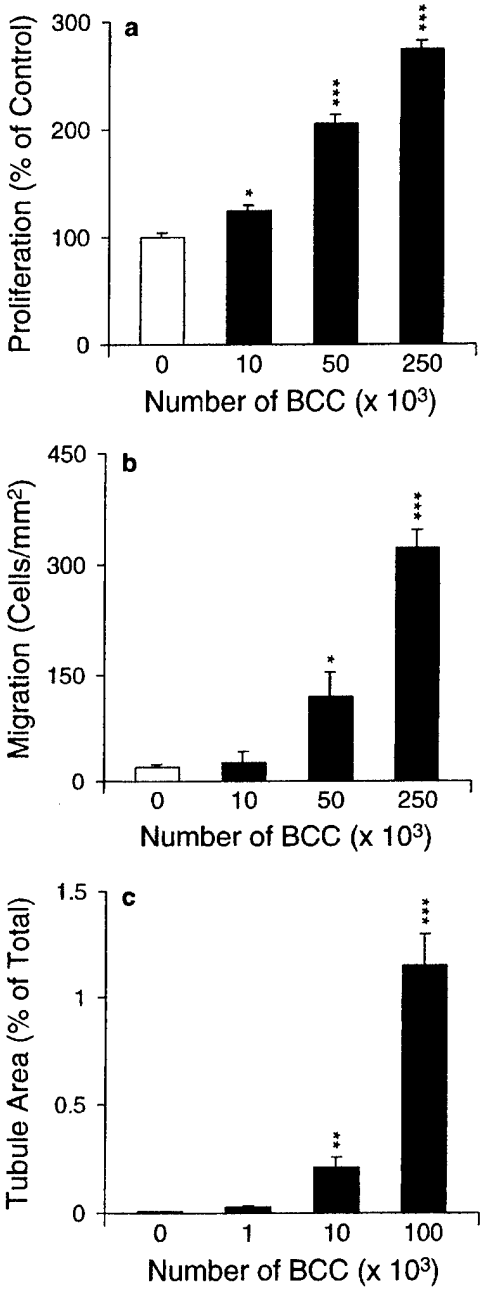

Fig. 5a–c Co-cultures of breast cancer and endothelial cells. **a** The diagram shows the proliferation of endothelial cells, measured as radiolabeled thymidine incorporation into DNA, in response to indirect co-culture with breast cancer cells (BCC). The proliferation is expressed as mean level ± SEM of thymidine incorporation after normalization to control values. The experiments were repeated three times with similar results. **b** The number of endothelial cells, migrating through a thin layer of type I collagen gel on a membrane insert, was significantly and dose dependently increased by indirect co-culture with BCC. **c** Likewise, the area of endothelial tubule-like structures, formed in a three-dimensional artificial basal-membrane (Matrigel), was significantly and dose dependently increased when plated onto increasing numbers of BCC. Results are expressed as mean ± SEM. Significance levels, $*P < 0.05$, $**P < 0.01$, $***P < 0.001$

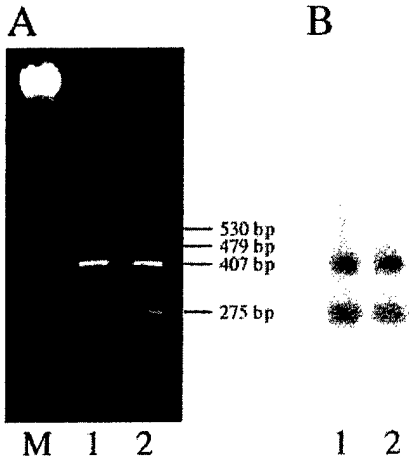

Fig. 6A, B Expression of VEGF isoforms in the human breast cancer cell line MDA-231. **A** RT-PCR demonstrating the expression of the two VEGF isoforms, $VEGF_{121}$ and $VEGF_{165}$, of the expected product size of 275 and 407 base pairs, respectively. No clear RT-PCR products were observed for the two higher isoforms of VEGF, $VEGF_{189}$, and $VEGF_{206}$, of expected product size of 479 and 530 base pairs, respectively. *Lane M*: 123 bp DNA marker; *lane 1*: MDA-231/P RNA; *lane 2*: MDA-231/B RNA. **B.** Southern blotting confirming the identity of $VEGF_{121}$ and $VEGF_{165}$

cytokine in normal OCl development (Tanaka et al. 1993). This has been highlighted by the fact that mice lacking the gene for M-CSF become osteopetrotic due to a very low number of matured OCls in the skeleton (Felix et al. 1990a,b). It is, therefore, likely that breast cancer cell-derived M-CSF participate as a paracrine factor in the recruitment and maturation of OCls from the bone marrow. This has been supported by recent data from our laboratories, where monoclonal antibodies raised against human M-CSF were found to decrease the breast cancer cell-induced recruitment of OCls by 40% (Misander et al. 1999).

IL-6 was found to be expressed by breast cancer cells in culture at moderate levels. IL-6 is involved in the early stages of OCl development, while its role in the regulation of the activity of mature OCls is controversial and the results depend on the system used for evaluation (de la Mata et al. 1995; Kurihara et al. 1990; Lowik et al. 1989; Ohsaki et al. 1992; Roodman 1996). Moreover, IL-6 has been implicated in several diseases involving increased bone resorption, such as osteoporosis, Paget's disease, myelomatosis, and Gorham-Stout disease (Roodman 1996; Jilka et al. 1992). In co-culture with breast cancer cells, the bone marrow was found to secrete tenfold higher levels of mouse IL-6 than bone marrow cultures alone (Fig. 4). The results suggest that breast cancer cells induce an up-regulation of bone marrow expression of IL-6, which subsequently can act as a co-factor in OCl recruitment.

Other potent stimulators of osteoclastogenesis and OCl activity in vivo and in vitro, i.e., IL-1β, and TNF-α, were expressed at low or undetectable levels by breast cancer cells and by bone marrow in co-cultures or when

cultured alone. PTHrP, which has been suggested to be important for breast cancer cell-induced osteolysis in vivo (Guise 1997; Guise et al. 1996), was not secreted in detectable levels by the MDA-231/B cells in culture nor could it be detected by RT-PCR. It is possible that cytokines other than those selected for analysis in this study, such as transforming growth factor-beta (TGF-β), IGF-II, and IL-11 (Pederson et al. 1999; Lacroix et al. 1998; Morinaga et al. 1997), may also participate in the observed breast cancer cell-induced increase in OCl number and activity.

Cancer cell-induced angiogenesis is essential for sustained tumor growth as it allows tumor oxygenation and nutrient perfusion and the removal of tumor waste products. Recent studies have shown that angiogenesis in breast cancer assessed by microvessel count is a significant prognostic factor (Bosari et al. 1992; Horak et al. 1992; Toi et al. 1995). In line with the human studies (Horak et al. 1992; Shibusa et al. 1998), antibodies directed against mouse CD31 and mouse CD34 can be used to assess the amount of neo-vascularization in tumors in the in vivo bone metastasis model. It has previously been suggested that the MEC 14.7 antibody, recognizing mouse CD34, can be used to discriminate between larger blood vessels and smaller blood vessels including newly formed capillaries in tumors in mice (Garlanda et al. 1997). Our observations in nude mice with bone metastasis support this finding. Indeed, the distinct reaction of the MEC 14.7 antibody with small, newly formed capillaries in both the peripheral and central part of osteolytic tumors implies that the cancer cells – not only in vitro, as shown clearly by our co-culture experiments, but also in vivo – have the capacity to induce endothelial cell proliferation, migration, and differentiation. The induction of an endothelial cell response may be mediated solely by cancer cell derived cytokines and growth factors or may be concerted in action by growth factors, such as TGF-β1 and insulin-like growth factors, released from the bones during osteoclastic resorption (Oursler 1994). TGF-β has been implicated as being a very potent co-factor to VEGF in the induction of angiogenesis in cancer (Tsujii et al. 1998; Nakanishi et al. 1997; Donovan et al. 1997; Benefield et al. 1996). The high levels of VEGF expression in the human breast cancer cell line MDA-231/B (Fig. 6, Table 2) suggest that this growth factor may be involved in the paracrine communication between breast cancer cells and endothelial cells as has been shown for colon cancer cell-induced angiogenesis (Tsujii et al. 1998). This hypothesis is currently being studied in our laboratory.

The feasibility of targeted drug delivery to tumor vasculature has previously been elegantly demonstrated by Ruoslahti and co-workers, taking advantage of the selective expression of several proteins in endothelial cells in the angiogenic vessels within solid tumors as compared to endothelial cells located in established blood vessels (Arap et al. 1998; Pasqualini et al. 1997; Pasqualini and Ruoslahti 1996). Although skepticism regarding the success of this approach has recently been called for by Schnitzer (1998), similar results have been found by several other investigators (Hammes et al. 1996; Strawn et al. 1996; Spragg et al. 1997; Molema et al. 1997). Using targeted drug delivery to bone metastasis vasculature, inhibition of OCl activity, tumor growth, and/or angiogenesis could be achieved with improved efficacy and tolerability and with reduced systemic toxicity and side effects.

Matrix destruction and neo-vascularization are necessary for all solid tumors to expand. This study has shown that breast cancer cells arrested in the bone marrow accomplish this by two events. First, the hard calcified bone matrix is removed by osteoclasts increased in number and activity by cancer-derived factors and, second, new blood vessel formation is enhanced due to a cancer-stimulated increase in endothelial cell proliferation, invasion, and differentiation.

Acknowledgements The continuous help from Professor Toshiyuki Yoneda and Paul Williams, Texas University, San Antonio, is highly appreciated.

References

Arap W, Pasqualini R, Ruoslahti E (1998) Cancer treatment by targeted drug delivery to tumor vasculature in a mouse model. Science 279: 377–380

Arguello F, Baggs RB, Frantz CN (1988) A murine model of experimental metastasis to bone and bone marrow. Cancer Res 48: 6878–6881

Benefield J, Petruzzelli GJ, Fowler S, Taitz A, Kalkanis J, Young MR (1996) Regulation of the steps of angiogenesis by human head and neck squamous cell carcinomas. Invasion Metastasis 16: 291–301

Bosari S, Lee AK, DeLellis RA, Wiley BD, Heatley GJ, Silverman ML (1992) Microvessel quantitation and prognosis in invasive breast carcinoma. Hum Pathol 23: 755–761

Brown KJ, Maynes SF, Bezos A, Maguire DJ, Ford MD, Parish CR (1996) A novel in vitro assay for human angiogenesis. Lab Invest 75: 539–555

Chomczynski P, Sacchi N (1987) Single-step method of RNA isolation by acid guanidinium thiocyanate-phenol-chloroform extraction. Anal Biochem 162: 156–159

Clohisy DR, Palkert D, Ramnaraine ML, Pekurovsky I, Oursler MJ (1996) Human breast cancer induces osteoclast activation and increases the number of osteoclasts at sites of tumor osteolysis. J Orthop Res 14: 396–402

Coleman RE (1997) Skeletal complications of malignancy. Cancer 80: 1588–1594

Diel IJ, Solomayer EF, Costa SD, Gollan C, Goerner R, Wallwiener D, Kaufmann M, Bastert G (1998). Reduction in new metastases in breast cancer with adjuvant clodronate treatment. N Engl J Med 339: 357–363

Donovan D, Harmey JH, Toomey D, Osborne DH, Redmond HP, Bouchier-Hayes DJ (1997) TGF beta-1 regulation of VEGF production by breast cancer cells. Ann Surg Oncol 4: 621–627

Felix R, Cecchini MG, Fleisch H (1990a) Macrophage colony stimulating factor restores in vivo bone resorption in the op/op osteopetrotic mouse. Endocrinology 127: 2592–2594

Felix R, Cecchini MG, Hofstetter W, Elford PR, Stutzer A, Fleisch H (1990b) Impairment of macrophage colony-stimulating factor production and lack of resident bone marrow macrophages in the osteopetrotic op/op mouse. J Bone Miner Res 5: 781–789

Fidler IJ, Ellis LM (1994) The implications of angiogenesis for the biology and therapy of cancer metastasis. Cell 79: 185–188

Foged NT, Delaisse JM, Hou P, Lou H, Sato T, Winding B, Bonde M (1996) Quantification of the collagenolytic activity of isolated osteoclasts by enzyme-linked immunosorbent assay. J Bone Miner Res 11: 226–237

Garlanda C, Berthier R, Garin J, Stoppacciaro A, Ruco L, Vittet D, Gulino D, Matteucci C, Mantovani A, Vecchi A, Dejana E (1997) Characterization of MEC 14.7, a new monoclonal antibody recognizing mouse CD34: a useful reagent for identifying and characterizing blood vessels and hematopoietic precursors. Eur J Cell Biol 73: 368–377

Guise TA (1997) Parathyroid hormone-related protein and bone metastasis. Cancer 80: 1572–1580

Guise TA, Yin JJ, Taylor SD, Kumagai Y, Dallas M, Boyce BF, Yoneda T, Mundy GR (1996) Evidence for a clausal role of parathyroid hormone-related protein in the pathogenesis of human breast cancer-mediated osteolysis. J Clin Invest 98: 1544–1549

Hammes HP, Brownlee M, Jonczyk A, Sutter A, Preissner KT (1996) Subcutaneous injection of a cyclic peptide antagonist of vitronectin receptor-type integrins inhibits retinal neovascularization. Nat Med 2: 529–533

Hanahan D, Folkman J (1996) Patterns and emerging mechanisms of the angiogenic switch during tumorigenesis. Cell 86: 353–364

Horak ER, Leek R, Klenk N, LeJeune S, Smith K, Stuart N, Greenall M, Stepniewska K, Harris AL (1992) Angiogenesis, assessed by platelet/endothelial cell adhesion molecule antibodies, as indicator of node metastases and survival in breast cancer. Lancet 340: 1120–1124

Jilka RL, Hangoc G, Girasole G, Passeri G, Williams DC, Abrams JS, Boyce B, Broxmeyer H, Manolagas SC (1992) Increased osteoclast development after estrogen loss: mediation by interleukin-6. Science 257: 88–91

Kanis JA, Powles T, Paterson AH, McCloskey EV, Ashley S (1996) Clodronate decreases the frequency of skeletal metastases in women with breast cancer. Bone 19: 663–667

Kurihara N, Bertolini D, Suda T, Akiyama Y, Roodman GD (1990) IL-6 stimulates osteoclast-like multinucleated cell formation in long-term human marrow cultures by inducing IL-1 release. J Immunol 144: 4226–4230

Lacroix M, Siwek B, Marie PJ, Body JJ (1998) Production and regulation of interleukin-11 by breast cancer cells. Cancer Lett 127: 29–35

Löwik CWGM, van der Pluijm G, Bloys H, Hoekman K, Bijvoet OL, Aarden LA, Papapoulos SE (1989) Parathyroid hormone (PTH) and PTH-like protein (PLP) stimulate interleukin-6 production by osteogenic cells: a possible role of interleukin-6 in osteoclastogenesis. Biochem Biophys Res Commun 162: 1546–1552

de la Mata J, Uy HL, Guise TA, Story B, Boyce BF, Mundy GR, Roodman GD (1995) Interleukin-6 enhances hypercalcemia and bone resorption mediated by parathyroid hormone-related protein in vivo. J Clin Invest 95: 2846–2852

Misander H, Jakobsen M, Winding B (1999) A possible role for M-CSF in breast cancer-induced osteolysis. Second International Conference: Cancer-Induced Bone Diseases, March 27–29, Davos, Switzerland, p 26 (Abstract)

Molema G, de Leij LF, Meijer DK (1997) Tumor vascular endothelium: barrier or target in tumor directed drug delivery and immunotherapy. Pharm Res 14: 2–10

Morinaga Y, Fujita N, Ohishi K, Tsuruo T (1997) Stimulation of interleukin-11 production from osteoblast-like cells by transforming growth factor-beta and tumor cell factors. Int J Cancer 71: 422–428

Mundy GR (1997) Mechanisms of bone metastasis. Cancer 80: 1546–1556

Nakanishi Y, Kodama J, Yoshinouchi M, Tokumo K, Kaminura S, Okuda H, Kudo T (1997) The expression of vascular endothelial growth factor and transforming growth factor-beta associated with angiogenesis in epithelial ovarian cancer. Int J Gynecol Pathol 16: 256–262

Ohsaki Y, Takahashi S, Scarcez T, Demulder A, Nishihara T, Williams R, Roodman GD (1992) Evidence for an autocrine/paracrine role for interleukin-6 in bone resorption by giant cells from giant cell tumors of bone. Endocrinology 131: 2229–2234

Oursler MJ (1994) Osteoclast synthesis and secretion and activation of latent transforming growth factor beta. J Bone Miner Res 9: 443–452

Pasqualini R, Ruoslahti E (1996) Organ targeting in vivo using phage display peptide libraries. Nature 380: 364–366

Pasqualini R, Koivunen E, Ruoslahti E (1997) Alpha v integrins as receptors for tumor targeting by circulating ligands. Nat Biotechnol 15: 542–546

Pederson L, Kremer M, Foged NT, Winding B, Ritchie C, Fitzpatrick LA, Oursler MJ (1997) Evidence of a correlation of estrogen receptor level and avian osteoclast estrogen responsiveness. J Bone Miner Res 12: 742–752

Pederson L, Winding B, Foged NT, Spelsberg TC, Oursler MJ (1999) Identification of breast cancer cell line-derived paracrine factors that stimulate osteoclast activity. Cancer Res 59: 5849–5855

Roodman GD (1996) Advances in bone biology: the osteoclast. Endocr Rev 17: 308–332

Sasaki A, Boyce BF, Story B, Wright KR, Chapman M, Boyce R, Mundy GR, Yoneda T (1995) Bisphosphonate risedronate reduces metastatic human breast cancer burden in bone in nude mice. Cancer Res 55: 3551–3557

Scheven BAA, Kawilarang-de Haas EWM, Wassenaar AM, Nijweide PJ (1986) Differentiation kinetics of osteoclasts in the periosteum of embryonic bones in vivo and in vitro. Anat Rec 214: 418–423

Schnitzer JE (1998) Vascular targeting as a strategy for cancer therapy. N Engl J Med 339: 472–474

Shibusa T, Shijubo N, Abe S (1998) Tumor angiogensis and vascular endothelial growth factor expression in stage I lung adenocarcinoma. Clin Cancer Res 4: 1483–1487

Spragg DD, Alford DR, Greferath R, Larsen CE, Lee KD, Gurtner GC, Cybulsky MI, Tosi PF, Nicolau C, Gimbrone MA Jr (1997) Immunotargeting of liposomes to activated vascular endothelial cells: a strategy for site-selective delivery in the cardiovascular system. Proc Natl Acad Sci USA 94: 8795–9800

Strawn LM, McMahon G, App H, Schreck R, Kuchler WR, Longhi MP, Hui TH, Tang C, Levitzki A, Gazit A, Chen I, Keri G, Orfi L, Risau W, Flamme I, Ullrich A, Hirth KP, Shawver LK (1996) Flk-1 as a target for tumor growth inhibition. Cancer Res 56: 3540–3545

Takahashi N, Akatsu T, Udagawa N, Sasaki T, Yamaguchi A, Moseley JM, Martin TJ, Suda T (1988) Osteoblastic cells are involved in osteoclast formation. Endocrinology 123: 2600–2602

Tanaka S, Takahashi N, Udagawa N, Tamura T, Akatsu T, Stanley ER, Kurokawa T, Suda T (1993) Macrophage colony-stimulating factor is indispensable for both proliferation and differentiation of osteoclast progenitors. J Clin Invest 91: 257–263

Toi M, Inada K, Suzuki H, Tominaga T (1995) Tumor angiogenesis in breast cancer: its importance as a prognostic indicator and the association with vascular endothelial growth factor expression. Breast Cancer Res Treat 36: 193–204

Tsujii M, Kawano S, Tsuji S, Sawaoka H, Hori M, DuBois RN (1998) Cyclooxygenase regulates angiogenesis induced by colon cancer cells. Cell 93: 705–716

Vecchi A, Garlanda C, Lampugnani MG, Resnati M, Matteucci C, Stoppacciaro A, Schnurch H, Risau W, Ruco L, Mantovani A, et al (1994) Monoclonal antibodies specific for endothelial cells of mouse blood vessels. Their application in the identification of adult and embryonic endothelium. Eur J Cell Biol 63: 247–254

Winding B, Wiltink A, Foged NT (1997) Pituitary adenylyl cyclase-activating polypeptides and vasoactive intestinal peptide inhibit bone resorption by isolated rabbit osteoclasts. Exp Physiol 82: 871–886

Woodhouse EC, Chuaqui RF, Liotta LA (1997) General mechanisms of metastasis. Cancer 80: 1529–1537

Yoneda T, Sasaki A, Mundy GR (1994) Osteolytic bone metastasis in breast cancer. Breast Cancer Res Treat 32: 73–84

Zipori D, Krupsky M, Resnitzky P (1987) Stromal cell effects on clonal growth of tumors. Cancer 60: 1757–1762

JOURNAL OF BONE AND MINERAL RESEARCH
Volume 16, Number 6, 2001

The Src Signaling Pathway Regulates Osteoclast Lysosomal Enzyme Secretion and Is Rapidly Modulated by Estrogen

DAVID PASCOE and MERRY JO OURSLER

ABSTRACT

To investigate the role of the pp60*src* signaling pathway in osteoclast activity, we have used dominant negative pp60*src*, c-*ras*, and c-*raf* expression vectors to individually disrupt their functions in osteoclasts. Osteoclasts were transiently transfected and secretions of cathepsin B/K and tartrate-resistant acid phosphatase (TRAP) were monitored. Expression of these constructs increased secretion of lysosomal enzymes. In contrast, constitutively active pp60*src* expression caused decreased lysosomal enzyme secretion. Osteoclasts respond to 17-β estradiol ($17\beta E_2$) treatment with decreased lysosomal enzyme secretion. Therefore, we investigated the effects of E_2 on pp60*src* kinase activity and observed an E_2 time- and dose-dependent decrease in cytoskeletal membrane-associated pp60*src* tyrosine kinase activity. We have shown that estrogen decreases lysosomal enzyme gene expression and secretion; so we have examined the effects of the expression constructs on estrogen regulation of enzyme secretion. Constitutively active pp60*src* blocked E_2 effects on secretion whereas expression of dominant negative pp60*src*, c-*Ras*, or c-*Raf* enhanced E_2 effects. These data support that the kinase domain of cytoskeletal-associated pp60*src* is likely to be involved in the regulation of lysosomal enzyme secretion. (J Bone Miner Res 2001;16:1028–1036)

Key words: osteoclast, lysosomal enzymes, Src, tyrosine kinase, estrogen

INTRODUCTION

OSTEOCLASTS, THE cells responsible for metabolic bone degradation, form on the bone surface by fusion of postmitotic precursors. Once formed, the cells adhere to the bone through attachment foci that form around the perimeter of the cell.[1] Large numbers of acidifying vesicles are transported to the plasma membrane adjacent to the bone, fusing to form a ruffled membrane that acidifies the extracellular compartment.[2] Lysosomal enzymes are transported from the Golgi to this compartment and the combination of these enzymes and the low pH of the compartment efficiently degrade the bone juxtaposed to the ruffled membrane. Over the past several years, it has become increasingly apparent that the phosphoprotein pp60*src* is critical to normal osteoclast functioning. Evidence began to mount in 1991 when Soriano et al.[3] generated $src^{-/-}$ transgenic mice that developed osteopetrosis as the result of defective osteoclast activity. After this observation, Boyce et al.[4] demonstrated that pp60*src* expression is required for ruffled border formation in osteoclasts and that the in vitro osteoclast generation from the $src^{-/-}$ mutant tissues were not able to form ruffled borders and resorb bone. Lowe et al.[5] transplanted liver (a source of osteoclast precursors) from normal mice to the $src^{-/-}$ mutant mice and restored normal osteoclast activity, showing that the defect in osteoclast function was caused by the lack of pp60*src* in the osteoclast lineage. Recently, chemical inhibition of pp60*src* kinase activity was shown to inhibit resorption in fetal rat long bone cultures and partially prevent bone loss in young rats

Departments of Biology, Medical Microbiology and Immunology, and Biochemistry and Molecular Biology, University of Minnesota, Duluth, Minnesota, USA.

after ovariectomy.[6] Importantly, the phenotype of the $src^{-/-}$ mice have been rescued by transgenic expression of a kinase-defective *Src* construct.[7] This supports that the critical pp60*src* function is independent of its kinase activity. Recently, two pieces of evidence have pointed to the importance of other regions of pp60*src* in its functions in osteoclasts. Violette et al.[8] have shown that a synthetic compound that binds selectively to the SH2 (*src* homology 2) domain of pp60*src* inhibits osteoclast activity and Gray et al.[9] have shown that the SH3 (*src* homology 3) domain of pp60*src* is required for macrophage colony–stimulating factor 1 induction of osteoclast migration. The SH3 domain is a proline-rich region present on many second messengers that binds homologous regions on target protein while the SH2 domain specifically binds phosphotyrosine regions of target proteins. Recently, Furuyama and Fujisawa[10] have shown that inhibition of the second messenger PI3 kinase or inhibition of actin polymerization suppressed lysosomal enzyme secretion without altering synthesis. PI3 kinase is involved in multiple signaling pathways including the pp60*src* pathway. Taken together, these data implicate pp60*src* in regulating the movement of lysosomal enzymes to the external resorption lacuna. Collectively, these data support an involvement of pp60*src* tyrosine kinase activity in osteoclast bone resorption, but the role of this kinase in osteoclasts remains unresolved. An exciting clue to this is the recent demonstration that a member of the small guanosine triphosphate phosphatases (GTPases) involved in regulating exocytosis localizes with the H^+ adenosine triphosphate phosphatase (ATPase) and pp60*src* in acidifying vesicles that may be involved in forming a ruffled membrane.[11] To better understand the involvement of this cytosolic kinase in osteoclast activity, we have examined the role of pp60*src* in osteoclast secretion of lysosomal enzymes.

MATERIALS AND METHODS

Materials

Unless otherwise noted, reagents were from Sigma Chemical Co. (St. Louis, MO, USA).

Osteoclast isolation and culture

Five-week-old chick osteoclasts: Osteoclasts were isolated from white leg horn hatchlings that were maintained on a low-calcium diet for a period of 5 weeks.[12] All animals were treated as humanely as possible and treatment followed the National Institutes of Health (NIH) and institutional guidelines for care and use of experimental animals. Multinucleated cells from human giant cell tumors of the bone were isolated as previously described.[13] An osteoclast-directed monoclonal antibody, 121F (a gift from Dr. Philip Osdoby, Washington University, St. Louis, MO, USA), coupled to immunomagnetic beads (Dynal, Inc., Oslo, Norway) was used to obtain cell populations that consist of at least 90% pure multinucleated cells and 10% or less unidentified mononuclear cells.[12,13] The purified osteoclasts exhibit all the phenotypic attributes of osteoclasts including multinucleation, attachment and ruffled border formation when cultured with bone particles and the ability to attach and form resorption pits when cultured on slices of cortical bone. Osteoclasts were cultured in phenol red–free α-modified minimal essential medium (Gibco/BRL, Gaithersburg, MD, USA) supplemented with 0.25% (wt/vol) bovine serum albumin (BSA; culture media) on bone slices prepared as previously described (for transfections)[14] or with 1 mg of bone particles per 10^6 cells as described (for kinase assays and co-immunoprecipitations[15]).

Egg-laying hen osteoclasts: Osteoclasts were isolated as previously described.[14] Briefly, egg-laying hens were maintained on a low-calcium diet as outlined previously. After death, osteoclasts were isolated and cultured as detailed previously.

Transient transfection

Isolated osteoclasts were resuspended in culture media on bone slices. The expression vector (dominant interfering [K295M][16] and constitutively active [Y527F][17] pp60*src* constructs were gifts from Dr. Courtneidge EMBL; dominant interfering *Ras* [*ras*N17][18] and *Raf* [K375M][19] were gifts from Dr. Karin, University of California at San Diego) or the corresponding empty expression vector was transiently transfected into the osteoclasts using the Lipofectamine Reagent System (Gibco/BRL) according to the manufacturer's instructions. After 5 h of culture, media was supplemented by the addition of charcoal-stripped fetal bovine serum to a final concentration of 10% and the cells were cultured for an additional 18 h before treatment or harvest for activity studies.

Analysis of successful transfection

The success of osteoclast transfection was monitored by analysis of overexpression (comparing cultures transfected with constructs to vector-only transfected cultures) as follows. Transfection was done as outlined previously. After culture, cell pellets on bone slices were detergent-extracted with cold lysis buffer [NaH_2PO_4, 100 mM; ethylene glycol-bis(β-amino ethyl ether)-*N*,*N*,*N*′,*N*′-tetracetic acid (EGTA), 10 mM; EDTA, 10; phenylmethylsulfonyl fluoride, (PMSF), 1 mM with 1% Triton X-100 (Tx-100); 1% sodium deoxycholate; 0.1% sodium dodecyl sulfate; and 10 μg/ml of the following: leupeptin, chymostatin, antipain, and pepstatin A, pH 7.4]. The extracts were desalted to remove detergents and plated for ELISA analysis as previously described.[20] Antibodies to pp60src, c-Ras, and c-Raf were from Upstate Biotechnology (Lake Placid, NY, USA). We have previously published that a cell-by-cell analysis of this transfection protocol showed a transfection efficiency of greater than 90%.[14]

Lysosomal enzyme assays

Osteoclasts plated on bone slices were transfected and cultured as detailed in the figure legends. The conditioned

media were harvest for assay as previously described.[21] Tartrate-resistant acid phosphatase (TRAP) activity was measured using an assay based on the work of Hofstee.[22] The initial rate of hydrolysis of *o*-carboxy phenylphosphate was determined by following the increase in absorbency at 300 nM resulting from the liberation of salicylic acid. One unit hydrolyzes 1 μmol of *o*-carboxy phenylphosphate per minute at 24°C, pH 5.0. The assay was performed in the presence of 1 mM tartrate. Cathepsin B/K levels were measured using a substrate that is cleaved by both cathepsins by measuring Na-CBZ-lysine *p*-nitrophenyl ester hydrolysis as measured by 520 nM absorbance as outlined by Barrett and Kirschke.[23] To standardize for relative cell number, the protein content of the solubilized cell pellet was determined using the Bio-Rad protein detection system (Bio-Rad, Hercules, CA, USA).

Membrane preparation

Osteoclasts were cultured with bone particles as mentioned previously and treated with either vehicle or steroid as detailed in the figure legends. Cell pellets were extracted and the membranes were fractionated to separate Tx-100 insoluble and soluble components as detailed by Oda et al.[24] Briefly, cell pellets were resuspended in cold lysis buffer. The cell lysates were centrifuged at 10,000*g* at 4°C for 30 minutes. The resulting pellet was washed with an equal volume of lysis buffer and recentrifuged. The supernatant was centrifuged at 100,000*g* at 4°C for 4 h. Pellets were resuspended in 200 mM HEPES, pH 7, containing 10% glycerol and 0.1% NP-40. The immunomagnetic beads were removed by magnetic sorting and the protein concentrations of the samples were determined by the Bio-Rad protein quantitation system.

Immunoprecipitation

Equal protein in equal volumes within each experiment were used in the immunoprecipitations to standardize for relative cell number as mentioned previously. Sodium dodecyl sulfate (SDS) was added to a final concentration of 0.3%. The extracts were precleared for nonspecific binding by incubation with protein A/G (Oncogene Research Products, Cambridge, MA, USA) for 60 minutes, followed by centrifugation at 13,000 rpm at 4°C for 30 minutes. Kinase immunoprecipitation was carried out using specific antibodies (anti-pp60*src*, Oncogene Science, Uniondale, NY; anti-*Yes*: a gift of M. Sudol, Rockefeller University; anti-*Fyn* and anti-*Lyn*: Upstate Biotechnology) as suggested by Oncogene Science in the product literature using a protein A/G complex to aggregate the immunoprecipitate.

Kinase assay

Tyrosine kinase activity was assayed using a kit from Upstate Biotechnology according to the manufacturer's instructions. Briefly, pellets were resuspended in 25 ml of 200 mM HEPES, pH 7, with 10% (vol/vol) glycerol, 0.1% NP-40, and 0.1% SDS and the specific tyrosine kinase (c-*Src*, c-*Yes*, c-*Fyn*, or c-*Lyn* immunoprecipitated using the protocol provided by Upstate Biotechnology with the c-*Src*, c-*Fyn*, and c-*Lyn* antibodies). Samples were resuspended in 50 mM Tris, pH7, 25 mM $MgCl_2$, 5 mM $MnCl_2$, and 0.05 mM Na_3VO_4. Substrate (KVRKIGEGTYGVVKK), 0.03 mM in water or an equal volume of water, was added to equal aliquots. ^{32}P-γ ATP (NEN, Boston, MA; final concentration of 0.1 mM ATP, specific activity, 1000 cpm/pmol) was added and the samples were transferred to a 30°C water bath to initiate the reaction. The reaction was stopped after 20 minutes by the addition of trichloroacetic acid to a final concentration of 15%. The samples were centrifuged at 300 rpm for 5 minutes to remove precipitated proteins. Equal volumes of the supernatant were spotted onto 1.5 cm × 1.5 cm p80 phosphocellulose filter paper squares (Fisher Scientific, Pittsburgh, PA, USA). The squares were washed four times with excess 0.75% phosphoric acid, immersed in scintillation fluid, and counted.

Statistical analysis

The results represent the mean ± SEM of three separate experiments. The effect of treatment was compared with control values by one-way analysis of variance (ANOVA); significant treatment effects were further evaluated by the Fisher's least significant difference method of multiple comparisons in a one-way ANOVA. Tests were carried out using Apple software, obtained from StatView II (Abacus Concepts, Inc., Cupertino, CA, USA).

RESULTS

The role of pp60src/c-Ras/c-Raf in osteoclast lysosomal enzyme secretion

We have used transient expression of either dominant interfering pp60*src*, c-*Ras*, or c-*Raf* constructs to explore the potential role of pp60*src* signal transduction in osteoclast lysosomal enzyme secretion (Fig. 1). Transient expression of individual dominant interfering constructs increased secretion of cathepsin B/K and TRAP. In contrast, a constitutively active pp60*src* construct decreased lysosomal enzyme secretion of the isolated osteoclasts (Fig. 2).

Estrogen effects on pp60src tyrosine kinase activity

It has been well documented that pp60*src* association with the cytoskeletal network is important in its cellular functions.[24–29] Moreover, recent data have shown that the SH2 domain of pp60*src* is required for osteoclast function.[8] Our data have documented that estrogen decreases lysosomal enzyme gene expression and secretion while increasing intracellular levels of the enzymes.[21] In consideration of these facts, we have examined the time course of the influence of 17βE_2 on osteoclast Tx-100) soluble and insoluble membrane localization of pp60*src* tyrosine kinase activity. There was a rapid decrease in Tx-100 insoluble membrane–associated activity, which was detected within 1 minute of treatment and decreased progressively throughout

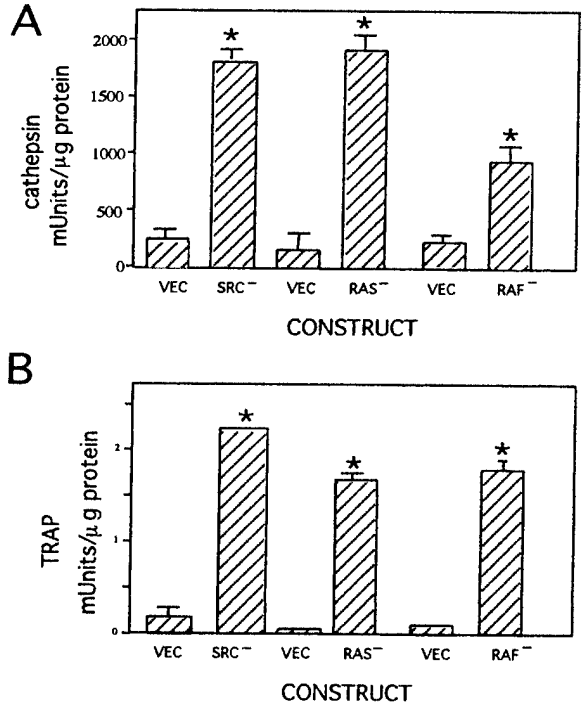

FIG. 1. Effects of dominant interfering pp60*src*, c-*Ras*, or c-*Raf* on lysosomal enzyme secretion. Isolated osteoclasts were plated on bone and transiently transfected with either the respective empty vector (VEC), a vector containing a constitutively active pp60*src* construct (SRC+), c-*Ras*, or c-*Raf* as described. Influences of expression on (A) cathepsin B and (B) TRAP secretion were carried out as described. In all cases, there was a minimum of a 100-fold increase in expression of the respective protein compared with vector-transfected cultures. $*p <$ 0.01 comparing vector-transfected cells to respective expression vector-transfected cells.

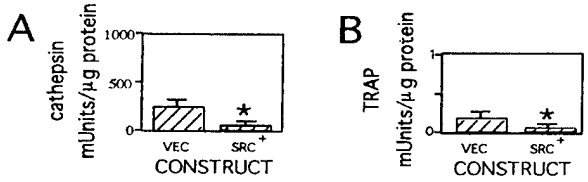

FIG. 2. Effects of pp60*src* on estrogen regulation of osteoclast lysosomal enzyme secretion. Isolated osteoclasts were plated on bone and transiently transfected with either empty vector (VEC) or a vector containing a constitutively active pp60*src* construct (SRC+) on (A) cathepsin B and (B) TRAP secretion were carried out as described. In all cases, there was a minimum of a 100-fold increase in expression of pp60*src* comparing SRC+ to vector-transfected cultures. $*p < 0.01$ comparing vector-transfected cells to expression vector-transfected cells.

the maximum culture period of 24 h of 10^{-8} M $17\beta E_2$ treatment (Fig. 3). The detergent soluble membrane pp60*src* tyrosine kinase activity increased over this time period. The total amount of pp60*src* protein in each of these fractions

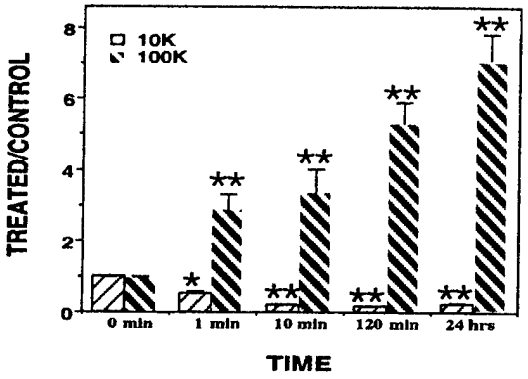

FIG. 3. Effects of $17\beta E_2$ on pp60*src* tyrosine kinase activity. time course of response. Isolated osteoclasts were cultured with either vehicle (control) or 10^{-8} M $17\beta E_2$ (treated) for the indicated time period. Cell pellets were harvested and assayed for pp60*src* kinase activity in the TX-100 insoluble (10K) and soluble (100K) fractions as described. The results are the mean ± SEM of three separate experiments. $*p <$ 0.05; $**p < 0.001$ comparing treated with zero time.

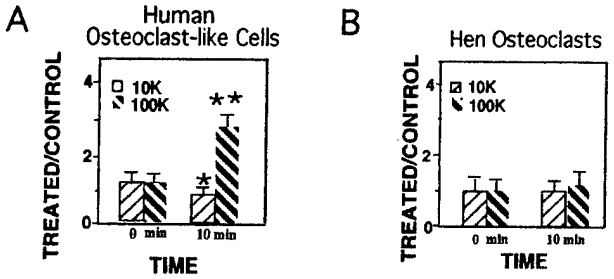

FIG. 4. (A) Effects on human osteoclast-like cells. Isolated cells were cultured with either vehicle (control) or 10^{-8} M $17\beta E_2$ (treated) for 10 minutes and assayed for pp60*src* kinase activity in the TX-100 insoluble (10K) and soluble (100K) fractions as described. The results are the mean ± SEM of three separate experiments. (B) Effects on egg-laying hen osteoclasts. Isolated osteoclasts were cultured with either vehicle (control) or 10^{-8} M $17\beta E_2$ (treated) for 10 minutes and assayed for pp60*src* kinase activity in the TX-100 insoluble (10K) and soluble (100K) fractions as described. The results are the mean ± SEM of three separate experiments. $*p < 0.05$; $**p < 0.001$ comparing treated with zero time

was not significantly altered with treatment (data not shown). To determine whether 10^{-8} M $17\beta E_2$ had a similar effect on mammalian osteoclast-like cells, we used multinucleated cells isolated from human giant cell tumors of the bone. In this model, we observed a response similar to the avian osteoclasts (Fig. 4A). We and others have shown that osteoclasts isolated from egg-laying hens do not respond to estrogen treatment with altered resorption activity.[14] Our studies have shown that there is no evidence of nuclear binding of estrogen in these cells. We have examined the effects of 10^{-8} M $17\beta E_2$ on pp60src kinase activity and similarly are unable to detect any influence on Tx-100 soluble or insoluble–associated activity (Fig. 4B). We next

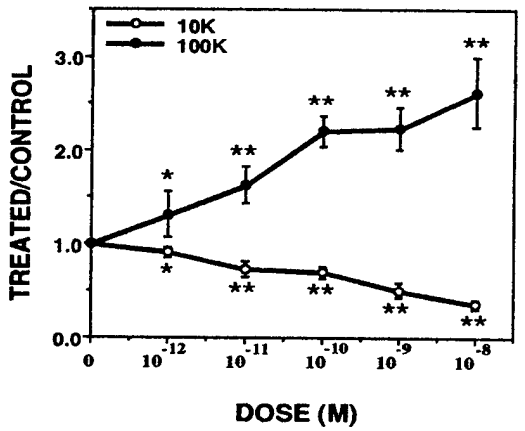

FIG. 5. Influence of $17\beta E_2$ dose on response. Isolated osteoclasts were cultured with either vehicle (0) or the indicated concentration of $17\beta E_2$ for 10 minutes. Cell pellets were harvested and assayed for pp60*src* kinase activity in the TX-100 insoluble (10K) and soluble (100K) fractions as described. The results are the mean ± SEM of three separate experiments. $*p < 0.05$; $**p < 0.001$ comparing treated with vehicle (0).

examined a broad range of $17\beta E_2$ concentrations for effects on Tx-100 soluble and insoluble membrane association of pp60*src* kinase activity (Fig. 5). At 10^{-12} M $17\beta E_2$, there was a significant decrease in Tx-100 insoluble membrane association of pp60*src* kinase activity. This decrease progressively expanded up to the maximum concentration examined, 10^{-8} M. Moreover, there was a dose-dependent increase in detergent soluble membrane–associated tyrosine kinase activity. For subsequent studies, we elected to examine osteoclast responses after 10 minutes of 10^{-8} M steroid treatment.

To further examine the involvement of the estrogen receptor in this $17\beta E_2$-induced response, we examined the influence of the inactive estrogen stereoisomer $17\alpha E_2$ and cotreatment with E_2 and the receptor antagonist ICI 182–780 (Fig. 6A). Neither the inactive stereoisomer nor the estrogen antagonist had any significant effect on Tx-100 soluble and insoluble membrane–associated pp60*src* Tx-100 kinase activity. In contrast to the expected effects of $17\beta E_2$ alone, cotreatment with $17\beta E_2$ and the estrogen antagonist inhibited the $17\beta E_2$ response. To determine the steroid specificity of Tx-100 insoluble membrane–associated pp60*src* kinase activity changes, the response to treatment with 10^{-8} M of dexamethasone, dihydroxy testosterone, or the progestin R5020 responses were compared with the response to $17\beta E_2$ after 10 minutes of treatment (Fig. 6B). The responses to treatment with the other steroids did not follow a pattern similar to that with estrogen treatment.

Osteoclasts contain high levels of c-*Fyn*, c-*Lyn*, and c-*Yes* in addition to pp60*src*[30]; so we have examined how $17\beta E_2$ effects the membrane localization of tyrosine kinase activity of these members of the *Src* family (Fig. 6C). In contrast to the decrease measured after immunoprecipitation of

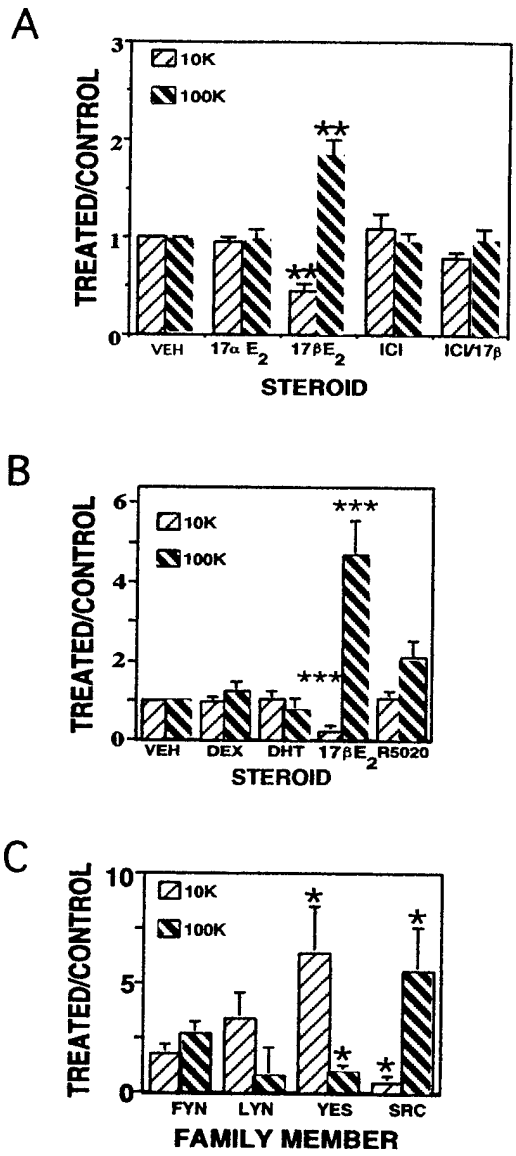

FIG. 6. (A) Response specificity. Isolated osteoclasts were treated with either vehicle (VEH), 10^{-8} M $17\alpha E_2$, 10^{-8} M $17\beta E_2$, 10^{-6} M ICI 182–780 (ICI), or 10^{-8} M 17β E_2 plus 10^{-6} M ICI 182–780 (ICI/17β). Cell pellets were harvested and assayed for pp60*src* kinase activity as described. (B) Steroid response specificity. Isolated osteoclasts were treated either with vehicle (VEH), dexamethasone (DEX), dihydroxy testosterone (DHT), $17\beta E_2$, or a synthetic progestin (R5020) each at 10^{-8} M for 10 minutes. Cell pellets were harvested and assayed for pp60*src* kinase activity as described. The results are the mean ± SEM of three separate experiments. (C) $17\beta E_2$ on *Src* family members. Osteoclasts were treated with either vehicle (control) or 10^{-8} M E_2 (treated) for 10 minutes. Cell pellets were harvested and assayed for kinase activity after precipitation of the kinase with specific antibodies to the *Src* family members indicated as described. The results are the mean ± SEM of three separate experiments. $*p < 0.05$; $**p < 0.005$; $***p < 0.001$ comparing treated with vehicle.

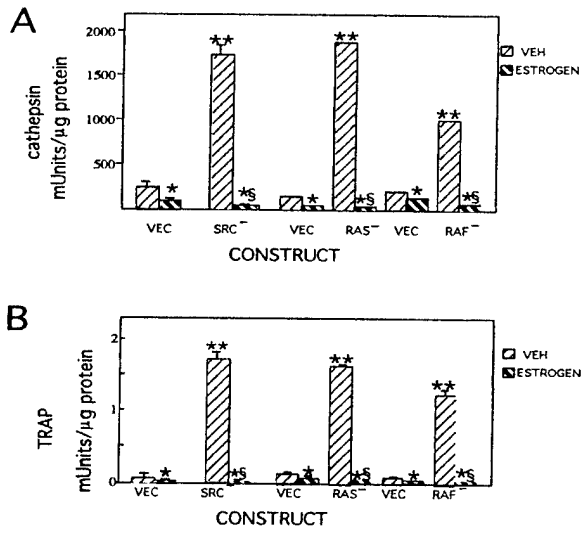

FIG. 7. Effects of dominant interfering expression of either pp60*src*, c-*Ras*, or c-*Raf* on estrogen regulation of osteoclast lysosomal enzyme secretion. Isolated osteoclasts were plated on bone and transiently transfected with either the respective empty vector (VEC), a vector containing a dominant interfering expression construct for pp60*src* (SRC-), c-*Ras* (Ras-), or c-*Raf* (Raf-) before $17\beta E_2$ treatment as described. Influences of expression with and without $17\beta E_2$ treatment on (A) cathepsin B and (B) TRAP secretion were carried out as described. In all cases, there was a minimum of a 100-fold increase in expression of the respective protein compared with vector-transfected cultures. $*p < 0.01$ comparing vehicle (VEH) to $17\beta E_2$-treated cells; $**p < 0.01$ comparing vehicle-treated transfected cells to vehicle-treated vector-only transfected cells; $\S p < 0.01$ comparing 17βE2-treated transfected cells to $17\beta E_2$-treated vector-only transfected cells.

pp60*src*, there appeared to be an increase in Tx-100 insoluble membrane-associated c-*Yes* kinase activity after E_2 treatment, but no significant influence of $17\beta E_2$ on the localization of c-*Fyn* and c-*Lyn*. Moreover, there was a significant decrease in c-*Yes* kinase activity and no significant effects on c-*Fyn* or c-*Lyn* kinase activity in Tx-100 soluble membranes.

To further explore the interactions of $17\beta E_2$, pp60src signal transduction and the regulation of lysosomal enzyme secretion, we have examined the interactions of the dominant interfering and constitutively active constructs on $17\beta E_2$ regulation of lysosomal enzyme secretion. Dominant interfering pp60*src*, c-*Ras*, or c-*Raf* individually enhanced the $17\beta E_2$ effects on osteoclast activity (Fig. 7) whereas constitutively active pp60*src* blocked $17\beta E_2$ effects on lysosomal enzyme secretion (Fig. 8).

DISCUSSION

For several years, it has been apparent that osteoclast function was dependent on the presence of pp60*src*. Mice lacking pp60*src* contained osteoclasts that were nonfunctional and failed to form a clear zone when present adjacent to bone surfaces.[3] Recent data have revealed two key factors important in the progress of understanding the role of pp60*src* in osteoclast activity. One key element in this was the observation that kinase-defective pp60*src* could replace wild-type pp60*src* in restoring osteoclast function in transgenic $src^{-/-}$ mice.[7] Another important observation was that the SH2 domain of pp60*src* is critical for osteoclast migration, not the kinase domain.[8] The SH3 domains of proteins are involved in protein-protein interactions through interactions with other SH3 domains.[31] In pp60*src*, the SH3 domain also localizes pp60*src* in the cytosol and participates in interactions between the tail and the SH2 domain when the protein is inactivated.[32 36] The conformation of the SH3 domain of pp60*src* alters after phosphorylation of Y527 and subsequent interactions of the tail region with the SH2 domain.[36] Thus, although pp60*src* kinase activity is not required for pp60*src* function in osteoclasts, phosphorylation and inactivation of wild-type pp60*src* will alter conformation of the SH3 domain, blocking efficient function of the SH3 domain and blocking pp60*src* function in osteoclasts.

Signaling after activation of pp60*src* may involve a number of pp60*src* substrates.[37] Many of these pathways lead to activation of c-*Ras* and subsequent activation of c-*Raf*.[38] These events ultimately can lead to alteration in a number of cellular processes, depending on the interactions and integration of the variety of stimuli a cell encounters. We have used dominant interfering constructs of pp60*src*, c-*Ras*, and c-*Raf* to investigate the role of this signaling pathway in regulating osteoclast lysosomal enzyme secretion. The dominant interfering pp60*src* mutation functionally blocks the kinase activity without interfering with the SH2 or SH3 domain amino acid sequences. Interestingly, blocking the *Src/Ras/Raf* signaling pathway greatly stimulated secretion of lysosomal enzymes while expression of a constitutively active pp60*src* construct decreased secretion. These data, taken together with the ability of kinase-defective pp60*src* to rescue the $src^{-/-}$ phenotype, suggests multiple roles of pp60*src* in osteoclast activity.[7] The kinase domain is not involved in the ability of osteoclasts to form ruffled borders and resorb bone.[7] The data presented here supports that activation of the *Src/Ras/Raf* pathway is involved either in regulation of the rate at which lysosomal enzymes are secreted or directional targeting. The later possibility is raised by the fact that we measure lysosomal enzyme accumulation in the conditioned media, not the amount of enzyme in the resorption lacunae. Thus, inappropriate targeting of lysosomal enzymes could cause an increased accumulation in the overall media while decreasing release juxtaposed to the bone surface.

The pp60*src* association with the membrane cytoskeleton has been well documented.[25 29,39,40] Several investigations have shown that in platelets, pp60*src* cytoskeletal association changes in response to multiple stimuli including platelet-activating factor; thrombin and interaction with IIb-IIIa[25,39] have shown that association of pp60*src* with the platelet cytoskeletal membrane requires platelet aggregation and actin polymerization. This response is very rapid, occurring within less than 10 minutes of treatment, suggesting

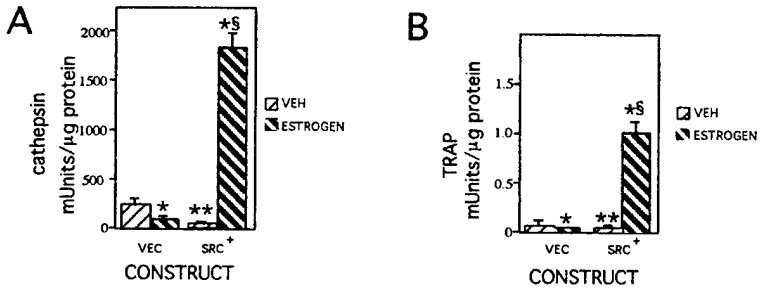

FIG. 8. Effects of expression of constitutively active pp60*src* on estrogen regulation of osteoclast lysosomal enzyme secretion. Isolated osteoclasts were plated on bone and transiently transfected with either empty vector (VEC) or a vector containing a constitutively active pp60*src* construct (SRC+) on (A) cathepsin B and (B) TRAP secretion were carried out as described. In all cases, there was a minimum of a 100-fold increase in expression of pp60*src* comparing SRC+ to vector-transfected cultures. $*p < 0.01$ comparing vehicle (VEH) to $17\beta E_2$-treated cells; $**p < 0.01$ comparing vehicle-treated–transfected cells to vehicle-treated vector-only transfected cells; $\S p < 0.01$ comparing $17\beta E_2$-treated–transfected cells to $17\beta E_2$-treated vector-only transfected cells.

that this is a very early response to stimulation. Migliaccio et al.[41] have showed that $17\beta E_2$ rapidly increases transient protein tyrosine phosphorylation (PTP) in estrogen target cells and that the kinase involved is closely related to pp60*src*. Our data shows a rapid and sustained dose-dependent decrease in cytoskeletal pp60*src* kinase activity and an increase in noncytoskeletal pp60*src* kinase activity that is specific to $17\beta E_2$ and antagonized with a specific estrogen antagonist. The ability of the estrogen receptor antagonist to block $17\beta E_2$ effects successfully supports that the response is mediated by estrogen receptors. This point is further strengthened by the lack of a response in hen osteoclasts because we and others have shown that hen osteoclasts do not contain estrogen receptors.[14] Interestingly, Brubaker and Gay[42] have shown rapid $17\beta E_2$-mediated translocation to the plasma membrane and phosphorylation of pp60*src* in osteoclasts. They also documented a transitory increase in pp60*src* kinase activity. The transitory nature of these responses is in contrast to the sustained changes in pp60*src* kinase activity shown here. The cause of this discrepancy may be that osteoclasts in the studies detailed here were engaged actively in bone degradation whereas the studies of Brubaker and Gay were carried out with osteoclasts not plated on bone. These differences in the osteoclast state of activation may account for these differences.

Several steroids have been shown to cause rapid responses in target cells that are presumed to use nongenomic mechanisms, because the responses are too rapid to be the result of the classical genomic effects of steroids. Nanomolar concentrations of estrogen caused a rapid alteration in osteoclast acidification.[43,44] These data confirm that $17\beta E_2$ treatment activates nongenomic responses in osteoclasts. Several of the nongenomic effects of steroids in other cells involve activation of protein kinase C and/or changes in intracellular calcium levels. Our initial attempts to examine intracellular calcium changes as well as cyclic adenosine monophosphate (cAMP) and cyclic guanosine monophosphate (cGMP) changes have not shown any effect of $17\beta E_2$ on these second messenger systems (data not shown).

In addition to high levels of pp60*src*, osteoclasts contain high levels of c-*Fyn*, c-*Yes*, and c-*Lyn*, all of which are at levels similar to that of platelets.[30] In $src^{-/-}$ mice, there are no apparent defects in platelet function, supporting that other members of the *Src* family are able to substitute for the lack of pp60*src* in platelets. As noted previously, osteoclasts are present but nonfunctional in $src^{-/-}$ mice. This suggests that other members of the *Src* family are unable to functionally replace pp60*src* in $src^{-/-}$ osteoclasts. Interestingly, $17\beta E_2$-induced change in membrane localization of pp60*src* kinase activity is not paralleled by similar alterations in c-*Lyn*, c-*Yes*, or c-*Fyn* tyrosine kinase activity, supporting that the decreased cytoskeletal-associated and increase noncytoskeletal-associated tyrosine kinase activity alterations may be restricted to pp60*src* changes. Although the pattern differed from that of pp60*src*, there were striking changes in the phosphorylation activity of c-*Yes*. Clarification of the role of these changes in osteoclast activity awaits further study.

Because dominant interfering pp60*src*, c-*Ras*, or c-*Raf* expression stimulated lysosomal enzyme secretion and estrogen altered pp60*src* activity, we examined the interaction of these with $17\beta E_2$. Dominant interfering constructs increased secretion of lysosomal enzymes yet estrogen treatment of cells expressing these constructs enhanced repression of lysosomal enzyme secretion. During normal bone resorption, lysosomal enzyme secretion is modulated by the interplay of signals from growth factors, attachment proteins, and other stimuli. Overexpression of the dominant interfering pp60*src* construct shifted this interplay to result in the elevation of lysosomal enzyme secretion. In the presence of E_2, normal osteoclasts respond to the interplay of stimulatory and repressive signals with lower lysosomal enzyme secretion. Overexpression of dominant interfering pp60*src* enhanced estrogen effects on the repression of lysosomal enzyme secretion. This paradoxical effect leads us to the conclusion that the decrease in osteoclast lysosomal enzyme secretion caused by treatment with $17\beta E_2$ is not the result of $17\beta E_2$-mediated activation of noncytoskeletal membrane-associated pp60*src*. However, estrogen-mediated decreased cytoskeletal-associated pp60*src* activity may be involved in these responses. Interestingly, transfection with the constitutively active pp60*src* construct during

$17\beta E_2$ treatment caused an elevation in lysosomal enzyme secretion. These data suggest that activation of pp60*src* by external signaling from sources such as growth factors or binding to the extracellular matrix are able to overcome $17\beta E_2$-stimulated decreases in lysosomal enzyme steady-state messenger RNA (mRNA) levels.

The data presented here support that the pp60*src*/*Ras*/*Raf* signaling pathway is important in osteoclast lysosomal enzyme secretion and the role of pp60*src* in regulating osteoclast activity is likely to be complex and multiple factors must interplay in influencing this activity.

ACKNOWLEDGMENTS

The authors gratefully acknowledge the technical support of Mr. Larry Pederson, Mr. Joseph Trowbridge, and Ms. Debra Erickson. We also thank the NIH, The University of Minnesota, The Duluth Clinic, The Minnesota Medical Foundation, and The American Heart Association for their support.

REFERENCES

1. Roodman GD 1999 Cell biology of the osteoclast. Exp Hematol **27:**1229–1241.
2. Baron R, Neff L, Louvard D, Courtoy PJ 1985 Cell-mediated extracellular acidification and bone resorption: Evidence for a low pH in resorbing lacunae and localization of a 100-kDa lysosomal membrane protein at the osteoclast ruffled border. J Cell Biol **101:**2210–2222.
3. Soriano P, Montgomery C, Geske R, Bradley A 1991 Targeted disruption of the c-src proto-oncogene leads to osteopetrosis in mice. Cell **64:**693–702.
4. Boyce BF, Yoneda T, Lowe C, Soriano P, Mundy GR 1992 Requirement of pp60c-src expression for osteoclasts to form ruffled borders and resorb bone in mice. J Clin Invest **90:** 1622–1627.
5. Lowe C, Yoneda T, Boyce BF, Chen H, Mundy GR, Soriano P 1993 Osteopetrosis in *Src*-deficient mice is due to an autonomous defect of osteoclasts. Proc Natl Acad Sci USA **90:** 4485–4489.
6. Missbach M, Jeschke M, Feyen J, Muller K, Glatt M, Green J, Susa M 1999 A novel inhibitor of the tyrosine kinase Src suppresses phosphorylation of its major cellular substrates and reduces bone resorption in vitro and in rodent models in vivo. Bone **24:**437–449.
7. Schwartzberg PL, Xing L, Hoffmann O, Lowell CA, Garrett L, Boyce BF, Varmus HE 1997 Rescue of osteoclast function by transgenic expression of kinase- deficient Src in $src^{-/-}$ mutant mice. Genes Dev **11:**2835–2844.
8. Violette SM, Shakespeare WC, Bartlett C, Guan W, Smith JA, Rickles RJ, Bohacek RS, Holt DA, Baron R, Sawyer TK 2000 A Src SH2 selective binding compound inhibits osteoclast-mediated resorption Chem Biol **7:**225–235.
9. Grey A, Chen Y, Paliwal I, Carlberg K, Insogna K 2000 Evidence for a functional association between phosphatidylinositol 3-kinase and c-src in the spreading response of osteoclasts to colony-stimulating factor-1. Endocrinology **141:** 2129–2138.
10. Furuyama N, Fujisawa Y 2000 Regulation of collagenolytic protease secretion through c-Src in osteoclasts. Biochem Biophys Res Commun **272:**116–124.
11. Abu-Amer Y, Teitelbaum SL, Chappel JC, Schlesinger P, Ross FP 1999 Expression and regulation of RAB3 proteins in osteoclasts and their precursors. J Bone Miner Res **14:**1855–1860.
12. Collin-Osdoby P, Oursler MJ, Webber D, Osdoby P 1991 Osteoclast-specific monoclonal antibodies coupled to magnetic beads provide a rapid and efficient method of purifying avian osteoclasts. J Bone Miner Res **6:**1353–1365.
13. Oursler MJ, Pederson L, Fitzpatrick L, Riggs BL, Spelsberg T 1994 Human giant cell tumors of the bone (osteoclastomas) are estrogen target cells. Proc Natl Acad Sci USA **91:**5227–5231.
14. Pederson L, Kremer M, Foged NT, Winding B, Ritchie C, Fitzpatrick LA, Oursler MJ 1997 Evidence of a correlation of estrogen receptor level and avian osteoclast estrogen responsiveness. J Bone Miner Res **12:**742–752.
15. Oursler MJ, Osdoby P, Pyfferoen J, Riggs BL, Spelsberg TC 1991 Avian osteoclasts as estrogen target cells. Proc Natl Acad Sci USA **88:**6613–6617.
16. Twamley-Stein GM, Pepperkok R, Ansorge W, Courtneidge SA 1993 The Src family tyrosine kinases are required for platelet-derived growth factor-mediated signal transduction in NIH 3T3 cells. Proc Natl Acad Sci USA **90:**7696–7700.
17. Roche S, Koegl M, Barone MV, Roussel MF, Courtneidge SA 1995 DNA synthesis induced by some but not all growth factors requires Src family protein tyrosine kinases. Mol Cell Biol **15:**1102–1109.
18. Rayter SI, Woodrow M, Lucas SC, Cantrell DA, Downward J 1992 p21ras mediates control of IL-2 gene promoter function in T cell activation. Embo J **11:**4549–4556.
19. Dent P, Reardon DB, Morrison DK, Sturgill TW 1995 Regulation of Raf-1 and Raf-1 mutants by Ras-dependent and Ras-independent mechanisms in vitro. Mol Cell Biol **15:**4125–4135.
20. Oursler M, Collin-Osdoby P, Anderson F, Li L, Webber D, Osdoby P 1991 Isolation of avian osteoclasts: Improved techniques to preferentially purify viable cells. J Bone Miner Res **6:**375–385.
21. Kremer M, Judd J, Rifkin B, Auszmann J, Oursler MJ 1995 Estrogen modulation of osteoclast lysosomal enzyme secretion. J Cell Biochem **57:**271–279.
22. Hofstee BHJ 1954 Direct and continuous spectrophotometric assay of phosphomonoesterases. Arch Biochem Biophys **51:** 139–144.
23. Barrett A, Kirschke H 1981 Proteases of diverse origin and function, cathepsin B, cathepsin D, cathepsin H, and cathepsin L. Methods Enzymol **80:**535–561.
24. Oda A, Druker BJ, Smith M, Salzman EW 1992 Association of pp60src with Triton X-100-insoluble residue in human blood platelets requires platelet aggregation and actin polymerization. J Biol Chem **267:**20075–20081.
25. Fox JE, Lipfert L, Clark EA, Reynolds CC, Austin CD, Brugge JS 1993 On the role of the platelet membrane skeleton in mediating signal transduction. Association of GP IIb-IIIa, pp60c-src, pp62c-yes, and the p21ras GTPase-activating protein with the membrane skeleton. J Biol Chem **268:**25973–25984.
26. Grondin P, Plantavid M, Sultan C, Breton M, Mauco G, Chap H 1991 Interaction of pp60c-src, phospholipase C, inositol-lipid, and diacyglycerol kinases with the cytoskeletons of thrombin-stimulated platelets. J Biol Chem **266:**15705–15709.
27. Helmke S, Pfenninger KH 1995 Growth cone enrichment and cytoskeletal association of non-receptor tyrosine kinases. Cell Motil Cytoskeleton **30:**194–207.
28. Horvath AR, Muszbek L, Kellie S 1992 Translocation of pp60c-src to the cytoskeleton during platelet aggregation. Embo J **11:**855–861.

29. Okamura H, Resh MD 1994 Differential binding of pp60c-src and pp60v-src to cytoskeleton is mediated by SH2 and catalytic domains. Oncogene **9**:2293–2303.
30. Horne WC, Neff L, Chatterjee D, Lomri A, Levy JB, Baron R 1992 Osteoclasts express high levels of pp60c-src in association with intracellular membranes. J Cell Biol **119**:1003–1013.
31. Sparks AB, Rider JE, Hoffman NG, Fowlkes DM, Quillam LA, Kay BK 1996 Distinct ligand preferences of Src homology 3 domains from Src, Yes, Abl, Cortactin, p53bp2, PLCgamma, Crk, and Grb2. Proc Natl Acad Sci USA **93**: 1540–1544.
32. Koegl M, Courtneidge SA, Superti-Furga G 1995 Structural requirements for the efficient regulation of the Src protein tyrosine kinase by Csk. Oncogene **11**:2317–2329.
33. Erpel T, Superti-Furga G, Courtneidge SA 1995 Mutational analysis of the Src SH3 domain: The same residues of the ligand binding surface are important for intra- and intermolecular interactions. Embo J **14**:963–975.
34. Okada M, Howell BW, Broome MA, Cooper JA 1993 Deletion of the SH3 domain of Src interferes with regulation by the phosphorylated carboxyl-terminal tyrosine. J Biol Chem **268**: 18070–18075.
35. Superti-Furga G, Courtneidge SA 1995 Structure-function relationships in Src family and related protein tyrosine kinases. Bioessays **17**:321–330.
36. Superti-Furga G, Fumagalli S, Koegl M, Courtneidge SA, Draetta G 1993 Csk inhibition of c-Src activity requires both the SH2 and SH3 domains of Src. Embo J **12**:2625–2634.
37. Tatosyan Ab, Mizenina OA 2000 Kinases of the Src family: Structure and function. Biochemistry **65**:49–58.
38. Porter AC, Vaillancourt RR 1998 Tyrosine kinase receptor-activated signal transduction pathways which lead to oncogenesis. Oncogene **17**:1343–1352.
39. Dhar A, Shukla SD 1991 Involvement of pp60c-src in platelet-activating factor-stimulated platelets. Evidence for translocation from cytosol to membrane. J Biol Chem **266**:18797–18801.
40. Walker F, deBlaquiere J, Burgess AW 1993 Translocation of pp60c-src from the plasma membrane to the cytosol after stimulation by platelet-derived growth factor. J Biol Chem **268**:19552–19558.
41. Migliaccio A, Pagano M, Auricchio F 1993 Immediate and transient stimulation of protein tyrosine phosphorylation by estradiol in MCF-7 cells. Oncogene **8**:2183–2191.
42. Brubaker KD, Gay CV 2000 Estrogen stimulates protein tyrosine phosphorylation and src kinase activity in avian osteoclasts. J Cell Biochem **76**:206–216.
43. Gay CV, Kief NL, Bekker PJ 1993 Effect of estrogen on acidification in osteoclasts. Biochem Biophys Res Commun **192**:1251–1259.
44. Brubaker KD, Gay CV 1999 Depolarization of osteoclast plasma membrane potential by 17beta-estradiol. J Bone Miner Res **14**:1861–1866.

Address reprint requests to:
Merry Jo Oursler, Ph.D.
University of Minnesota
211 Life Science
10 University Drive
Duluth, MN 55812, USA

Received in original form February 28, 2000; in revised form November 16, 2000; accepted January 12, 2001.

ELSEVIER

Journal of Orthopaedic Research 20 (2002) 58–65

Journal of Orthopaedic Research

www.elsevier.com/locate/orthres

Temporal expression patterns of BMP receptors and collagen II (B) during periosteal chondrogenesis

Arunik Sanyal [a], Merry Jo Oursler [b], Victoria R. Clemens [a], Takumi Fukumoto [a], James S. Fitzsimmons [a], Shawn W. O'Driscoll [a,*]

[a] *Department of Orthopedics, Cartilage and Connective Tissue Research Laboratory, Mayo Clinic and Mayo Foundation, 200 First Street SW, MS 3-69, Rochester, MN 55905, USA*

[b] *Departments of Biology, Medical Microbiology and Immunology, and Biochemistry and Molecular Biology, University of Minnesota, Duluth, MN, USA*

Received 8 May 2000; accepted 15 May 2001

Abstract

Articular cartilage has a limited ability to repair itself. Periosteal grafts have chondrogenic potential and are used clinically to repair defects in articular cartilage. An organ culture model system for in vitro rabbit periosteal chondrogenesis has been established to study the molecular events of periosteal chondrogenesis in vitro. In this model, bone morphogenetic protein-2 (BMP2) mRNA expression was found to be upregulated in the first 12 h. BMPs usually transduce their signals through a receptor complex that includes type II and either type IA or type IB BMP receptors. Receptors IA and IB play distinct roles during limb development. We have examined the temporal expression patterns for the mRNAs of these receptors using our experimental model. The mRNA expression patterns of these three BMP receptors differed from one another in periosteal explants during chondrogenesis. When these explants were cultured under chondrogenic conditions (agarose suspension with TGF-β1 added to the media for the first 2 days), the expression of BMPRII mRNA and that of BMPRIA mRNA varied only slightly and persisted over a long time. In contrast, the expression of BMPRIB mRNAwas upregulated within 12 h, peaked at day 5, and fell to a level that was barely detected beyond day 21. Moreover, the expression of BMPRIB mRNA preceded that of collagen type IIB mRNAs, a marker for matrix-depositing chondrocytes. These data support a role for coordinate expression of BMP2 and its receptors early during periosteal chondrogenesis.

Keywords: BMP receptor; Collagen II (B); Chondrogenesis; Periosteum

Introduction

Since articular cartilage lacks both blood supply and mesenchymal progenitor cells, it has a limited potential for self-repair [7]. Autologous periosteal transplantation is a viable approach to repair a defect in articular cartilage since periosteum, the thick outer layer of bone, has both osteogenic and chondrogenic potential [15–18]. The molecular mechanisms regulating periosteal chondrogenesis are, however, poorly understood. We have established an organ culture model system to study periosteal chondrogenesis in vitro [14]. In this model, periosteal explants produce cartilage when cultured in agarose and this process is enhanced by exogenously added TGF-β1. During our search for the expression of potential regulatory factors in this model, we observed an upregulation of bone morphogenetic protein-2 (BMP2) mRNA during culture in agarose [23]. This upregulation was enhanced by the exogenous addition of TGF-β1 and was transcriptionally regulated, implicating BMP2 signaling in this process.

Bone morphogenetic proteins (BMPs) are members of the TGF-β superfamily of proteins and are involved in a variety of developmental processes including chondrogenesis [3]. They were originally detected and purified from bone for their ability to induce ectopic cartilage and bone formation [29–31]. The upregulation of BMP2 supports our hypothesis that members of the TGF-β superfamily of growth factors are regulators of periosteal chondrogenesis. BMPs transduce signals through transmembrane serine–threonine kinase receptors [8,9]. The BMP receptor complex is a heterodimer

* Corresponding author. Tel.: +1-507-284-4570; fax: +1-507-266-4234.

E-mail address: odriscoll.shawn@mayo.edu (S.W. O'Driscoll).

0736-0266/02/$ - see front matter
PII: S0736-0266(01)00078-X

consisting of type I (BMPRI) and type II (BMPRII) receptors. There are two type I receptors, BMPRIA and BMPRIB [6,26]. Similar to TGF-β, BMPs first bind to a type II receptor followed by the recruitment of a type I receptor to form the heteromeric complex. Transphosphorylation of the type I receptor by the type II receptor then takes place triggering the downstream signaling [9,12,19]. BMPR IA and IB have distinct functions during the formation and differentiation of cartilage. BMPRIA appears to regulate chondrocyte differentiation whereas BMPRIB initiates apoptosis and cartilage formation [32].

To ascertain which type I receptor could be acting during periosteal chondrogenesis in our system, investigation of the temporal mRNA expression patterns is necessary. Because of limited availability of the starting material (rabbit periosteal explants) and hence the amount of total RNA, we employed RT-PCR instead of northern blot analysis or RNase protection assay to study the expression patterns of the three types of mRNAs. Since the experimental model for in vitro periosteal chondrogenesis is rabbit-based and RT-PCR relies on the use of species-specific sequences, we report, in this paper, the isolation of rabbit-specific partial cDNA sequences of BMPRIA, IB and BMPRII. We found that during periosteal chondrogenesis the expression of all the three mRNAs is modulated. Interestingly, the mRNA for collagen IIB, a marker for chondrogenesis, was increased subsequent to the peaks in BMPR expression.

Materials and methods

Culture of periosteal explants

A total of 336 periosteal explants (2×3 mm^2) were harvested from proximal tibiae of 21 rabbits (two months old). Three hundred and twelve explants were cultured in agarose in the presence of 10% fetal bovine serum (FBS) with or without TGF-β1 (10 ng/ml) as described by O'Driscoll et al. [14]. TGF-β1, however, was present in the medium only for the first two days of culture. Periosteal explants, after culture for a desired period, were washed with phosphate buffered saline (PBS) and then pooled (12 explants/group).

Preparation of total RNA and synthesis of cDNA

Total RNA from rabbit tibiae pulverized in liquid nitrogen or from pooled periosteal explants was prepared using Trizol™ reagent as described by Sanyal et al. [21]. 2 μg of total RNA was treated with DNase I and then converted to cDNA using superscript II reverse transcriptase and random primers as described previously [21].

Polymerase chain reaction

20 μl reaction mix for polymerase chain reaction (PCR) contained 10 mM *tris*-HCl pH 8.3, 50 mM KCl, 1.5 mM $MgCl_2$, 0.001% gelatin, 200 μM dNTPs, 2 pmol of each sense (S) and antisense (AS) primers, 1 μl cDNA (40 ng of RNA) as template, and 0.5 units of Taq DNA polymerase. The template was initially denatured at 94°C for 7 min. PCR was performed (for different numbers of cycles as described in the legends to figures) with annealing at 60°C (or as described in the legends to figures) for 2 min, elongation at 72°C for 3 min and denaturation at 94°C for 1 min.

Isolation of rabbit-specific cDNA sequences

Rabbit-specific cDNA sequences of BMPRIA, IB and BMPRII were isolated using the method of gene digging [22] which involved two rounds of PCR using sense (S) and antisense (AS) primers designed based on the stretches of nucleotide sequences conserved across species for which the corresponding cDNAs are known. In each case cDNA from rabbit tibiae was used as a template for the 1st round of PCR with a 5′ sense (S) and a 3′ antisense (AS) primers. The product of the 1st round of PCR was used as the template for the 2nd round of PCR, also called seminested PCR, with either the sense or the antisense primer (as described above) and an internal primer. The following primers were used for gene digging:

For BMPRIA
- 5′S T(T/C)(A/G)(A/G)ACAATGACTCAGCTATACA,
- 3′AS GTCC(T/G)GCGTAGCTGGGCTTT,
- 3′AS (internal) GCA(T/C)TGAAAATCAGA(T/G)CCTTCATA.

For BMPRIB
- 5′S C(A/T)GGAAAATTAAATGTGGGCACC,
- 3′AS GG(T/C)CCATCAACAAAATCTCTGT,
- 3′AS (internal) T(A/G)GGGTG(T/G)AGGTCTTTATTACA.

For BMPRII
- 5′S GAAGACTCTATCCATCATACTGA,
- 3′AS TGCTCCATGAGATTCTCATCA,
- 3′AS (internal) AGGTTCTTATCAACTTCTTTTGG.

Both 1st and 2nd round of PCRs were performed for 35 cycles with annealing temperature at 50°C. The other parameters for PCR remained same as described above. The amplified products after seminested PCR were electrophoresed on an agarose gel and the expected DNA band was excised, purified and then subjected to automated sequencing using the primers that were used for seminested PCR.

Densitometry

Densitometry was performed on autoradiographs depicting the time courses of expression of BMPRIB and collagen type IIB presented in Fig. 5. Digital scans were obtained of the autoradiographs that were then analyzed using the "Gel Plotting" macro of NIH Image 1.62 image analysis software. Band densities, less background, were obtained in arbitrary units and normalized to percent maximum expression for the time period examined.

Results

Isolation of rabbit-specific partial cDNA sequences of BMPRIA, BMPRIB and BMPRII mRNAs

We have employed the method of gene-digging [22], as described in methods section, to isolate rabbit-specific partial cDNA sequences of BMPRIA and IB (from the ligand binding domain) and BMPRII (from the cytoplasmic tail region) mRNAs. This method involves amplification of a gene segment in the coding region by PCR using primers designed from the stretches of conserved nucleotide sequences of the same gene from other species. A DNA segment of the expected size was amplified with semi-nested PCR (Fig. 1(A), lane 2) using the primers designed based on human, mouse and rat BMPRIA cDNA sequences [6,24,25]. The nucleotide sequence of this fragment was 90% identical to human

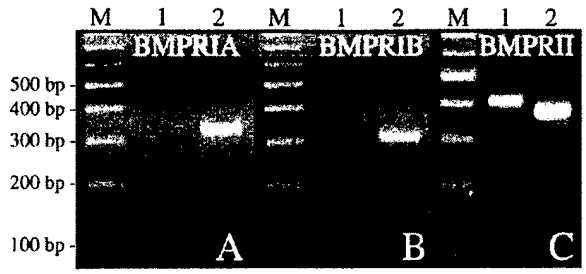

Fig. 1. Isolation of rabbit-specific cDNA fragments for three BMP receptor mRNAs by gene digging. Photographs of ethidium bromide stained agarose gels containing the products of 1st round and seminested PCRs are shown for the isolation of rabbit-specific cDNA fragments for (A) BMPRIA, (B) BMPRIB and (C) BMPRII, components of the BMP receptor complex. In each case, lane 1, 1st round PCR product obtained by using rabbit tibia cDNA as a template, and lane 2, seminested PCR product obtained by using 10-fold diluted 1st PCR product as a template. *M* indicates 100 bp DNA ladder (Boehringer Mannheim). The specific cDNA band appeared in the seminested PCR in each case was used for sequencing.

and 89% identical to mouse BMPRIA cDNA sequences (Fig. 2(A)). The deduced amino acid sequence was 93% and 91% identical to that of human and mouse cDNAs, respectively. Similarly, when primers designed based on human and mouse BMPRIB cDNAs [4,27] were used, a DNA segment of expected size was amplified in the semi-nested PCR (Fig. 1(B), lane 2). The nucleotide sequence of this fragment was 90% identical to human cDNA (Fig. 2(B)). The deduced amino acid sequence of this fragment was 99% and 97% identical to that of mouse and human cDNAs, respectively. Again, the nucleotide sequence of the amplified product (Fig. 1(C), lane 2), isolated using primers designed based on human and mouse BMPRII cDNAs [5], was 88% homologous to human and 85% homologous to mouse cDNA sequences (Fig. 2(C)). Deduced amino acid sequence of this fragment was 91% and 92% identical to that of human and mouse cDNAs, respectively. These results suggest the acquisition of rabbit-specific partial cDNA sequences of the aforementioned mRNAs.

Basal level of expression of BMPRIA, IB and BMPRII mRNAs in periosteum

To determine if periosteum expresses BMPRIA, BMPRIB and BMPRII mRNAs, the total RNA from periosteal explants (used right after harvest and not cultured) was analyzed by RT-PCR using rabbit-specific primers for these mRNAs (Table 1) designed based on the above-mentioned sequences. PCRs were performed separately for different numbers of cycles for each receptor mRNA. The results show that all three receptor mRNAs were amplified indicating their presence in the periosteal explants (Fig. 3). The identity of each PCR-amplified band of the expected size was determined by direct sequencing. This indicates that the primers we have designed based on the isolated sequences, can be used to study the patterns of expression of three BMP receptor mRNAs by RT-PCR. The data from this experiment were also used to determine the exponential phase of amplification by log plot analysis for each mRNA (data not shown) based on which we chose 30 cycles of amplification for later experiments.

Upregulation of BMPRIA, IB and BMPRII mRNAs early during periosteal chondrogenesis

Since BMP2 mRNA expression is upregulated in periosteal explants within 12 h (i.e. 0.5 days) of culture in agarose with and without TGF-β1 and remained upregulated more than a week [23], we sought to determine if any of the BMP receptor mRNAs were expressed during this time. To address this issue we cultured periosteal explants in agarose in the presence of FBS with and without TGF-β1. The explants were harvested after 0.5, 1, 2 and 5 days of culture. Initially the expression of BMPRIA, IB and BMPRII mRNAs was examined by RT-PCR on RNAs prepared from these explants. RNA from day 0 explants (used right after harvest) was also included. The results presented in Fig. 4 indicate that the mRNAs of all the three BMP receptors were present in the explants at all the time points tested with and without TGF-β1 treatment. In explants cultured without TGF-β1 (Fig. 4, lanes 2, 4, 6, and 8), the levels of BMPRII and BMPRIB mRNAs were below their respective basal levels up to day 2 followed by a pronounced increase on day 5 for both. The level of BMPRIA mRNA in these same explants, on the other hand, was close to its basal level at these time points. Explants treated with TGF-β1 (Fig. 4, lanes 3, 5, 7, and 9), which enhances chondrogenesis, contained more mRNAs than the untreated explants for all the three types of receptor mRNAs at all the time points tested during culture. Altogether, the results suggest that, during periosteal chondrogenesis all the three mRNAs are upregulated. Since TGF-β1 influences the timing and magnitude of the process, we chose to perform the rest of our experiments with TGF-β1 treated explants for subsequent studies.

Upregulated BMPRIB mRNA expression precedes collagen type IIB mRNA expression

To determine how long the expression of BMP receptor mRNAs persist, we examined the expression of all the three receptor mRNAs in TGF-β1 treated explants over a longer period of time (to include the time of cartilage production by the explants). For this, we cultured the periosteal explants in agarose in the presence of FBS with TGF-β1. The explants were harvested after 0.5, 1, 2, 5, 7, 10, 14, 21, and 28 days of culture.

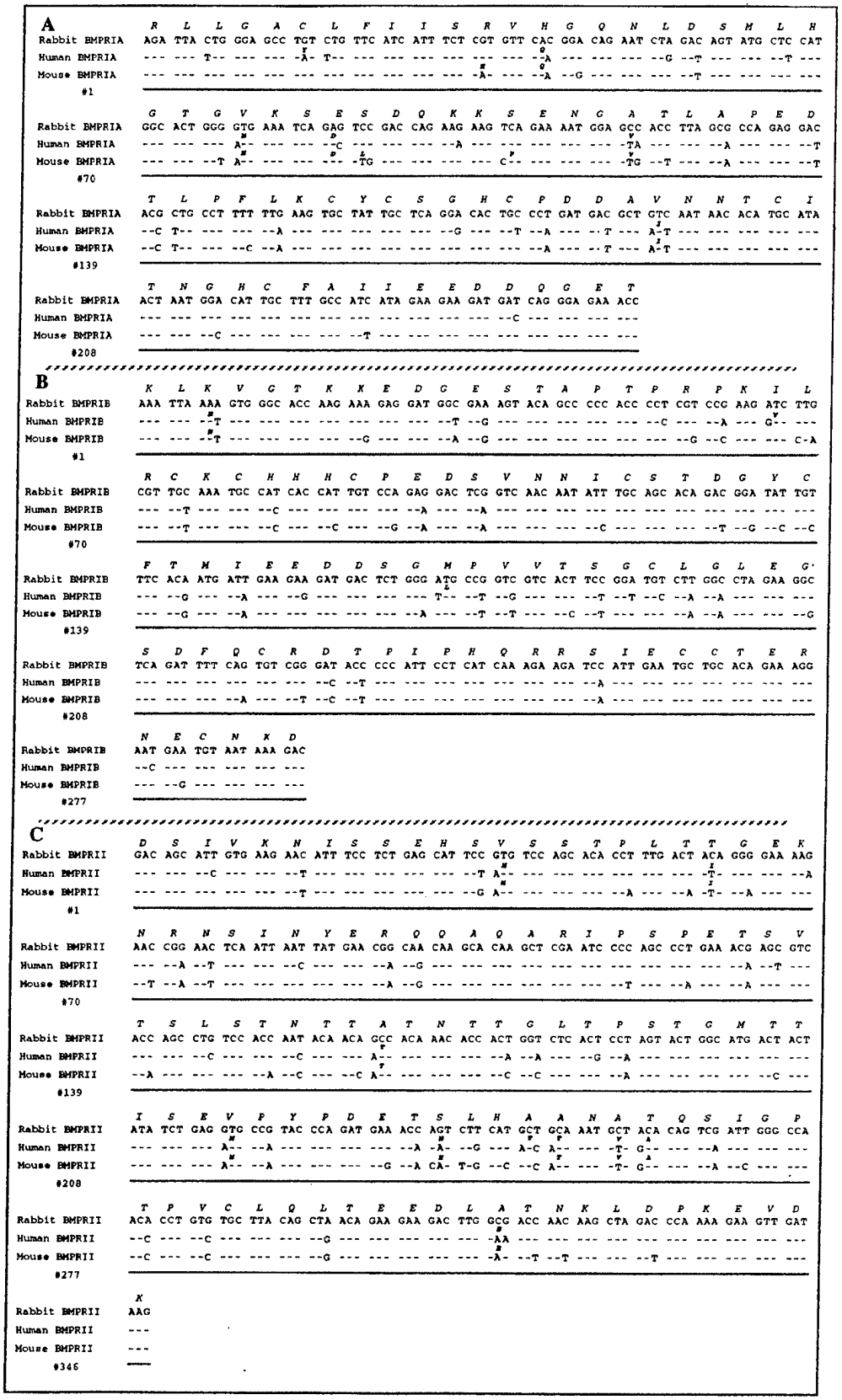

Fig. 2. Alignment of the rabbit (rb), human (hu), and mouse (m) partial cDNA sequences of BMPRIA (A), BMPRIB (B), and BMPRII (C). Identical nucleotides are indicated by dashes. The deduced amino acid sequence of the rabbit-specific cDNA is shown on top of the rabbit nucleotide sequence in italics. The amino acids that distinguish mouse and human homologues from the rabbit one are indicated (bold italics).

Table 1
Nucleotide sequences of the rabbit-specific primers used for specific amplification of segments of different mRNAs

cDNA		Primer sequence	Target size
BMPRIA	S	5′GTTCATCATTTCTCGTGTTCACGGA3′	209 bp
	AS	5′GGCAAAGCAATGTCCATTAGTTATG3′	
BMPRIB	S	5′GTGGGCACCAAGAAAGAGGATGG3′	246 bp
	AS	5′GGATCTTCTTTGATGAGGAATGGG3′	
BMPRII	S	5′CGTGTCCAGCACACCTTTGACTA3′	276 bp
	AS	5′AAGTCTTCTTCTGTTAGCTGTAAGC3′	
COLIIB[a]	S	5′GGGCCAGGATGTCCGGAAACCA3′	215 bp
	AS	5′CCAGGGGGGCCCGGATTTCCA3′	
GAPDH[b]	S	5′CTGGCCAAGGTCATCCACGAC3′	400 bp
	AS	5′GAGGAGTGGGTGGCACTGTTG3′	

[a] Sanyal et al. [20].
[b] Applequist et al. [1].

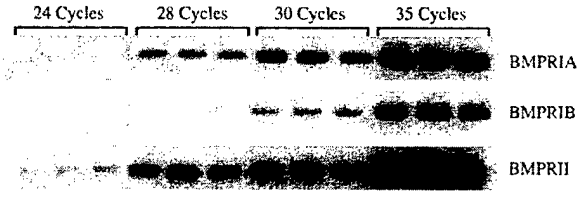

Fig. 3. Autoradiograms of agarose gels showing the expression of BMPRIA, BMPRIB and BMPRII mRNAs in native periosteum taken from the rabbits on day 0 and not cultured. PCR was performed on cDNAs from the explants (day 0) for different numbers of cycles for each mRNA in the presence of ^{32}P dCTP. The radioactive products were electrophoresed, in triplicate, on agarose gels, dried under vacuum, then imaged by autoradiography.

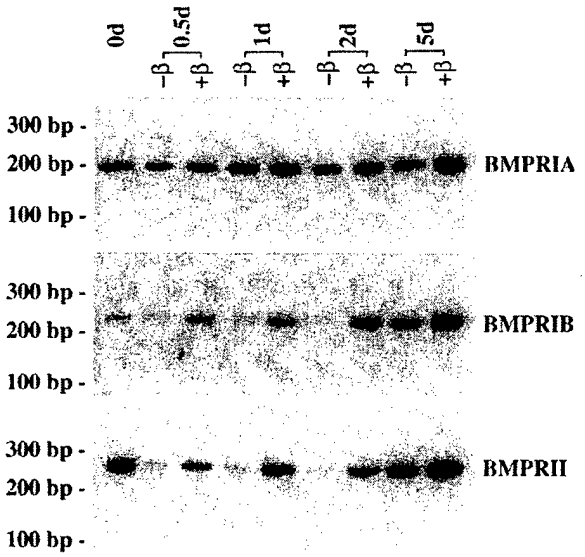

Fig. 4. Autoradiograms of agarose gels showing expression of BMPRIA, BMPRIB and BMPRII mRNAs early during periosteal chondrogenesis in the absence (−β) or presence (+β) of TGF-β1 (added only for the first two days). cDNAs from periosteal explants, cultured in agarose for the first 5 days, were used for the amplification of the three BMP receptor mRNAs by PCR for 30 cycles with the corresponding rabbit-specific primers in the presence of ^{32}P dCTP. The radioactive products were electrophoresed in agarose gels, dried under vacuum followed by autoradiography. The results show upregulation of all three mRNAs during periosteal chondrogenesis and the process is enhanced by TGF-β1.

The expression of BMPRIA, IB and BMPRII mRNAs were examined by RT-PCR on RNAs prepared from these explants. Expressions of GAPDH mRNA, an internal control to monitor the quality of the cDNA preparations, and collagen type IIB mRNA, a marker for articular cartilage, were also examined. Our results show that levels of BMPRIB mRNAs were upregulated, reached a peak on day 5 and then markedly down regulated (Fig. 5). In fact, BMPRIB mRNAs were barely detected by day 21. Expression of BMPRII mRNAs, however reached a peak between day 5 and day 10 and persisted at an elevated level for the rest of the time periods tested (Fig. 5). The pattern of expression of BMPRIA mRNA was closer to that of BMPRII than that of BMPRIB. Collagen type IIB mRNAs were expressed predominantly from day 10 onwards, indicating the onset of chondrogenesis in periosteal explants (Fig. 5).

Discussion

BMPs exert their influences through a BMP-specific receptor complex [8,9]. As is the case with the prototype TGF-β, BMPs bind to the type II receptor subunit, causing complexing and phosphorylation of a type I subunit. This activates signal transduction and biological effects. Unlike TGF-β, there are two type I isoforms capable of activating BMP signaling. Data suggest that BMPRIA and IB play distinct roles in limb development. By transfecting chicken embryos with kinase defective and constitutively active BMPRIA and

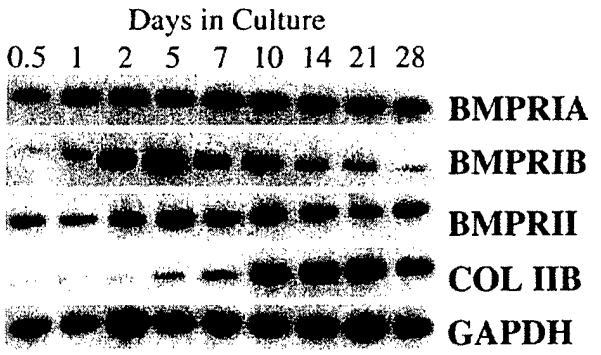

Fig. 5. Time courses of expression of three BMP receptor mRNAs compared to that for collagen type IIB and GAPDH mRNAs during periosteal chondrogenesis in the presence of TGF-β1. PCR was performed for 30 cycles with rabbit-specific primers (col IIB primers were annealed at 72°C) for each mRNA using cDNAs from explants, cultured in agarose for 0.5–28 days. TGF-β1 was added to the medium only for the first two days. The radioactive products were electrophoresed in agarose gels, dried under vacuum followed by autoradiography. BMPRIB mRNA, unlike BMPRIA and BMPRII mRNAs, was expressed mainly before collagen type IIB mRNA.

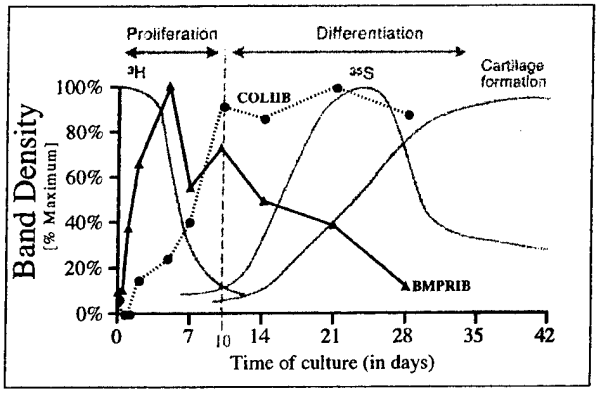

Fig. 6. Relationship of BMPRIB and collagen IIB mRNA expression in our proposed model of chondrogenesis [13]. Densitometric analysis from Fig. 5 was calculated as the percentage of maximum intensity for each time point examined. These were overlayed on profiles of proliferation as determined by ^{3}H thymidine incorporation, sulfation as determined by ^{35}S incorporation, and cartilage formation as determined by histomorphometry.

BMPRIB, Zou et al. [32] have demonstrated that these two receptors function distinctly during chick limb development. While BMPRIA regulated chondrocyte differentiation, BMPRIB was required for the initial steps of chondrogenesis and mediated programmed cell death. Expression studies of the two type I receptors using in situ and immunohistochemistry also support distinct roles of BMPRIA and BMPRIB during embryonic development. While BMPRIB is expressed in the precartilage condensations, BMPRIA is expressed in the rapidly growing loose mesenchymal cells surrounding the precartilaginous condensations [2] and in the prehypertrophic zone [32]. Interestingly, Volk et al. have utilized dominant negative BMPRs and shown that BMPR IB blocked BMP-induced hypertrophy more effectively than BMPRIA in upper sternal chondrocytes [28].

In our system, BMP2 mRNA is upregulated within 12 h and is barely detected after 14 days of culture during periosteal chodrogenesis [23]. As a result of this observation, we have sought to elucidate the expression patterns of the components of the BMP receptor complex during this process. Isolation of rabbit-specific partial cDNA sequences of the three types of BMP receptor mRNAs was a prerequisite for our investigation. The cDNA sequences, obtained by gene-digging, showed strong homologies at both nucleotide and amino acid level to the corresponding cDNAs of other species, suggesting the acquisition of rabbit homologues of those mRNAs.

Examination of the short-term culture of explants reveals that BMPRIA mRNA is expressed and the level increases gradually, but this increase is slight. Moreover, TGF-β, which greatly stimulates chondrogenesis, has only modest influences on the expression of BMPRIA. This suggests that, while BMPRIA may be important in chondrogenesis in this system, its expression is not sufficient to produce extensive cartilage. In contrast to BMPRIA, BMPRIB mRNA is expressed at low levels initially, then rise by day 5 of culture. However, its expression is elevated with TGF-β treatment within 12 h. BMPRII mRNA levels, while high in uncultured tissue, fall rapidly in the absence of TGF-β. Intriguingly, TGF-β appears to maintain BMPRII mRNA expression with a gradual rise by day 5. Even in the absence of TGF-β, explant expression of BMPRII mRNA is elevated by day 5 of culture.

When periosteum was cultured in conditions conducive to chondrogenesis (in the presence of TGF-β1), the expression of BMPRIB mRNA was upregulated within the first 24 h of culture. While the expressions of BMPRIA and BMPRII mRNAs persisted over a prolonged period of time, the expression of BMPRIB was barely detectable beyond day 14. Upregulation of BMPRIB mRNA by TGF-β1 in chondrogenesis is not unprecedented. TGF-β1 implanted into the interdigital mesoderm of chick embryo induces ectopic extra digits and this chondrogenesis is preceded by the expression of BMPRIB [10].

Fig. 6 presents relative densitometric intensities of the mRNAs for collagen type IIB and BMPRIB from Fig. 5 in relationship to proliferation, ^{35}S incorporation, and cartilage formation profiles in our model [13]. Since BMP2 mRNA increases within 12 h of culture, the relatively constant expression of BMPRIA and BMPRII mRNAs prior to the elevation in BMPRIB suggests that early BMP2 influences are likely to include promotion of chondrocyte differentiation. Once BMPRIB appears,

influences of BMP2 may expand to include initiation of chondrogenesis and induction of apoptosis. Our preliminary data demonstrates that apoptotic cells begin to appear in our model by week two, suggesting a role of BMPRIB in mediating this process (unpublished observations). During limb outgrowth, BMP2 antagonizes the proliferative effects of fibroblast growth factor on mesenchymal cells [11]. The timing of the appearance of BMP2 and its cognate receptors relative to proliferation in our model supports the possibility that BMP2 may function similarly in chondrogenesis. Collagen type IIB mRNA, a marker for matrix-depositing chondrocytes, is expressed mainly from day 7 onwards, indicating a time point when osteochondroprogenitor cells in periosteum are differentiated into chondrocytes [20]. BMPRIB mRNA is expressed mainly before the appearance of collagen type IIB mRNA, supporting the possible role of BMPRIB in chondrogenesis. By 21 days in culture, ^{35}S incorporation peaks in conjunction with the expression of collagen protein, followed by cartilage formation, which rises rapidly between days 21 and 35 [13]. This profile suggests a potential coordinate expression of BMP2 and its receptors in modulating early events during periosteal chondrogenesis. The data presented in this study open up interesting possiblilities regarding the roles of coordinate expression of BMPs and their receptors, but it is clear that any firm conclusion as to their respective roles will require more definitive examination. Thus, studies blocking the expression of BMPRIA, BMPRIB, and BMP2 with subsequent analysis for periosteal chondrogenesis inhibition are necessary to prove this unequivocally. Since BMPRIB has been found to be expressed in precartilaginous condensation zones in the developing limb, and its expression precedes collagen type II expression [32], we suggest the existence of similar regulatory mechanisms for both embryonic and periosteal chondrogenesis.

Periosteum contains undifferentiated mesenchymal cells, with both osteogenic and chondrogenic potential in its cambium layer [13]. It is unknown neither how and when these cells are committed to become chondrocytes. Our observations of upregulation of mRNAs for BMP2 and for components of the BMP receptor complex during periosteal chondrogenesis may help in elucidating this commitment step. Understanding this initial event will be important not only for improving cartilage repair by autologous periosteal transplantation but also for callus (cartilage) formation during fracture healing.

Acknowledgements

This work was funded by National Institute of Health Grant AR43890. We thank Dr. Gobinda Sarkar for his valuable comments and suggestions.

References

[1] Applequist SE, Keyna U, Calvin MR, Beck-Engeser GB, Raman C, Jack HM. Sequence of the rabbit glyceraldehyde-3-phosphate dehydrogenase-encoding cDNA. Gene 1995;163:325–6.

[2] Dewulf N, Verschueren K, Lonnoy O, Moren A, Grimsby S, Spiegle K, Miyazono K, Huylebroeck D, ten Dijke P. Distinct spatial and temporal expression patterns of two type I receptors for bone morphogenetic proteins during mouse embryogenesis. Endocrinology 1995;136:2652–63.

[3] Hogan BLM. Bone morphogenetic proteins:multifunctional regulators of vertebrate development. Genes Dev 1996;10:1580–94.

[4] Ide H, Katoh M, Sasaki H, Yoshida T, Aoki K. Cloning of human bone morphogenetic protein type IB receptor (BMPRIB) and its expression in prostate cancer in comparison with other BMPRs. Oncogene 1997;14:1377–82.

[5] Kawabata M, Chytil A, Moses H. Cloning of a novel type II serine/threonine kinase receptor through interaction with the type I transforming growth factor-β receptor. J Biol Chem 1995; 270:5625–30.

[6] Koenig B, Cook J, Wolsing D, Ting J, Thiesmann J, Correa P, Olson C, Pecquet A, Ventura F, Grant R, Chen G-X, Wrana J, Massague J, Rosenbaum J. Characterization and cloning of a receptor for BMP-2 and BMP-4 from NIH3T3 cells. Mol Cell Biol 1994;14:5961–74.

[7] Mankin HJ, Mow VC, Buckwalter JA, Iannotti JP, Ratcliffe A. Form and function of articular cartilage. In: Simon SR, editor. Orthopaedic basic science. American Academy of Orthopedic Surgeons, Rosemont, IL; 1994. p. 1–44.

[8] Massagué J. TGF-β signaling: receptors, transducers, and mad proteins. Cell 1996;85:947–50.

[9] Massagué J, Weis-Garcia F. Serine/threonine kinase receptors: mediators of transforming growth factor beta family signals. Cancer Surv 1996;27:41–64.

[10] Merino R, Ganan Y, Macias D, Economides A, Sampath K, Hurle J. Morphogenesis of digits in the avian limb is controlled by FGFs, TGF-βs and Noggin through BMP signaling. Dev Biol 1998;200:35–45.

[11] Niswander L, Martin GR. FGF-4 and BMP-2 have opposite effects on limb growth. Nature 1993;361:68–71.

[12] Nohno T, Ishikawa T, Saito T, Hosokawa K, Noji S, Wolsing DH, Rosenbaum JS. Identification of a human type II receptor for bone morphogenetic protein-4 that forms differential heteromeric complexes with bone morphogenetic protein type I receptors. J Biol Chem 1995;270:22522–6.

[13] O'Driscoll S. Articular cartilage regeneration using periosteum. Clin Orthop 1999;367(Suppl):186–203.

[14] O'Driscoll S, Recklies A, Poole A. Chondrogenesis in periosteal explants. An organ culture model for in vitro study. J Bone Joint Surg 1994;76A:1042–51.

[15] O'Driscoll SW, Keeley FW, Salter RB. The chondrogenic potential of free autogenous periosteal grafts for biological resurfacing of major full-thickness defects in joint surfaces under the influence of continuous passive motion. An experimental investigation in the rabbit. J Bone Joint Surg 1986;68A:1017–35.

[16] O'Driscoll SW, Salter RB. The induction of neochondrogenesis in free intra-articular periosteal autografts under the influence of continuous passive motion. An experimental investigation in the rabbit. J Bone Joint Surg 1984;66A:1248–57.

[17] O'Driscoll SW, Salter RB. The repair of major osteochondral defects in joint surfaces by neochondrogenesis using autogenous osteoperiosteal grafts stimulated by continuous passive motion. An experimental investigation in the rabbit. Clin Orthop 1986; 208:131–40.

[18] Rubak JM. Reconstruction of articular cartilage defects with free periosteal grafts. An experimental study. Acta Orthop Scand 1982;53:175–80.
[19] Ruberte E, Marty T, Nellen D, Affolter M, Basler K. An absolute requirement for both the type II and type I receptors, punt and thick veins, for dpp signaling in vivo. Cell 1995;80:889–97.
[20] Sanyal A, Davis C, Sarkar G, O'Driscoll S. Temporal pattern of expression of collagen type IIA and IIB mRNAs during the early stages of periosteal chondrogenesis (Abstract). Trans Orthop Res Soc 1999;24:687.
[21] Sanyal A, O'Driscoll S, Bolander M, Sarkar G. An effective method of completely removing contaminating genomic DNA from an RNA sample to be used for PCR. Mol Biotechnol 1997;8:135–7.
[22] Sanyal A, O'Driscoll S, Fitzsimmons J, Bolander M, Sarkar G. Gene-digging: a method for obtaining species-specific sequence based on conserved segments of nucleotides in open reading frames. Mol Biotechnol 1998;10:223–30.
[23] Sanyal A, Sarkar G, Saris D, Fitzsimmons J, Bolander M, O'Driscoll S. Initial evidence for the involvement of Bone Morphogenetic Protein-2 early during periosteal chondrogenesis. J Orthop Res 1999;17:926–34.
[24] Takeda K, Oida S, Ichijo H, Iimura T, Maruoka Y, Amagasa T, Sasaki S. Molecular cloning of rat bone morphogenetic protein (BMP) type IA receptor and its expression during ectopic bone formation induced by BMP. BBRC 1994;204:203–9.
[25] ten Dijke P, Ichijo H, Franzen P, Schultz P, Saras J, Toyoshima H, Heldin C-H, Miyazono K: Activin receptor-like kinases: a novel subclass of cell surface receptors with predicted serine/threonine kinase activity. Oncogene 1993;8:2879–87.
[26] ten Dijke P, Yamashita H, Sampath T, Reddi A, Estevez M, Riddle D, Ichijo H, Heldin C-H, Miyazono K: Identification of type I receptors for osteogenic protein-1 and bone morphogenetic protein-4. J Biol Chem 1994;269:16985–8.
[27] ten Dijke P, Yamashita M, Ichijo H, Franzen P, Laiho M, Miyazono K, Heldin C-H. Characterization of type I receptors for transforming growth factor-β and activin. Science 1994;264:101–4.
[28] Volk SW, D'Angelo M, Diefenderfer D, Leboy PS. Utilization of bone morphogenetic protein receptors during chondrocyte maturation [In Process Citation]. J Bone Miner Res 2000;15:1630–9.
[29] Wang EA, Rosen V, Cordes P, Hewick RM, Kriz MJ, Luxenberg DP, Sibley BS, Wozney JM. Purification and characterization of other distinct bone-inducing factors. Proc Natl Acad Sci USA 1988;85:9484–8.
[30] Wang EA, Rosen V, D'Alessandro JS, Bauduy M, Cordes P, Harada T, Israel DI, Hewick RM, Kerns KM, LaPan P, Luxenberg DP, McQuaid D, Moutsatsos IK, Nove J, Wozney JM. Recombinant human bone morphogenetic protein induces bone formation. Proc Natl Acad Sci USA 1990;87:2220–4.
[31] Wozney JM, Rosen V, Celeste AJ, Mitsock LM, Whitters MJ, Kriz RW, Hewick RM, Wang EA. Novel regulators of bone formation: molecular clones and activities. Science 1988;242:1528–34.
[32] Zou H, Wieser R, Massague J, Niswander L. Distinct roles of type I bone morphogenetic protein receptors in the formation and differentiation of cartilage. Genes Dev 1997;11:2191–203.

ELSEVIER

Journal of Orthopaedic Research 20 (2002) 562–574

Journal of Orthopaedic Research

www.elsevier.com/locate/orthres

The spatiotemporal expression of TGF-β1 and its receptors during periosteal chondrogenesis in vitro

Hiroshi Mizuta [a,b], Arunik Sanyal [a], Takumi Fukumoto [a,b], James S. Fitzsimmons [a], Nobuzo Matsui [a], Mark E. Bolander [a], Merry Jo Oursler [c], Shawn W. O'Driscoll [a,*]

[a] *Department of Orthopedics, Cartilage and Connective Tissue Research Laboratory, Mayo Clinic, Mayo Foundation, 200 First Street SW, MS 3-69, Rochester, MN 55905, USA*

[b] *Department of Orthopaedic Surgery, Kumamoto University School of Medicine, Kumamoto, Japan*

[c] *Departments of Biology, Medical Microbiology and Immunology, and Biochemistry and Molecular Biology, University of Minnesota, Duluth, MN, USA*

Received 20 September 2000; accepted 29 August 2001

Abstract

Transforming growth factor-β1 (TGF-β1) has been shown to stimulate chondrogenesis in periosteal explants cultured in agarose suspension. TGF-βs exert their cellular effects through a heteromeric cell membrane receptor complex consisting of TGF-β type I and type II receptors. In this study, the spatial and temporal expressions of the type I receptor (TβR-I), type II receptor (TβR-II) and endogenous TGF-β1 in periosteal explants cultured in vitro were examined using reverse transcription polymerase chain reaction (RT-PCR) and immunohistochemistry. The temporal changes in the expression of the TβR-I and TβR-II mRNAs correlated with that of TGF-β1. Exogenous administration of TGF-β1 upregulated the expression of both receptors and of the TGF-β1 ligand in a biphasic pattern. The earlier peak of upregulation was observed at 7 days in culture. A later peak of upregulation was seen at 42 days, at which time cartilage formation reached a maximum. Immunohistochemical studies demonstrated co-localization of TβR-I and TβR-II simultaneously among the same cells expressing TGF-β1. TGF-β1 treatment increased the expression of TGF-β1, TβR-I and TβR-II in mesenchymal cells in the cambium layer at 7 days in culture. Small round chondrocytes showed widely distributed immunoreactivity of TGF-β1, TβR-I and TβR-II in the 42-day explants treated with TGF-β1. These observations support the hypothesis that TGF-β1 regulates the initiation and formation of cartilage during periosteal chondrogenesis.

Introduction

Recent advances concerning cell-based and tissue-based methods for biological repair of damaged articular cartilage have evoked tremendous interest among clinicians, scientists and industry. Autologous periosteal transplantation is one such method under investigation for the repair of defects in articular cartilage [8,9,13,19,20,26,33,38,40–45,52,53,64]. Periosteum contains undifferentiated mesenchymal stem cells and periosteal grafting has been shown to be capable of producing new cartilage in animal experiments [42,52,61] and clinical studies [13,26,38]. A thorough understanding, which presently is only elementary, of the molecular and cellular events in this process would, therefore, be helpful in optimizing cartilage formation for the repair of a damaged joint surface.

An organ culture model system has been established to study periosteal chondrogenesis in vitro [41]. In this model periosteal explants from rabbit tibiae produce cartilage when cultured in agarose suspension. This process is significantly enhanced by exogenously added Transforming growth factor-β1 (TGF-β1) [31,41]. To date, the location of the cells in the periosteum that are responsive to TGF-β have not been identified nor have the mechanisms of action of TGF-β. Achieving these steps would clarify how periosteal chondrogenesis might be regulated and optimized for cartilage repair.

TGF-β1 is a multifunctional polypeptide that regulates a variety of biological functions, including cell proliferation, differentiation, and extracellular matrix synthesis [30,58,59]. In previous in vitro and in vivo studies, TGF-β1 has been implicated as a critical regulatory molecule in a sequence of events during

* Corresponding author. Tel.: +1-507-284-2763; fax: +1-507-284-3826.

E-mail address: odriscoll.shawn@mayo.edu (S.W. O'Driscoll).

0736-0266/02/$ - see front matter
PII: S0736-0266(01)00130-9

chondrogenesis, but the mechanistic basis of this regulation has not been fully elucidated [23]. In our organ culture model, enhancement of periosteal chondrogenesis by TGFβ1 was identical when 2 days of treatment with TGF-β1 was compared to 14 days of treatment [32]. In addition, brief exposure to TGF-β1 for just 30 min at the initiation of the culture period induced a 300% increase in the amount of cartilage that the explants formed during 6 weeks in culture [33]. These findings suggest that TGF-β1 may trigger a cascade of processes regulated by autocrine/paracrine mechanisms during periosteal chondrogenesis that can be induced at an early stage.

Recent studies have demonstrated that TGF-βs exert their effects by forming a heteromeric complex with two distinct transmembrane serine/threonine kinase receptors called type I and type II receptors [3,4,28]. TGF-βs bind directly to the extracellular domain of the TGF-β type II receptor (TβR-II). The TGF-β type I receptor (TβR-I) then binds to the ligand-bound TβR-II, and is phosporylated by TβR-II, resulting in the initiation of the intracellular TGF-β signal transduction [5,37,66]. The presence of these receptors is obviously a prerequisite for TGF-β to exert its regulatory function. Therefore, identification and localization of these receptors will permit a better understanding of the role and mechanisms of TGF-βs function.

As a first step in addressing the molecular mechanisms involved in the regulatory function of TGF-β1 during periosteal chondrogenesis, we investigated the expression of TβR-I and TβR-II, as well as the expression of endogenous TGF-β1 with use of a previously established organ culture model.

Materials and methods

Periosteal explants and tissue cultures

A total of 320 periosteal explants were obtained from 40 2-month-old New Zealand White rabbits weighing an average of 1.75 kg. Each animal was given a lethal injection of sodium pentobarbital. The leg was then shaved, prepared, draped, and exposed in a sterile manner. All periosteal explants were obtained within 30 min after death. From each rabbit, 8 (2 × 3 mm) explants were taken from the proximal media tibia by subperiosteal dissection with a sharp periosteal elevator. These 8 explants were assigned to be cultured for 8 different time periods, as described below, so that the rabbits were controlled for as a variable.

The culture conditions were as reported in the periosteal agarose explant model by O'Driscoll, et al. [41]. Once harvested, the explants were suspended in 1 ml of a 1:1 mixture of 1.0% low Tm agarose gel (Bio-Rad Laboratories) and ×2 normal concentration DMEM (12100-046; Life Technologies, Grand Island, NY, USA). Once the agarose had solidified, it was layered with 1.0 ml of "nutrient" media consisting of DMEM with 10% fetal bovine serum (Life Technologies), 1 mM proline (an essential protein for type II collagen production) (Sigma Chemical, St. Louis, MO, USA), penicillin/streptomycin (50 U/ml and 50 μg/ml) (15145-014; Life Technologies), 50 μg/ml ascorbic acid and 10 ng/ml TGF-β1. The control explants were cultured in an identical fashion but without the addition of TGF-β1.

The medium above the gel layer was replaced every other day with nutrient media as described above. No TGF-β was added after the second day. In other words, the explants that were treated with TGF-β1 were exposed to it only for the first 48 h. Vitamin C, 25 μg/ml, was added daily to each well. The cultures were maintained at 37 °C and 5% carbon dioxide mixed with room air.

Seventeen to twenty explants treated with and without TGF-β1, respectively, were removed from culture on each of the following days: 2, 5, 7, 14, 21, 28, 42, and 56. Twelve explants from each time point were randomly selected for analysis of gene expression and the remainder was analyzed histologically and immunohistochemically as described below.

Total RNA extraction and cDNA preparation

Total RNA from 192 of the aforementioned 320 cultured periosteal explants (12 explants per time point) was extracted as previously described [54]. A single pool of total RNA was obtained for each time point and TGF-β treatment (i.e., 16 total RNA pools in all). From each of these total RNA pools 2 pools of first strand cDNA were synthesized by reverse transcription [54]. Synthesized cDNA (20 μl) was diluted with 30 μl of 1×TE (10 mM Tris-HCl, 0.1 mM EDTA) and stored at −20 °C.

Polymerase chain reaction

Polymerase chain reaction (PCR) was carried out in a 20 μl reaction mixture 10 mM Tris-HCl (pH 8.3), 50 mM KCl, 1.5 mM $MgCl_2$, 200 μM dNTPs, 2 pmol of each primer, 1 μl of cDNA and 0.5 units of AmpliTaq DNA polymerase. Amplification was carried out with initial denaturation for 5 min at 94 °C followed by 35 cycles of annealing at 50 °C (or as described in the figure legends) for 2 min, elongation at 72 °C for 3 min and denaturation at 94 °C for 1 min. Quantitative PCRs were carried out in the presence of 2 μCi of α^{32}P dCTP. The number of cycles used for the PCRs were confirmed to be in the log phase of the amplifications (data not shown).

Isolation of rabbit-specific partial cDNA sequences

Partial cDNA sequences were isolated using the method of gene digging as described before [55]. In this method rabbit liver cDNA was used as a template for PCR with 5'S (sense) and 3'AS (antisense) primers. The product of the 1st round of PCR was used as a template for nested PCR using one of these 5'S or 3'AS primers and an internal primer. Both 1st round and nested PCRs were performed using the same parameters as described above. For the isolation of rabbit-specific TGF-β1 cDNA sequence the primers were chosen based on conserved nucleotide sequences between human, mouse, rat and chicken. The primers were:

5'S primer CCT(G/C)GA(T/C)ACC(A/G)ACTA(T/C)TGCTT
3'AS primer GCTGCACTTGCAGG(A/C)(A/G)CG
and an internal 3'AS primer ATGTTGGA(G/C)A(A/G)CTGCTC-CAC.

For the TβR-I, the primers, designed based on conserved nucleotide sequences between mouse and human, the primers were:

5'S primer CCACAGAGT(A/G)GG(C/A)AC(T/A)AAAAGG
3'AS primer TTACATTTTGATGCCTTCCTGTTG
and an internal 5'S primer CCTGAAGTTT(A/C)GATGATTC-CAT.

For the TβR-II the 1st round PCR amplified the product to a detectable and analyzable level. For isolating the sequence of this gene the primers, chosen based on the conserved nucleotide sequences between human and chicken, were:

5'S primer TGCA(A/T)GAGCAACTGCA(A/G)CAT
3'AS primer TCAS(A/C)(T/G)CTACAGGAACACATGAA.

In each case, the products were electrophoresed on agarose gel and the desired bands were excised and eluted using the Wizard™ Kit (Promega, Madison, WI) and sequenced by direct automated sequencing using the same primers that had been used for PCR.

Noncompetitive quantitative PCR

Noncompetitive quantitative PCR was performed by coamplifying the desired segments of the mRNAs of the target gene and the glyceraldehyde-3-phosphate dehydrogenase (GAPDH) gene (an endogenously expressed gene as an internal reference) using rabbit-specific

primers for both genes under conditions as described above. The rabbit-specific primers, used for amplifying a segment of TGF-β1 mRNA, were as follows:
5′S primer CTTCCGCAAGGACCTGGG
3′AS primer CGGGTTGTGCTGGTTGTAC.
The rabbit-specific primers, used for amplifying a segment of TβR-I mRNA, were:
5′S primer GAATCCTTCAAACGTGCTGACATC
3′AS primer CCATTGGCATACCAACATTCTCTC.
The rabbit-specific primers, used for amplifying a segment of TβR-II mRNA, were:
5′S primer CAACTGCAGCATCACGTCCATCT
3′AS primer TACAGGAACACATGAAGAAAGTCTC.
The rabbit-specific primers, used for amplifying a segment of GAPDH mRNA [1], were:
5′S primer CTGGCCAAGGTCATCCACGAC
3′AS primer GAGGAGTGGGTGGCACTGTTG.

Quantitation of the radioactive amplified products

The amplified products from noncompetitive quantitative PCRs (i.e., the first strand cDNA pools) were electrophoresed on agarose gels which were then dried under vacuum and the radioactive bands were quantitated using a phosphorimager (Molecular Dynamics, Sunnyvale, CA) [7]. Each cDNA pool was assayed three times in this manner.

Histology and immunohistochemical analysis

The explants were fixed in 10% formalin and embedded in paraffin. Serial sections 3 μm thick were prepared for routine histological, histochemical staining with safranin O and fast green, and immunohistochemical analysis for TGF-β1, TβR-I, TβR-II and proliferating cell nuclear antigen (PCNA) using the Vectastain ABC kit (Vector Laboratories, Burlingame, CA). For immunohistochemical studies, polyclonal antibodies against synthetic peptides of human TβR-I and TβR-II were obtained from Santa Cruz Biotechnology (Santa Cruz, CA). TGF-βR-I (V-22) and TGF-βR-II (C-16) were used in this study. Immunostaining of rabbit kidney demonstrated specific patterns of tubular and glomerular epithelial staining, confirming antibody specificity for TβR-I and TβR-II [15] (data not shown). To assess the cellular expression of endogenous TGF-β1 in periosteal explants, polyclonal antibodies were used against human TGF-β1 LAP (i.e., the endogenously produced, inactive form of TGF-β1 bound to "latency-associated peptides" [10]) (R&D Systems). This was done so that latent TGF-β1 produced endogenously could be distinguished from the active form of TGF-β1 administrated for the first 2 days of culture. The specificity and cross-reactivity of this antibody to latent rabbit TGF-β1 was confirmed using rabbit growth plate [22] (data not shown). PCNA monoclonal antibodies were purchased from Sigma Chemical (St. Louis, MO).

The procedures for the immunostaining of TβR-I and TβR-II were performed using the primary–secondary antibody complex method designed by Gu, et al. [11] to permit the use of polyclonal antibodies raised in rabbit on rabbit tissue. In this method, the formation of primary and secondary antibody complex is performed prior to its application to tissue sections to avoid nonspecific binding of the secondary antibody to the endogenous rabbit IgG of the tissue. Briefly, the specific polyclonal antibodies (primary antibodies) were mixed with pre-diluted biotinylated goat-raised anti-rabbit secondary antibody (Vector) in Tris-buffered saline (TBS)/0.5% bovine serum albumin (BSA) to final dilutions of 1:150 for TβR-I and TβR-II, and incubated for 60 min at 37 °C. Nonimmune rabbit serum was then added to the mixture at a ratio of 1:100 and incubated for 60 min at 37 °C. The mixture was stored at 4 °C before applying it to the tissue sections. The tissue sections were deparaffinized and dehydrated. Endogenous peroxidase activity was blocked by incubation with 0.3% hydrogen peroxide in methanol for 60 min at room temperature, and the tissue sections were then treated with 500 U/ml hyaluronidase (Sigma Chemical, St. Louis, MO) for 30 min at 37 °C. Nonspecific immunoglobulin binding was blocked with 1.5% normal goat serum (Vector) in TBS/0.5% BSA for 15 min at room temperature. The above antibody mixtures were applied to the tissue sections which were then incubated overnight at 4 °C. Following extensive washing with TBS/0.1% BSA, the slides were incubated with avidin–biotin complex (Vector) for 30 min. Antibody binding was demonstrated by reacting the sections with a mixture of 0.5 mg/ml diaminobenzidine tetrahydrochloride (Sigma) in 50 mmol/l Tris-HCl buffer (pH 7.4) and 0.01% hydrogen peroxide for 4 min. The sections were dehydrated and mounted.

Immunostaining for TGF-β1 and PCNA was performed using the conventional ABC method. Sections were deparaffinized, dehydrated, and treated with 0.3% hydrogen peroxide in methanol. The sections were then treated with 500 U/ml hyaluronidase, as described earlier. Nonspecific staining was reduced by incubation with normal horse serum. The sections were incubated with PCNA monoclonal antibodies at a dilution of 1:400, or polyclonal antibodies against TGF-β1 at a dilution of 1:150 overnight at 4 °C, followed by incubation with biotinylated horse anti-mouse IgG and avidin–biotin complex and developed with diaminobenzidine tetrahydrochloride.

The immunohistochemical specificity of the reaction between antibodies against TβR-I and TβR-II and rabbit tissue was proven by absorption tests (data not shown). Each antiserum was pre-incubated with a ten-fold (by weight) excess of corresponding immunogenic peptide (Santa Cruz) overnight at 4 °C according to the manufacture's directions. After centrifugation at 4500 rpm for 10 min, the supernatant was used instead of primary antiserum. The specificity of the antibodies against TGF-β1 and PCNA was confirmed by substituting purified mouse IgG (Sigma) for the primary antibody.

Quantification of the immunohistochemical expression

Histomorphometric quantification of immunostaining for TGF-β1, TβR-I, TβR-II, or PCNA was performed by cell counting on three explants from each group. For this purpose, periosteal explants were analyzed by cambium layer, fibrous layer, and neocartilage region. In each region, three fields were selected at random under a magnification of 200×. Positive and negative cells were counted in each field, and the number of positive cells was divided by the total number of cells (the sum of positive and negative cells) to calculate the positive ratio in each field. The positive ratio for each tissue section was expressed as the mean of the positive ratio of the three fields. The measurements were carried out in three sections, and the average measurement obtained was used as the positive ratio. In cartilaginous tissues, chondrocytes were subclassified as flattened chondrocytes, small round chondrocytes (diameter less than 25 μm and thus expected to be less differentiated and more actively proliferating), or large round chondrocytes (diameter more than 25 μm and thus expected to be closer to terminal differentiation and less actively proliferating) based on their morphology and size [18]. The positive ratio was evaluated as negative or −/+ to 4+ according to the criteria described by Horner et al. [14].

Statistical analysis

All data were expressed as the mean ± one standard deviation. The gene expression data by PCR were analyzed using repeated measures analysis of variance (ANOVA) and post-hoc testing with Duncan's Multiple Range Test.

Results

Periosteal chondrogenesis in this organ culture model followed the same general time course as has been reported in our previous studies [34,41]. Briefly, in explants treated with TGF-β1 for the first 2 days, cartilage formation was observed by the fourth week, and increased during the period of culture, reaching a maximum at 42 days (Fig. 1(A)). In contrast, explants treated without TGF-β1 exhibited little cartilage up to the sixth week in culture (Fig. 1(B)).

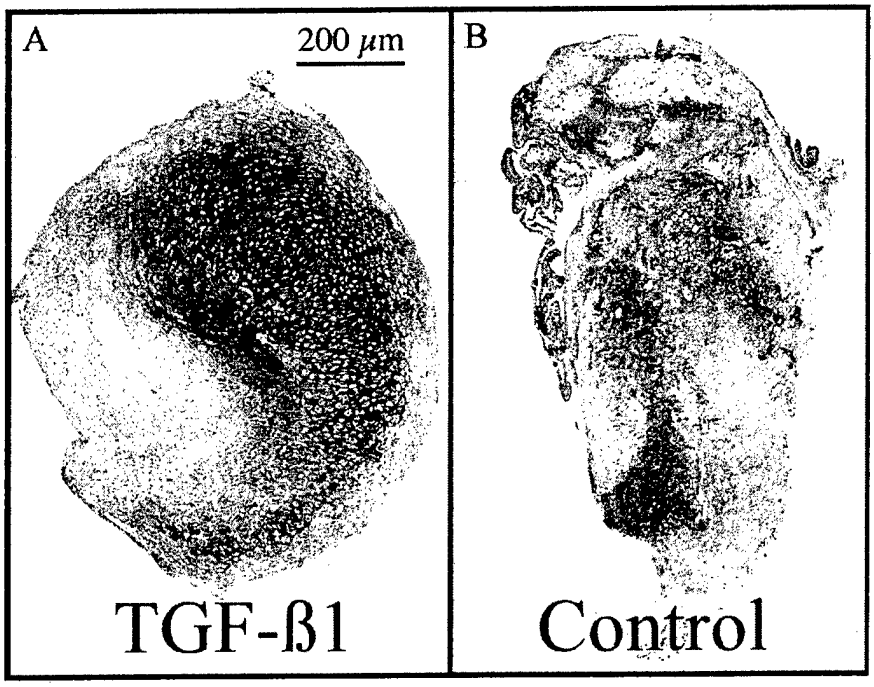

Fig. 1. Photomicrographs of periosteal explants after 42 days of culture in agarose (safranin O, ×50). (A) Representative histology of periosteal explant cultured with transforming growth factor-β1 (TGF-β1). (B) Representative histology of periosteal explant cultured without TGF-β1 (control).

Isolation of partial cDNA sequences of rabbit TGF-β1, TβR-I and TβR-II

Using rabbit liver cDNA as a template and primers based on human mouse and rat TGF-β1 cDNA sequences, we isolated a 246 bp fragment by PCR. Genebank accession number are as follows:

Mouse TGF-β type I receptor Accession No. L15436
Human TGF-β type I receptor Accession No. Z22534
Rat TGF-β type I receptor Accession No. L19341
Human TGF-β type II receptor Accession No. M85079
Mouse TGF-β type II receptor Accession No. D32072
Rat TGF-β type II receptor Accession No. L09653
Chicken TGF-β type II receptor Accession No. L18784.

This fragment is homologous to human (92.7%) and mouse (90.3%) TGF-β1 cDNA sequences, confirming the isolation of a partial cDNA sequence of rabbit TGF-β1 (Fig. 2(B)). The isolation of a 320 bp fragment for TβR-I and a 214 bp fragment for TβR-II, was performed using primers chosen from the corresponding human, mouse and chicken cDNAs. The 320 bp fragment was homologous to human (96.3%) and mouse (92.9%) TGF-β type I receptor cDNA sequences (Fig. 2(B)) while the 214 bp fragment was 84.4% homologous to both human and mouse TGF-β type II cDNA sequences (Fig. 2(C)). These data confirmed the isolation of partial rabbit-specific cDNA sequences for the corresponding genes. Based on these isolated sequences we then designed rabbit-specific primers for TGF-β1, TβR-I and TβR-II mRNAs. These primers were used to specifically amplify the corresponding mRNAs as determined by the direct sequencing of the amplified products (data not shown).

Expression patterns of mRNAs for TGF-β1, TβR-I and TβR-II during periosteal chondrogenesis

Next we examined the patterns of expression of the mRNAs for TGF-β1 ligand and its receptors, TβR-I and TβR-II, during periosteal chondrogenesis. We cultured periosteal explants in agarose with and without exogenous TGF-β1 added for the first 48 h of culture in the presence of FBS for different periods of time from 2 to 56 days. The expressions of the aforementioned mRNAs were measured on cDNAs prepared from these explants (containing both fibrous and cambium layers) by noncompetitive quantitative PCR. The mRNAs for TGF-β1, TβR-I and TβR-II were detected in periosteal explants treated with or without TGF-β1 at all the time points tested (Fig. 3). The expression patterns of these three genes are presented in Fig. 4. The most dramatic difference between the explants treated with TGF-β and the untreated controls was a delayed but very significant rise in the mRNA expression levels of TGF-β, TβR-I, and TβR-II at 42 days in the TGFβ1 treated explants.

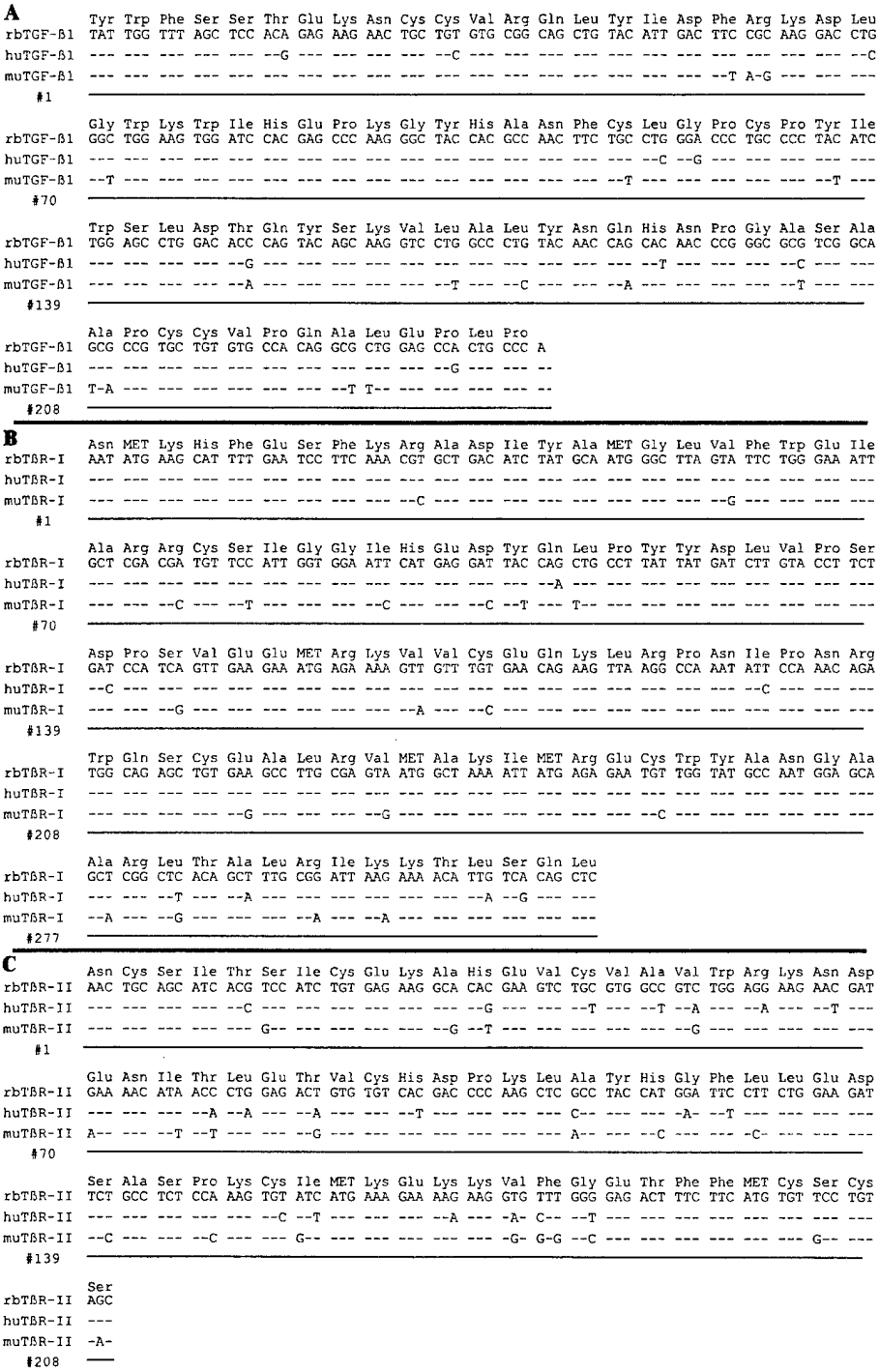

Fig. 2. Alignment of the rabbit (rb), human (hu) and mouse (mu) partial cDNA sequences of TGF-β1 (A), TβR-I (B) and TβR-II (C). Identical nucleotides are indicated by dashes. Deduced amino acid sequences are shown on top of the corresponding rabbit-specific cDNA sequences.

The temporal changes in expression of the TβR-I, TβR-II and TGF-β1 mRNAs correlated with each other. In the TGF-β1 treated explants, the expression of these genes showed a biphasic pattern with a small peak at 7 days and a significantly higher peak at 42 days ($p < 0.0001$). The only exception to this consistent pattern was that at day 7 the TβR-I mRNA rose from day 5 but did not demonstrate a true peak (Fig. 4(B)). In contrast, this biphasic pattern of change in gene expression over time was not seen in the absence of

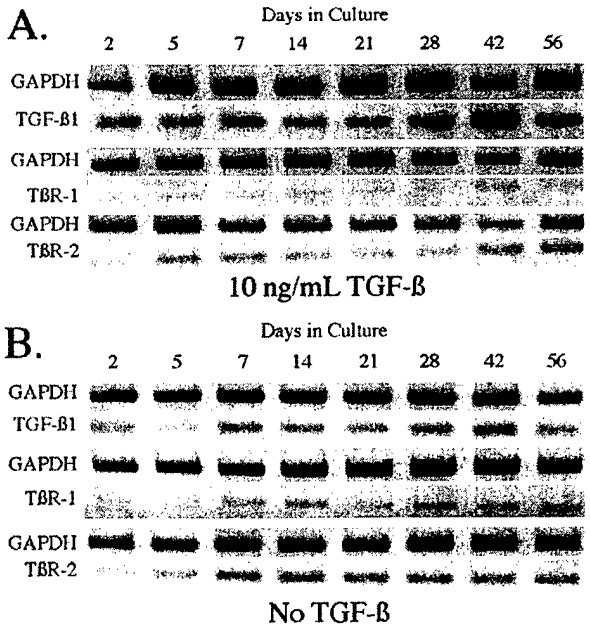

Fig. 3. Photographs of gels used for the analysis of PCR products. Representative gels from (A) explants treated with 10 ng/ml TGF-β1 and (B) explants cultured without TGF-β1. GAPDH = glyceraldehyde-3-phosphate dehydrogenase. TβR-I = TGF-β type I receptor. TβR-II = TGF-β type II receptor.

exogenous TGF-β1 treatment. Instead, from day 21 to day 56, there was a gradual increase in the expression of both TGF-1 ligand and TβR-II mRNA, with no identifiable change in the expression of TβR-I mRNA over time (Fig. 4). The endogenous TGF-β1 ligand mRNA levels were significantly higher in the explants that were treated with TGF-β1 than in the controls that were not exposed to TGF-β1 ($p < 0.0001$). At day 42, when cartilage formation reached a plateau, the mRNA levels for both TGF-β receptors, TβR-I and TβR-II, were significantly higher in those explants treated with TGF-β1 for the first 2 days in culture than in the controls not treated with TGF-β1 ($p < 0.0001$) (Fig. 4). The ratio of the expression of TGF-β1 mRNA in explants with TGF-β1 to that in the explants without TGF-β1 demonstrated a time-dependent biphasic upregulation of these genes upon TGF-β1 treatment with double peaking at 7 days and 42 days (Fig. 4(A)). Seven days after the initial exogenous TGF-β1 treatment, a 2.7 fold increase TGF-β1 expression was measured. At 42 days, in explants treated with TGF-β1, the relative gene expression of TGF-β1, and TβR-I was 3 times higher while the expression of TβR-II was 2 times higher than the expression of these same genes in the explants without exogenous TGF-β1 treatment. At day 56 no difference in gene expression was observed between explants treated with and without TGF-β.

Immunohistochemical localization of TGF-β1, and TGF-β receptors

The spatial patterns of expression of TGF-β1, TβR-I and TβR-II during periosteal chondrogenesis as determined by immunohistochemistry in vitro are summarized in Tables 1 and 2. The histomorphometry data enumerating the positively immunostained cells as a percentage of the total cells are summarized in Table 3 and Fig. 5. TGF-β1, TβR-I and TβR-II were detectable in the periosteal explants at all time points tested. TβR-I and TβR-II were simultaneously observed and generally co-distributed with those cells producing TGF-β1. In the first few days of agarose culture, endogenous TGF-β1, TβR-I and TβR-II were localized diffusely in both the cambium and fibrous layers, although a greater percentage was present in the fibrous layer compared to the cambium layer. However, by day 7, when the first peak was seen in the expression of TGF-β1, significant

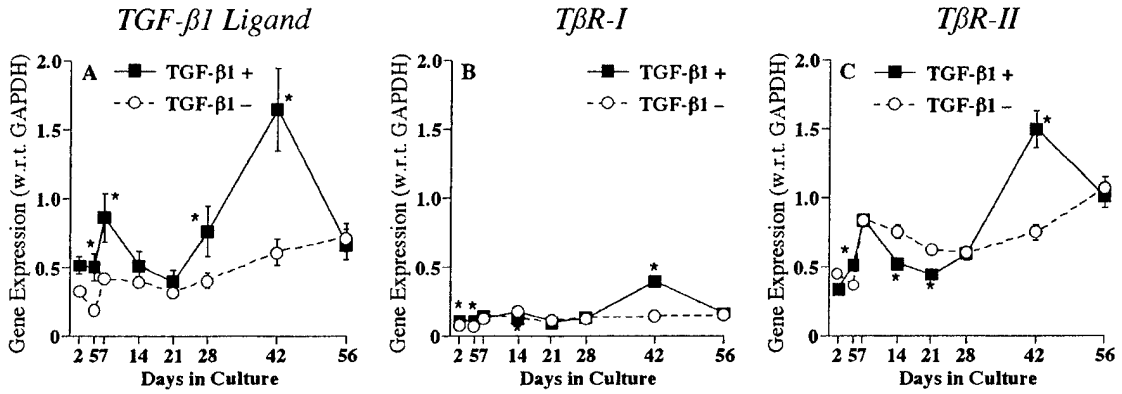

Fig. 4. The relative levels of mRNA expression (normalized to GAPDH) for TGF-β1 ligand, the type I receptor (TβR-I) and the type II receptor (TβR-II) in periosteal explants treated with TGF-β1 compared to those not treated with TGF-β1. A biphasic pattern of expression was observed in the explants treated with TGF-β1, but not in the control explants not treated with TGF-β1. Each specimen was evaluated in triplicate. The graph shows mean values ± S.D.

Table 1
Quantification of expression of proliferating cell nuclear antigen (PCNA), transforming growth factor-β1 (TGF-β1), TGF-β type I receptor (TβR-I) and TGF-β type II receptor (TβR-II) in periosteal explants cultured with TGF-β1

Days in culture	Tissue	PCNA	TGF-β1	TβR-I	TβR-II
2	Cambium	+	+	+	+
	Fibrous	+++	++	++	++
5	Cambium	+	+	+	+
	Fibrous	+++	++	++	+
7	Cambium	+++	+++	+++	+++
	Fibrous	+++	+++	+++	++
14	Cambium	+	+	+	+
	Fibrous	++	+	±	±
21	Cambium	++	+	+	+
	Fibrous	++	+	+	+
28	Fibrous	++	++	±	++
	Flattened	+	+	+	+
	Small round	++	++	+	++
42	Fibrous	++	+	±	±
	Flattened	+	+	±	+
	Small round	+++	+++	+++	+++
	Large round	++	+	+	+
56	Fibrous	+	+	+	+
	Flattened	±	+	+	+
	Small round	++	+	+	+
	Large round	+	+	+	+

The positive ratio was evaluated as follows: (−) no staining; (±) <5% cells stained; (+) 5–25% cells stained; (++) 25–50% cells stained; (+++) 50–75% cells stained; (++++) >75% cells stained. Cambium = cells in the cambium layer; fibrous = cells in the fibrous layer; flattened = flattened chondrocytes; small round = small round chondrocytes; large round = large round chondrocytes.

Table 2
Quantification of expression of proliferating cell nuclear antigen (PCNA), Transforming growth factor-β1 (TGF-β1), TGF-β type I receptor (TβR-I) and TGF-β type II receptor (TβR-II) in periosteal explants cultured without TGF-β1

Days in culture	Tissue	PCNA	TGF-β1	TβR-I	TβR-II
2	Cambium	+	+	+	+
	Fibrous	+++	++	+	+
5	Cambium	+	+	+	+
	Fibrous	+++	++	+	++
7	Cambium	+	+	+	+
	Fibrous	+++	+++	+++	++
14	Cambium	+	+	±	+
	Fibrous	++	+	+	+
21	Cambium	+	+	±	+
	Fibrous	++	++	±	+
28	Cambium	++	+	+	+
	Fibrous	++	++	±	+
42	Fibrous	+	+	±	+
	Flattened	±	+	±	±
	Small round	+	+	+	+
56	Fibrous	+	+	±	±
	Flattened	±	+	±	±
	Small round	++	+	+	+
	Large round	+	±	±	±

The positive ratio was evaluated as follows: (−) no staining; (±) <5% cells stained; (+) 5–25% cells stained; (++) 25–50% cells stained; (+++) 50–75% cells stained; (++++) >75% cells stained. Cambium = cells in the cambium layer; fibrous = cells in the fibrous layer; flattened = flattened chondrocytes; small round = small round chondrocytes; large round = large round chondrocytes.

Table 3
Positive cells (as % of total) immunostained for TGF-β1 and its receptors

Antigen	TGF-β1 ligand				TβR-I				TβR-II			
TGF-β1 treament	+TGF-β1		−TGF-β1		+TGF-β1		−TGF-β1		+TGF-β1		−TGF-β1	
Day	C	F	C	F	C	F	C	F	C	F	C	F
2	11	43	11	42	10	27	14	23	16	31	19	23
5	16	32	12	34	14	26	8	23	15	20	15	27
7	50	58	9	53	50	57	19	56	51	47	11	36
14	15	13	9	21	6	5	2	7	10	3	8	9
21	18	18	25	41	9	7	4	2	13	10	7	7
28	29	31	20	39	16	2	5	3	29	3	13	9
42	57	20	8	17	54	4	6	3	59	4	8	5
63	21	13	4	8	23	11	5	2	21	6	10	2

C = cambium layer; F = fibrous layer.

changes and effects of exogenously administered TGF-β1 were identified. In the TGF-β1-treated explants 50%, 50% and 51% of the cambium layer cells were positive for TGF-β1, TβR-I, and TβR-II, respectively, at day 7 (Fig. 5(A)–(C), Fig. 6), while only 9%, 19% and 11%, respectively, of the cambium layer cells were positive in the explants not treated with TGF-β1 (Figs. 5(D)–(F) and 6). The presence or absence of TGF-β1 treatment had no identifiable effect on the number of positively stained cells in the fibrous layer. With the progression of cartilage formation, TGF-β1, TβR-I and TβR-II were expressed by increasing numbers of neochondrocytes. At 42 days, immunostaining for their proteins was greatest in the small round chondrocytes and decreased as the chondrocytes increased in size (Fig. 7). At day 42 in the TGF-β1-treated explants, 57%, 54% and 59% of

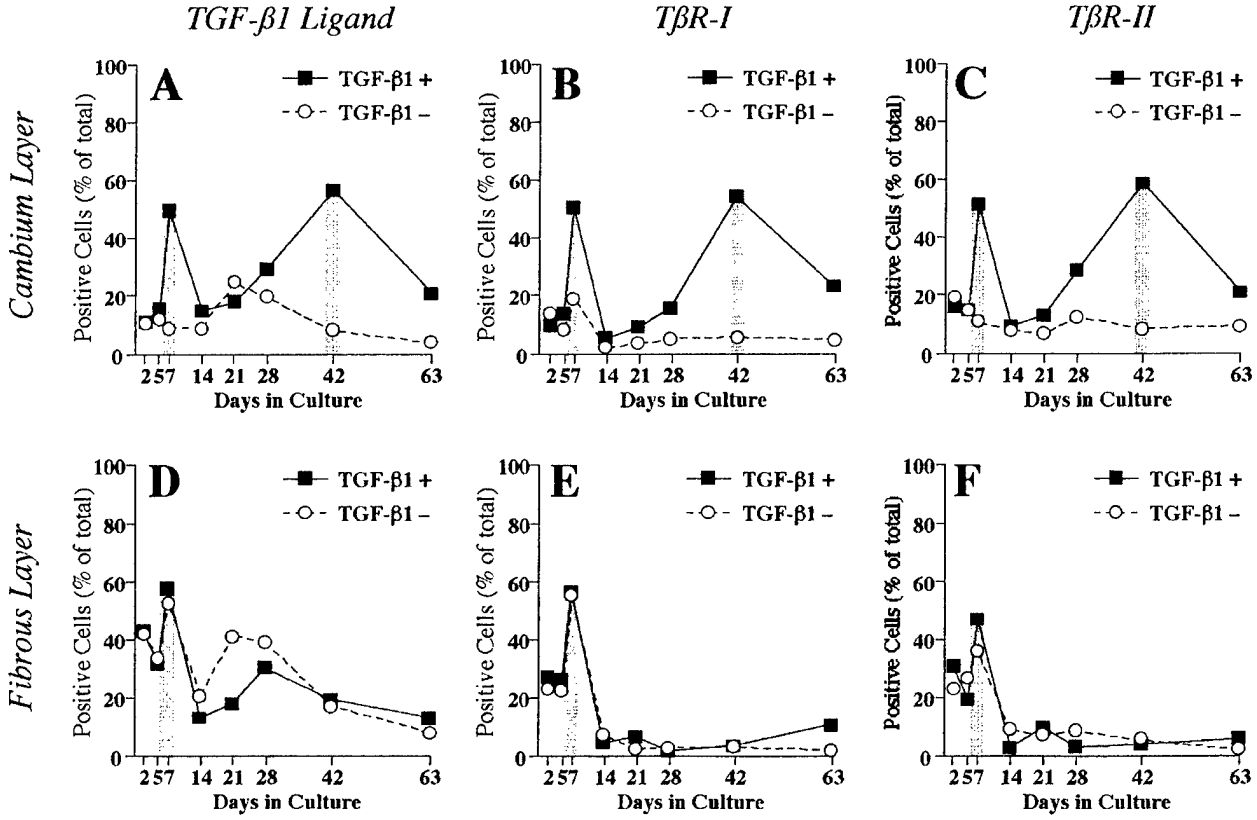

Fig. 5. Immunohistochemical results showing the percentage of cells in the fibrous and cambium layers staining positive for TGF-β1. An initial peak at 7 days was seen in all explants; those stimulated with TGF-β1 in the first 48 h of culture had a delayed peak of expression of TGF-β1 and its receptors in the cambium layer on day 42.

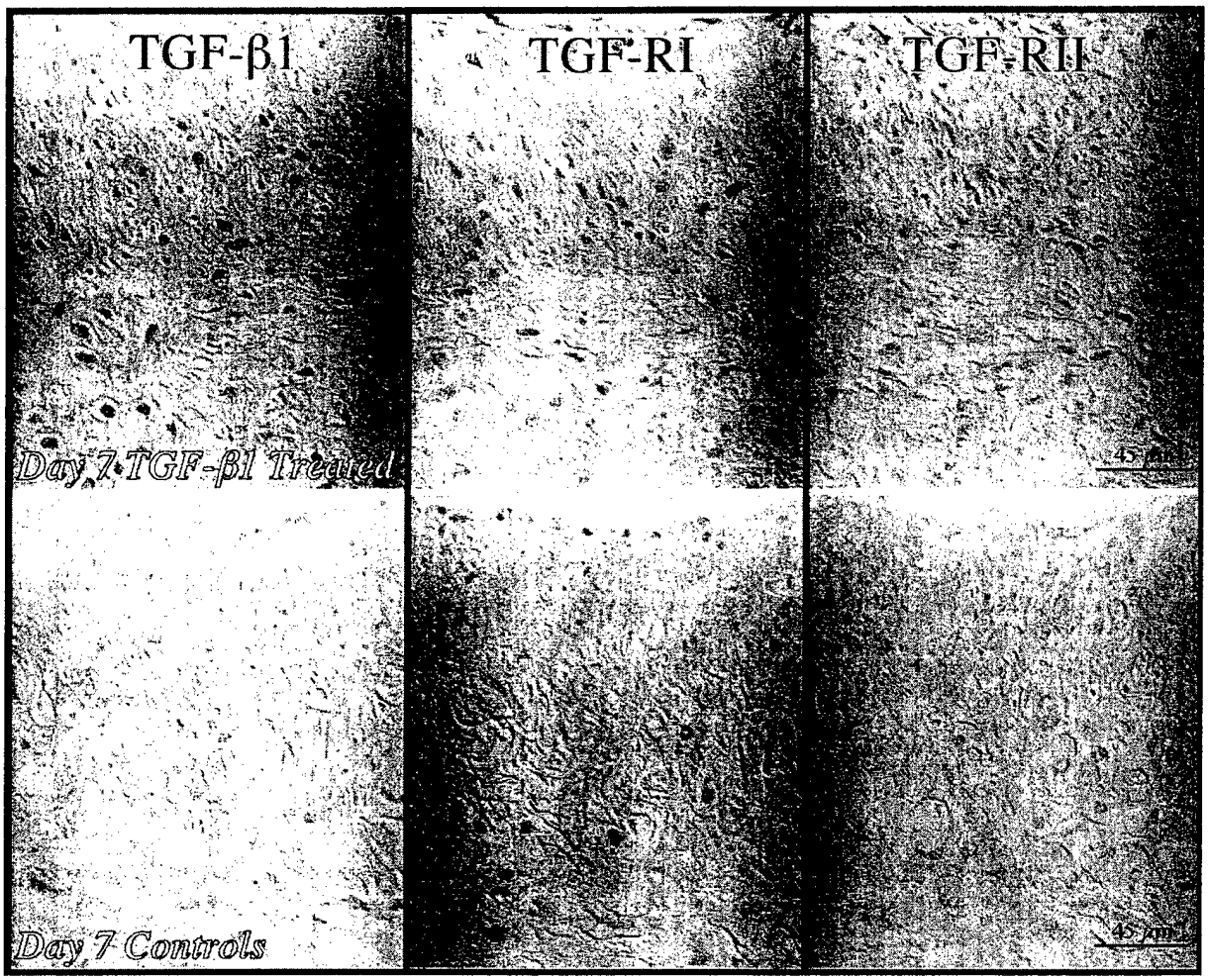

Fig. 6. Cambium layer immunolocalization of transforming growth factor-β1 (TGF-β1), TGF-β type I receptor (TβR-I), and TGF-β type II receptor (TβR-II) in periosteal explants after 7 days of culture in agarose with and without TGF-β1 supplementation.

the cambium layer cells were positive for TGF-β1, TβR-I, and TβR-II, respectively. In the absence of exogenous TGF-β1 treatment, however, these proteins were detected only in a minority of the neochondrocytes (TGF-β1 = 8%, TβR-I = 6%, and TβR-II = 8%). The three sets of immunohistochemistry data were very repeatable. The three values in each group were within a 5% range more than half the time. Most of the remainder were within a 10% range. Consistency was high early and late in culture. At 21–28 days of culture, the results were more variable from one specimen to the next. Taken together, these expression patterns were biphasic, with initial peaks of TβR-I and TβR-II at day 7 then again at day 42 immunohistochemistry.

Discussion

The present study documents the spatiotemporal expression patterns of the TGF-β receptors, TβR-I and TβR-II, during periosteal chondrogenesis in vitro and the correlation between these and the endogenous expression of the TGF-β1 ligand. Periosteal explants expressed TβR-I and TβR-II at both the mRNA and protein levels throughout the period of agarose culture for 56 days. Three primary observations were made. First, the expressions of the TGF-β receptors, and the ligand itself, were significantly upregulated by endogenous TGF-β1 treatment. Second, the pattern of expression was biphasic, with an initial peak as chondrogenic differentiation was taking place, and a larger peak again later during extracellular matrix deposition during cartilage formation. Third, the temporal and spatial patterns of expression of the TGF-β receptors coincided with those of the ligand itself.

In both the experimental and control groups, the expression of TGF-β and its receptors rose to an initial peak at 7 days, in the pre-cartilage stage, when cell proliferation is decreasing and chondrogenic differentiation is commencing. This is consistent with the report

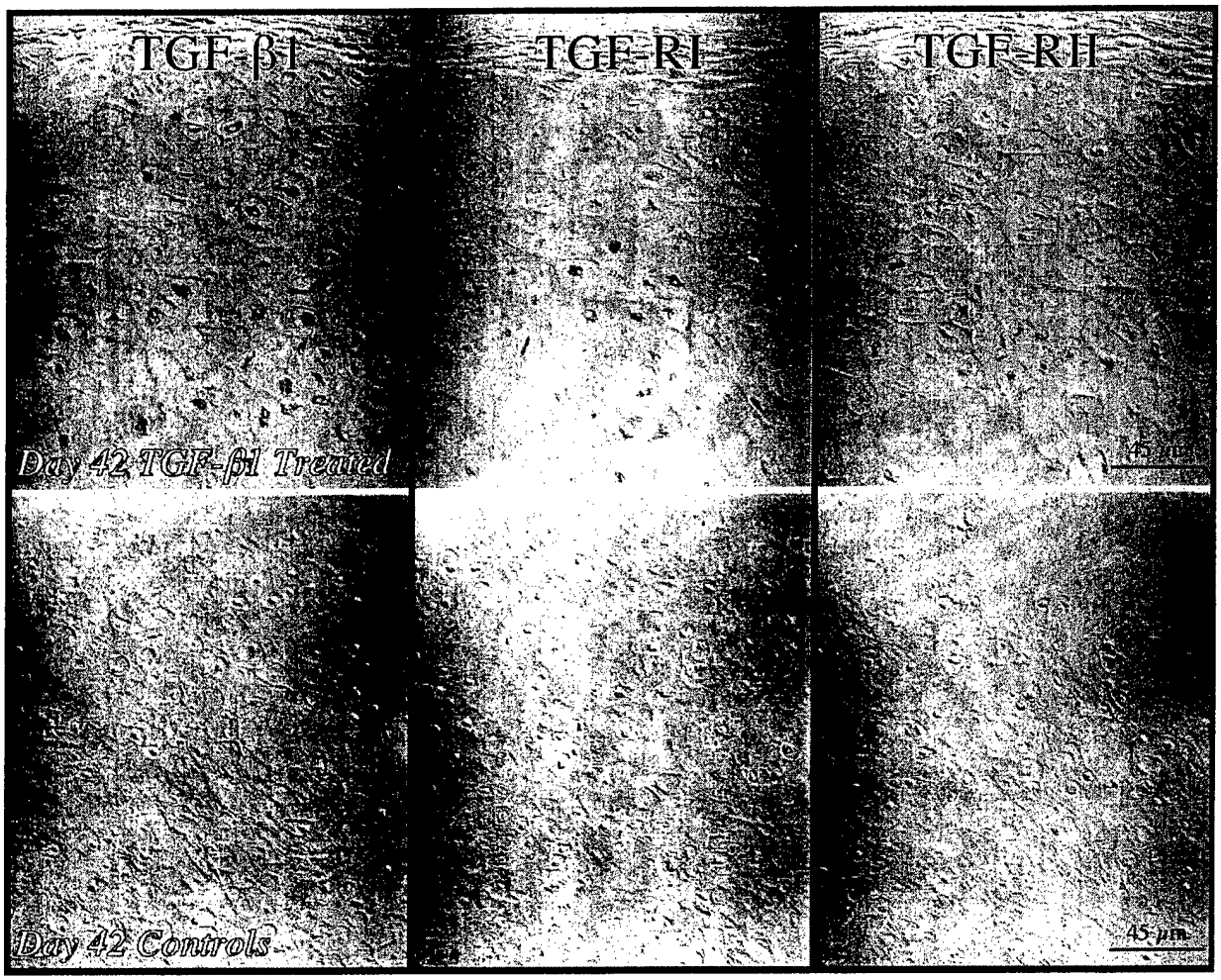

Fig. 7. Immunolocalization of transforming growth factor-β1 (TGF-β1), TGF-β type I receptor (TβR-I), TGF-β type II receptor (TβR-II) in periosteal explants after 42 days of culture in agarose with and without TGF-β1 supplementation.

of Miura, et al. [31] who showed that TGF-β1 strongly stimulated chondrogenic differentiation in periosteal explants. Exogenous administration of TGF-β1 stimulates cell proliferation among the chondrocyte precursor in the cambium layer of the periosteum, and this initial phase of cell proliferation is thought to be responsible for later chondrogenic differentiation [56]. It is presumably this initial proliferative response that sets off an autocrine or paracrine response in the chondrocyte precursor cells in the cambium layer of the periosteum to differentiate into the chondrocyte lineage. Previous in vitro [2,63] and in vivo [48,49] studies have shown that TGF-β1 autoregulates its own expression. The fact that expression of the TGF-β1 receptors was upregulated following treatment with TGF-β1 suggests that the biological response to TGF-β1 was indeed directly mediated by it.

The second observation was that the patterns of expression of TGF-β1 and its receptors were biphasic, with an initial peak as chondrogenic differentiation was taking place, and a larger peak again later during extracellular matrix deposition during cartilage formation. In the explants treated with TGF-β for just the first 48 h in culture, there was a dramatic rise to a second peak in mRNA levels of TGF-β, TβR-I, and TβR-II at 42 days. This biphasic pattern of expression was not seen in the untreated controls. The prolonged interval between exposure to exogenously added TGF-β1 and the eventual upregulation suggests that TGF-β1 acts early in periosteal chondrogenesis, presumably during the commitment phase. Immunohistochemical studies demonstrated that TβR-I and TβR-II were generally expressed by the same type of cells expressing the TGF-β1 ligand. Initially, TGF-β1 was expressed endogenously in both the fibrous and cambium layers, whereas later during cartilage matrix formation, such expression was seen principally in the chondrocytes. Although the immunolocalization of TGF-β1 presented in this study doesn't directly indicate

expression of the active form of TGF-β1, these findings suggest that endogenous TGF-β1 acts in either (or both) an autocrine or a paracrine fashion to regulate periosteal chondrogenesis. In a separate study, Saris et al. [56] identified a sequential pattern of cell proliferation that commenced in the fibrous layer and progressed into the cambium layer in a manner strongly suggestive of a paracrine signaling mechanism between the cells in these two layers. The dynamic spatiotemporal changes in the patterns of expression of TβR-I and TβR-II, as well as that of endogenous TGF-β1, reported in the present study support the concept of an autocrine/paracrine mechanism involving TGF-β1 in the regulation of periosteal chondrogenesis in vitro.

The third observation was that the temporal and spatial patterns of expression of the TGF-β receptors coincided with those of the ligand itself. Several recent in vitro studies have demonstrated the capacity of TGF-β1 to regulate the expression of its own receptors [16,36,39]. Upregulation of the expression of TGF-β1, TβR-I and TβR-II seen in the early stages of periosteal chondrogenesis with TGF-β1 treatment indicates a positive autocrine feedback mechanism that is induced by exogenous TGF-β1. This would be similar to the effects of TGF-β1 on the expression of its own ligand and its receptors, consistent with these previous studies.

This early action of TGF-β might affect proliferation of the chondrocyte precursors and/or mesenchymal stem cells. Previous studies have reported conflicting effects of TGF-β1 on the proliferation of mesenchymal cells in periosteum. Joyce et al. [24] have shown that exogenous subperiosteal injections of TGF-β1 in vivo stimulate the proliferation of mesenchymal cells in the periosteum. Conversely, Izumi et al. [21] and Iwasaki et al. [19] have demonstrated that TGF-β1 stimulates chondrogenic differentiation of periosteal-derived cells but has no effect on their proliferation in vitro. One possible explanation for these contradictions may be that different cell types and environments were studied. TGF-β1 has been well documented to have a multitude of effects that depend on the type of cell upon which it is acting and the conditions of its application [46,51]. Also, the behavior of cells released from their extracellular matrix is not necessarily the same as that of cells in their matrix. We have previously shown that ^{3}H-thymidine incorporation in periosteal explants treated with TGF-β1 increases significantly during the initial period in culture using our organ culture model [35].

Previous studies have shown that TGF-β1 guides a variety of mesenchymal stem cells into chondrocyte differentiation [6,27,57]. The mechanism involved in such regulatory functions are not fully elucidated, but it has been suggested that TGF-βs facilitate the initiation of prechondrogenic condensation, a prerequisite stage of chondrogenic differentiation, by stimulating production of cell adhesion molecules [29,47,60]. Transient exposure to TGF-β1 in chick wing bud mesenchyme in vitro has been shown to stimulate mesenchymal condensation and subsequent cartilage differentiation, consistent with the elevation of fibronectin mRNA expression [29]. It has been demonstrated both in vitro and in vivo that N-cadherin is expressed in the limb mesenchymal cells and that blocking N-cadherin activity inhibits their chondrogenic differentiation [47]. Upregulation of N-cadherin expression with TGF-β1 treatment has been shown in chick limb bud mesenchymal cells in vitro [60]. We have also found in preliminary studies that TGF-β enhances the expression of N-cadherin mRNA in cultured periosteal explants between day 2 and day 10 in culture, with a peak at day 5 [65]. Taken together with the temporal expression of TGF-β1 and its receptors presented in this study, exogenous TGF-β1 and/or endogenous TGF-β1 upregulated by exogenous TGF-β1, appear to be related to this critical step for chondrogenic differentiation. Clearly, more direct evidence is required to elucidate the role of TGF-β1 in the stimulation of chondrogenic differentiation in periosteal chondrogenesis.

Previous immunohistochemical studies have shown proliferative chondrocytes have greatest immunoreactivity for TGF-β1 in cartilaginous tissues, including growth plate [22], neonatal rib and osteophyte [14]. By contrast, immunoreactivity for TGF-β receptors in cartilaginous tissues is somewhat conflicting [14,25]. Kabasawa et al. [25] have shown immunolocalization of TβR-II was observed more intensely in maturing and hypertrophic chondrocytes than in proliferating chondrocytes in rat growth plate. Horner et al. [14] have demonstrated that immunoreactivity for TβR-I and TβR-II in human osteophytes is maximum in proliferating chondrocytes. The present study showed that TβR-I and TβR-II, as well as TGF-β1, were more highly expressed in small round chondrocytes, which were thought to correspond to proliferative chondrocytes based on ongoing studies of cell proliferation during periosteal chondrogenesis. In a separate investigation, Ito et al. [17] have identified these small round chondrocytes as having maintained their capacity for proliferation and as having avoided terminal differentiation into hypertrophic chondrocytes. Previous studies by other investigators have shown the stimulatory effect of TGF-β1 on the proliferation of chondrocytes [12] and the production of extracellular matrix protein synthesis by chondrocytes [50,62].

In conclusion, the present study has documented the spatial and temporal patterns of expression of TβR-I and TβR-II, as well as that of TGF-β1, during periosteal chondrogenesis in vitro. The expression of this growth factor, and of its receptors, is upregulated in response to exogenous administration of TGF-β1. The most dramatic effects are delayed, indicating that TGF-β1 is involved early in the regulation of initiating and

promoting cartilage formation during periosteal chondrogenesis. These data will be useful in planning further studies to elucidate molecular mechanism of TGF-β1 function for regulating periosteal chondrogenesis.

Acknowledgements

This study was funded by NIH Grant AR43890.

References

[1] Applequist SE, Keyna U, Calvin MR, Beck-Engeser GB, Raman C, Jack HM. Sequence of the rabbit glyceraldehyde-3-phosphate dehydrogenase-encoding cDNA. Gene 1995;163:325–6.

[2] Bascom CC, Wolfshohl JR, Coffey Jr. RJ, Madisen L, Webb NR, Purchio AR, Derynck R, Moses HL. Complex regulation of transforming growth factor beta 1, beta 2, and beta 3 mRNA expression in mouse fibroblasts and keratinocytes by transforming growth factors beta 1 and beta 2. Mol Cell Biol 1989;9: 5508–15.

[3] Bassing CH, Howe DJ, Segarini PR, Donahoe PK, Wang XF. A single heteromeric receptor complex is sufficient to mediate biological effects of transforming growth factor-beta ligands. J Biol Chem 1994;269:14861–4.

[4] Bassing CH, Yingling JM, Howe DJ, Wang T, He WW, Gustafson ML, Shah P, Donahoe PK, Wang XF. A transforming growth factor beta type I receptor that signals to activate gene expression. Science 1994;263:87–9.

[5] Chen F, Weinberg RA. Biochemical evidence for the autophosphorylation and transphosphorylation of transforming growth factor beta receptor kinases. Proc Natl Acad Sci USA 1995; 92:1565–9.

[6] Denker AE, Nicoll SB, Tuan RS. Formation of cartilage-like spheroids by micromass cultures of murine C3H10T1/2 cells upon treatment with transforming growth factor-beta 1. Differentiation 1995;59:25–34.

[7] Dukas K, Sarfati P, Vaysse N, Pradayrol L. Quantitation of changes in the expression of multiple genes by simultaneous polymerase chain reaction. Anal Biochem 1993;215:66–72.

[8] Fujii K, Sai S, Tanak T, Tsuji M, Mori M, Murota K. Biological resurfacing of full-thickness defects in patellar cartilage utilizing autogenous periosteal grafts. In: Combined Meeting of the Orthopaedic Research Societies of USA, Japan, and Canada, Alberta, 1991. p. 144.

[9] Gallay SH, Miura Y, Commisso CN, Fitzsimmons JS, O'Driscoll SW. Relationship of donor site to chondrogenic potential of periosteum in vitro. J Orthop Res 1994;12:515–25.

[10] Gentry LE, Webb NR, Lim GJ, Brunner AM, Ranchalis JE, Twardzik DR, Lioubin MN, Marquardt H, Purchio AF. Type 1 transforming growth factor beta amplified expression and secretion of mature and precursor polypeptides in Chinese hamster ovary cells. Mol Cell Biol 1987;7:3418–27.

[11] Gu J, Agrawal N, Wang PP, Cohen MV, Downey J. A primary–secondary antibody complex method of immunocytochemistry using rabbit polyclonal antibodies to detect antigens in rabbit tissue. Cell Vision 1995;2:52–9.

[12] Guerne PA, Sublet A, Lotz M. Growth factor responsiveness of human articular chondrocytes: distinct profiles in primary chondrocytes, subcultured chondrocytes, and fibroblasts. J Cell Physiol 1994;158:476–84.

[13] Hoikka VEJ, Jaroma HJ, Ritsilä VA. Reconstruction of the patellar articulation with periosteal grafts. 4-year follow-up of 13 cases. Acta Orthop Scand 1990;61:36–9.

[14] Horner A, Kemp P, Summers C, Bord S, Bishop NJ, Kelsall AW, Coleman N, Compston JE. Expression and distribution of transforming growth factor-beta isoforms and their signaling receptors in growing human bone. Bone 1998;23:95–102.

[15] Horvath LZ, Friess H, Schilling M, Borisch B, Deflorin J, Gold LI, Korc M, Buchler MW. Altered expression of transforming growth factor-beta S in chronic renal rejection. Kidney Int 1996; 50:489–98.

[16] Inagaki M, Wang Z, Carr BI. Transforming growth factor beta 1 selectively increases gene expression of the serine/threonine kinase receptor 1 (SKR1) in human hepatoma cell lines. Cell Struct Funct 1994;19:305–13.

[17] Ito Y, Fitzsimmons J, O'Driscoll S. Proliferative characterization of developing periosteal neochondrocytes. Trans Orthop Res Soc 1999;24:673.

[18] Ito Y, Sanyal A, Fitzsimmons JS, Mello MA, O'Driscoll SW. Histomorphological and proliferative characterization of developing periosteal neochondrocytes in vitro. J Orthop Res 2001;19: 405–13.

[19] Iwasaki M, Nakahara H, Nakata K, Nakase T, Kimura T, Ono K. Regulation of proliferation and osteochondrogenic differentiation of periosteum-derived cells by transforming growth factor-β and basic fibroblast growth factor. J Bone Jt Surg 1995;77A: 543–54.

[20] Iwasaki M, Nakata K, Nakahara H, Nakase T, Kimura T, Kimata K, Caplan AI, Ono K. Transforming growth factor-beta 1 stimulates chondrogenesis and inhibits osteogenesis in high density culture of periosteum-derived cells. Endocrinology 1993;132:1603–8.

[21] Izumi T, Scully SP, Heydemann A, Bolander ME. Transforming growth factor-β1 stimulates type II collagen expression in cultured periosteum-derived cells. J Bone Miner Res 1992;7:115–21.

[22] Jingushi S, Scully SP, Joyce ME, Sugioka Y, Bolander ME. Transforming growth factor-β1 and fibroblast growth factors in rat growth plate. J Orthop Res 1995;13:761–8.

[23] Joyce ME, Roberts AB, Sporn MB, Bolander ME. Transforming growth factor-beta and the initiation of chondrogenesis and osteogenesis in the rat femur. J Cell Biol 1990;110:2195–207.

[24] Joyce ME, Roberts AB, Sporn MB, Bolander ME. Transforming growth factor-beta and the initiation of chondrogenesis and osteogenesis in the rat femur. J Cell Biol 1990;110:2195–207.

[25] Kabasawa Y, Ejiri S, Matsuki Y, Hara K, Ozawa H. Immunoreactive localization of transforming growth factor-beta type II receptor-positive cells in rat tibiae. Bone 1998;22:93–8.

[26] Korkala OL. Periosteal primary resurfacing of joint surface defects of the patella due to injury. Injury 1988;19:216–8.

[27] Kulyk WM, Rodgers BJ, Greer K, Kosher RA. Promotion of embryonic chick limb cartilage differentiation by transforming growth factor-β. Dev Biol 1989;135:424–30.

[28] Laiho M, Weis F, Boyd F, Ignotz R, Massague J. Responsiveness to transforming growth factor beta restored by genetic complementation between cells defective in TGF-beta receptors I and II. J Biol Chem 1991;266:9108–12.

[29] Leonard CM, Fuld HM, Frenz DA, Downie SA, Massagué J, Newman SA. Role of transforming growth factor-beta in chondrogenic pattern formation in the embryonic limb: stimulation of mesenchymal condensation and fibronectin gene expression by exogenenous TGF-beta and evidence for endogenous TGF-beta-like activity. Dev Biol 1991;145:99–109.

[30] Lyons RM, Moses HL. Transforming growth factors and the regulation of cell proliferation. Eur J Biochem 1990;187:467–73.

[31] Miura Y, Fitzsimmons JS, Commisso C, Gallay SH, O'Driscoll SW. Enhancement of periosteal chondrogenesis in vitro: Dose-response for transforming growth factor-beta 1 (TGF-β1). Clin Orthop 1994;301:271–80.

[32] Miura Y, Gallay SH, Commisso CN, Fitzsimmons JS, O'Driscoll SW. Periosteal organ culture model: 2 vs.14 days exposure to (TGF-β1). Orthop Trans 1994;18:143–4.

[33] Miura Y, O'Driscoll SW. Brief (30 min) exposure to high dose TGF-β1 enhances periosteal chondrogenesis in vitro. Orthop Trans 1993;17:713.
[34] Miura Y, O'Driscoll SW. General time course of periosteal chondrogenesis in vitro with TGF-β1. Orthop Trans 1994;18:686.
[35] Miura Y, O'Driscoll SW. The role of TGF-β1 in induction, proliferation and phenotypic expression during chondrogenesis. Trans Orthop Res Soc 1995;20:55.
[36] Moreland RB, Traish A, McMillin MA, Smith B, Goldstein I, Saenz de Tejada I. PGE1 suppresses the induction of collagen synthesis by transforming growth factor-beta 1 in human corpus cavernosum smooth muscle. J Urol 1995;153:826–34.
[37] Nakao A, Roijer E, Imamura T, Souchelnytskyi S, Stenman G, Heldin CH, ten Dijke P. Identification of Smad2, a human mad-related protein in the transforming growth factor beta signaling pathway. J Biol Chem 1997;272:2896–900.
[38] Niedermann B, Boe S, Lauritzen J, Rubak JM. Glued periosteal grafts in the knee. Acta Orthop Scand 1985;56:457–60.
[39] Norgaard P, Spang-Thomsen M, Poulsen HS. Expression and autoregulation of transforming growth factor beta receptor mRNA in small-cell lung cancer cell lines. Br J Cancer 1996; 73:1037–43.
[40] O'Driscoll S, Commisso C, Fitzsimmons J. Type II collagen quantification in experimental chondrogenesis. Osteoarthritis Cartilage 1995;3:197–203.
[41] O'Driscoll S, Recklies A, Poole A. Chondrogenesis in periosteal explants. An organ culture model for in vitro study. J Bone Jt Surg 1994;76A:1042–51.
[42] O'Driscoll SW, Keeley FW, Salter RB. The chondrogenic potential of free autogenous periosteal grafts for biological resurfacing of major full-thickness defects in joint surfaces under the influence of continuous passive motion. An experimental investigation in the rabbit. J Bone Jt Surg 1986;68A:1017–35.
[43] O'Driscoll SW, Keeley FW, Salter RB. Durability of regenerated articular cartilage produced by free autogenous periosteal grafts in major full-thickness defects in joint surfaces under the influence of continuous passive motion. A follow-up report at one year. J Bone Jt Surg 1988;70A:595–606.
[44] O'Driscoll SW, Marx RG, Beaton DE, Miura Y, Gallay SH, Fitzsimmons JS. Validation of a simple histological–histochemical cartilage scoring system. Tissue Eng 2001;7:313–320.
[45] O'Driscoll SW, Salter RB. The repair of major osteochondral defects in joint surfaces by neochondrogenesis using autogenous osteoperiosteal grafts stimulated by continuous passive motion. An experimental investigation in the rabbit. Clin Orthop 1986;208:131–40.
[46] O'Keefe RJ, Puzas JE, Brand JS, Rosier RN. Effect of transforming growth factor-β on DNA synthesis by growth plate chondrocytes: modulation by factors present in serum. Calcif Tissue Int 1988;43:352–8.
[47] Oberlender SA, Tuan RS. Expression and functional involvement of N-cadherin in embryonic limb chondrogenesis. Development 1994;120:177–87.
[48] Quaglino Jr. D, Nanney LB, Ditesheim JA, Davidson JM. Transforming growth factor-beta stimulates wound healing and modulates extracellular matrix gene expression in pig skin: incisional wound model. J Invest Dermatol 1991;97:34–42.
[49] Quaglino Jr. D, Nanney LB, Kennedy R, Davidson JM. Transforming growth factor-beta stimulates wound healing and modulates extracellular matrix gene expression in pig skin. I. Excisional wound model. Lab Invest 1990;63:307–19.
[50] Redini F, Galera P, Mauviel A, Loyau G, Pujol JP. Transforming growth factor beta stimulates collagen and glycosaminoglycan biosynthesis in cultured rabbit articular chondrocytes. FEBS Lett 1988;234:172–6.
[51] Rollins BJ, O'Connell TM, Bennett G, Burton LE, Stiles CD, Rheinwald JG. Environment-dependent growth inhibition of human epidermal keratinocytes by recombinant human transforming growth factor-beta. J Cell Physiol 1989;139:455–62.
[52] Rubak JM, Poussa M, Ritsilä V. Chondrogenesis in repair of articular cartilage defects by free periosteal grafts in rabbits. Acta Orthop Scand 1982;53:181–6.
[53] Rubak JM, Poussa M, Ritsilä V. Effects of joint motion on the repair of articular cartilage with free periosteal grafts. Acta Orthop Scand 1982;53:187–91.
[54] Sanyal A, O'Driscoll S, Bolander M, Sarkar G. An effective method of completely removing contaminating genomic DNA from an RNA sample to be used for PCR. Mol Biotechnol 1997;8:135–7.
[55] Sanyal A, O'Driscoll S, Fitzsimmons J, Bolander M, Sarkar G. Gene-digging: a method for obtaining species-specific sequence based on conserved segments of nucleotides in open reading frames. Mol Biotechnol 1998;10:223–30.
[56] Saris D, Sanyal A, An K-N, Fitzsimmons J, O'Driscoll S. Periosteum responds to dynamic fluid pressure (DFP) by proliferating in vitro. J Orthop Res 1999;17:668–77.
[57] Seyedin SM, Thomas TC, Thompson AY, Rosen DM, Piez KA. Purification and characterization of two cartilage-inducing factors from bovine demineralized bone. Proc Natl Acad Sci USA 1985;82:2267–71.
[58] Sporn MB, Roberts AB, Wakefield LM, Assolan RK. Transforming growth factor-β: Biological function and chemical structure. Science 1986;233:532–4.
[59] Sporn MB, Roberts AB, Wakefield LM, de Crombrugghe B. Some recent advances in the chemistry and biology of transforming growth factor-beta. J Cell Biol 1987;105:1039–45.
[60] Tsonis PA, Del R-TK, Millan JL, Wheelock MJ. Expression of N-cadherin and alkaline phosphatase in chick limb bud mesenchymal cells: regulation by 1,25-dihydroxyvitamin D3 or TGF-beta 1. Exp Cell Res 1994;213:433–7.
[61] Vachon A, McIlwraith CW, Trotter GW, Norrdin RW, Powers BE. Neochondrogenesis in free intra-articular, periosteal, and perichondrial autografts in horses. Am J Vet Res 1989;50:1787–94.
[62] van Beuningen HM, van der Kraan PM, Arntz OJ, van den Berg WB. Transforming growth factor-beta 1 stimulates articular chondrocyte proteoglycan synthesis and induces osteophyte formation in the murine knee joint. Lab Invest 1994;71:279–90.
[63] Van Obberghen-Schilling E, Roche NS, Flanders KC, Sporn MB, Roberts AB. Transforming growth factor-β1 positively regulates its own expression in normal and transformed cells. J Biol Chem 1988;263:7741–6.
[64] Wakitani S, Goto T, Pineda SJ, Young RG, Mansour JM, Caplan AI, Goldberg VM. Mesenchymal cell-based repair of large, full-thickness defects of articular cartilage. J Bone Jt Surg 1994;76A: 579–92.
[65] Ward M, Sanyal A, Sarkar G, O'Driscoll S. N-cadherin is expressed during periosteal chondrogenesis. Orthop Trans 1998; 23:501.
[66] Wrana JL, Attisano L, Wieser R, Ventura F, Massague J. Mechanism of activation of the TGF-beta receptor. Nature 1994;370:341–7.

In: *Signal Transduction by Reactive Oxygen and Nitrogen Species: Pathways and Chemical Principles*. M. Torres, J. Fukuto, and H. J. Forman, eds. Kluwer Press, New York.

CHAPTER X

ROLE OF MITOCHONDRIAL OXYGEN AND NITROGEN REACTIVE SPECIES IN SIGNALING

Cecilia Giulivi and Merry Jo Oursler

1. INTRODUCTION

The four-electron reduction of oxygen to water by cytochrome *c* oxidase is a reaction performed with high precision and rapidity; however, during the transfer of electrons throughout the electron transport chain, oxygen is partially reduced, yielding oxygen species that readily react with a variety of cellular components. The term "reactive oxygen species" (ROS) includes superoxide anion, hydrogen peroxide, and hydroxyl radical. Superoxide anion radical is the one-electron reduction product of oxygen and is a precursor of other reactive species. Hydrogen peroxide is formed from superoxide anion dismutation. Probably the most potent oxygen species in biological systems is the hydroxyl radical. This species forms from relatively harmless hydrogen peroxide. Although most free radicals are extremely short-lived (1 ns to 1 μs), they react readily with other molecules, transferring the radical character, converting them to free radicals and thereby initiating chain reactions.

On the basis that uni- or divalent reduction products of oxygen are produced during normal oxidative metabolism, it is possible to speculate that either an increase in the production of these species, or decrease in the antioxidant defenses, will lead to ROS injury. Considering the manifestations of ROS toxicity, it is likely that sequential processes would be involved; these include (a) the primary injury at the molecular level followed by (b) the defence mechanisms that normally respond to the initial injury. If the defence mechanisms are exhausted or after what may be accounted for as the accumulation of errors in the handling of oxygen intermediates, the biological target (enzyme, cell, or tissue) cannot adequately perform their physiologic function. Considering the concentration of the normal biological antioxidant defences -usually 2-3 orders of magnitude higher than those of the corresponding substrates- it seems that the free-radical reactions arising during the course of normal oxidative metabolism are at least partially responsible for the aging process [1,2]. Because the mitochondrion is the site of the bulk of the cell's oxidative metabolism, mitochondrial biomolecules (e.g., DNA, lipids, and proteins) probably sustain most of free-radical damage. In this regard, several

degenerative diseases, including Parkinson's, Alzheimer's, and Huntington's diseases, are associated with oxidative damage to mitochondria.

The high reactivity of free radicals makes it difficult to characterize their reaction products, for all classes of biological molecules are susceptible to oxidative damage by free radicals. As a consequence of their high reactivity, their short half-life limits the target radius. Thus, a role for ROS as initiators or participants in signal transduction pathways has been controversial. However, accumulating evidence indicates some important functions for reactive oxygen and nitrogen species (RONS) in signalling pathways [3-5]. Their actions seem to be attributed either to reduction-oxidation reactions or binding to target molecules. These signalling mechanisms are entirely different from those attributed to, for example, calcium-activated and phosphorylation-dependent pathways.

In this Chapter we will review the sources of oxygen- and nitrogen species in mitochondria, the modulation of their production, and describe some examples in which mitochondrial RONS have been implicated in signal transduction pathways.

2. MITOCHONDRIAL OXYGEN FREE RADICALS

Almost 40 years ago, an increased formation of hydrogen peroxide it was observed from mitochondria exposed to hyperbaric conditions [6]. In the following years, the generation of hydrogen peroxide was demonstrated in mitochondria isolated from various sources also under normoxic conditions [7-10]. Both NAD- and FAD-linked substrates support rates of hydrogen peroxide production (0.2-0.8 nmol hydrogen peroxide/min mg protein [9]) modulated by various metabolic states [9,10]. The production of hydrogen peroxide by submitochondrial particles (i.e., constituted only by inner membrane fraction) suggested that a member of the respiratory chain was responsible for hydrogen peroxide generation. Studies performed with inhibitors of the mitochondrial respiratory chain pointed to a carrier on the substrate side of succinate dehydrogenase-ubiquinone segment [9,11] as a potential generator of hydrogen peroxide. Among the different components of this segment, a main role for ubiquinone in for hydrogen peroxide generation in mitochondria was supported by the linear correlation between ubiquinone supplementation and rate of for hydrogen peroxide production in ubiquinone-depleted mitochondria [8,9]. Later, a second site, albeit quantitatively less significant, was found at the NADH dehydrogenase segment [12].

Besides mitochondria, other subcellular fractions have been identified as intracellular sources of for hydrogen peroxide: microsomes, peroxisomes, and soluble enzymes, among others [8]. However, the rate of ROS production by mitochondria at biologically relevant pO_2 constitutes the most important contribution to the cellular/organ rate of ROS production, therefore, these organelles should be considered as the main source of ROS under physiological conditions [13]. Supporting this view, experimental rates of for hydrogen peroxide production by perfused rat liver were found to be mostly of mitochondrial origin [14].

2.1. Modulation of mitochondrial ROS production

Mitochondria are dynamic organelles whose morphology, composition and function adapt to changes in physiological signals [14]. These physiological signals include nutritional variations, different workloads, oxygen availability, and

development. Responses to physiological signals are fundamental at maintaining homeostasis and as such, are typically reversible and serve to optimise energy production relative to energy demand. In this regard, formation of hydrogen peroxide by mitochondria shows generally similar characteristics across species/tissues. All mitochondria exhibit lower (or negligible) rates of hydrogen peroxide production in State 3 (active ATP production), whereas is maximum in State 4 (resting, nonphosphorylating mitochondria). Hyperbaric oxygen and hyperoxia exposure results in a marked increase in for hydrogen peroxide production by isolated heart and liver mitochondria [7,8,15]. However, owed to mitochondrial plasticity and the consequent heterogeneity, assessment of ROS production by mitochondria necessitates consideration of specific aspects of mitochondrial characteristics. For example, presence of uncoupler and inhibitors are required to exert maximal rates of ROS production in heart but not in liver mitochondria. Phenotypic changes occur in cellular energetics during cell culture, thus results obtained with mitochondria isolated from organs might not be comparable to those obtained with mitochondria isolated from cultured cells. In addition, rates of ROS production obtained with isolated mitochondria are lacking the cell-specific and tissue-specific interaction, availability of chemically different substrates and the presence of regulatory pathways.

Focusing on isolated mitochondria, and considering the succinate dehydrogenase-ubiquinone segment as the most important source of ROS (60-80%), then the rate of ROS production is modulated by the steady-state concentrations of ubisemiquinone and oxygen (eq. 1; assuming that superoxide anion is the chemical precursor of for hydrogen peroxide) for the production of hydrogen peroxide is formulated as a non-enzymatic oxidation of ubisemiquinone ($UQ^{\bullet-}$) by oxygen [16]:

$$+d[O_2^{\bullet-}]/dt = 2 \times +d[H_2O_2]/dt = k\,[UQ^{\bullet-}]\,[O_2] \qquad [1]$$

As a consequence, several metabolic conditions that result in an increased level of ubiquinone (fasting, chronic treatment with dinitrophenol, cortisone treatment [17]) or higher availability of oxygen (e.g., hyperoxia) are expected to have increased rates of ROS.

2.2. Availability of intracellular oxygen and the role of nitric oxide

Hyperoxia and hyperbaric oxygen enhance hydrogen peroxide generation at the subcellular and cellular levels at different extents (from 60 to 200%). However, the hyperbaric response appears to be greatly diminished at the organ level *in vivo*. The level of oxygen in a tissue may be limited by the microvascular response, probably modulated by endogenous factors such as nitric oxide.

Nitric oxide, a reactive free radical molecule, is generated *in vivo* by nitric oxide synthase (NOS) during the conversion of L-Arg to citrulline. Several isoforms of NOS have been isolated [18-21], namely the neuronal, endothelial, and macrophage forms. The constitutive forms, *i.e.*, neuronal and endothelial, account for the rapid, transient, Ca^{2+}-dependent production of nitric oxide [19-21]; the inducible form, *i.e.*, macrophage NOS, causes the slow onset of Ca^{2+}-independent nitric oxide synthesis in inflammatory cells (after stimulation with cytokines or lipopolysaccharides [18,22].

Nitric oxide functions as an intercellular signal in regulating blood vessel dilation (among other important functions [23-25]), thus facilitating oxygen delivery and removal of metabolic end products from tissues. The stimulatory action of vasodilators on the phosphoinositide signalling system in endothelial cells

produces an influx of calcium resulting in the synthesis of nitric oxide. Nitric oxide rapidly diffuses across membranes [26], although its high reactivity prevents it from getting far away from its site of synthesis (e.g., it reacts efficiently with heme proteins and oxygen [27]). The physiological target of nitric oxide in smooth muscle cells is guanylate cyclase, which catalyzes the reaction of GTP to yield cGMP [28], an intracellular second messenger similar to cAMP. Nitric oxide reacts with guanylate's cyclase heme prosthetic group to yield nitrosoheme, increasing the enzyme's activity by 50- to 200-fold [29], presumably via a conformation change that allows the release of transaxial histidine ligand, which presumably, participates in catalysis. In turn, cGMP causes smooth muscle relaxation through its stimulation of protein phosphorylation by cGMP-dependent protein kinase. In other biological settings, nerve stimulation causes calcium increases at nerve terminals, thereby stimulating NOS activity. The resultant nitric oxide diffuses to nearby smooth muscle cells, where it binds to guanylate cyclase and activates it to synthesize cGMP as described above [30,31].

The vasodilating effects mediated by nitric oxide are understood as part of intercellular signalling pathways, in which nitric oxide is produced by one cell type and acts on another one. However, the recent finding that mitochondria are endowed with a NOS has extended the role of this free radical as an intracellular signal molecule.

3. MITOCHONDRIAL NITROGEN REACTIVE SPECIES

Our [32-37]] and others' [38-41] studies provided evidence for the occurrence of a NOS (mtNOS) in mitochondria. Based on MALDI-ToF and Q-ToF analyses of tryptic digests, mtNOS has been identified as nNOS isoform alpha [36]. mtNOS is constitutively expressed, following a particulate distribution [32,35], probably favoured by its acylation with myristic acid [36]. The rate of nitric oxide production by intact, coupled mitochondria is L-Arg-dependent; the apparent K_m for L-Arg and V_{max} values were 5 μM and 1.4 nmol/min per mg protein, respectively, in agreement with the values published for the purified brain isoform [32]. Given that the experimental K_m is 30-40 times below the reported pool of L-Arg in mitochondrial matrix (about 200 μM), the modulation of mtNOS activity by L-Arg seems unlikely under physiological conditions. The production of nitric oxide is also sustained by endogenous NADPH, the specific electron donor for NOS. Under our experimental conditions, the energy-dependent transhydrogenase seems to represent the main source of NADPH because uncoupling conditions (overload of Ca^{2+} or FCCP) significantly decreased the levels of NADPH, halting nitric oxide production [32].

Although nitric oxide is produced by mitochondria, the target molecule for this free radical was unknown for these organelles do not contain guanylate cyclase. Intact coupled mitochondria, when stimulated to produce nitric oxide, exhibited a decrease in their respiratory rates from 30 to 50% (at pO_2 = 0.2 atm), which was completely reversed upon the addition of an inhibitor of NOS or the removal of L-Arg [33]. Conversely, oxygen uptake increased in the presence of an inhibitor of NOS, *N*-monomethyl-L-arginine, indicating the involvement of nitric oxide in the modulation of oxygen consumption. Concomitantly to the decline in the respiratory rate, an inhibition of ATP synthesis was also observed (40-50%), a decrease not attributable to a direct effect of nitric oxide on Complex V [33]. The dependence of the respiratory rates of mitochondria in State 3 and cytochrome oxidase activities on oxygen concentrations indicated that both processes were

linked and competitively inhibited by nitric oxide at the cytochrome oxidase level. Thus, the target molecule of nitric oxide in mitochondria is cytochrome oxidase: nitric oxide by binding to the oxidase, increases the apparent K_m for oxygen (decreasing the affinity for oxygen), thereby decreasing the oxygen consumption at a given pO_2. This inhibition of cytochrome oxidase by nitric oxide was explained primarily by the catabolism of nitric oxide to N_2O, and secondarily, by the direct binding of nitric oxide to the bimolecular center.

The main impact of this finding is that nitric oxide produced by mitochondria may constitute the main participant at regulating the oxygen uptake in organs. The intracellular level of oxygen may be estimated in 10-20 μM, thus, under normal physiological conditions, tissues are under hypoxic environments. A gradient of oxygen as high as 1000-fold [42] is expected from the capillaries toward mitochondria, and the steady-state concentration of oxygen in the latter compartment may be lower than those in either the peroxisomal and cytosolic spaces [14]. The critical oxygen concentration for bioenergetic function of mitochondria corresponds to approximately to 50% reduction of pyridine nucleotide being 60 and 80 nM in State 4 and 3, respectively [42]. Thus, when oxygen levels are adequate, the ratio [oxygen]/[nitric oxide] is high, and cytochrome oxidase activity is maximal. When oxygen levels are low, then the ratio [oxygen]/[nitric oxide] is lower, nitric oxide competitively inhibits cytochrome oxidase, thereby decreasing oxygen consumption. By this mechanism, the oxygen gradient is extended to other mitochondria/cells, thus allowing a more homogeneous distribution of oxygen throughout the cell/organ.

Therefore, the production of nitric oxide by mitochondria gains significance given the modulatory role that this molecule might have on energy metabolism, oxygen consumption, and consequently, on oxygen free radicals production (see below).

3.1. Mitochondrial nitric oxide and cytochrome oxidase modulation

In the case of oxidative phosphorylation, the pathway from NADH to cytochrome *c* functions near equilibrium. In the cytochrome oxidase reaction, however, the terminal step of the electron transport chain is irreversible and is therefore a prime candidate as the control site of the pathway. It is believed that cytochrome oxidase, in contrast to most regulatory enzyme systems, appears to be controlled exclusively by the availability of one of its substrates, reduced cytochrome *c*. Since this substrate is in equilibrium with the rest of the coupled oxidation phosphorylation system, its concentration ultimately depends on the intramitochondrial [NADH]/[NAD^+] ratio and the ATP mass action ratio ([ATP]/[ADP][Pi]). Consequently, the higher the [NADH]/[NAD^+] ratio and the lower the ATP mass action ratio, the higher the concentration of ferrocytochrome *c* and thus the higher the cytochrome oxidase activity.

ATP production is controlled by mass action: an increased ATP utilization increases ATP synthesis, oxygen consumption, and substrate oxidation, simply by providing the substrates (ADP and Pi) for oxidative phosphorylation. By following this process, mass action stimulates the respiratory chain back to substrate oxidation. Several factors have been proposed to regulate respiration; among them Ca^{2+} mobilization, adenine nucleotide carriers, oxygen supply, and cytosolic ATP mass action ratio. However, cytochrome oxidase can serve as a potential control point of oxidative phosphorylation for it catalyzes an irreversible reaction (the reduction of oxygen to water. In this regard, several molecules have

been proposed as regulators or inhibitors of cytochrome *c* oxidase, among them cyanide, azide, formate, sulfide, carbon monoxide and nitric oxide. From these, carbon monoxide has similar chemical characteristics to nitric oxide: it is synthesized by an enzyme (*i.e.*, heme oxygenase) and binds to guanylate cyclase. In contrast to nitric oxide, carbon monoxide has a higher affinity for myo- or hemoglobins than for cytochrome oxidase, thus the concentration required to exert a significant inhibition of cytochrome oxidase activity would be higher that that achieved under physiological conditions. Nitric oxide is the only one that satisfies all the requirements as an allosteric effector of cytochrome oxidase [35]: it is produced at a fair rate by a specific enzyme (mtNOS), located close to the target site (cytochrome oxidase), and it is formed at levels (10-220 nM) that effectively affect the respiratory rate (K_I = 6-10 nM).

As a consequence of the high affinity of nitric oxide for cytochrome oxidase, the cytotoxic role of nitric oxide observed in other systems could be explained as a sustained inhibition of cytochrome oxidase by high concentrations of nitric oxide - like those achieved by activated macrophages- or a formation of the powerful oxidant peroxynitrite (the product between superoxide anion and nitric oxide) which would favor mitochondrial dysfunction, leading probably to cell death.

3.2. Modulation of ROS production by mitochondrial nitric oxide

Changes in hydrogen peroxide production by L-Arg-supplemented mitochondria indicated that nitric oxide affected the rate of oxygen radicals' production by modulating the rate of oxygen consumption at the cytochrome oxidase level [37]. This mechanism was supported by two observations: (1) changes in hydrogen peroxide production correlated with the effect of nitric oxide on the respiratory rates, and (2) the pattern of oxidized/reduced carriers in the presence of nitric oxide indicated cytochrome oxidase as the crossover point according to the crossover theorem [45]. Although the rate of hydrogen peroxide production by mitochondria increased in the presence of L-Arg, the increase was not as high as that obtained with other inhibitors (e.g., antimycin A) used to stimulate ROS production. This could be explained by the catabolism of nitric oxide by cytochrome oxidase, which allowed electrons to go through the chain without resulting in the full reduction of respiratory carriers.

Elucidation of the effect of nitric oxide on the mitochondrial ROS production brought a more dynamic view at the way oxygen consumption and ROS formation occurs, considering not only availability of ADP but also other regulatory devices (Fig. 1). As it has been indicated in previous sections, historically the mitochondrial production of ROS has been considered as a side-process of the normal oxidative metabolism; its rate alternating between two levels determined by physiologically relevant mitochondrial metabolic states, namely States 4 (maximum) and 3 (minimum). However, our studies demonstrated that the mitochondrial production of ROS is not limited to these two values and may exhibit a degree of values modulated by endogenous nitric oxide.

The balance between producing slightly higher hydrogen peroxide when low levels of nitric oxide are available (which probably could be handle by endogenous peroxidases, minimizing organelle damage) to peroxynitrite when sustained production of nitric oxide are attained (which will produce damage to biomolecules)

will be maintained by cellular conditions that would influence the availability of either Arg or other cofactors required for NOS activity as well as the concentration of oxygen.

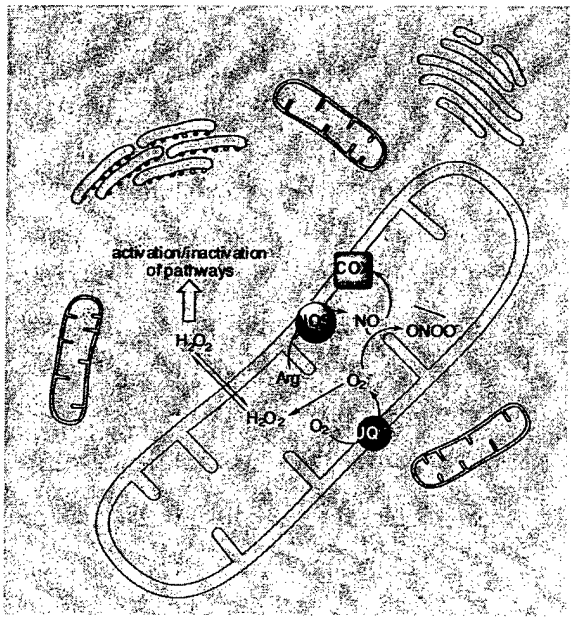

FIGURE 1: MITOCHONDRIAL RONS

4. SIGNAL TRANSDUCTION ELICITED BY RONS

A variety of extracellular and intracellular signals including the presence or absence of specific growth factors/cytokines and DNA damage result in elevation of mitochondria-derived ROS and subsequent apoptosis (reviewed in [5,43,44]). As discussed in detail elsewhere in this book, apoptosis is a controlled and regulated process involving caspase-mediated degradation of many cellular components that is often driven by elevated levels of mitochondria-derived ROS in the cytosol (reviewed in [45]). The mitochondria may serve to integrate multiple signalling events to focus the interactions that result in apoptosis and/or it may be the target of the apoptotic signal to drive caspase activation [46]. Many of these signalling pathways impact ROS levels by influencing Bcl-2 family member expression and/or localization. Pro-survival members of the Bcl2 family, including Bcl-2 and Bcl-xl, block apoptosis by blocking changes in the mitochondria membrane to prevent release of apoptosis-promoting factors and preserving mitochondria integrity [47]. In many instances, pro-apoptotic family members such as BAD, Bik, and Bid, alter the mitochondria membrane potential, resulting in elevations of cytosolic ROS. In addition, pathways that activate sphingomylinase to produce ceramide, disrupt mitochondria membrane integrity and influence ROS levels in the cytosol [48-52]. As discussed elsewhere in this book, activation of members of the MAPK kinase family of signalling molecules promotes apoptosis, to a large extent by

influencing the Bcl-2 family members transcription or cellular localization. These members include MEK1/2, which activates ERK1/2, and ASK1, which activates both the JNK and p38 MAPK pathways [53-56]. The MEK/ERK pathway has been implicated in both survival and apoptosis induction, depending on the signal and the cell system under study [57-61]. ASK1 is an integral component of the apoptotic response following TNF-α and FAS treatment [54,62-64]. Recently, ASK1 has been implicated in the apoptotic response in sympathetic neurons following NGF withdrawal, supporting a role in stress-induced apoptosis as well [65].

4.1. Molecular basis for RONS signalling

The starting point for signal transduction pathways is the ligand/receptor recognition step. This recognition is the result of a delicate balance among powerful countervailing forces of noncovalent interactions (electrostatic, hydrogen bonding, and hydrophobic forces). Conversely, the basis for free radical signalling does not entail protein-protein interaction but usually either a reduction-oxidation process or a binding reaction between the free radical and the target molecule. The specificity of free radical-mediated pathway then relies essentially on steric exposure, reduction potential (e.g., thiol group), rate constant, and binding capacity (dissociation constant of, for example, nitric oxide to heme) of the target molecule, in addition to spatial distribution of RONS production. This last condition is important for free radicals that diffuse to target molecules. Since the transport rate of diffusing substance varies inversely with the square of the distance it must diffuse, the diffusion rate of a free radical through a tissue thicker than 1 mm is too slow to support a reaction. Indeed, assuming a lifetime of a free radical of 1 ns, it can be calculated from Einstein's equation that the average distance a free radical can diffuse is about one-third of a membrane thickness or protein diameter. Thus, the target molecule must be in close proximity to the free radical source; otherwise pathway activation will be halted.

There are several mechanisms by which ROS can impact protein function. As discussed before, the nucleophilic cysteine side chains are reactive to RONS and modifications of these can alter protein functions (Reviewed in [66]). ROS can also modulate intracellular calcium ion concentrations or modify protein-protein interactions of redox-sensitive proteins [67]. There has been a massive influx of studies of the impact of ROS on cellular activity. Many of the studies that have been published on the impacts of ROS on cellular events have been done with relatively high treatment levels, so the physiological relevance of these effects remains unclear. Importantly, intracellular glutathione levels can determine whether a cell responds to ROS [68-71]. Thus discrepancies in published data may in part be the result of subtle shifts in the redox state of the cells under study.

4.2. Molecular targets of RONS

The RONS-mediated signalling pathways can be divided on the basis of their molecular target. In this Chapter, we will focus on cytosolic and nuclear proteins of relevant signal transduction pathways as targets of RONS.

4.2.1. Cytosolic proteins as molecular targets of RONS

4.2.1.1. Tyrosine phosphatase

Protein tyrosine phosphatases appear to be particularly sensitive to inactivation by RONS [66,72,73]. This inactivation is reversible, providing a basis for the speculation that regulation of phosphatase activity by ROS participates in regulation of cell signalling [72]. The impact of this is potentially enormous, as it could result in amplification of all activated signalling pathways since the removal of phosphates from phosphotyrosines in both receptors and downstream signalling molecules is integral to either activation or inactivation of several components of these pathways. This may be the case in many instances, particularly at high ROS levels used for cell response studies, but there is evidence of selective activation of specific pathways in response to ROS when studies are carried out using physiologically relevant ROS levels.

4.2.1.2. Receptor Activation

Although non-physiological hydrogen peroxide levels have been shown to activate several types of receptors, physiological levels do not have similar effects on receptor activation [74]. Physiological hydrogen peroxide levels can, however, amplify receptor responses under conditions where ligand levels are low [74]. Moreover, in the case of the insulin receptor, prolonged exposure to low hydrogen peroxide levels results in decreased signalling, suggesting that ROS impacts on receptor activity are complex [75].

4.2.1.3. MAPK pathways

The MAPK pathways are complex, intersecting pathways that impact a broad spectrum of cellular processes including proliferation, differentiation, and apoptosis (reviewed in [53,76-78]). Below are discussed components of these pathways that have been shown to be influenced by ROS. Many of the aspects of these pathways are covered in more detail elsewhere in this book.

4.2.1.3.1. c-Src family

The members of the c-Src family of tyrosine kinases act as second messengers in a broad spectrum of signalling pathways originating from both receptor kinases and receptors that do not have intrinsic kinase activity (reviewed in [76,79,80]). At millimolar levels, hydrogen peroxide activates several members of the Src family [81-85]. However, when examining lower levels of hydrogen peroxide, Lck is selectively activated [83]. The selective activation of Lck suggests that inactivation of tyrosine phosphatases is unlikely to be the Lck activation mechanism, although phosphorylation at the autophosphorylation site is required [83]. Nitric oxide selectively activates c-Src by causing aggregation of c-Src, promoting cross-

phosphorylation and amplified activation [86]. Activation of members of the c-Src family can result in activation of several pathways. A key c-Src family member activation target is Ras (reviewed in [76]). In addition, *S*-nitrosylation of cysteine 118 in by nitric oxide can also lead to Ras activation independent of Src activation [87-90]. Hydrogen peroxide stimulates Ras and JAK2 activation, but only in mice with functional c-Fyn, another member of the c-Src family that can also activate Ras [91]. Activated Ras can target the MEK/ERK, JNK, and p38 MAPK pathways (reviewed in [56,77,78,92-94]). ROS have been documented to activate all of these pathways [88,91,95-103]. Treatment with hydrogen peroxide results in Src-mediated activation of JNK, ERK1/2, and p38 MAPK [95,99,101,102]. Others have shown that superoxide anion, but not hydrogen peroxide, activates ERK 1/2, so the responses are likely to be cell type or condition-specific [98]. Superoxide anion activates p38 MAPK, most likely by activation of c-Src [102,104]. Nitric oxide activates ERK1/2, JNK, and p38 MAPK pathways [88,96,100]. The mechanisms of hydrogen peroxide-mediated activation of JNK include targeted disruption of a complex of JNK and glutathione-*S*-transferase Pi [103]. While incorporated in this complex, JNK is inactive. Hydrogen peroxide caused oligomerization of the glutathione-*S*-transferase Pi, which dissociates from the complex with JNK, leading to JNK activation.

4.2.1.3.2. Protein Kinase C

The PKC pathway is mainly impacted by ROS influences on intracellular calcium levels. ROS have been shown to increase intracellular calcium ion levels by both mobilization of intracellular stores and increases influx of calcium from the extracellular environment [105-112].

4.2.1.3.3.. Apoptosis Signalling-regulated Kinase 1 (ASK1)

The amino terminus of ASK1 can bind with Trx, blocking ASK1 activation [113]. Trx is an oxidoreductase that in induced by oxidative stress and is redox sensitive [114-116]. ROS causes Trx dimerization, resulting in release of ASK1, which forms multimers and becomes active [117,118].

4.2.2. Nuclear proteins as targets for RONS

4.2.2.1. Transcription factor AP-1

AP-1 is a dimer of members of the Fos and Jun families and regulates expression of a number of genes (reviewed in [119-124]). In yeast, hydrogen peroxide activates yAP-1, which activates genes involved in protection against oxidative stress [125]. In higher organisms, ROS also activate AP-1 [90,94,103,119,126-128]. There are several levels of AP-1 activation that are potential ROS targets: expression of Fos and Jun family members, phosphorylation of Jun members by JNK, and oxidative state of Trx. ROS increases in c-Fos and c-Jun mRNA levels, perhaps through increasing intracellular calcium levels [72,129-135]. As noted above, oxidative-mediated JNK activation has been documented. JNK specifically phosphorylates the amino terminus of Jun, promoting dimerization of with Fos family members and AP-1 activation (reviewed in [136]). AP-1 is also sensitive to oxidized Trx levels and activity is thus impacted by this redox sensitive protein [137]. The role of AP-1 in promoting stress-induced apoptosis is not fully resolved, but has been shown to activate FAS-ligand, a well-known apoptosis inducing agent (reviewed in [120-124]).

One possible mechanisms is that AP-1 has been implicated in repression of pro-survival Bcl-3 [138] and activation of the pro-apoptotic Bcl-2 family member Bax [139]. Further, AP-1 has also been shown to promote survival of cells in some instances, but the mechanisms of this are also not fully determined [120,122].

4.2.2.2. Transcription factor STATS

STAT transcription factors regulate a number of protooncogenes including c-fos and c-myc [140-142]. The JAK-STAT pathway is activated by hydrogen peroxide, raising the likelihood of regulation of transcriptional activity by ROS [143].

4.2.2.3.Transcription factor NFκB

ROS have been shown to activate NFκB in many cell types [89,94,103,126-128,144]. The mechanisms by which activation takes place appears to vary with the cell type. Inactive NFκB is sequestered in the cytosol in a complex with IκB and activation in response to external stimuli involves phosphorylation and targeted degradation of IκB (reviewed in [145]). A number of studies have supported ROS-mediated targeted degradation of IκB, either with or without increased IκB phosphorylation [84,104,146-150]. In several cell types, NFκB responds directly to oxidative stress [85,128,131,151]. Additionally, physiological levels of glutathione disulfide decrease NFκB binding to DNA, suggesting another mechanism by which NFκB responds to the redox state of the cell [137]. NFκB has been most classically associated with pro-survival responses, but activation has also been associated with apoptosis induction in some instances (reviewed in [152-156]). Pro-survival Bcl-xL and Bcl-2 increase as a result of NFκB activation in many of the systems in which NFκB is involved in promoting survival [157]. In systems where NFκB promotes apoptosis, this may be, at least in part, due to increase FAS transcription [158].

5. CONCLUSIONS

Thus, a spectrum of signalling pathways both regulate mitochondria-derived RONS in the cytosol and are downstream targets of RONS. This creates the potential for a positive feedback amplification loop, significantly impacting the rate of apoptosis. In addition, the observations that several of these pathways may promote or suppress apoptosis and are regulated by RONS further suggests that the ultimate survival of a cell is dependent on the redox state of the intracellular environment.

Acknowledgements: This work was supported by grants ES011407-01 from the National Institutes of Health, 37470-B4 Petroleum Research Fund (American Chemical Society), and CC5675 Cottrell Research Corporation to C. G and the Department of the Army Grant DAMD17-00-1-0346, the Minnesota Medical Foundation, and the Lilly Center for Women's Health to M. J. O..

6. REFERENCES

1. Menzel, D.B. Toxicity of ozone, oxygen, and radiation. *Annu Rev Pharmacol* **10**, 379-94 (1970).
2. Gerschman, R. Biological Effects of Oxygen. in *Oxygen in the Animal Organism* (eds. Dickens, F. & Niel, E.) 475-494 (Pergamon Press, London, 1964).
3. Lander, H.M. An essential role for free radicals and derived species in signal transduction. *Faseb J* **11**, 118-24 (1997).
4. Finkel, T. Oxygen radicals and signaling. *Curr Opin Cell Biol* **10**, 248-53 (1998).
5. Nose, K. Role of reactive oxygen species in the regulation of physiological functions. *Biol Pharm Bull* **23**, 897-903 (2000).
6. Chance, B., Jamieson, D. & Coles, H. Energy-linked pyridine nucleotide reduction: inhibitory effects of hyperbaric oxygen in vitro and in vivo. *Nature* **206**, 257-63 (1965).
7. Loschen, G., Flohe, L. & Chance, B. Respiratory Chain Linked H2O2 Production in Pigeon Heart Mitochondria. *FEBS Lett* **18**, 261-264 (1971).
8. Boveris, A., Oshino, N. & Chance, B. The Cellular Production of Hydorgen Peroxide. *Biochem J* **128**, 617-630 (1972).
9. Boveris, A. & Chance, B. The Mitochondrial Generation of Hydrogen Peroxide: General Properties and Effect of Hyperbaric Oxygen. *Biochem J.* **134**, 707-716 (1973).
10. Loschen, G., Azzim, A., Richter, C. & Flohe, L. Mitochondial H2O2 Formation: Relationship with Energy Conservation. *FEBS Lett* **33**, 84-88 (1973).
11. Loschen, G., Azzim, A. & Richter, C. Superoxide Radicals as Precursors of Mitochondrial Hydrogen Peroxide. *FEBS Lett* **42**, 68-72 (1974).
12. Turrens, J.F. & Boveris, A. Generation of superoxide anion by the NADH dehydrogenase of bovine heart mitochondria. *Biochem J* **191**, 421-7 (1980).
13. Giulivi, C., Boveris, A. & Cadenas, E. Oxygen Radicals in Mitochondria: Critical Evaluation of the Methodology Availabe for Estimating Steady-State Concentrations of Oxygen Radidals. in *Reactive Oxygen Species in Biological Systems: Selected Topics* (eds. Gilbert, D.L. & Colton, C.A.) 77-102 (Plenum Press, New York, 1999).
14. Oshino, N., Jamieson, D., Sugano, T. & Chance, B. Optical measurement of the catalase-hydrogen peroxide intermediate (Compound I) in the liver of anaesthetized rats and its implication to hydrogen peroxide production in situ. *Biochem J* **146**, 67-77 (1975).
15. Chance, B., Boveris, A., Oshino, N. & Loschen, G. The Nature of the Catalase Intermediate in its Biological Function. in *Oxidases and Related Redox Systems*, Vol. I (eds. King, T.E., Mason, H.S. & Morrison, M.) 350-353 (University Park Press, Baltimore, 1971).
16. Boveris, A., Cadenas, E. & Stoppani, A.O. Role of ubiquinone in the mitochondrial generation of hydrogen peroxide. *Biochem J* **156**, 435-44. (1976).

17. Beyer, R.E., Noble, W.M. & Hirschfeld, T.J. Alterations of Rat-Tissue Coenxymes Q (Ubiquinone) Levels by Various Treatments. *Biochim Biophys Acta* **57**, 376-379 (1962).
18. Bredt, D.S. & Snyder, S.H. Isolation of nitric oxide synthetase, a calmodulin-requiring enzyme. *Proc Natl Acad Sci U S A* **87**, 682-5 (1990).
19. Mayer, B., John, M. & Bohme, E. Purification of a Ca2+/calmodulin-dependent nitric oxide synthase from porcine cerebellum. Cofactor-role of tetrahydrobiopterin. *FEBS Lett* **277**, 215-9 (1990).
20. Schmidt, H.H. et al. Purification of a soluble isoform of guanylyl cyclase-activating-factor synthase. *Proc Natl Acad Sci U S A* **88**, 365-9 (1991).
21. Stuehr, D.J. & Marletta, M.A. Induction of nitrite/nitrate synthesis in murine macrophages by BCG infection, lymphokines, or interferon-gamma. *J Immunol* **139**, 518-25 (1987).
22. Forstermann, U., Schmidt, H.H., Kohlhaas, K.L. & Murad, F. Induced RAW 264.7 macrophages express soluble and particulate nitric oxide synthase: inhibition by transforming growth factor-beta. *Eur J Pharmacol* **225**, 161-5 (1992).
23. Feldman, P.L., Griffith, O.W. & Struehr, D.J. The surprising life of nitric oxide. *Chem. Eng. News* **20**, 26-38 (1993).
24. Gally, J.A., Montague, P.R., Reeke, G.N., Jr. & Edelman, G.M. The NO hypothesis: possible effects of a short-lived, rapidly diffusible signal in the development and function of the nervous system. *Proc Natl Acad Sci U S A* **87**, 3547-51 (1990).
25. Moncada, S., Palmer, R.M. & Higgs, E.A. Nitric oxide: physiology, pathophysiology, and pharmacology. *Pharmacol Rev* **43**, 109-42 (1991).
26. Wise, D.L. & Houghton, G. Diffusion coefficients of neon, krypton, xenon, carbon monoxide and nitric oxide in water at 10-60 degrees C. *Chem. Eng. Sci.* **23**, 1211-1216 (1968).
27. Furchgott, R.F. & Vanhoutte, P.M. Endothelium-derived relaxing and contracting factors. *Faseb J* **3**, 2007-18 (1989).
28. Craven, P.A. & DeRubertis, F.R. Restoration of the responsiveness of purified guanylate cyclase to nitrosoguanidine, nitric oxide, and related activators by heme and hemeproteins. Evidence for involvement of the paramagnetic nitrosyl-heme complex in enzyme activation. *J Biol Chem* **253**, 8433-43 (1978).
29. Ignarro, L.J., Adams, J.B., Horwitz, P.M. & Wood, K.S. Activation of soluble guanylate cyclase by NO-hemoproteins involves NO-heme exchange. Comparison of heme-containing and heme-deficient enzyme forms. *J Biol Chem* **261**, 4997-5002 (1986).
30. Garthwaite, J., Charles, S.L. & Chess-Williams, R. Endothelium-derived relaxing factor release on activation of NMDA receptors suggests role as intercellular messenger in the brain. *Nature* **336**, 385-8 (1988).
31. Shibuki, K. & Okada, D. Endogenous nitric oxide release required for long-term synaptic depression in the cerebellum. *Nature* **349**, 326-8 (1991).
32. Giulivi, C., Poderoso, J.J. & Boveris, A. Production of nitric oxide by mitochondria. *J Biol Chem* **273**, 11038-43 (1998).
33. Giulivi, C. Functional implications of nitric oxide produced by mitochondria in mitochondrial metabolism. *Biochem J* **332 (Pt 3)**, 673-9 (1998).

34. Giulivi, C., Sarkela, T.M., Berthiaume, J. & Elfering, S. Modulation of mitochondrial respiration by endogenous nitric oxide. *FASEb J* **13**, A1554 (1999).
35. Tatoyan, A. & Giulivi, C. Purification and characterization of a nitric-oxide synthase from rat liver mitochondria. *J Biol Chem* **273**, 11044-8 (1998).
36. Elfering, S.L., Sarkela, T.M. & Giulivi, C. Biochemistry of mitochondrial nitric-oxide synthase. *J Biol Chem* (2002).
37. Sarkela, T.M., Berthiaume, J., Elfering, S., Gybina, A.A. & Giulivi, C. The modulation of oxygen radical production by nitric oxide in mitochondria. *J Biol Chem* **276**, 6945-9 (2001).
38. Bates, T.E., Loesch, A., Burnstock, G. & Clark, J.B. Immunocytochemical evidence for a mitochondrially located nitric oxide synthase in brain and liver. *Biochem Biophys Res Commun* **213**, 896-900 (1995).
39. Kobzik, L., Stringer, B., Balligand, J.L., Reid, M.B. & Stamler, J.S. Endothelial type nitric oxide synthase in skeletal muscle fibers: mitochondrial relationships. *Biochem Biophys Res Commun* **211**, 375-81 (1995).
40. Ghafourifar, P. & Richter, C. Nitric oxide synthase activity in mitochondria. *FEBS Lett* **418**, 291-6 (1997).
41. Ghafourifar, P., Schenk, U., Klein, S.D. & Richter, C. Mitochondrial nitric-oxide synthase stimulation causes cytochrome c release from isolated mitochondria. Evidence for intramitochondrial peroxynitrite formation. *J Biol Chem* **274**, 31185-8 (1999).
42. Sugano, T., Oshino, N. & Chance, B. Mitochondrial functions under hypoxic conditions. The steady states of cytochrome c reduction and of energy metabolism. *Biochim Biophys Acta* **347**, 340-58 (1974).
43. Dormann, S. et al. Intercellular induction of apoptosis through modulation of endogenous survival factor concentration: a review. *Anticancer Res* **19**, 87-103. (1999).
44. Carmody, R.J. & Cotter, T.G. Signalling apoptosis: a radical approach. *Redox Rep* **6**, 77-90 (2001).
45. Leist, M. & Jaattela, M. Four deaths and a funeral: from caspases to alternative mechanisms. *Nat Rev Mol Cell Biol* **2**, 589-98. (2001).
46. Ranger, A.M., Malynn, B.A. & Korsmeyer, S.J. Mouse models of cell death. *Nat Genet* **28**, 113-8. (2001).
47. Quaglino, D. & Ronchetti, I.P. Cell death in the rat thymus: A minireview. *Apoptosis* **6**, 389-401. (2001).
48. Zha, J., Harada, H., Yang, E., Jockel, J. & Korsmeyer, S.J. Serine phosphorylation of death agonist BAD in response to survival factor results in binding to 14-3-3 not BCL-X(L) [see comments]. *Cell* **87**, 619-28 (1996).
49. Yang, E. et al. Bad, a heterodimeric partner for Bcl-XL and Bcl-2, displaces Bax and promotes cell death. *Cell* **80**, 285-91 (1995).
50. Roberts, M.L., Virdee, K., Sampson, C.P., Gordon, I. & Tolkovsky, A.M. The combination of bcl-2 expression and NGF-deprivation facilitates the selective destruction of BAD protein in living sympathetic neurons. *Mol Cell Neurosci* **16**, 97-110 (2000).

51. Scheid, M.P., Schubert, K.M. & Duronio, V. Regulation of bad phosphorylation and association with Bcl-x(L) by the MAPK/Erk kinase. *J Biol Chem* **274**, 31108-13 (1999).
52. Zhou, X.M., Liu, Y., Payne, G., Lutz, R.J. & Chittenden, T. Growth factors inactivate the cell death promoter BAD by phosphorylation of its BH3 domain on Ser155. *J Biol Chem* **275**, 25046-51 (2000).
53. Cross, T.G. et al. Serine/threonine protein kinases and apoptosis. *Exp Cell Res* **256**, 34-41. (2000).
54. Tobiume, K. et al. ASK1 is required for sustained activations of JNK/p38 MAP kinases and apoptosis. *EMBO Rep* **2**, 222-8. (2001).
55. Davis, R.J. Signal transduction by the c-Jun N-terminal kinase. *Biochem Soc Symp* **64**, 1-12 (1999).
56. Kolch, W. Meaningful relationships: the regulation of the Ras/Raf/MEK/ERK pathway by protein interactions. *Biochem J* **351 Pt 2**, 289-305 (2000).
57. Mitsui, H. et al. The MEK1-ERK map kinase pathway and the PI 3-kinase-Akt pathway independently mediate anti-apoptotic signals in HepG2 liver cancer cells. *Int J Cancer* **92**, 55-62. (2001).
58. Wang, X., Martindale, J.L. & Holbrook, N.J. Requirement for ERK activation in cisplatin-induced apoptosis. *J Biol Chem* **275**, 39435-43. (2000).
59. Ishikawa, Y. & Kitamura, M. Dual potential of extracellular signal-regulated kinase for the control of cell survival. *Biochem Biophys Res Commun* **264**, 696-701. (1999).
60. Moreno-Manzano, V., Ishikawa, Y., Lucio-Cazana, J. & Kitamura, M. Suppression of apoptosis by all-trans-retinoic acid. Dual intervention in the c-Jun n-terminal kinase-AP-1 pathway. *J Biol Chem* **274**, 20251-8. (1999).
61. Iryo, Y., Matsuoka, M., Wispriyono, B., Sugiura, T. & Igisu, H. Involvement of the extracellular signal-regulated protein kinase (ERK) pathway in the induction of apoptosis by cadmium chloride in CCRF-CEM cells. *Biochem Pharmacol* **60**, 1875-82. (2000).
62. Liu, Y., Yin, G., Surapisitchat, J., Berk, B.C. & Min, W. Laminar flow inhibits TNF-induced ASK1 activation by preventing dissociation of ASK1 from its inhibitor 14-3-3. *J Clin Invest* **107**, 917-23. (2001).
63. Liu, W. et al. Endothelial cell survival and apoptosis in the tumor vasculature. *Apoptosis* **5**, 323-8. (2000).
64. Ichijo, H. et al. Induction of apoptosis by ASK1, a mammalian MAPKKK that activates SAPK/JNK and p38 signaling pathways. *Science* **275**, 90-4. (1997).
65. Kanamoto, T. et al. Role of apoptosis signal-regulating kinase in regulation of the c-Jun N- terminal kinase pathway and apoptosis in sympathetic neurons. *Mol Cell Biol* **20**, 196-204. (2000).
66. Barrett, W.C. et al. Regulation of PTP1B via glutathionylation of the active site cysteine 215. *Biochemistry* **38**, 6699-705 (1999).
67. Droge, W. Free radicals in the physiological control of cell function. *Physiol Rev* **82**, 47-95 (2002).
68. Roth, S. & Droge, W. Regulation of T-cell activation and T-cell growth factor (TCGF) production by hydrogen peroxide. *Cell Immunol* **108**, 417-24 (1987).

69. Roth, S. & Droge, W. Regulation of interleukin 2 production, interleukin 2 mRNA expression and intracellular glutathione levels in ex vivo derived T lymphocytes by lactate. *Eur J Immunol* **21**, 1933-7 (1991).
70. Roth, S., Gmunder, H. & Droge, W. Regulation of intracellular glutathione levels and lymphocyte functions by lactate. *Cell Immunol* **136**, 95-104 (1991).
71. Axline, S.G. Functional biochemistry of the macrophage. *Semin Hematol* **7**, 142-60 (1970).
72. Beiqing, L., Chen, M. & Whisler, R.L. Sublethal levels of oxidative stress stimulate transcriptional activation of c-jun and suppress IL-2 promoter activation in Jurkat T cells. *J Immunol* **157**, 160-9 (1996).
73. Berlett, B.S., Levine, R.L. & Stadtman, E.R. Comparison of the effects of ozone on the modification of amino acid residues in glutamine synthetase and bovine serum albumin. *J Biol Chem* **271**, 4177-82 (1996).
74. Schmid, E., Holtz-Wagenblatt, A., Hack, V. & Droge, W. Phosphorylation of the insulin receptor kinase by phosphocreatine in combination with hydrogen peroxide. The structural basis of redox priming. *FAseb J* **13**, 1491-1500 (1999).
75. Tirosh, A., Potashnik, R., Bashan, N. & Rudich, A. Oxidative stress disrupts insulin-induced cellular redistribution of insulin receptor substrate-1 and phosphatidylinositol 3-kinase in 3T3-L1 adipocytes. A putative cellular mechanism for impaired protein kinase B activation and GLUT4 translocation. *J Biol Chem* **274**, 10595-602 (1999).
76. Porter, A.C. & Vaillancourt, R.R. Tyrosine kinase receptor-activated signal transduction pathways which lead to oncogenesis. *Oncogene* **17**, 1343-52 (1998).
77. Avruch, J. et al. Ras activation of the Raf kinase: tyrosine kinase recruitment of the MAP kinase cascade. *Recent Prog Horm Res* **56**, 127-55 (2001).
78. Campbell, S.L., Khosravi-Far, R., Rossman, K.L., Clark, G.J. & Der, C.J. Increasing complexity of Ras signaling. *Oncogene* **17**, 1395-413. (1998).
79. Superti-Furga, G. & Courtneidge, S.A. Structure-function relationships in Src family and related protein tyrosine kinases. *Bioessays* **17**, 321-30 (1995).
80. Brown, M.T. & Cooper, J.A. Regulation, substrates and functions of src. *Biochim Biophys Acta* **1287**, 121-49 (1996).
81. Brumell, J.H., Burkhardt, A.L., Bolen, J.B. & Grinstein, S. Endogenous reactive oxygen intermediates activate tyrosine kinases in human neutrophils. *J Biol Chem* **271**, 1455-61 (1996).
82. Hayashi, T., Ueno, Y. & Okamoto, T. Oxidoreductive regulation of nuclear factor kappa B. Involvement of a cellular reducing catalyst thioredoxin. *J Biol Chem* **268**, 11380-8 (1993).
83. Nakamura, K. et al. Redox regulation of a src family protein tyrosine kinase p56lck in T cells. *Oncogene* **8**, 3133-9 (1993).
84. Schoonbroodt, S. et al. Crucial role of the amino-terminal tyrosine residue 42 and the carboxyl-terminal PEST domain of I kappa B alpha in NF-kappa B activation by an oxidative stress. *J Immunol* **164**, 4292-300 (2000).

85. Schreck, R., Rieber, P. & Baeuerle, P.A. Reactive oxygen intermediates as apparently widely used messengers in the activation of the NF-kappa B transcription factor and HIV-1. *Embo J* **10**, 2247-58 (1991).
86. Akhand, A.A. et al. Nitric oxide controls src kinase activity through a sulfhydryl group modification-mediated Tyr-527-independent and Tyr-416-linked mechanism. *J Biol Chem* **274**, 25821-6 (1999).
87. Lander, H.M. et al. A molecular redox switch on p21(ras). Structural basis for the nitric oxide-p21(ras) interaction. *J Biol Chem* **272**, 4323-6 (1997).
88. Lander, H.M., Jacovina, A.T., Davis, R.J. & Tauras, J.M. Differential activation of mitogen-activated protein kinases by nitric oxide-related species. *J Biol Chem* **271**, 19705-9 (1996).
89. Lander, H.M. et al. Redox regulation of cell signalling. *Nature* **381**, 380-1 (1996).
90. Lander, H.M., Ogiste, J.S., Pearce, S.F., Levi, R. & Novogrodsky, A. Nitric oxide-stimulated guanine nucleotide exchange on p21ras. *J Biol Chem* **270**, 7017-20 (1995).
91. Abe, J. & Berk, B.C. Fyn and JAK2 mediate Ras activation by reactive oxygen species. *J Biol Chem* **274**, 21003-10 (1999).
92. Yordy, J.S. & Muise-Helmericks, R.C. Signal transduction and the Ets family of transcription factors. *Oncogene* **19**, 6503-13 (2000).
93. Segal, R.A. & Greenberg, M.E. Intracellular signaling pathways activated by neurotrophic factors. *Annu Rev Neurosci* **19**, 463-89 (1996).
94. Adler, V., Yin, Z., Tew, K.D. & Ronai, Z. Role of redox potential and reactive oxygen species in stress signaling. *Oncogene* **18**, 6104-11 (1999).
95. Abe, J., Kusuhara, M., Ulevitch, R.J., Berk, B.C. & Lee, J.D. Big mitogen-activated protein kinase 1 (BMK1) is a redox-sensitive kinase. *J Biol Chem* **271**, 16586-90 (1996).
96. Callsen, D., Pfeilschifter, J. & Brune, B. Rapid and delayed p42/p44 mitogen-activated protein kinase activation by nitric oxide: the role of cyclic GMP and tyrosine phosphatase inhibition. *J Immunol* **161**, 4852-8 (1998).
97. Elbirt, K.K., Whitmarsh, A.J., Davis, R.J. & Bonkovsky, H.L. Mechanism of sodium arsenite-mediated induction of heme oxygenase-1 in hepatoma cells. Role of mitogen-activated protein kinases. *J Biol Chem* **273**, 8922-31 (1998).
98. Baas, A.S. & Berk, B.C. Differential activation of mitogen-activated protein kinases by H2O2 and O2- in vascular smooth muscle cells. *Circ Res* **77**, 29-36 (1995).
99. Ushio-Fukai, M., Alexander, R.W., Akers, M. & Griendling, K.K. p38 Mitogen-activated protein kinase is a critical component of the redox-sensitive signaling pathways activated by angiotensin II. Role in vascular smooth muscle cell hypertrophy. *J Biol Chem* **273**, 15022-9 (1998).
100. Pfeilschifter, J. & Huwiler, A. Nitric oxide stimulates stress-activated protein kinases in glomerular endothelial and mesangial cells. *FEBS Lett* **396**, 67-70 (1996).
101. Yoshizumi, M., Abe, J., Haendeler, J., Huang, Q. & Berk, B.C. Src and Cas mediate JNK activation but not ERK1/2 and p38 kinases by reactive oxygen species. *J Biol Chem* **275**, 11706-12 (2000).
102. Pu, M. et al. Evidence of a novel redox-linked activation mechanism for the Src kinase which is independent of tyrosine 527-mediated regulation. *Oncogene* **13**, 2615-22 (1996).

103. Adler, V. et al. Regulation of JNK signaling by GSTp. *Embo J* **18**, 1321-34 (1999).
104. Hehner, S.P. et al. Enhancement of T cell receptor signaling by a mild oxidative shift in the intracellular thiol pool. *J Immunol* **165**, 4319-28 (2000).
105. Doan, T.N., Gentry, D.L., Taylor, A.A. & Elliott, S.J. Hydrogen peroxide activates agonist-sensitive Ca(2+)-flux pathways in canine venous endothelial cells. *Biochem J* **297 (Pt 1)**, 209-15 (1994).
106. Dreher, D. & Junod, A.F. Role of oxygen free radicals in cancer development. *Eur J Cancer* **32A**, 30-8 (1996).
107. Hallbrucker, C., Ritter, M., Lang, F., Gerok, W. & Haussinger, D. Hydroperoxide metabolism in rat liver. K+ channel activation, cell volume changes and eicosanoid formation. *Eur J Biochem* **211**, 449-58 (1993).
108. Kumasaka, S., Shoji, H. & Okabe, E. Novel mechanisms involved in superoxide anion radical-triggered Ca2+ release from cardiac sarcoplasmic reticulum linked to cyclic ADP-ribose stimulation. *Antioxid Redox Signal* **1**, 55-69 (1999).
109. Okabe, E. et al. Calmodulin participation in oxygen radical-induced cardiac sarcoplasmic reticulum calcium uptake reduction. *Arch Biochem Biophys* **255**, 464-8 (1987).
110. Okabe, E. et al. The effect of ryanodine on oxygen free radical-induced dysfunction of cardiac sarcoplasmic reticulum. *J Pharmacol Exp Ther* **256**, 868-75 (1991).
111. Okabe, E., Sugihara, M., Tanaka, K., Sasaki, H. & Ito, H. Calmodulin and free oxygen radicals interaction with steady-state calcium accumulation and passive calcium permeability of cardiac sarcoplasmic reticulum. *J Pharmacol Exp Ther* **250**, 286-92 (1989).
112. Roveri, A. et al. Effect of hydrogen peroxide on calcium homeostasis in smooth muscle cells. *Arch Biochem Biophys* **297**, 265-70 (1992).
113. Saitoh, M. et al. Mammalian thioredoxin is a direct inhibitor of apoptosis signal-regulating kinase (ASK) 1. *Embo J* **17**, 2596-606 (1998).
114. Matsui, M. et al. Early embryonic lethality caused by targeted disruption of the mouse thioredoxin gene. *Dev Biol* **178**, 179-85 (1996).
115. Sachi, Y. et al. Induction of ADF/TRX by oxidative stress in keratinocytes and lymphoid cells. *Immunol Lett* **44**, 189-93 (1995).
116. Taniguchi, Y., Taniguchi-Ueda, Y., Mori, K. & Yodoi, J. A novel promoter sequence is involved in the oxidative stress-induced expression of the adult T-cell leukemia-derived factor (ADF)/human thioredoxin (Trx) gene. *Nucleic Acids Res* **24**, 2746-52 (1996).
117. Gopalakrishna, R. & Anderson, W.B. Ca2+- and phospholipid-independent activation of protein kinase C by selective oxidative modification of the regulatory domain. *Proc Natl Acad Sci U S A* **86**, 6758-62 (1989).
118. Konishi, H. et al. Activation of protein kinase C by tyrosine phosphorylation in response to H2O2. *Proc Natl Acad Sci U S A* **94**, 11233-7 (1997).
119. Angel, P. & Karin, M. The role of Jun, Fos and the AP-1 complex in cell-proliferation and transformation. *Biochim Biophys Acta* **1072**, 129-57 (1991).
120. Shaulian, E. & Karin, M. AP-1 as a regulator of cell life and death. *Nat Cell Biol* **4**, E131-6 (2002).

121. Karin, M. & Shaulian, E. AP-1: linking hydrogen peroxide and oxidative stress to the control of cell proliferation and death. *IUBMB Life* **52**, 17-24 (2001).
122. Shaulian, E. & Karin, M. AP-1 in cell proliferation and survival. *Oncogene* **20**, 2390-400 (2001).
123. Shaulian, E. et al. The mammalian UV response: c-Jun induction is required for exit from p53-imposed growth arrest. *Cell* **103**, 897-907 (2000).
124. Shaulian, E. & Karin, M. Stress-induced JNK activation is independent of Gadd45 induction. *J Biol Chem* **274**, 29595-8 (1999).
125. Kuge, S. & Jones, N. YAP1 dependent activation of TRX2 is essential for the response of Saccharomyces cerevisiae to oxidative stress by hydroperoxides. *Embo J* **13**, 655-64 (1994).
126. Flohe, L., Brigelius, R., Saliou, C. & Traber, M. Redox regulation of NF-kB activation. *Free Radic Biol Med* **22**, 1115-1126 (1997).
127. Piette, J. et al. Multiple redox regulation in NF-kappaB transcription factor activation. *Biol Chem* **378**, 1237-45 (1997).
128. Sen, C. & Packer, L. Antioxidant and redox regulation of gene transcription. *Faseb J* **10**, 709-720 (1996).
129. Crawford, D., Zbinden, I., Amstad, P. & Cerutti, P. *Expression of oxidant stress-related genes in tumor promotion of mouse epidermal cells JB6.*, 183-190 (Plenum, New York, 1987).
130. Janssen, Y.M., Matalon, S. & Mossman, B.T. Differential induction of c-fos, c-jun, and apoptosis in lung epithelial cells exposed to ROS or RNS. *Am J Physiol* **273**, L789-96 (1997).
131. Meyer, M., Schreck, R. & Baeuerle, P.A. H2O2 and antioxidants have opposite effects on activation of NF-kappa B and AP-1 in intact cells: AP-1 as secondary antioxidant-responsive factor. *Embo J* **12**, 2005-15 (1993).
132. Maki, A., Berezesky, I.K., Fargnoli, J., Holbrook, N.J. & Trump, B.F. Role of [Ca2+]i in induction of c-fos, c-jun, and c-myc mRNA in rat PTE after oxidative stress. *Faseb J* **6**, 919-24 (1992).
133. Morris, B.J. Stimulation of immediate early gene expression in striatal neurons by nitric oxide. *J Biol Chem* **270**, 24740-4 (1995).
134. Muehlematter, D., Ochi, T. & Cerutti, P. Effects of tert-butyl hydroperoxide on promotable and non-promotable JB6 mouse epidermal cells. *Chem Biol Interact* **71**, 339-52 (1989).
135. Shibanuma, M., Kuroki, T. & Nose, K. Induction of DNA replication and expression of proto-oncogene c-myc and c-fos in quiescent Balb/3T3 cells by xanthine/xanthine oxidase. *Oncogene* **3**, 17-21 (1988).
136. Weston, C.R. & Davis, R.J. The JNK signal transduction pathway. *Curr Opin Genet Dev* **12**, 14-21 (2002).
137. Galter, D., Mihm, S. & Droge, W. Distinct effects of glutathione disulphide on the nuclear transcription factor kappa B and the activator protein-1. *Eur J Biochem* **221**, 639-48 (1994).
138. Rebollo, A. et al. Bcl-3 expression promotes cell survival following interleukin-4 deprivation and is controlled by AP1 and AP1-like transcription factors. *Mol Cell Biol* **20**, 3407-16 (2000).
139. Lei, K. et al. The Bax subfamily of Bcl2-related proteins is essential for apoptotic signal transduction by c-Jun NH(2)-terminal kinase. *Mol Cell Biol* **22**, 4929-42 (2002).

140. Jenab, S. & Quinones-Jenab, V. The effects of interleukin-6, leukemia inhibitory factor and interferon-gamma on STAT DNA binding and c-fos mRNA levels in cortical astrocytes and C6 glioma cells. *Neuroendocrinol Lett* **23**, 325-8 (2002).
141. Kolonics, A. et al. Unregulated activation of STAT-5, ERK1/2 and c-Fos may contribute to the phenotypic transformation from myelodysplastic syndrome to acute leukaemia. *Haematologia (Budap)* **31**, 125-38 (2001).
142. Servidei, T. et al. Coordinate regulation of STAT signaling and c-fos expression by the tyrosine phosphatase SHP-2. *J Biol Chem* **273**, 6233-41 (1998).
143. Simon, A.R., Rai, U., Fanburg, B.L. & Cochran, B.H. Activation of the JAK-STAT pathway by reactive oxygen species. *Am J Physiol* **275**, C1640-52 (1998).
144. Monteiro, H.P. & Stern, A. Redox modulation of tyrosine phosphorylation-dependent signal transduction pathways. *Free Radic Biol Med* **21**, 323-33 (1996).
145. Cramer, P. & Muller, C.W. A firm hand on NFkappaB: structures of the IkappaBalpha-NFkappaB complex. *Structure Fold Des* **7**, R1-6 (1999).
146. Beg, A.A., Finco, T.S., Nantermet, P.V. & Baldwin, A.S., Jr. Tumor necrosis factor and interleukin-1 lead to phosphorylation and loss of I kappa B alpha: a mechanism for NF-kappa B activation. *Mol Cell Biol* **13**, 3301-10 (1993).
147. Kretz-Remy, C., Bates, E.E. & Arrigo, A.P. Amino acid analogs activate NF-kappaB through redox-dependent IkappaB-alpha degradation by the proteasome without apparent IkappaB-alpha phosphorylation. Consequence on HIV-1 long terminal repeat activation. *J Biol Chem* **273**, 3180-91 (1998).
148. Kretz-Remy, C., Mehlen, P., Mirault, M.E. & Arrigo, A.P. Inhibition of I kappa B-alpha phosphorylation and degradation and subsequent NF-kappa B activation by glutathione peroxidase overexpression. *J Cell Biol* **133**, 1083-93 (1996).
149. Manna, S.K., Zhang, H.J., Yan, T., Oberley, L.W. & Aggarwal, B.B. Overexpression of manganese superoxide dismutase suppresses tumor necrosis factor-induced apoptosis and activation of nuclear transcription factor-kappaB and activated protein-1. *J Biol Chem* **273**, 13245-54 (1998).
150. Traenckner, E.B., Wilk, S. & Baeuerle, P.A. A proteasome inhibitor prevents activation of NF-kappa B and stabilizes a newly phosphorylated form of I kappa B-alpha that is still bound to NF-kappa B. *Embo J* **13**, 5433-41 (1994).
151. Mihm, S., Ennen, J., Pessara, U., Kurth, R. & Droge, W. Inhibition of HIV-1 replication and NF-kappa B activity by cysteine and cysteine derivatives. *Aids* **5**, 497-503 (1991).
152. Romas, E., Gillespie, M.T. & Martin, T.J. Involvement of receptor activator of NFkappaB ligand and tumor necrosis factor-alpha in bone destruction in rheumatoid arthritis. *Bone* **30**, 340-6 (2002).
153. Said, S.I. & Dickman, K.G. Pathways of inflammation and cell death in the lung: modulation by vasoactive intestinal peptide. *Regul Pept* **93**, 21-9 (2000).
154. Leong, K.G. & Karsan, A. Signaling pathways mediated by tumor necrosis factor alpha. *Histol Histopathol* **15**, 1303-25 (2000).

155. Hatada, E.N., Krappmann, D. & Scheidereit, C. NF-kappaB and the innate immune response. *Curr Opin Immunol* **12**, 52-8 (2000).
156. Li, X. & Stark, G.R. NFkappaB-dependent signaling pathways. *Exp Hematol* **30**, 285-96 (2002).
157. Glasgow, J.N. et al. Transcriptional regulation of the BCL-X gene by NF-kappaB is an element of hypoxic responses in the rat brain. *Neurochem Res* **26**, 647-59 (2001).
158. Kuhnel, F. et al. NFkappaB mediates apoptosis through transcriptional activation of Fas (CD95) in adenoviral hepatitis. *J Biol Chem* **275**, 6421-7 (2000).

Journal of Cellular Biochemistry 89:165–179 (2003)

Phosphatidylinositol 3-Kinase Coordinately Activates the MEK/ERK and AKT/NFκB Pathways to Maintain Osteoclast Survival

Anne Gingery,[1] Elizabeth Bradley,[1] Aubie Shaw,[1] and Merry Jo Oursler[1,2]*

[1]Department of Biochemistry and Molecular Biology, University of Minnesota, Duluth, Minnesota 55812
[2]Departments Biology, and Medical Microbiology and Immunology, University of Minnesota, Duluth, Minnesota 55812

Abstract We have examined highly purified osteoclasts that were generated in vitro from murine co-culture of marrow precursors with stromal support cells and have found evidence of activation of the MEK/ERK and AKT/NFκB survival pathways. Many mature marrow-derived osteoclasts survived for at least 48 h in culture whether or not they are maintained with stromal cells. Moreover, supplementing purified osteoclasts with RANKL and/or M-CSF had no impact on their survival pattern. In addition, spleen-derived osteoclasts generated with RANKL and M-CSF treatment exhibited a similar survival pattern. Blocking MEK, AKT, or NFκB activity resulted in apoptosis of many, but not all, of the osteoclasts in purified marrow-derived osteoclasts, marrow-derived osteoclasts co-cultured with stromal cells, and spleen-derived osteoclasts maintained with RANKL and M-CSF. These data support that both the MEK/ERK and AKT/NFκB pathways contribute to osteoclast survival. Since PI3K has been shown to activate either of these pathways, we have examined its role in osteoclast survival. PI3K inhibition caused apoptosis of nearly all osteoclasts in purified and co-cultured marrow-derived osteoclasts and spleen-derived osteoclasts maintained with RANKL and M-CSF. Interestingly, in marrow-derived co-cultures, the apoptotic response was restricted to osteoclasts as there was no evidence of stromal support cell apoptosis. PI3K inhibition also blocked MEK1/2, ERK1/2, and AKT phosphorylation and NFκB activation in purified osteoclasts. Simultaneous blockage of both AKT and MEK1/2 caused rapid apoptosis of nearly all osteoclasts, mimicking the response to PI3K inhibition. These data reveal that PI3K coordinately activates two distinct survival pathways that are both important in osteoclast survival. J. Cell. Biochem. 89: 165–179, 2003.

Key words: osteoclast; apoptosis; PI3K; MEK; ERK; AKT; NFκB

Osteoclasts are the multinucleated hematopoetic cells that are responsible for most, if not all, cellular-based bone destruction in vertebrates. Osteoclast numbers are the main determinant of the rate of bone resorption and it is of great interest to understand how osteoclast numbers are controlled [Suda et al., 1997]. It is becoming increasingly evident that osteoclast disappearance in vivo is the result of apoptosis [Lutton et al., 1996; Roodman, 1999]. Apoptosis is a controlled series of events that results in biochemical and morphological changes including membrane blebbing, cell shrinkage, DNA fragmentation, chromatin condensation, and formation of apoptotic bodies. The mechanisms by which mature osteoclasts survive remains unresolved, but conflicting studies have implicated either the PI3K/AKT/NFκB or the MEK/ERK pathways in osteoclast survival [Ozaki et al., 1997; Lacey et al., 2000; Miyazaki et al., 2000; Lee et al., 2001, 2002a,b; Lee and McCubrey, 2002].

The MEK/ERK pathway has been implicated in both survival and apoptosis induction, depending on the signal and the cell system under study [Ishikawa and Kitamura, 1999; Moreno-Manzano et al., 1999; Iryo et al., 2000; Wang et al., 2000; Mitsui et al., 2001]. Miyazaki et al. [2000] examined the roles of MEK in osteoclast survival. This study documented that

Grant sponsor: Department of the Army; Grant number: DAMD17-00-1-0346; Grant sponsor: Minnesota Medical Foundation; Grant sponsor: Lilly Center for Women's Health.

*Correspondence to: Merry Jo Oursler, PhD, University of Minnesota, 211 Life Science, 10 University Drive, Duluth, MN 55812. E-mail: moursler@d.umn.edu

Received 25 November 2002; Accepted 16 January 2003
DOI 10.1002/jcb.10503

expression of constitutively active MEK caused enhanced osteoclast survival. In support of a role for this pathway in osteoclast survival, others have demonstrated that ERK activation is important in IL-1 and TNF-α-mediated osteoclast survival [Lee et al., 2001, 2002b].

The AKT/NFκB pathway is important in promoting survival of a spectrum of cell types [Romashkova and Makarov, 1999; Jones et al., 2000; Lee et al., 2000; Madge and Pober, 2000; Madrid et al., 2000; Reddy et al., 2000]. The role of AKT in preventing apoptosis following growth factor withdrawal is well documented, but there is also evidence implicating it in survival in a number of other systems. These include IGF-I, EGF, oxygen stress, TNF-α, IL-1, and PDGF-BB responses in various cells such as osteoblasts, endothelial cells, and epithelial cells [Ahmad et al., 1999; Ushio-Fukai et al., 1999; Madge and Pober, 2000; Wang et al., 2000; Chaudhary and Hruska, 2001; Hong et al., 2001]. There are conflicting reports of the role of NFκB in osteoclast survival. Ozaki et al. [1997] have shown that chemical inhibition of NFκB stimulated osteoclast apoptosis and inhibited resorption, suggesting that NFκB activation regulation is a key component in controlling osteoclast apoptosis. In contrast, Miyazaki et al. [2000] used expression of a dominant interfering form of IKK to inhibit NFκB activation and found that this had no impact on osteoclast survival. Thus, the role of NFκB in the regulation of osteoclast survival and apoptosis is unresolved.

PI3K is a lipid kinase that activates a variety of signaling pathways including the MEK/ERK as well as the AKT/NFκB pathways [Klippel et al., 1997; Scheid and Duronio, 1998; Kelley et al., 1999; Burow et al., 2000; Kuwahara et al., 2000; Lederer et al., 2000; Bisotto and Fixman, 2001; Mograbi et al., 2001; Nosaka et al., 2001; Agazie et al., 2002]. Some studies have documented that PI3K is involved in activation of the MEK/ERK pathway while others have demonstrated that ligand concentration determines whether PI3K impacts this pathway [King et al., 1997; Wennstrom and Downward, 1999; McCubrey et al., 2001; Sheng et al., 2001; von Gise et al., 2001]. There have also been instances in which cross-talk between these pathways have been reported in which the PI3K target AKT directly phosphorylates and inactivates Raf-1 to repress the MEK/ERK pathway [Rommel et al., 1999; Zimmermann and Moelling, 1999; Reusch et al., 2001; Moelling et al., 2002]. Since studies have documented that NFκB and MEK may be involved in modulating osteoclast survival by blocking apoptosis, we have investigated the relationship of these pathways in promoting osteoclast survival.

MATERIALS AND METHODS

Materials

Unless otherwise noted, all chemicals were from Sigma Chemical Co., St. Louis, MO.

Osteoclast Culture and Purification

Mouse marrow and spleen containing osteoclast precursors were obtained from female BalB/c mice (Taconic, Germantown, NY). Four- to six-week-old mice were sacrificed and long bones of the hind limbs and spleen were aseptically removed. The distal ends of bones were clipped and the marrow was flushed out by injecting sterile Mosconas buffer (8% NaCl, 0.2% KCl, 0.06% $NaH_2PO_4 + H_2O$, 2% glucose, 0.02% bicarbonate) into the marrow cavity with a 27-gauge needle. Marrow cells were counted and stored at 2.4×10^6 cells/tube in liquid nitrogen until used. Freezing media consisted of 12% dimethylsulfoxide (DMSO) in fetal bovine serum (FBS) as has been previously reported [Wesolowski et al., 1995]. To generate marrow-derived osteoclasts, precursors were cultured with ST2 stromal cells (Riken Cell Bank, Tsukuba, Japan) during differentiation as follows: apoptosis assessment: ST2 cells were plated in alpha-modified minimal essential media (αMEM, Gibco BRL, Grand Island, NY) supplemented with 10% FBS (Hyclone, Logan, UT) and antibiotic/antimycotic in 24-well plates on glass coverslips at a density of 1.6×10^5 cells/well. Biochemical assessments (Western blotting and electrophoretic mobility shift assay (EMSA) analysis): ST2 cells were plated in 6-well plates at a density of 6.4×10^5 cells/well. After 24 h of culture, marrow precursors were plated as follows: for 24-well plates, marrow were added at 1.18×10^5 cells/well, and for 6-well plates, marrow cells were added at 4.75×10^5 cells/well. Precursors were added to the stromal cells using MEM, 10% FBS, 1% nonessential amino acids, and 1% penicillin/streptomycin (base medium). Base medium was supplemented with 7×10^{-3} M ascorbic acid (Gibco BRL, Rockville, MD), 1×10^{-7} M dexamethasone, and 1×10^{-5} M vitamin D_3 (BioMol,

Plymouth Meeting, PA) immediately before use [Takahashi et al., 1988; Udagawa et al., 1990]. Cells were fed every 3 days until 13 days of culture. Osteoclast-like cells are purified by treatment for 15 min at 37°C with 0.2 mg/ml collagenase (Worthington Biochemicals, Lakewood, NJ) in Ham's F12 media (Gibco BRL) followed by 30 min at 37°C with 0.2 mg/ml dispase (Boehringer Mannheim, Framingham, MA) in Ham's F12 media to remove support cells. For generating spleen-derived osteoclasts, spleen cells were plated at 4×10^6 spleen cells per well in a 24-well plate as published papers have detailed for this model system [Sells Galvin et al., 1999]. Base medium was supplemented with 7×10^{-3} M ascorbic acid prior to plating the cells and cultures were supplemented with 30 ng/ml of RANKL (Calbiochem, La Jolla, CA) and 25 ng/ml of macrophage colony stimulating factor (M-CSF) (R&D, Minneapolis, MN). For both marrow- and spleen-derived cultures, media was changed every 3 days and cells were either fixed in 1% paraformaldehyde in phosphate buffered saline to terminate culture or treated as detailed below for individual experiments.

Western Blotting

Osteoclasts were purified as above and either harvested immediately for Western blotting or cultured in MEM for the indicated time period, rinsed with Mosconas buffer, and harvested for Western blotting. Harvesting was accomplished by scraping into SDS sample buffer lacking ß-mercaptoethanol and sodium dodecyl sulfate. To insure that equal cell protein was analyzed, equal (40 μg) cell protein (as determine using BioRad's Protein Quantitation in Detergent Analysis kit) was loaded in each lane. Following protein quantitation, ß-mercaptoethanol and sodium dodecyl sulfate were added to the samples. Parallel Western blotting was carried out as directed in the product literature using antibodies directed against phospho- or total ERK1/2, MEK1/2, or AKT at a 1: 2,000 dilution and secondary antibodies at a 1:10,000 dilution with chemiluminescent detection using the Pierce (Rockford, IL). All antibodies were from Cell Signaling (Beverly, MA).

Apoptosis Detection

Marrow-derived osteoclasts that were either maintained with stromal cells or purified as above were cultured in base media for the indicated time period, fixed with 1% paraformaldehyde and stained. Staining for two apoptotic measures was as given below.

Chromatin condensation. Fixed osteoclasts were stained for 60 min with Hoechst 33258 diluted to 5 μg/ml in phosphate buffered saline with 0.01% Tween 20. The cells were then TRAP stained using a kit from Sigma Chemical Co.

DNA fragmentation. Terminal deoxynucleotide transferase (TdT)-mediated labeling of fragmented DNA with fluorochrome conjugated nucleotides was carried out using the FragEL detection kit, following manufacturer's instructions (Calbiochem). After labeling, cells were examined with fluorescent microscopy, and cells displaying strongly labeled/condensed nuclei were scored as apoptotic.

Pattern of Osteoclast Survival

To examine the timing of osteoclast apoptosis, mature marrow-derived osteoclasts were either maintained with stromal cells or purified as above, and culture conditions were continued as indicated in the figure legend. Spleen-derived osteoclasts were maintained with RANKL and M-CSF throughout culture and treatments. Cells were fixed and then Hoechst and TRAP stained as above.

Inhibition of Signaling Pathway Components

Osteoclasts were generated and then either pretreated for 45 min or purified in the presence of either vehicle (DMSO), the PI3K inhibitors LY294002 (50 μM) or wortmannin (10 μM), the MEK 1 inhibitor PD98059 (50 μM), the MEK1/2 inhibitor U0126 (10 μM), an AKT inhibitor, a phosphatidylinositol ether analog (Calbiochem, San Diego, CA) (5 μM), or the NFκB activation inhibitor pyrrolidine dithiocarbamate (PDTC) (0.2 mM). Osteoclasts were either fixed (time zero) or cultured for 90 min in the continued presence of either vehicle or the indicated inhibitor, and assessed for apoptosis using chromatin condensation as above or analyzed by Western blotting (MEK inhibition and antiphospho ERK Western blot) or EMSA (NFκB inhibition and NFκB activation analysis) as detailed below.

EMSA

Purified osteoclasts were cultured for 0, 5, 10, or 15 min and harvested on ice. Cell pellets were scraped with hypotonic buffer (10 mM Tris-HCl,

pH 7.4, 10 mM NaCl, 30 mM $MgCl_2$, 0.02% sodium azide, and 1 mM each of phenylmethanesulfonyl fluoride, pepstatin, aprotinin, and leupeptin). After 10 min on ice, 0.05% non-idet P-40 was added and nuclei pelleted by centrifugation at 2,500*g* for 5 min. Pellets were washed in the above buffer and resuspended in 20 mM HEPES, pH 7.4, 420 mM NaCl, 1.5 mM $MgCl_2$, 0.2 mM EDTA, 25% glycerol, 0.01% sodium azide with the above proteinase inhibitors. Nuclear proteins were recovered from the supernatant following centrifugation at 12,000*g* for 10 min. A double stranded oligonucleotide containing the site of interest was end labeled with T4 polynucleotide kinase using γ^{32}P[ATP]. The NFκB target sequence used was: 5′-AGTTGAGGGGACTTTCCCAGGC-3′. The binding assay was performed by incubation of 5 μg of nuclear proteins with 10,000 dpm of the labeled oligonucleotide and 0.5 μg of oligo (dI-dT) in 8.5 mM HEPES, pH 7, 104 mM NaCl, 0.2 mM DTT, 8.5% glycerol for 20 min at 25°C. Treatment was followed by polyacrylamide gel electrophoresis in a 7% non-denaturing gel. Gels were dried and examined by autoradiography. Parallel EMSA of the 15-min nuclear extract in the presence of antibodies (2 μg; Santa Cruz Biotechnology, Santa Cruz, CA) directed against the p65 subunit (p65) was also examined.

Statistical Analysis

The results represent the mean ± SEM of three replicates from one experiment. Each experiment was carried out a minimum of three times and the results shown are representative of all results obtained. The effect of treatment was compared with control values by one-way analysis of variance (ANOVA); significant treatment effects were further evaluated by the Fisher's least significant difference method of multiple comparisons in a ANOVA. Tests were carried out using Apple software, obtained from Statview II, Abacus Concepts, Inc., Cupertino, CA.

RESULTS

Examination of Active Signaling Pathways in Purified Osteoclasts

As an initial study to characterize these cells, osteoclasts were generated from co-culture of marrow and ST2 support cells and purified by enzymatic removal of stromal cells. Cells were immediately harvested and analyzed by

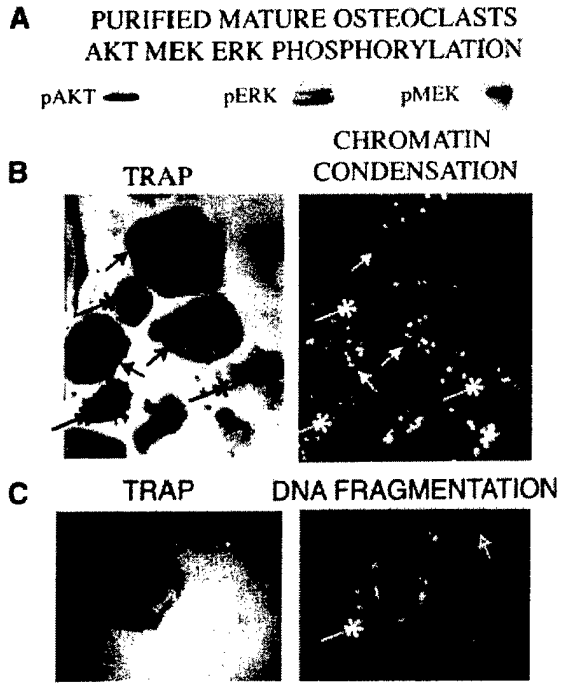

Fig. 1. Characterization of purified osteoclasts. **A:** Mature marrow-derived osteoclasts were purified and immediately harvested. Forty micrograms of protein were analyzed by Western blotting for phospho-AKT (pAKT), phospho-MEK (pMEK), phospho-ERK1/2 (pERK1/2). Evaluation of osteoclast apoptosis. **B, C:** Purified marrow-derived osteoclasts were cultured for 90 min, fixed, and stained for TRAP and apoptosis by detecting either chromatin condensation by Hoechst staining (B) or DNA fragmentation staining (C). Arrows point to selected non-apoptotic osteoclasts. The stars indicate selected apoptotic osteoclasts.

Western blotting using phospho-specific antibodies to pAKT, pMEK, and pERK1/2 (Fig. 1A). We observed that there was phosphorylation of AKT, MEK, and ERK1/2 in these cells. By 90 min of culture, there was no detectable phosphorylation of these proteins (data not shown). These data documented that mature osteoclasts showed evidence of transiently activated AKT, MEK, and ERK1/2, intracellular proteins that are reported to promote osteoclast survival. We, therefore, initiated studies to examine whether activation of these proteins in mature osteoclasts had an impact on their survival, the focus of this manuscript. For our first studies, we examined purified osteoclast survival following 90 min of culture using two measures for osteoclast apoptosis, chromatin condensation and DNA fragmentation (Fig. 1B,C). The condensed nuclei (Fig. 1B) and DNA fragmentation staining (Fig. 1C) distinguish apoptotic osteoclasts. Stars point to selected apoptotic osteoclasts

based on Hoechst staining (Fig. 1B) or DNA fragmentation detection (Fig. 1C). The arrows point to selected surviving osteoclasts.

Pattern of Osteoclast Survival in Culture

Having observed that many mature osteoclasts contain active pro-survival intracellular proteins and survived following stromal cell removal, we examined how long osteoclasts could maintain themselves in vitro with and without the presence of stromal cells using TRAP and Hoechst staining. For these studies, we examined mouse osteoclasts from two sources for their survival patterns in vitro: marrow-derived osteoclasts generated in co-culture as above and spleen-derived osteoclasts differentiated in vitro with RANKL and M-CSF (Fig. 2). Once mature, marrow cells co-cultured with stromal cells were either purified as above (Fig. 2A) or maintained in co-culture (Fig. 2B). As documented in the purified osteoclasts graph there was rapid apoptosis of approximately 25% of the osteoclasts present during 90 min of further culture. With longer culture, a significant proportion of surviving osteoclasts continued to show no indication of apoptosis. We have examined cultures for detached osteoclasts by cytospinning culture supernatants and have found a few apoptotic bodies. Due to the inability to determine cell numbers from these, we are restricting our analysis to counting apoptotic intact osteoclasts. However, the total number of osteoclasts did not appreciably decrease over time, suggesting that there were few cells released from the

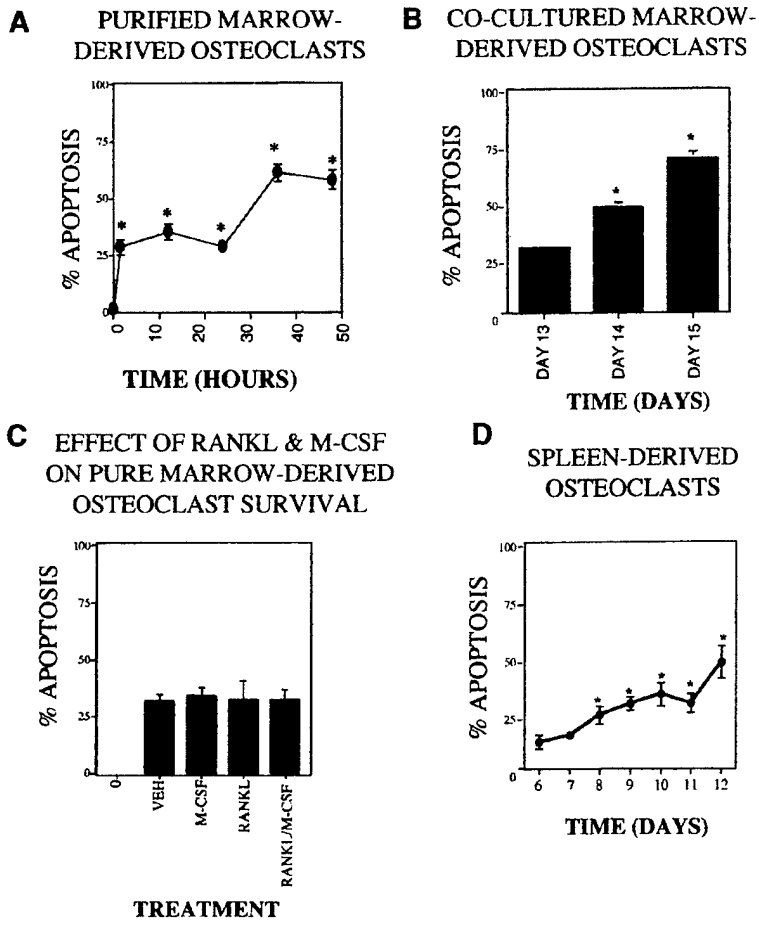

Fig. 2. The pattern of osteoclast apoptosis. Marrow-derived osteoclasts were either purified and cultured for the indicated time (**A**), fixed at the indicated time as co-cultures (**B**), or purified and cultured with 10 ng/ml RANKL and/or 25 ng/ml M-CSF as indicated (**C**). Spleen-derived osteoclasts were maintained with RANKL and M-CSF and analyzed on the indicated day of culture (**D**). The cells were stained for TRAP and chromatin condensation. Apoptotic osteoclasts were identified as TRAP stained cells having highly condensed nuclei. The percentage of apoptotic osteoclasts is shown (mean ± SEM of three replicates). $*P < 0.05$ compared to earliest time point.

coverslip. These studies raised the possibility that stromal cell removal may be a trigger for osteoclast apoptosis. Since osteoclasts do not exist in vivo in the absence of stromal cells, we have examined mature osteoclast cultures maintained with stromal cells for apoptotic osteoclasts over a time period similar to the above studies (Fig. 2B). On culture day 13, approximately 25% of the osteoclasts were apoptotic. Over the following 2 days, the proportion of apoptotic osteoclasts further increased on each successive day during co-culture with support cells. The discrepancy between the purified (Fig. 2A) and co-culture day 13 time point (Fig. 2B) is likely due to removal of apoptotic osteoclasts from the coverslip when the stromal cells were enzymatically removed. We have also examined the influence of replacing RANKL and/or M-CSF to the purified osteoclasts (Fig. 2C) and observed that replacing RANKL or M-CSF or both for 90 min of culture had no impact on apoptosis. To examine mouse osteoclasts from a precursor population that has few, if any, stromal cells, we used spleen cells cultured without stromal cells as another model systems (Fig. 2D). Spleen-derived osteoclasts were fixed after the indicated time in culture, stained, and evaluated as outlined above. As documented in Figure 2D, there were some apoptotic osteoclasts appearing by the first day of analysis, day 6. There was a significant elevation in apoptosis above this level beginning at day 8 and lasting throughout the analysis time. As with the marrow-derived osteoclasts above, there was significant numbers of surviving osteoclasts in these cultures as well.

Examination of Osteoclast Survival Mechanisms

Our time course studies document that significant numbers of osteoclasts were surviving in culture whether or not stromal cells, M-CSF or RANKL were present and we have, therefore, pursued the mechanisms by which they survive. We have focused on the MEK/ERK and AKT/NFκB pathways as they are two signaling pathways that have been well-documented to promote survival in a number of cell systems and our data above support that they are activated in purified osteoclasts.

Role of the MEK/ERK pathway in osteoclast survival. Initial studies of whether the MEK/ERK pathway might be involved in osteoclast survival focused on examining the cultures for evidence of activation of MEK and ERK (Fig. 3). Due to the need to utilize the model system with the purest osteoclast population, Western blot analyses were carried out on purified marrow-derived osteoclasts. We are cognizant that this is an artificial system in that osteoclasts do not exist in vivo in the absence of stromal cells, so all inhibition analyses are being done with marrow-derived osteoclasts with and without stromal cells and spleen-derived osteoclasts maintained with M-CSF and RANKL. As seen by Western blot analysis (Fig. 3A), within 5 min of culture, there was increased phosphorylation of MEK1/2 and ERK1/2. The most likely explanation for this observation is that the addition of serum (following its absence as the result of the 45 min of culture during the treatment period when stromal cells were removed) caused this response. At time zero, there was some evidence of MEK and ERK phosphorylation, although to a lesser extent than the culture response. To verify that inhibiting MEK1/2 blocked ERK activation in our cultures we initially determined whether 10 μM of the MEK1/2 inhibitor U0126 blocked ERK phosphorylation. As shown in Figure 3B, this dose effectively blocked phosphorylation of ERK1/2. These data documented that we were effectively blocking MEK-mediated ERK activation, so we examined the impact of blocking MEK1/2- and Raf (which can activate MEK) on osteoclast survival. As revealed in Figure 3C,D, inhibition of either Raf or MEK1/2 resulted in apoptosis of over half of the osteoclasts within 90 min of treatment independent of whether the osteoclasts were purified or maintained with stromal cells, supporting an involvement of the Raf/MEK1/2-ERK1/2 pathway in marrow-derived osteoclast survival. Following purification in Figure 3C, there was a significant level of apoptosis in the cultures (0 time). This is likely due to the inclusion of the inhibitors during the 45-min purification process. We next examine spleen-derived osteoclasts and observed that inhibition of either Raf or MEK1/2 for 2 h significantly increased osteoclast apoptosis in these cultures (Fig. 3E), supporting a role for the Raf/MEK/ERK pathway in spleen-derived osteoclast survival.

Role of the AKT/NFκB pathway in osteoclast survival. Since we detected phosphorylated AKT in freshly isolated osteoclasts and the AKT/NFκB pathway has also been implicated in promoting survival of a spectrum

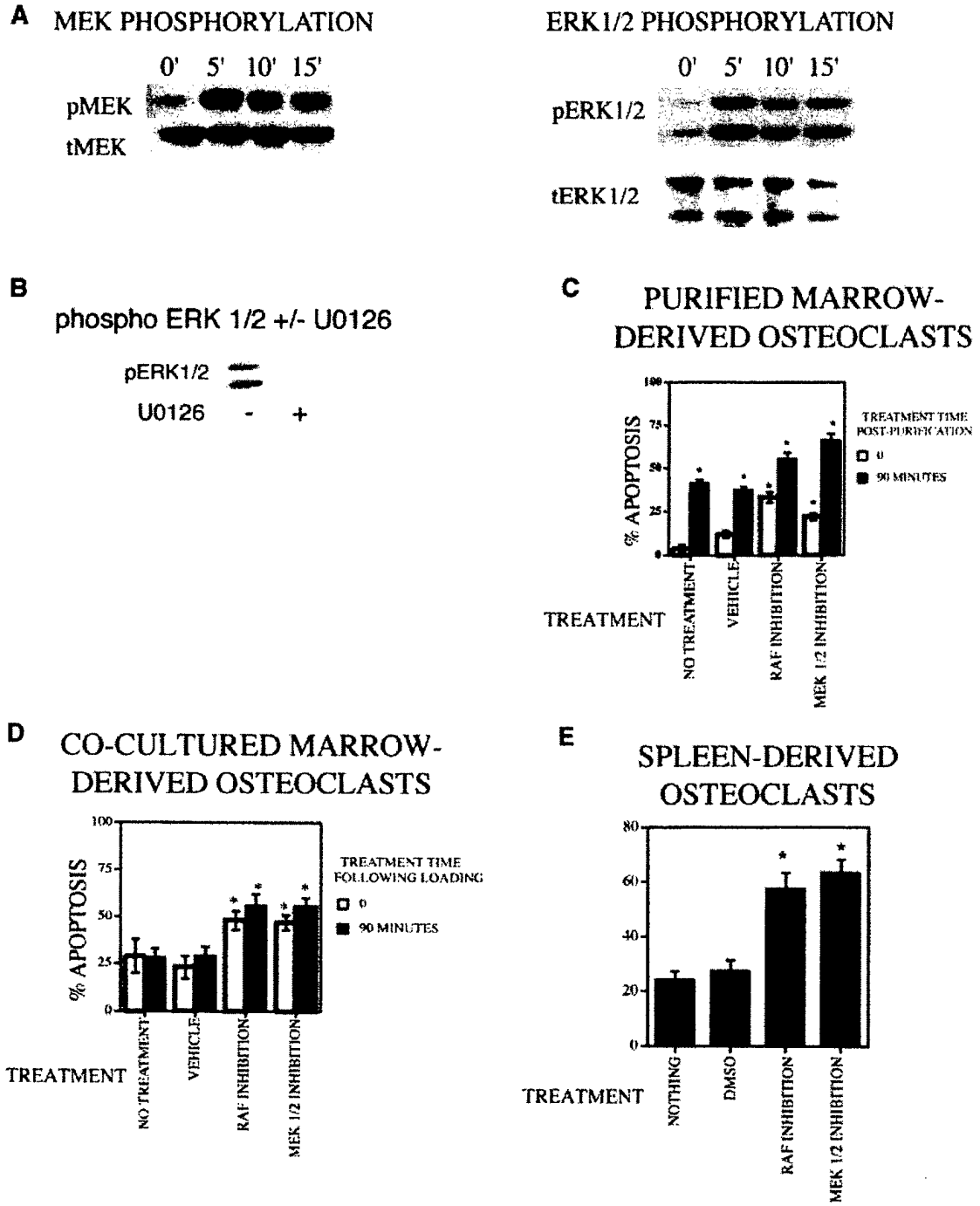

Fig. 3. The MEK/ERK pathway is involved in osteoclast survival. Activation of MEK1/2 and ERK1/2 during culture. **A**: Purified marrow-derived osteoclasts were cultured for 0–15 min as indicated and harvested for Western blotting for pMEK or total MEK (tMEK), pERK or total ERK (tERK) as described. The effects of inhibition. **B**: Marrow-derived osteoclasts were treated with the MEK1/2 inhibitor U0126 during purification and subsequent 15 min of culture. Cells were harvested for Western blotting for pERK as described. **C, D**: Marrow-derived osteoclasts were purified in the presence of vehicle, a Raf inhibitor, or the MEK1/2 inhibitor (C) or pre-treated with vehicle or the inhibitors for co-culture analysis (D). Cells were either fixed (0 culture time) or cultured in the presence of the same treatment for 90 min. **E**: Spleen-derived osteoclasts were cultured for 2.5 h with vehicle or the indicated inhibitor. After fixation, cells were stained for TRAP and chromatin condensation. Apoptotic osteoclasts were identified as above. The percentage of apoptotic osteoclasts is shown (mean ± SEM of three replicates). $^*P < 0.05$: for 0 time, compared to vehicle and for 90 min cultures, compared to both vehicle and 0 time of same treatment.

of cell types, we explored this pathway for whether it may have a role in osteoclast survival (Fig. 4). As above, we utilized purified osteoclasts from co-cultures of marrow precursors with stromal cells for Western blot analyses and examined the impact of blocking pathway components using multiple model systems. We first examined the impact of culture on osteoclast AKT phosphorylation (Fig. 4A). Within 5 min of culture, there was a striking increase in AKT phosphorylation that persisted through 15 min of culture. Note that the time zero sample again showed evidence of AKT phosphorylation. Following the indication of AKT activation, we examined the AKT target NFκB since it influences survival in many cell types [Ozes et al., 1999; Xie et al., 2000; Madrid et al., 2001]. We initially sought to determine if NFκB had a potential role in osteoclast survival by assaying for changes in NFκB activation during culture (Fig. 4B). EMSA analysis of purified osteoclast nuclear extracts revealed that there was evidence of activation at time zero and a rapid elevation in NFκB activation and nuclear localization when cultured further. To verify that we were detecting NFκB, we performed parallel EMSA of the 15-min nuclear extract in the presence of antibodies directed against the p65 subunit (Fig. 4C). Based on the appearance of a higher molecular weight complex concomitant with a decrease in the intensity of the band at the shifted location, we have documented that this band in this EMSA is the complex of NFκB and labeled oligo. Conflicting reports have suggested that NFκB may be involved in osteoclast activation but perhaps not in survival [Ozaki et al., 1997; Miyazaki et al., 2000]. We have, therefore, employed chemical blocking of both AKT and NFκB to study the role of the AKT/NFκB pathway in osteoclast survival in culture. Initially, we examined 0.2 mM of the NFκB activation inhibitor PDTC to determine that it was effective at blocking NFκB activation and found that we were using an effective blocking dose (Fig. 4D). We then examined the impact of blocking AKT or NFκB on osteoclast survival (Fig. 4E–G). Within 90 min of culture with either inhibitor, roughly half of the osteoclasts were apoptotic in all model systems examined, documenting that AKT and NFκB participate in osteoclast survival independent of whether osteoclasts are cultured as purified cells (Fig. 4E), maintained with support cells (Fig. 4F), or maintained with RANKL and M-CSF (Fig. 4G). As above, the apoptosis that was measured at treatment time 0 in purified osteoclasts (Fig. 4E) is likely due to the 45-min pretreatment during purification. AKT promotes survival by phosphorylating a number of targets including caspase 9, Bad, GSK-3, and FRAP/mTOR, which targets p70 S6 kinase [Datta et al., 1997; Fujita et al., 1999; Gingras et al., 1999; Khaleghpour et al., 1999; Raught and Gingras, 1999; Beitner-Johnson et al., 2001; Gingras et al., 2001]. Our data do not support that these targets are activated in osteoclasts, so these have not been pursued further (data not shown). We conclude from these data that AKT and NFκB are involved in promoting osteoclast survival.

Role of PI3K in osteoclast survival. Since PI3K is a multifunctional second messenger that has been implicated in activating a number of different survival signaling pathways, we examined whether blocking PI3K activity influenced osteoclast survival. As with the preceding blocking studies, we examined pathway blocking using marrow-derived osteoclasts with and without purification as well as spleen-derived osteoclasts. Figure 5A is a photograph of a co-culture of marrow-derived osteoclasts cultured with stromal support cells that has been incubated with 10 μM wortmannin for 2.5 h. In the picture, the TRAP staining photograph taken with visible light was over-layered with the fluorescent Hoechst stained same field of view. The larger nuclei (selected ones are indicated with arrows) that are surrounding and over-laying the osteoclasts are the nuclei of the TRAP-negative mononuclear stromal cells that overlay and surround the purple TRAP-positive multinucleated osteoclasts (indicated with the stars). Interestingly, the 2.5-h treatment that resulted in apoptosis of nearly all of the osteoclasts co-cultured with stromal cells, there was no detectable apoptosis of the stromal cells. We quantitated the apoptotic response of purified osteoclasts, osteoclasts maintained with stromal cells, and spleen-derived osteoclast. Inhibition of PI3K activity with either LY294002 or wortmannin resulted in apoptosis of nearly all of the osteoclasts in each of the model systems examined (Fig. 5B–D).

Role of PI3K in regulating the MEK/ERK and AKT/NFκB pathways. To determine whether PI3K was involved in activation of either the MEK/ERK or AKT/NFκB pathway in surviving osteoclasts, we examined the impact of PI3K inhibition on both of these

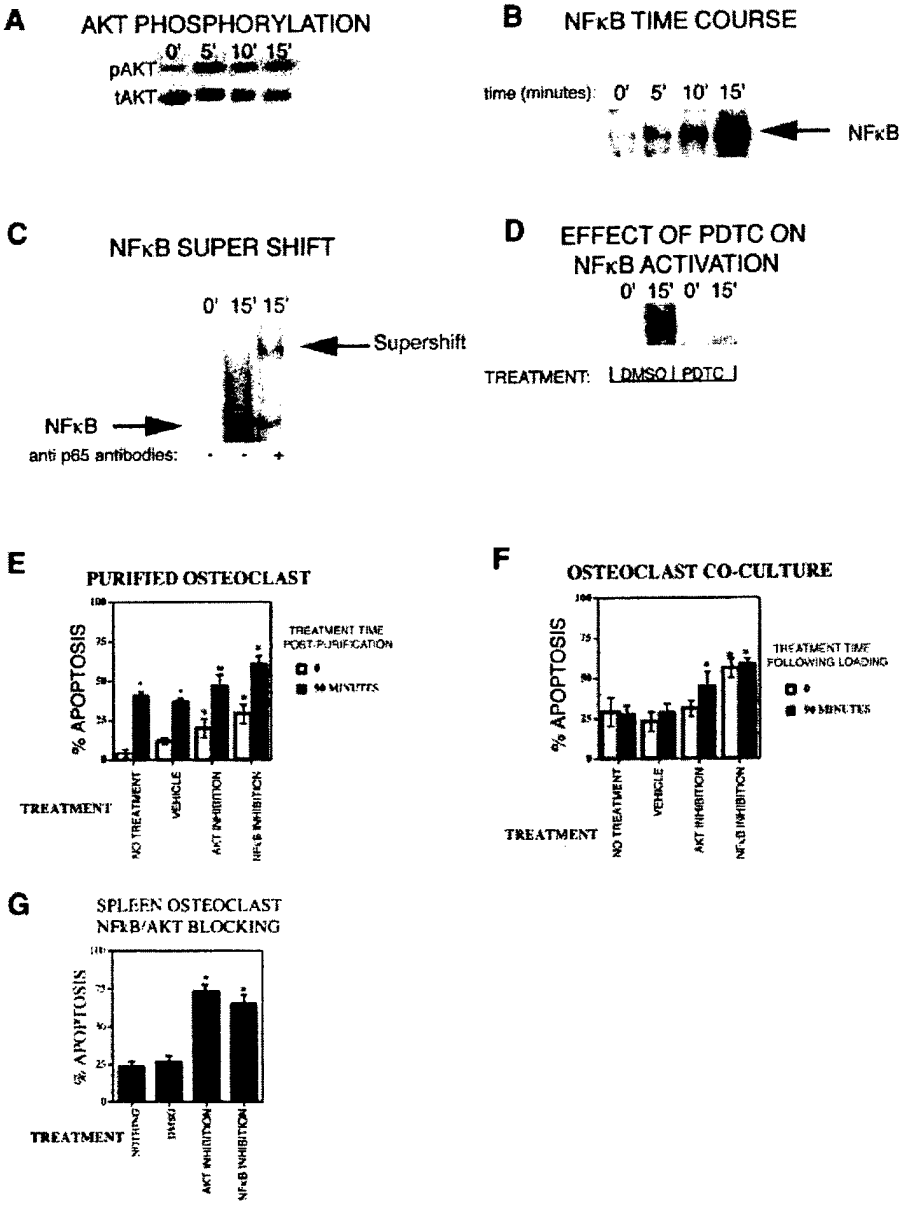

Fig. 4. The AKT/NFκB pathway is involved in osteoclast survival. Activation of AKT/NFκB during culture. **A–C**: Purified marrow-derived osteoclasts were cultured for 0–15 min as indicated and harvested for Western blotting for pAKT or total AKT (tAKT) as described (A). Purified marrow-derived osteoclasts were cultured for 0–15 min as indicated and harvested for nuclear extraction and electrophoretic mobility shift assay (EMSA) analysis as described (B). As detailed in Experimental Procedures, 15-min extracts were assessed for the presence of p65 subunit by the addition of anti-p65 antibodies prior to gel analysis (+ lane) (C). The effects of inhibition. **D–G**: Marrow-derived osteoclasts were treated with either vehicle or 0.2 mM of the NFκB activation inhibitor pyrrolidine dithiocarbamate (PDTC) during purification and subsequent 15 min of culture. Cells were harvested after purification or culture for NFκB activation as described (D). Marrow-derived osteoclasts were either purified in the presence of vehicle, AKT or NFκB activation inhibitor (E) or pre-treated with the inhibitors for co-culture analysis (F). Spleen-derived osteoclasts were cultured for 2.5 h with vehicle or the indicated inhibitor (G). Cells were either fixed (0 culture time) or cultured in the presence of the same treatment for 90 min. After fixation, cells were stained for TRAP and chromatin condensation. Apoptotic osteoclasts were identified as above. The percentage of apoptotic osteoclasts is shown (mean ± SEM of three replicates). $^*P < 0.05$: for 0 time, compared to vehicle and for 90 min cultures, compared to both vehicle and 0 time of same treatment.

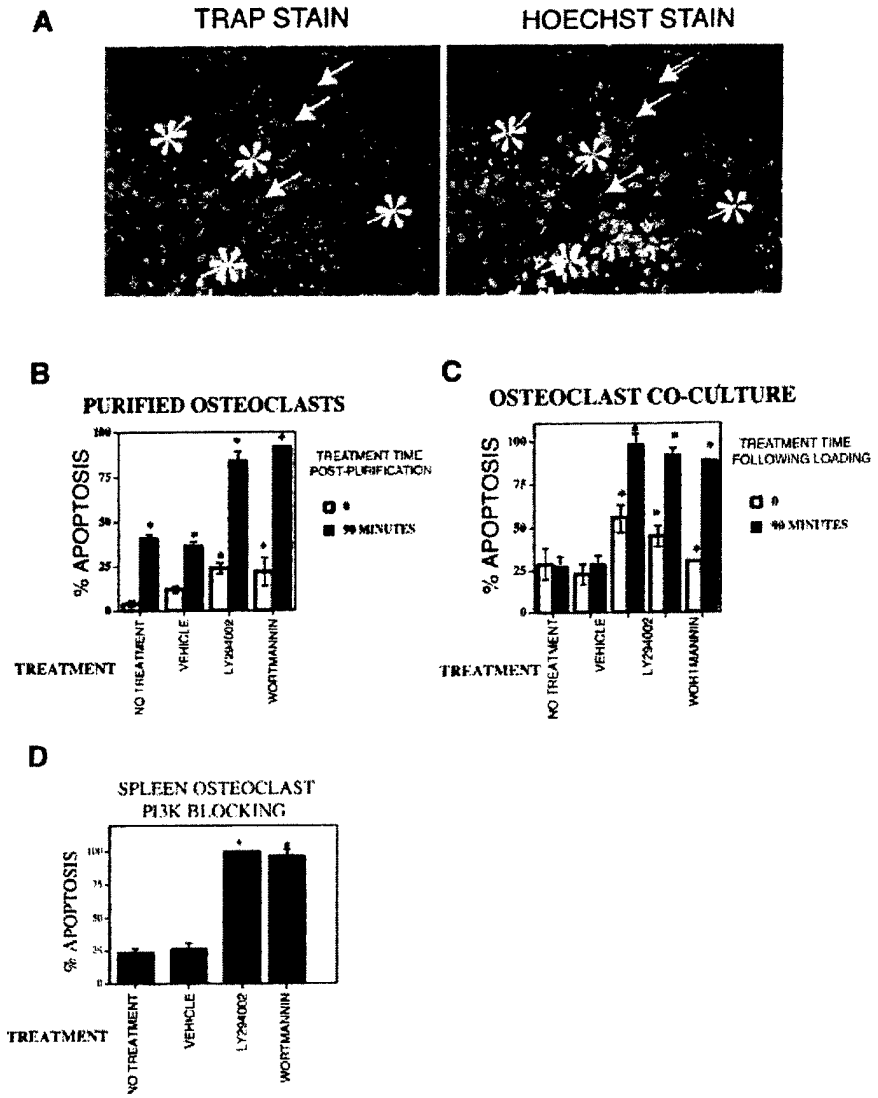

Fig. 5. PI3K mediates osteoclast survival. Examination of the impact of PI3K inhibition of co-cultures. **A:** Marrow-derived osteoclasts maintained with ST2 cells were treated for 2.5 h with wortmannin, fixed and stained for TRAP and chromatin condensation. Arrows point to selected non-apoptotic ST2 cells in the co-cultured cells. The stars indicate selected apoptotic osteoclasts in both pure and co-cultures. The effects of inhibition. **B–D:** Marrow-derived osteoclasts were either purified in the presence of vehicle or one of two PI3K inhibitors LY294002 or wortmannin (B) or pre-treated with the inhibitors for co-culture analysis (C). Cells were either fixed (0 culture time) or cultured in the presence of the same treatment for 90 min. Spleen-derived osteoclasts were cultured for 2.5 h with vehicle or the indicated inhibitor (D). After fixation, cells were stained for TRAP and chromatin condensation. Apoptotic osteoclasts were identified as above. The percentage of apoptotic osteoclasts is shown (mean ± SEM of three replicates). $^*P < 0.05$: at 0 time, compared to vehicle and at 90 min cultures, compared to both vehicle and 0 time of same treatment.

pathways. As documented in Figure 6A, both PI3K inhibitors blocked phosphorylation of AKT. Since the PI3K inhibitors blocked basal osteoclast survival and AKT phosphorylation, we examined if blocking PI3K also blocked osteoclast NFκB activation (Fig. 6B). Blocking PI3K effectively blocked osteoclast NFκB activation, verifying that PI3K was initiating a cascade that results in NFκB activation in cultured osteoclasts. In many cell types, PI3K activation results in stimulation of MEK-mediated phosphorylation of ERK1/2, so we examined whether blocking PI3K impacted the rapid phosphorylation of MEK1/2 and ERK1/2 that we detected (Fig. 6C,D). We observed that PI3K inhibition blocked phosphorylation of both

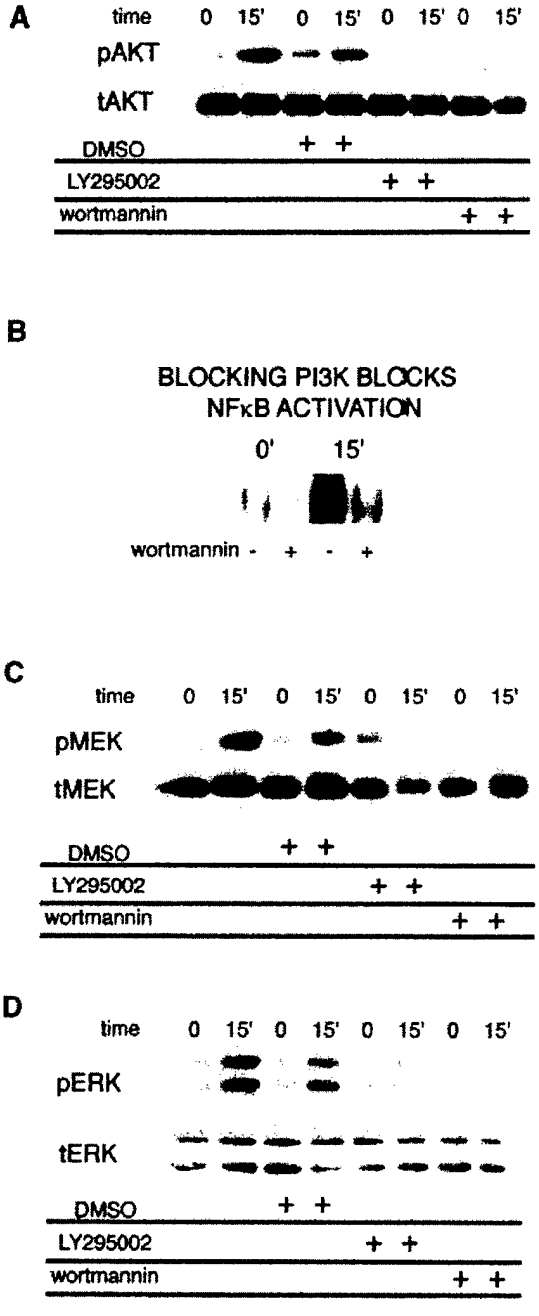

Fig. 6. PI3K coordinately regulates both MEK/ERK and AKT/NFκB pathway activation. The effects of PI3K inhibition on phosphoprotein levels. **A–D**: Osteoclasts were either purified in the presence of vehicle or one of two PI3K inhibitors LY294002 or wortmannin and either harvested (0) or cultured for 15 min (15') with the same treatment. Cells were harvested for Western blotting for pAKT or tAKT (A), pMEK or tMEK (C), or pERK or tERK (D) as described. The effects of PI3K inhibition on NFκB activation. B: Osteoclasts were either purified in the presence of vehicle or wortmannin and either harvested (0) or cultured for 15 min (15') with the same treatment. Nuclear extracts were assessed for activation and nuclear localization of NFκB by EMSA analysis as described.

MEK and ERK in the osteoclast cultures. We conclude from these data that PI3K coordinately activates both the AKT/NFκB and MEK/ERK pathways to promote osteoclast survival.

Impact of blocking both AKT and MEK1/2 on osteoclast survival. Since individual blocking of AKT or MEK1/2 did not induce apoptosis of all of the osteoclasts, we examined the impact of blocking both of these pathways together (Fig. 7). Simultaneous blockage of both pathways resulted in apoptosis of nearly all osteoclasts in both purified cultures (Fig. 7A), co-cultures with stromal cells (Fig. 7B), or spleen-derived osteoclasts maintained with M-CSF and RANKL (Fig. 7C). This pattern mimics the pattern observed when the PI3K pathway was blocked with either LY294002 or wortmannin.

DISCUSSION

We have examined mature osteoclast survival using a well-documented in vitro differentiation system to generate large numbers of mouse osteoclasts [Udagawa et al., 1990]. Others have reported that, once purified, these osteoclasts rapidly apoptose [Fuller et al., 1993]. We have examined these cultures and found that there was evidence of maintained activation of the AKT/NFκB and MEK/ERK pathways. These observations are in concordance with the studies of Miyazaki et al. [2000] and Xing et al. [2001] documenting activation of osteoclast ERK and AKT, respectively. Further study of the cultured osteoclasts derived from marrow or spleen precursors reveal that, although many mature osteoclasts apoptosed once support cells were removed, a significant number survived up to 48 h following purification. Examination of marrow-derived osteoclast cultures in which stromal cells were not removed revealed that, by day 13 of culture, there were significant numbers of apoptotic osteoclasts and that this number increased with culture time. In the purified day 13 osteoclasts, we were not able to detect these apoptotic cells prior to subsequent culturing. This discrepancy is most likely due to efficient removal of apoptotic osteoclasts during the purification steps on day 13. Further culture of both purified osteoclasts and co-cultures resulted in additional apoptotic osteoclasts, although significant numbers of osteoclasts survived. Moreover, addition of RANKL and/or M-CSF to purified osteoclasts

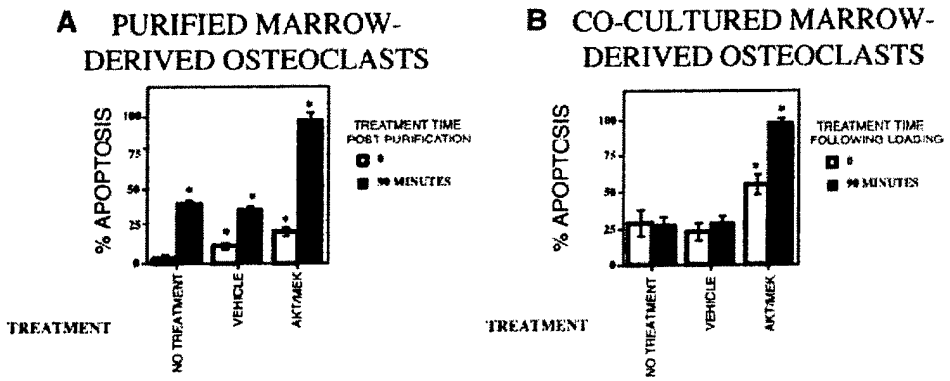

Fig. 7. Inhibition of both AKT and MEK mimic the effects of PI3K on osteoclast survival. Osteoclasts were either purified in the presence of vehicle, or the AKT and the MEK1/2 inhibitor U0126 combined together (AKT/MEK) (**A**) or pre-treated with the same inhibitors for co-culture analysis (**B**). Cells were either fixed (0 culture time) or cultured in the presence of the same treatment for 90 min. After fixation, cells were stained for TRAP and chromatin condensation. Apoptotic osteoclasts were identified as above. The percentage of apoptotic osteoclasts is shown (mean ± SEM of three replicates). $^*P < 0.05$: for 0 time, compared to vehicle and for 90 min cultures, compared to both vehicle and 0 time of same treatment.

did not measurably impact the rate of survival. These data support that the removal of the stromal cell-derived RANKL or M-CSF was not the trigger for apoptosis but, rather, that osteoclasts maintain a rate of apoptotic death independent of whether stromal cells were present. Spleen-derived osteoclasts were generated by culture with RANKL and M-CSF. Maintenance of these cultures with RANKL and M-CSF did not prevent apoptosis of some of the osteoclasts. Taken together, these data support that there is a sustained rate of apoptosis of some osteoclasts while others survive in culture. The focus of the remainder of this study was on the mechanisms by which the cultured osteoclasts survived.

Our studies provided evidence of activation of both the MEK/ERK and AKT/NFκB pathways in surviving osteoclasts. Chemical blocking of either of these pathways increased osteoclast apoptosis independent of stromal cells or RANKL and/or M-CSF. Interestingly, significant numbers of osteoclasts survived with separate blockage of each of these pathways whereas blocking PI3K resulted in apoptosis of nearly all osteoclasts. Combined blocking of the AKT/NFκB and MEK/ERK pathways mimicked the PI3K blocking response, suggesting that co-repression of these pathways induced apoptosis in more osteoclasts than separate blocking of each pathway osteoclast apoptosis. To better explore the integration of these signaling pathways, we examined the impact of blocking PI3K on phosphorylation of MEK, ERK, and AKT as well as NFκB activation and documented that inhibition effectively blocked activation of these downstream kinases. These data strongly support that PI3K coordinately activates two survival pathways that have been shown in many survival signaling systems to act independently [Xue et al., 2000; Mograbi et al., 2001; Tsakiridis et al., 2001; Agazie et al., 2002]. Recent studies have shown that cross-talk between the AKT and MEK/ERK pathways in muscle cells and breast cancer cells involves AKT-mediated inactivation of the MEK/ERK pathway. Direct phosphorylation of Raf-1 by AKT repressed the MEK pathway, switching MCF-7 breast cancer cell line response from proliferation cell cycle arrest [Zimmermann and Moelling, 1999]. Moreover, MCF-7 cells are regulated in a ligand- and concentration-dependent manner to either stimulate proliferation in response to insulin-like growth factor I, again by selective PI3K-mediated repression of the MEK/ERK pathway [Moelling et al., 2002]. In myoblasts, there was differentiation stage-specific inhibition of the MEK/ERK pathway in response to IGF-I-mediated AKT activation [Rommel et al., 1999]. In vascular smooth muscle cells, platelet-derived growth factor stimulation the PI3K/AKT pathway to promote differentiation required PI3K-mediated repression of the Raf/MEK/ERK pathway [Reusch et al., 2001]. Thus, to our knowledge, these are the first studies to report that PI3K activates both the AKT/NFκB and the MEK/ERK within the same time frame to participate coordinately in survival.

Although many cytokines and other growth factors impact osteoclast differentiation, there are a more restricted number of external stimuli

that have been documented to influence osteoclast survival. Among these, M-CSF, RANKL, IL-1, and TNF-α have all been shown to promote osteoclast survival. Interestingly, IL-1 and TNF-α both promote osteoclast survival by activation of both the ERK1/2 and the PI3K/AKT pathways. Surprisingly, TNF-α, although activating AKT, does not activate its well-documented target NFκB in osteoclasts [Lee et al., 2001]. Miyazaki et al. [2000] examined a role for NFκB in osteoclast survival using expression of a dominant interfering form of IKK to block NFκB activation. The data suggested that NFκB activation was not necessary for osteoclast survival. These results are in conflict with the results of Ozaki et al. [1997] using chemical inhibition of NFκB and Lacey et al. [2000] showing that RANKL-mediated activation of NFκB is important in osteoclast survival. In the studies reported here, blocking AKT or NFκB effectively blocked survival of a significant number of osteoclasts, although many cells survived this treatment. These data support that at least some osteoclasts require AKT/NFκB activation for survival.

The published literature supports a role for both AKT/NFκB and MEK/ERK in osteoclast survival following inflammatory cytokine stimulation. We report here for the first time that PI3K coordinately activate these pathways to promote osteoclast survival in the absence of inflammatory cytokine treatment. To our knowledge, this is the first report of the role of PI3K in coordinately activating these pathways to support osteoclast survival. Excessive bone loss is a major pathology in several diseases including periodontitis, postmenopausal osteoporosis, glucocorticoid-induced osteoporosis, and metastatic tumor-driven osteolysis. These disparate diseases share a common denominator in the elevation in the numbers of osteoclasts present during bone degradation. Since osteoclast numbers are controlled by impacting the rates of differentiation and elimination by apoptosis, understanding the mechanisms by which osteoclasts survive may be important to future therapeutic designs to limit the number of osteoclasts.

ACKNOWLEDGMENTS

The authors thank Genevieve Gorny for her tireless technical support. Also, Mr. Steven Johnsen, Dr. David Monroe, and Dr. Malayannan Subramaniam for their thoughtful review of this manuscript.

REFERENCES

Agazie Y, Ischenko I, Hayman M. 2002. Concomitant activation of the PI3K-Akt and the Ras-ERK signaling pathways is essential for transformation by the V-SEA tyrosine kinase oncogene. Oncogene 21:697–707.

Ahmad S, Singh N, Glazer RI. 1999. Role of AKT1 in 17beta-estradiol- and insulin-like growth factor I (IGF-I)-dependent proliferation and prevention of apoptosis in MCF-7 breast carcinoma cells. Biochem Pharmacol 58:425–430.

Beitner-Johnson D, Rust RT, Hsieh TC, Millhorn DE. 2001. Hypoxia activates Akt and induces phosphorylation of GSK-3 in PC12 cells. Cell Signal 13:23–27.

Bisotto S, Fixman ED. 2001. Src-family tyrosine kinases, phosphoinositide 3-kinase, and Gab1 regulate extracellular signal-regulated kinase 1 activation induced by the type A endothelin-1 G-protein-coupled receptor. Biochem J 360:77–85.

Burow ME, Weldon CB, Melnik LI, Duong BN, Collins-Burow BM, Beckman BS, McLachlan JA. 2000. PI3-K/AKT regulation of NF-kappaB signaling events in suppression of TNF-induced apoptosis. Biochem Biophys Res Commun 271:342–345.

Chaudhary LR, Hruska KA. 2001. The cell survival signal Akt is differentially activated by PDGF-BB, EGF, and FGF-2 in osteoblastic cells. J Cell Biochem 81:304–311.

Datta SR, Dudek H, Tao X, Masters S, Fu H, Gotoh Y, Greenberg ME. 1997. Akt phosphorylation of BAD couples survival signals to the cell-intrinsic death machinery. Cell 91:231–241.

Fujita E, Jinbo A, Matuzaki H, Konishi H, Kikkawa U, Momoi T. 1999. Akt phosphorylation site found in human caspase-9 is absent in mouse caspase-9. Biochem Biophys Res Commun 264:550–555.

Fuller K, Owens JM, Jagger CJ, Wilson A, Moss R, Chambers TJ. 1993. Macrophage colony-stimulating factor stimulates survival and chemotactic behavior in isolated osteoclasts. J Exp Med 178:1733–1744.

Gingras AC, Gygi SP, Raught B, Polakiewicz RD, Abraham RT, Hoekstra MF, Aebersold R, Sonenberg N. 1999. Regulation of 4E-BP1 phosphorylation: A novel two-step mechanism. Genes Dev 13:1422–1437.

Gingras AC, Raught B, Sonenberg N. 2001. Regulation of translation initiation by FRAP/mTOR. Genes Dev 15: 807–826.

Hong F, Kwon SJ, Jhun BS, Kim SS, Ha J, Kim SJ, Sohn NW, Kang C, Kang I. 2001. Insulin-like growth factor-1 protects H9c2 cardiac myoblasts from oxidative stress-induced apoptosis via phosphatidylinositol 3-kinase and extracellular signal-regulated kinase pathways. Life Sci 68:1095–1105.

Iryo Y, Matsuoka M, Wispriyono B, Sugiura T, Igisu H. 2000. Involvement of the extracellular signal-regulated protein kinase (ERK) pathway in the induction of apoptosis by cadmium chloride in CCRF-CEM cells. Biochem Pharmacol 60:1875–1882.

Ishikawa Y, Kitamura M. 1999. Dual potential of extracellular signal-regulated kinase for the control of cell survival. Biochem Biophys Res Commun 264:696–701.

Jones RG, Parsons M, Bonnard M, Chan VS, Yeh WC, Woodgett JR, Ohashi PS. 2000. Protein kinase B regulates T lymphocyte survival, nuclear factor kappaB activation, and Bcl-X(L) levels in vivo. J Exp Med 191: 1721–1734.

Kelley TW, Graham MM, Doseff AI, Pomerantz RW, Lau SM, Ostrowski MC, Franke TF, Marsh CB. 1999. Macrophage colony-stimulating factor promotes cell survival through Akt/protein kinase B. J Biol Chem 274: 26393–26398.

Khaleghpour K, Pyronnet S, Gingras AC, Sonenberg N. 1999. Translational homeostasis: Eukaryotic translation initiation factor 4E control of 4E-binding protein 1 and p70 S6 kinase activities. Mol Cell Biol 19:4302–4310.

King WG, Mattaliano MD, Chan TO, Tsichlis PN, Brugge JS. 1997. Phosphatidylinositol 3-kinase is required for integrin-stimulated AKT and Raf-1/mitogen-activated protein kinase pathway activation. Mol Cell Biol 17: 4406–4418.

Klippel A, Kavanaugh WM, Pot D, Williams LT. 1997. A specific product of phosphatidylinositol 3-kinase directly activates the protein kinase Akt through its pleckstrin homology domain. Mol Cell Biol 17:338–344.

Kuwahara K, Saito Y, Kishimoto I, Miyamoto Y, Harada M, Ogawa E, Hamanaka I, Kajiyama N, Takahashi N, Izumi T, Kawakami R, Nakao K. 2000. Cardiotrophin-1 phosphorylates akt and BAD, and prolongs cell survival via a PI3K-dependent pathway in cardiac myocytes. J Mol Cell Cardiol 32:1385–1394.

Lacey DL, Tan HL, Lu J, Kaufman S, Van G, Qiu W, Rattan A, Scully S, Fletcher F, Juan T, Kelley M, Burgess TL, Boyle WJ, Polverino AJ. 2000. Osteoprotegerin ligand modulates murine osteoclast survival in vitro and in vivo. Am J Pathol 157:435–448.

Lederer ED, Sohi SS, McLeish KR. 2000. Parathyroid hormone stimulates extracellular signal-regulated kinase (ERK) activity through two independent signal transduction pathways: Role of ERK in sodium-phosphate cotransport. J Am Soc Nephrol 11:222–231.

Lee JT, Jr., McCubrey JA. 2002. The Raf/MEK/ERK signal transduction cascade as a target for chemotherapeutic intervention in leukemia. Leukemia 16:486–507.

Lee J, Mira-Arbibe L, Ulevitch RJ. 2000. TAK1 regulates multiple protein kinase cascades activated by bacterial lipopolysaccharide. J Leukoc Biol 68:909–915.

Lee SE, Chung WJ, Kwak HB, Chung CH, Kwack KB, Lee ZH, Kim HH. 2001. Tumor necrosis factor-alpha supports the survival of osteoclasts through the activation of Akt and ERK. J Biol Chem 276:49343–49349.

Lee SE, Woo KM, Kim SY, Kim HM, Kwack K, Lee ZH, Kim HH. 2002a. The phosphatidylinositol 3-kinase, p38, and extracellular signal-regulated kinase pathways are involved in osteoclast differentiation. Bone 30: 71–77.

Lee ZH, Lee SE, Kim CW, Lee SH, Kim SW, Kwack K, Walsh K, Kim HH. 2002b. IL-1alpha stimulation of osteoclast survival through the PI 3-kinase/Akt and ERK pathways. J Biochem (Tokyo) 131:161–166.

Lutton JD, Moonga BS, Dempster DW. 1996. Osteoclast demise in the rat: Physiological versus degerative cell death. Exp Physiol 81:251–260.

Madge LA, Pober JS. 2000. A phosphatidylinositol 3-kinase/Akt pathway, activated by tumor necrosis factor or interleukin-1, inhibits apoptosis but does not activate NFkappaB in human endothelial cells. J Biol Chem 275:15458–15465.

Madrid LV, Wang CY, Guttridge DC, Schottelius AJ, Baldwin AS, Jr., Mayo MW. 2000. Akt suppresses apoptosis by stimulating the transactivation potential of the RelA/p65 subunit of NF-kappaB. Mol Cell Biol 20:1626–1638.

Madrid LV, Mayo MW, Reuther JY, Baldwin AS, Jr. 2001. Akt Stimulates the transactivation potential of the RelA/p65 subunit of NF-kappa B through utilization of the Ikappa B kinase and activation of the mitogen-activated protein kinase p38. J Biol Chem 276:18934–18940.

McCubrey JA, Lee JT, Steelman LS, Blalock WL, Moye PW, Chang F, Pearce M, Shelton JG, White MK, Franklin RA, Pohnert SC. 2001. Interactions between the PI3K and Raf signaling pathways can result in the transformation of hematopoietic cells. Cancer Detect Prev 25:375–393.

Mitsui H, Takuwa N, Maruyama T, Maekawa H, Hirayama M, Sawatari T, Hashimoto N, Takuwa Y, Kimura S. 2001. The MEK1-ERK map kinase pathway and the PI 3-kinase-Akt pathway independently mediate anti-apoptotic signals in HepG2 liver cancer cells. Int J Cancer 92:55–62.

Miyazaki T, Katagiri H, Kanegae Y, Takayanagi H, Sawada Y, Yamamoto A, Pando MP, Asano T, Verma IM, Oda H, Nakamura K, Tanaka S. 2000. Reciprocal role of ERK and NF-kappaB pathways in survival and activation of osteoclasts. J Cell Biol 148:333–342.

Moelling K, Schad K, Bosse M, Zimmermann S, Schweneker M. 2002. Regulation of Raf-Akt cross-talk. J Biol Chem 277:31099–31106.

Mograbi B, Bocciardi R, Bourget I, Busca R, Rochet N, Farahi-Far D, Juhel T, Rossi B. 2001. Glial cell line-derived neurotrophic factor-stimulated phosphatidylinositol 3-kinase and Akt activities exert opposing effects on the ERK pathway: Importance for the rescue of neuroectodermic cells. J Biol Chem 276:45307–45319.

Moreno-Manzano V, Ishikawa Y, Lucio-Cazana J, Kitamura M. 1999. Suppression of apoptosis by all-*trans*-retinoic acid. Dual intervention in the c-Jun n-terminal kinase-AP-1 pathway. J Biol Chem 274:20251–20258.

Nosaka Y, Arai A, Kanda E, Akasaki T, Sumimoto H, Miyasaka N, Miura O. 2001. Rac is activated by tumor necrosis factor alpha and is involved in activation of Erk. Biochem Biophys Res Commun 285:675–679.

Ozaki K, Takeda H, Iwahashi H, Kitano S, Hanazawa S. 1997. NF-kappaB inhibitors stimulate apoptosis of rabbit mature osteoclasts and inhibit bone resorption by these cells. FEBS Lett 410:297–300.

Ozes ON, Mayo LD, Gustin JA, Pfeffer SR, Pfeffer LM, Donner DB. 1999. NF-kappaB activation by tumour necrosis factor requires the Akt serine-threonine kinase. Nature 401:82–85.

Raught B, Gingras AC. 1999. eIF4E activity is regulated at multiple levels. Int J Biochem Cell Biol 31:43–57.

Reddy SA, Huang JH, Liao WS. 2000. Phosphatidylinositol 3-kinase as a mediator of TNF-induced NF-kappa B activation. J Immunol 164:1355–1363.

Reusch HP, Zimmermann S, Schaefer M, Paul M, Moelling K. 2001. Regulation of Raf by Akt controls growth and differentiation in vascular smooth muscle cells. J Biol Chem 276:33630–33637.

Romashkova JA, Makarov SS. 1999. NF-kappaB is a target of AKT in anti-apoptotic PDGF signalling. Nature 401: 86–90.

Rommel C, Clarke BA, Zimmermann S, Nunez L, Rossman R, Reid K, Moelling K, Yancopoulos GD, Glass DJ. 1999. Differentiation stage-specific inhibition of the Raf-MEK-ERK pathway by Akt. Science 286:1738–1741.

Roodman GD. 1999. Cell biology of the osteoclast. Exp Hematol 27:1229–1241.

Scheid MP, Duronio V. 1998. Dissociation of cytokine-induced phosphorylation of Bad and activation of PKB/akt: Involvement of MEK upstream of Bad phosphorylation. Proc Natl Acad Sci USA 95:7439–7444.

Sells Galvin RJ, Gatlin CL, Horn JW, Fuson TR. 1999. TGF-beta enhances osteoclast differentiation in hematopoietic cell cultures stimulated with RANKL and M-CSF. Biochem Biophys Res Commun 265:233–239.

Sheng H, Shao J, DuBois RN. 2001. Akt/PKB activity is required for Ha-Ras-mediated transformation of intestinal epithelial cells. J Biol Chem 276:14498–14504.

Suda T, Nakamura I, Jimi E, Takahashi N. 1997. Regulation of osteoclast function. J Bone Min Res 12:869–879.

Takahashi N, Yamana H, Yoshiki S, Roodman GD, Mundy GR, Jones SJ, Boyde A, Suda T. 1988. Osteoclast-like cell formation and its regulation by osteotropic hormones in mouse bone marrow cultures. Endocrinology 122:1373–1382.

Tsakiridis T, Tsiani E, Lekas P, Bergman A, Cherepanov V, Whiteside C, Downey GP. 2001. Insulin, insulin-like growth factor-I, and platelet-derived growth factor activate extracellular signal-regulated kinase by distinct pathways in muscle cells. Biochem Biophys Res Commun 288:205–211.

Udagawa N, Takahashi N, Akatsu T, Tanaka H, Sasaki T, Nishihara T, Koga T, Martin TJ, Suda T. 1990. Origin of osteoclasts: Mature monocytes and macrophages are capable of differentiating into osteoclasts under a suitable microenvironment prepared by bone marrow-derived stromal cells. Proc Natl Acad Sci USA 87:7260–7264.

Ushio-Fukai M, Alexander RW, Akers M, Yin Q, Fujio Y, Walsh K, Griendling KK. 1999. Reactive oxygen species mediate the activation of Akt/protein kinase B by angiotensin II in vascular smooth muscle cells. J Biol Chem 274:22699–22704.

von Gise A, Lorenz P, Wellbrock C, Hemmings B, Berberich-Siebelt F, Rapp UR, Troppmair J. 2001. Apoptosis suppression by Raf-1 and MEK1 requires MEK- and phosphatidylinositol 3-kinase-dependent signals. Mol Cell Biol 21:2324–2336.

Wang X, McCullough KD, Franke TF, Holbrook NJ. 2000. Epidermal growth factor receptor-dependent Akt activation by oxidative stress enhances cell survival. J Biol Chem 275:14624–14631.

Wennstrom S, Downward J. 1999. Role of phosphoinositide 3-kinase in activation of ras and mitogen-activated protein kinase by epidermal growth factor. Mol Cell Biol 19:4279–4288.

Wesolowski G, Duong LT, Lakkakorpu PT, Nagy RM, Tezuka K-I, Tanaka H, Rodan GA, Rodan SB. 1995. Isolation and characterization of highly enriched, prefusion mouse osteoclastic cells. Exp Cell Res 219:679–686.

Xie P, Browning DD, Hay N, Mackman N, Ye RD. 2000. Activation of NF-kappa B by bradykinin through a Galpha(q)- and Gbeta gamma-dependent pathway that involves phosphoinositide 3-kinase and Akt. J Biol Chem 275:24907–24914.

Xing L, Venegas AM, Chen A, Garrett-Beal L, Boyce BF, Varmus HE, Schwartzberg PL. 2001. Genetic evidence for a role for Src family kinases in TNF family receptor signaling and cell survival. Genes Dev 15:241–253.

Xue L, Murray JH, Tolkovsky AM. 2000. The Ras/phosphatidylinositol 3-kinase and Ras/ERK pathways function as independent survival modules each of which inhibits a distinct apoptotic signaling pathway in sympathetic neurons. J Biol Chem 275:8817–8824.

Zimmermann S, Moelling K. 1999. Phosphorylation and regulation of Raf by Akt (protein kinase B). Science 286:1741–1744.

J Musculoskel Neuron Interact 2003; 3(4):363-366

Perspective Article

Hylonome

Direct and indirect effects of estrogen on osteoclasts

M.J. Oursler

Departments of Biology, Medical Microbiology and Immunology, and Biochemistry and Molecular Biology, University of Minnesota, Duluth, MN, USA

Keywords: Osteoclasts, Osteoblasts, Estrogen, Genomic Responses, Non-genomic Responses

Extensive bone metabolism studies have shown that the rate at which osteoclasts resorb bone and osteoblasts replace the lost bone with new bone are tightly coupled, creating a scenario in which osteoclasts and osteoblasts communicate to maintain a balance of bone resorption and formation. Although it has been recognized for many years that estrogen depletion at menopause results in a net loss of bone and that this can be prevented by estrogen replacement therapy, the mechanisms by which estrogen has this impact have remained somewhat elusive. This breakdown in the balance of resorption and formation implies that estrogen loss uncouples the resorption and formation phases of bone metabolism. Discoveries of the mechanisms by which resorption and formation are coupled and how estrogen loss disrupts this coupling have been complicated by a number of factors including the fact that the tissue is mineralized, there is cellular heterogeneity of the tissue, a relatively small number of cells are available and they are difficult to recover intact from the tissue, and there is a lack of suitable cell lines for all stages of differentiation. In addition, the most powerful method for studying bone metabolism, dynamic histomorphometry, is invasive and cannot be accomplished on live tissue. Recent advances in all of these areas have allowed for a more complete picture of how estrogen modulates bone balance by directly and indirectly targeting bone resorbing osteoclasts. This summary will outline current knowledge of both of these mechanisms by which estrogen impacts bone resorption.

Estrogen targets osteoclast numbers

It is generally acknowledged that the rate of bone resorption over the long term is modulated effectively by controlling the number of osteoclasts present at the site of bone resorption. Since cell numbers are influenced by the rate at which they differentiate from precursors and the rate at which they are eliminated, in this case through apoptosis, both of these parameters are discussed.

Indirect estrogen effects on osteoclasts

Effects on differentiation: It is apparent that many of the paracrine and endocrine mechanisms that regulate bone metabolism do so, at least in part, by targeting management of osteoclast differentiation[1]. A wealth of data document that receptor activator of nuclear factor kappa B ligand (RANKL) is critical for osteoclast differentiation. Interactions between RANKL and its cognate receptor, RANK, are regulated by production of a decoy receptor, osteoprotegerin (OPG)[1]. Many paracrine factors influence osteoclast differentiation by regulating RANKL and OPG expression by stromal support cells[1-9]. Saika et al.[10] have documented that the mouse ST-2 stromal cell line responds to estrogen treatment with increased OPG expression. Since OPG is a decoy receptor for RANKL, this suggests that at least one mechanism by which estrogen regulates osteoclast differentiation would be by repressing RANKL binding to RANK on osteoclast precursors. Studies by Bord et al.[11] documenting that human osteoblasts respond to low dose estrogen treatment with repression of RANKL while maintaining OPG expression, support that modulating this mechanism may be key in estrogen effects on osteoclast differentiation in human cells as well. Whether these changes in the RANKL/OPG ratio are the direct result of estrogen modulation of either or both gene expressions or through estrogen modulation of cytokines and other growth factors that then impact this ratio is not resolved. Indeed, a number of other studies, both *in vivo* and *in vitro*, have implicated multiple cytokines and other growth factors as being involved in estrogen effects on osteoclast differentiation. These studies have highlighted IL-6[12,13], IL-1 and/or TNF-α[14-17], IL-11[18], and IL-7[19,20] as potential mediators of osteoclast differentiation. Evidence that estrogen also modulates TGF-ß production by osteoblasts, coupled with evidence that TGF-ß regulates osteoclast differentiation, suggests that this growth factor may also

The author has no conflict of interest.

Corresponding author: Merry Jo Oursler, Ph.D., Endocrine Research Unit, Mayo Clinic and Foundation, 200 First St. SW, Rochester, MN 55905, USA
E-mail: oursler.merryjo@mayo.edu

Accepted 1 August 2003

play a critical part in osteoblast-mediated estrogen effects on osteoclast differentiation[6,21-24].

Effects on apoptosis: Modulation of osteoclast survival may also be important in controlling the number of osteoclasts present at sites of bone resorption. Hughes et al. have shown that estrogen induces osteoclast apoptosis, a process that was inhibited by antibodies to TGF-ß[25,26]. Murakami et al. have demonstrated that TGF-ß treatment of co-cultures of osteoclasts and support cells causes apoptosis by increasing OPG[27]. Stromal cells respond to TGF-ß with increased OPG expression and this is consistent with that observation[27]. Since estrogen increases osteoblast TGF-ß production, estrogen-induced osteoclast apoptosis is likely, at least in part, to be mediated by osteoblast TGF-ß production[28].

Direct estrogen effects on osteoclasts

Effects on differentiation: There has not been extensive study of direct estrogen effects on osteoclast precursor differentiation. Shevde et al.[29] have documented that estrogen directly targets RANKL-induced osteoclast differentiation by repressing c-Jun activation and that this response was dependent on the estrogen receptor. Studies of Srivastava et al.[30] have shown that estrogen treatment of osteoclast precursors results in down regulation of the c-Jun activating kinase JNK. These data support a direct action of estrogen on osteoclast precursors to repress differentiation and, therefore, bone resorption levels.

Effects on apoptosis: The above discussion highlighted that estrogen effects on osteoclast apoptosis may be mediated, at least in part, by estrogen stimulation of osteoblast TGF-ß production causing OPG production. Interestingly, when stromal cells are removed from the mature osteoclasts in these studies, OPG was not involved in TGF-ß-induced osteoclast apoptosis[31]. Thus, it appears that stromal or osteoblast OPG production is not the sole mechanism by which estrogen causes osteoclast apoptosis. This intriguing observation raises the important question of how osteoclast TGF-ß-induced apoptosis is driven.

Estrogen targets osteoclast activity

Much research has focused on estrogen regulation of the number of osteoclasts as this is a likely major mechanism by which bone resorption in controlled *in vivo* over the span of many years. However, there is a body of data that support that, over the short term, modulation of osteoclast activity may also result from changes in estrogen levels. *In vivo* data examining the effects of estrogen withdrawal on young women support that decreased estrogen exposure may result in increased activity levels of individual osteoclasts[32]. In these studies, therapeutic lowering of serum estrogen levels caused increased bone loss and elevated TRAP activity of individual osteoclasts. *In vitro* studies of this possibility support this concept as well. Studies of mixed cell cultures consisting of osteoclasts and stromal or osteoblastic cells have shown that estrogen also modulates mature osteoclast bone resorption activity. In studies of this nature, the target cell for estrogen effects are impossible to discern due to the multiple cell types present in the cultures. Because of this, these studies are discussed below under the category of potential indirect effects. In studies using highly purified osteoclasts or studies comparing purified and co-culture responses, it is possible to attribute the responses to direct effects on osteoclasts and these studies are considered separately.

Potential indirect estrogen effects on osteoclasts

Studies have shown that RANKL can activate mature osteoclasts, so studies discussed above of estrogen modulation of osteoblast RANKL and/or OPG have relevance here in that increased RANKL and/or decreased OPG would activate mature osteoclasts. Moreover, an interesting study by Parikka et al.[33] examined mixed cultures plated on bone and found that estrogen treatment resulted in shallower pits that were filled with non-degraded collagen. Further examination of this collagen led to the conclusion, on the basis of enzyme specificity, that estrogen repressed cathepsin K activity. As noted above, the mixed nature of these cultures means that one cannot discern the estrogen responding cell. However, studies outlined below document that estrogen targets osteoclast cathepsin expression in highly purified cultures, supporting that at least some of this observed effect is likely due to direct estrogen effects on osteoclast cathepsin production.

Direct estrogen effects on osteoclasts

Pensler et al.[34] and Hoyland et al.[35] provided early evidence of estrogen receptors in human osteoclasts. Studies of chicken, mouse, and rabbit osteoclasts have confirmed that mature osteoclasts express estrogen receptors[36-39]. Human, mouse, rabbit, and avian osteoclasts have been shown to respond to estrogen treatment with decreased resorption activity[35-39]. Studies of the mechanisms of estrogen's impact on osteoclast activity can be divided into two categories: rapid effects that presumably are non-genomic in nature and more delayed effects that appear due to estrogen effects on osteoclast gene expression. Each of these will be considered separately.

Rapid non-genomic effects: Rapid estrogen responses include increased acidification and modulation of Src kinase activity[40-42]. Moreover, studies of rat osteoclasts have documented rapid inhibition of superoxide anion generation and inward rectifying K+ channel-mediated depolarization of the plasma membrane[43,44]. Although studies of non-genomic estrogen effects on mature osteoclasts are in their infancy, it appears that these cells are among those that exhibit estrogen responses too rapid to be genomic in nature.

Genomic effects: Direct estrogen effects on osteoclast gene expression include rapid stimulation of c-fos and c-jun expression, a response observed within 15 minutes of treatment[36]. More long-term responses include repression of

TRAP as well as cathepsins B, L and K[37,39,45]. These data support that estrogen modulation of mature osteoclast activity may be mediated, at least in part, by direct repression of expression of the genes for proteins involved in degrading bone matrix, the cathepsins.

Conclusions and future directions

Recent advances in technology, coupled with advances in model systems and our fundamental knowledge of osteoclast biology are creating an environment where we will be rapidly accumulating knowledge that, hopefully, will enable us to therapeutically address fundamental issues relating to controlling pathological bone loss. Undoubtedly, future therapies will focus on the regulation of both osteoclast numbers through targeting differentiation and survival as well as repressing activity of mature osteoclasts to control bone resorption.

Acknowledgment

Dr. Oursler is supported by the Department of the Army Grant DAMD17-00-1-0346 and the National Institutes of Health Grant DE14680.

References

1. Khosla S. Minireview: the OPG/RANKL/RANK system. Endocrinology 2001: 142:5050-5055.
2. Atkins GJ, Haynes DR, Geary SM, Loric M, Crotti TN, Findlay DM. Coordinated cytokine expression by stromal and hematopoietic cells during human osteoclast formation. Bone 2000; 26:653-661.
3. Atkins GJ, Haynes DR, Graves SE, Evdokiou A, Hay S, Bouralexis S, Findlay DM. Expression of osteoclast differentiation signals by stromal elements of giant cell tumors. J Bone Miner Res 2000; 15:640-649.
4. Mancino AT, Klimberg VS, Yamamoto M, Manolagas SC, Abe E. Breast cancer increases osteoclastogenesis by secreting M-CSF and upregulating RANKL in stromal cells. J Surg Res 2001; 100:18-24.
5. Massey HM, Scopes J, Horton MA, Flanagan AM. Transforming growth factor-beta1 (TGF-β) stimulates the osteoclast-forming potential of peripheral blood hematopoietic precursors in a lymphocyte-rich microenvironment. Bone 2001; 28:577-582.
6. Quinn JM, Itoh K, Udagawa N, Häusler K, Yasuda H, Shima N, Mizuno A, Higashio K, Takahashi N, Suda T, Martin TJ, Gillespie MT. Transforming growth factor beta affects osteoclast differentiation via direct and indirect actions. J Bone Miner Res 2001; 16:1787-1794.
7. Suda T, Kobayashi K, Jimi E, Udagawa N, Takahashi N. The molecular basis of osteoclast differentiation and activation. Novartis Found Symp 2001; 232:235-247; discussion 247-250.
8. Udagawa N, Takahashi N, Jimi E, Matsuzaki K, Tsurukai T, Itoh K, Nakagawa N, Yasuda H, Goto M, Tsuda E, Higashio K, Gillespie MT, Martin TJ, Suda T. Osteoblasts/stromal cells stimulate osteoclast activation through expression of osteoclast differentiation factor/RANKL but not macrophage colony-stimulating factor: receptor activator of NF-kappa B ligand. Bone 1999; 25:517-523.
9. Wei S, Wang MW, Teitelbaum SL, Ross FP. Interleukin-4 reversibly inhibits osteoclastogenesis via inhibition of NF-kappa B and mitogen-activated protein kinase signaling. J Biol Chem 2002; 277:6622-6630.
10. Saika M, Inoue D, Kido S, Matsumoto T. 17β-estradiol stimulates expression of osteoprotegerin by a mouse stromal cell line, ST-2, via estrogen receptor-alpha. Endocrinol 2001; 142:2205-2212.
11. Bord S, Ireland DC, Beavan SR, Compston JE. The effects of estrogen on osteoprotegerin, RANKL, and estrogen receptor expression in human osteoblasts. Bone 2003; 32:136-141.
12. Jilka RL, Hangoc C, Girasole G, Passeri G, Williams DC, Abrams JS, Boyce B, Broxmeyer H, Manolagas SC. Increased osteoclast development after estrogen loss: mediation by interleukin-6. Science 1992; 257:88-91.
13. Girasole G, Jilka RL, Passeri G, Boswell S, Boder G, Williams DC, MAnolagas SC. 17β-estradiol inhibits interleukin-6 production by bone marrow-derived stromal cells and osteoblasts *in vitro*: a potential mechanism for the anti-osteoporotic effect of estrogens. J Clin Invest 1992; 89:883-891.
14. Pacifici R, Rifas L, McCracken R, Vered I, McMurty C, Avioli LV, Peck WA. Ovarian steroid treatment blocks a postmenopausal increase in blood monocyte interleukin-1 release. Proc Natl Acad Sci USA 1989; 86:2398-2402.
15. Pacifici R, Brown C, Puscheck E, Friedrich E. Slatopolsky E, Maggio D, McCracken R, Avioli LV. Effect of surgical menopause and estrogen replacement on cytokine release from human blood mononuclear cells. Proc Natl Acad Sci USA 1991; 88:5134-5138 .
16. Kimble RB, Bain S, Pacifici R. The functional block of TNF but not of IL-6 prevents bone loss in ovariectomized mice. J Bone Miner Res 1997; 12:935-941.
17. Kimble RB, Matayoshi AB, Vannice JL, Kung VT, Williams C, Pacifici R. Simultaneous block of interleukin-1 and tumor necrosis factor is required to completely prevent bone loss in the early post-ovariectomy period. Endocrinology 1995; 136:3054-3061.
18. Shaughnessy SG, Walton KJ, Deschamps P, Butcher M, Beaudin SM. Neutralization of interleukin-11 activity decreases osteoclast formation and increases cancellous bone volume in ovariectomized mice. Cytokine 2002; 20:78-85.
19. Toraldo G, Roggia C, Qian WP, Pacifici R, Weitzmann MN. IL-7 induces bone loss *in vivo* by induction of receptor activator of nuclear factor kappa B ligand and tumor necrosis factor alpha from T cells. Proc Natl Acad Sci USA 2003; 100:125-130.
20. Weitzmann MN, Roggia C, Toraldo G, Weitzmann L,

Pacifici R. Increased production of IL-7 uncouples bone formation from bone resorption during estrogen deficiency. J Clin Invest 2002; 110:1643-1650.
21. Shinar DM, Rodan GA. Biphasic effects of transforming growth factor-β on the production of osteoclast-like cells in mouse bone marrow cultures: the role of prostaglandins in the generation of these cells. Endocrinology 1990; 126:3153-3158.
22. Yamaguchi K, Shirakabe K, Shibuya H, Irie K, Oishi I, Ueno N, Taniguchi T, Nishida E, Matsumoto K. Identification of a member of the MAPKKK family as a potential mediator of TGF-β signal transduction. Science 1995; 270:2008-2011.
23. Mundy GR. The effects of TGF-β on bone. Ciba Found Symp 1991; 157:137-143.
24. Heino TJ, Hentunen TA, Vaananen HK. Osteocytes inhibit osteoclastic bone resorption through transforming growth factor-β: enhancement by estrogen. J Cell Biochem 2002; 85:185-197.
25. Hughes DE, Wright KR, Mundy GR, Boyce BF. TGFβ1 induces osteoclast apoptosis *in vitro*. J Bone Miner Res 1994; 9:S138.
26. Hughes DE, Dai A, Tiffee JC, Li HH, Mundy GR, Boyce BF. Estrogen promotes apoptosis of murine osteoclasts mediated by TGF-β. Nat Med 1996; 2:1132-1136.
27. Murakami T, Yamamoto M, Ono K, Nishikawa M, Nagata N, Motoyoshi K, Akatsu T. Transforming growth factor-β 1 increases mRNA levels of osteoclastogenesis inhibitory factor in osteoblastic/stromal cells and inhibits the survival of murine osteoclast-like cells. Biochem Biophys Res Commun 1998; 252:747-752.
28. Oursler MJ, Cortese C, Keeting P, Anderson MA, Bonde SK, Riggs BL, Spelsber TC. Modulation of transforming growth factor-β production in normal human osteoblast-like cells by 17 β-estradiol and parathyroid hormone. Endocrinology 1991; 129:3313-3320.
29. Shevde NK, Bendixen AC, Dienger KM, Pike JW. Estrogens suppress RANK ligand-induced osteoclast differentiation via a stromal cell independent mechanism involving c-Jun repression. Proc Natl Acad Sci USA 2000; 97:7829-7834.
30. Srivastava S, Toraldo G, Weitzmann MN, Cenci S, Ross FP, Pacifici R. Estrogen decreases osteoclast formation by down-regulating receptor activator of NF-kappa B ligand (RANKL)-induced JNK activation. J Biol Chem 2001; 276:8836-8840.
31. Akatsu T, Murakami T, Nishikawa M, Ono K, Shinomiya N, Tsuda E. Mochizuki S, Yamaguchi K, Kinosaki M, Higashio K, Yamamoto M, Motoyoshi K, Nagata N. Osteoclastogenesis inhibitory factor suppresses osteoclast survival by interfering in the interaction of stromal cells with osteoclast. Biochem Biophys Res Commun 1998; 250:229-234.
32. Bell KL, Loveridge N, Lindsay PC, Lunt M, Garrahan N, Compston JE, Reeve J. Cortical remodeling following suppression of endogenous estrogen with analogs of gonadotrophin releasing hormone. J Bone Miner Res 1997; 12:1231-1240.
33. Parikka V, Lehenkari P, Sassi ML, Halleen J, Risteli J, Harkonen P, Vaananen HK. Estrogen reduced the depth of resorption pits by disturbing organic bone matrix degradation activity of mature osteoclasts. Endocrinology 2001; 142:5371-5378.
34. Pensler JM, Radosevich JA, Higbee R, Langman CB. Osteoclasts isolated from membranous bone in children exhibit nuclear estrogen and progesterone receptors. J Bone Miner Res 1990; 5:797-802.
35. Hoyland JA, Mee AP, Baird P, Braidman IP, Mawer EB, Freemont AJ. Demonstration of estrogen receptor mRNA in bone using *in situ* reverse-transcriptase polymerase chain reaction. Bone 1997; 20:87-92.
36. Oursler MJ, Osdoby P, Pyfferoen J, Riggs BL, Spelsberg TC. Avian osteoclasts as estrogen target cells. Proc Natl Acad Sci USA 1991; 88:6613-6617.
37. Oursler MJ, Pederson L, Fitzpatrick L, Riggs BL, Spelsberg T. Human giant cell tumors of the bone (osteoclastomas) are estrogen target cells. Proc Natl Acad Sci USA 1994; 91:5227-5231.
38. Mizuno Y, Hosoi T, Inoue S, Ikegami A, Kaneki M, Akedo Y, Nakamura T, Ouchi Y, Chang C, Orimo H. Immunocytochemical identification of androgen receptor in mouse osteoclast-like multinucleated cells. Calcif Tissue Int 1994; 54:325-326.
39. Mano H, Yuasa T, Kameda T, Miqazawa K, Nakamaru Y, Shiokawa M, Mori Y, Yamada T, Miyata Km Shindo H, Azuma H, Hakeda Y, Kumegawa M. Mammalian mature osteoclasts as estrogen target cells. Biochem Biophys Res Commun 1996; 223:637-642.
40. Brubaker KD, Gay CV. Specific binding of estrogen to osteoclast surfaces [published erratum appears in Biochem Biophys Res Commun 1994 15;202:643]. Biochem Biophys Res Commun 1994; 200:899-907.
41. Pascoe D, Oursler MJ. The Src signaling pathway regulates osteoclast lysosomal enzyme secretion and is rapidly modulated by estrogen. J Bone Miner Res 2001; 16:1028-1036.
42. Brubaker KD, Gay CV. Estrogen stimulates protein tyrosine phosphorylation and Src kinase activity in avian osteoclasts. J Cell Biochem 1999; 76:206-216.
43. Berger CE, Horrocks BR, Datta HK. Direct non-genomic effect of steroid hormones on superoxide anion generation in the bone resorbing osteoclasts. Mol Cell Endocrinol 1999; 149:53-59.
44. Okabe K, Okamoto F, Kajiya H, Takada K, Soeda H. Estrogen directly acts on osteoclasts via inhibition of inward rectifier K+ channels. Naunyn Schmiedebergs Arch Pharmacol 2000; 361:610-620.
45. Kremer M, Judd J, Rifkin B, Auszmann J, Oursler MJ. Estrogen modulation of osteoclast lysosomal enzyme secretion. J Cell Biochem 1994; 58:1-9.

Available online at www.sciencedirect.com
SCIENCE DIRECT®
Experimental Cell Research 294 (2004) 149–158
Experimental Cell Research
www.elsevier.com/locate/yexcr

IL-6, LIF, and TNF-α regulation of GM-CSF inhibition of osteoclastogenesis in vitro

Genevieve Gorny,[a] Aubie Shaw,[a] and Merry Jo Oursler[b,*]

[a] *Department of Biology, University of Minnesota Duluth, Duluth, MN 55812, USA*
[b] *Endocrine Research Unit, Mayo College of Medicine, Rochester, MN 55905, USA*

Received 16 July 2003, revised version received 24 October 2003

Abstract

During pathological bone loss, factors that are both stimulatory and inhibitory for osteoclast differentiation are over-expressed. Despite the presence of inhibitory factors, osteoclast differentiation is significantly enhanced to bring about bone loss. To examine the hypothesis that stimulatory growth factors overcome the effects of inhibitory factors, we have examined the ability of IGF-I, IGF-II, IL-6, LIF, and TNF-α to overcome osteoclast differentiation inhibition by GM-CSF in vitro. Osteoclast numbers were significantly elevated by treatment with IGF-I, IGF-II, IL-6, LIF, or TNF-α alone whereas GM-CSF treatment of stromal cell and osteoclast co-cultures inhibited osteoclast formation. IL-6, LIF, or TNF-α, individually overcame GM-CSF inhibition whereas neither IGF-I nor IGF-II treatment overcame GM-CSF inhibition. Interestingly, GM-CSF addition with either IL-6 or TNF-α increased osteoclast numbers beyond that seen with either IL-6 or TNF-α alone. Combined treatment with TNF-α and IL-6 showed a significant increase in osteoclast numbers with GM-CSF addition. Examination of the impacts of these growth factors individually or in combinations on stromal cell M-CSF, RANKL, and OPG expression revealed a complex pattern involving alterations in the ratio of RANKL to OPG and/or M-CSF expression as candidate mechanisms of action.

Keywords: Osteoclastogenesis; GM-CSF; IGF-I; IGF-II; IL-6; LIF; TNF-α

Introduction

Mature osteoclasts form by differentiation from hematopoietic stem cells found in the marrow cavity [1]. Among the growth factors that have been shown to individually stimulate osteoclast differentiation are the insulin-like growth factors (IGF-I and IGF-II), interleukin 6 (IL-6), leukemia inhibitory factor (LIF), and tumor necrosis factor alpha (TNF-α) [2–12]. One potent inhibitor of differentiation is granulocyte/macrophage colony stimulating factor (GM-CSF), which shifts a pluripotential progenitor population away from the osteoclast lineage [13–17]. Conditions in which pathological bone loss is seen include orthopedic implant loosening, metastatic cancer, periodontal disease, and myeloma. A number of studies have recently shown that pathological bone loss in many cases is due to the stimulation of osteoclastogenesis by growth factors. Increased secretion of IL-6 and TNF-α has been implicated in bone loss associated with periodontal disease [18]. Macrophage colony-stimulating factor (M-CSF) and TNF-α are suspected to play a role in aseptic loosening of total hip replacements due to their ability to stimulate osteoclast formation and bone resorption [19,20]. Growth factors secreted by metastatic breast tumors have the ability to induce osteoclastic bone resorption and cause focal bone loss or osteolysis [21,22]. During metastatic breast cancer, osteoclast precursors are exposed to high levels of a variety of growth factors that are secreted by the tumor cells as they proliferate including IGF-II, IL-6, and TNF-α [21]. In this mix of stimulatory growth factors, GM-CSF was found, a potent inhibitor of osteoclast differentiation.

The majority of data available support that the number of osteoclasts present dictates the amount of bone resorbed. Thus, factors that stimulate bone loss act primarily by increasing the number of osteoclasts [23,24]. It is increasingly apparent that many of the paracrine and endocrine mechanisms that regulate bone metabolism do so, at least in part, by targeting management of osteoclast differentiation. A wealth of recent data has accumulated to document that

* Corresponding author. Endocrine Research Unit, Mayo College of Medicine, 200 First Street SW, Rochester, MN 55905. Fax: +1-507-284-2053.
E-mail address: moursler@d.umn.edu (M.J. Oursler).

0014-4827/$ - see front matter © 2003 Elsevier Inc. All rights reserved.
doi:10.1016/j.yexcr.2003.11.009

M-CSF and receptor activator of nuclear factor kappa B ligand (RANKL) are critical paracrine factors required for osteoclast differentiation [25]. Interactions between RANKL and its cognate receptor, RANK, are regulated by production of a decoy receptor, osteoprotegerin (OPG). Many paracrine factors influence osteoclast differentiation by regulating M-CSF, RANKL, and/or OPG expression by stromal support cells [25–32]. Since M-CSF, RANKL, and OPG are key factors that regulate osteoclast differentiation, growth factor-mediated regulation of these is likely to be important in impacting osteoclast numbers.

The effects of individual growth factors on osteoclast formation have been studied extensively, but the effect of combinations of growth factors on osteoclast formation have been much more limited. A recent study by Ragab et al. [33] revealed that IL-1, IL-6, IL-11, and TNF-α treatment together resulted in a synergistic elevation in osteoclast differentiation that was lacking when any one of the factors was removed. During both normal bone metabolism and pathological bone loss, osteoclast precursors are exposed to a host of growth factors as they differentiate into functional osteoclasts and it is important to understand these potentially complex interactions. Our previous studies have documented that tumor cells that metastasize to bone secrete the IGF-II, IL-6, LIF, TNF-α, and GM-CSF [21]. Therefore, we have examined the effects of exposure to combinations of IGFs, IL-6, LIF, TNF-α, and GM-CSF on osteoclast differentiation using an in vitro model of osteoclast formation.

Materials and methods

Materials

ST2 mouse stromal cells were obtained from Riken (Ibaraki, Japan). Human IGF-I and IGF-II, murine GM-CSF, human TNF-α, LIF, and IL-6 were purchased from R&D Systems (Minneapolis, MN). Growth factors were reconstituted in phenol red-free minimum essential media containing 0.25% bovine serum albumin (Sigma Co, St. Louis, MO) at the concentration recommended by the manufacturer. A 1, 25-dihydroxyvitamin D_3 was purchased from Biomol (Plymouth Meeting, PA) and resuspended in ethanol at a concentration of 10^{-4} M. Dexamethazone was purchased from Sigma and resuspended in ethanol at a concentration of 10^{-4} M.

In vitro osteoclast differentiation

Osteoclast precursors were harvested by flushing the marrow from femurs of male Balb/C mice (Taconic, Germantown, NY), as we have described previously [34]. Marrow cells were centrifuged, resuspended in serum containing 12% dimethyl sulfoxide, and frozen in liquid nitrogen until use. Mouse osteoclast-like cells were generated from mouse marrow precursors using the method described previously [34]. ST2 mouse stromal cells served as support cells and were grown to confluence in alpha-modified minimum essential medium (Sigma Co.) supplemented with 10% fetal bovine serum (Hyclone, Logan, UT) at 37°C, 5% CO_2. ST2 cells were plated into 48-well plates at a density of 8×10^4 cells per well and allowed to attach for 8–18 h. Osteoclast precursors were thawed into phenol red-free minimum essential medium supplemented with 10% FBS, and 50 ng/ml ascorbic acid. 1,25-Dihydroxyvitamin D_3 and dexamethazone were added to achieve a final concentration of 10^{-7} M each. Precursors were plated at a density of 5×10^4 cells per well onto the attached ST2 cells and growth factors were added. Growth factors doses were determined from the midpoints of the 50% maximal effective doses (ED_{50}) for each factor as determined by the supplier in cell proliferation or cytotoxicity assays. These doses are 10 ng/ml IGF-I (MCF-7 cells), 10 ng/ml IGF-II (MCF-7 cells), 0.15 ng/ml GM-CSF (DA-3 cells), 0.05 ng/ml TNF-α (L-929 cells), 0.5 ng/ml IL-6 (T1165.85.2.1 cells), and 0.1 ng/ml LIF (TF-1 cells). Media were changed every third day and fresh 1,25-dihydroxyvitamin D_3, dexamethasone, ascorbic acid, and growth factors were added.

Visualization of osteoclasts

After 11 days in culture, cells were washed gently with phosphate-buffered saline (PBS), pH 7.4, and fixed in a solution of 1% paraformaldehyde in PBS. Cells were then washed twice with water and stained for tartrate-resistant acid phosphatase (TRAP) using a kit supplied by Sigma Co. Multinuclear TRAP-positive cells were counted using an inverted light microscope. Cells were counted by tabulating the number of osteoclasts seen at 200× magnification across a single diameter of a 48-well plate (12 fields of view). Each treatment within an experiment was completed in triplicate wells and all experiments were repeated at least once with similar results.

Real time polymerase chain reaction analyses

ST2 cells were plated into 6-well plates at a density of 6.4×10^5 cells per well and allowed to attach for 12 h before switching to phenol red-free minimum essential medium supplemented with 10% FBS and 50 ng/ml ascorbic acid. 1, 25-Dihydroxyvitamin D_3 and dexamethazone were added to achieve a final concentration of 10^{-7} M as indicated. Growth factors were added alone or in combination at the concentrations outlined above and the cells cultured for an additional 3 days. RNA was isolated using Trizol reagent according to manufacturer's protocol (Invitrogen, Carlsbad, CA). Following LiCl precipitation to remove DNA, cDNA was synthesized by standard protocol: 1 μg total RNA was heat denatured at 68°C for 15 min in reverse transcription reaction buffer (50 mM Tris–HCl, 75 mM KCl, 3 mM $MgCl_2$, 50 mM DTT, 1 μM dNTPs, 500 ng oligo-dT primer). Following heat denaturation, 1 unit of MMLV-RT

(Invitrogen) was added and the mixture incubated at 37°C for 45 min followed by a 68°C incubation for an additional 15 min. For real-time PCR, the resultant cDNA was diluted 10-fold before analysis and 2 μl used for each reaction as follows: PCR buffer (20 mM Tris–HCl, 50 mM KCl, 3 mM $MgCl_2$), 300 nM of both the upstream and downstream primers (see table below), and 1 unit of Taq Polymerase (Promega). As a control, tubulin was always amplified simultaneously in separate reactions. Message levels were examined using the BioRad iCycler according to the specifics recommended by the manufacturer. The amount of target cDNA in the sample, relative to tubulin, was calculated using the formula 2-ΔΔCt, where ΔΔCt is the difference between the target and tubulin levels. The results were calculated as the relative quantification of the target gene compared to a control (vehicle without vitamin D or dexamethazone) treatment. The table below is the primer sequences used for amplification.

Target mRNA	5′ Primer	3′ Primer
M-CSF	CTCTGGCTGGCTTGGCTTGG	GCAGAAGGATGAGGTTGTG
OPG	ACGGACAGCTGGCACACCAG	CTCACACACTCGGTTGTGGG
RANKL	GGAGGACCATGAACCCTTTCC	GCTGGCTGCTGCTTCACTGG
c-fms	GGACTATGCTAACCTGCCAAG	CTCTCCTCTTCTCCGTCAC
RANK	GGAGCCTCAGGGTCCG	GCCCGCTAGAGATGAACGTG
Tubulin	CTGCTCATCAGCAAGATCAGAG	GCATTATAGGGXTCCACCACAG

Ribonuclease protection assay

Osteoclast co-cultures or ST2 cells alone were treated with growth factors during the 11-day differentiation period. Total RNA was isolated using the acid guanidinium thiocyanate–phenol–chloroform method [35]. RNA was further purified by lithium chloride precipitation followed by ethanol precipitation. Purified RNA was quantitated by UV spectrophotometry. Ten micrograms of RNA was analyzed by ribonuclease protection assay (RPA). RPA probe templates were purchased from BD PharMingen (San Diego, CA). [α-^{32}P]UTP-labeled RNA probes were generated using in vitro transcription according to manufacturer's protocol (BD PharMingen). RNA probes were hybridized with the RNA by heating to 90°C and slowly cooling to 50°C overnight. RNase treatment was carried out according to manufacturer's protocol (BD PharMingen) and RNA–RNA duplexes were purified by phenol–chloroform extraction and ethanol precipitation. Fragments were separated by denaturing polyacrylamide gel electrophoresis, the gel was dried, and bands were visualized by autoradiography. The identity of the various protected fragments was determined by comparison with the undigested probe and positive control mRNA using NIH Image software.

Statistical analysis

Data are presented as the mean of triplicate wells ± standard errors (SEM). Data points were compared using a one-tailed Student's *t* test. Differences were considered to be statistically significant at a 0.05 level of significance.

Results

Growth factor impacts on osteoclast formation

As shown in Fig. 1, IGF-I, IGF-II, IL-6, LIF, or TNF-α treatment during differentiation dose-dependently stimulated osteoclast formation. Maximal stimulation was approximately 1.5- to 2-fold. In contrast, GM-CSF dose-dependently inhibited osteoclast formation with complete inhibition at 15 pg/ml. Osteoclast differentiation in this culture system is dependent on vitamin D and glucocorticoid (dexamethazone) induction of RANKL and M-CSF as well as repression of OPG in the stromal support cells. Since these are potent regulators of osteoclast differentiation, we have investigated the expression levels of these factors in our cultures. As documented in Table 1, vitamin D and dexamethazone increased RANKL while repressing OPG expression as expected. GM-CSF, IGF-I, LIF, and TNF-α each increased both RANKL and OPG expression whereas IGF-II and IL-6 showed lower expression levels for both RANKL and OPG compared to vitamin D and dexamethazone alone. Since the ratio of RANKL to OPG and M-CSF expression levels are critical to the impact on osteoclast differentiation, we examined growth factor impacts on these in our culture system. As seen in Fig. 2, vitamin D and dexamethazone increased both M-CSF expression and the ratio of RANKL to OPG, as expected. GM-CSF treatment lowered the RANKL/OPG ratio significantly as the result of higher levels of OPG expression. Likewise, GM-CSF decreased M-CSF expression. With IGF-I treatment, the ratio of RANKL to OPG was insignificantly higher than untreated cultures but lower than vitamin D- and dexamethazone-treated cells while this treatment significantly increased M-CSF expression. IGF-II or IL-6 elevated M-CSF levels significantly and also significantly increased the RANKL/OPG ratio, mainly due to decreased OPG expression. Both LIF and TNF-α elevated M-CSF expression and also increased the RANKL/OPG ratio due to increased RANKL expression.

Overcoming GM-CSF inhibition

The 50% effective dose (ED_{50}) for GM-CSF-mediated repression of osteoclast differentiation in our cultures was 1.59 pg/ml. In co-cultures treated with the partial inhibi-

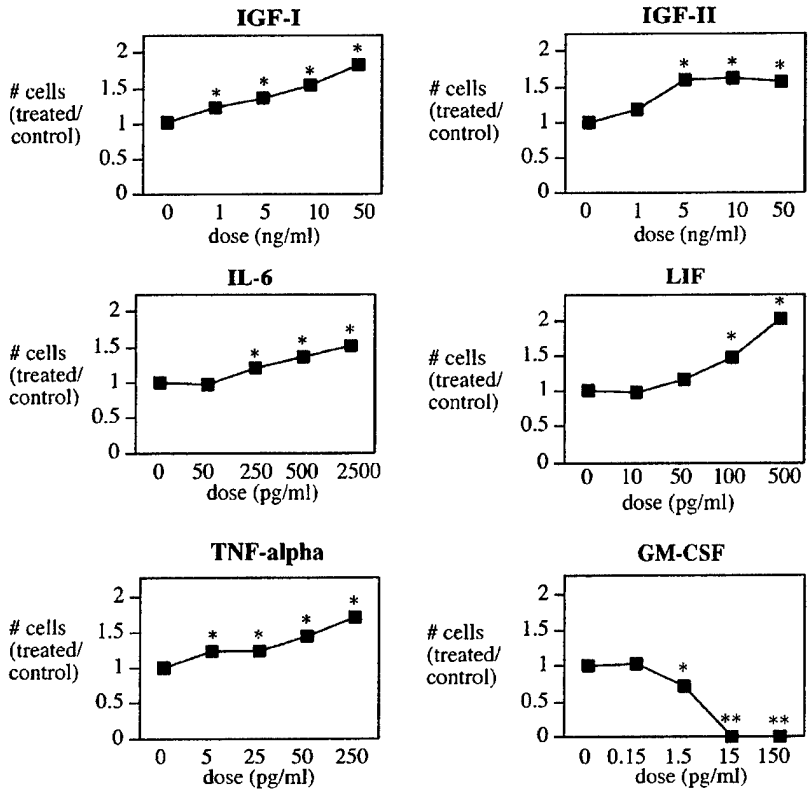

Fig. 1. Effects of growth factors on osteoclast differentiation. Mouse osteoclast-like cells were differentiated as described in the presence of vitamin D, dexamethazone, and either vehicle (0) or the indicated concentration of the indicated growth factor. Cells were TRAP stained after 11 days in culture and multinucleated cells were counted by light microscopy. The ratio of treated to control cells was calculated. The mean control osteoclast count was 144 ± 22. *$P < 0.05$, significantly different from vehicle-treated cells.

tory dose of GM-CSF (1.5 pg/ml), addition of the manufacturer's ED_{50} dose of IL-6, LIF, or TNF-α blocked GM-CSF-mediated repression (Fig. 3). Interestingly, the combination of GM-CSF with either IL-6 or TNF-α resulted in increased osteoclast formation above the levels observed without GM-CSF addition. Neither IGF-I nor IGF-II was able to overcome GM-CSF-mediated inhibition of osteoclast differentiation. Examination of stromal cell RANKL and OPG expression (Table 2) revealed that IGF-I combined with GM-CSF resulted in decreased expression of both factors compared to IGF-I treatment alone. For the IGF-II treated cells, the addition of GM-CSF resulted in increased expression of both RANKL and OPG. In the IL-

Table 1
Expression of RANKL and OPG following individual growth factor treatment

Treatment	–	Vit.D + Dex	GM-CSF	IGF-I	IGF-II	IL-6	LIF	TNF-α
RANKL	1.0	2.7	10.4	24.0	1.0	2.0	42.4	15.4
OPG	1.0	0.7	13.0	16.0	0.1	0.1	3.3	1.2

Real Time PCR analysis of RANKL and OPG mRNA levels. All samples were normalized to tubulin to ensure consistent loading of total RNA. Data are presented as treated/control (–) ratios of the mean of at least three experiments.

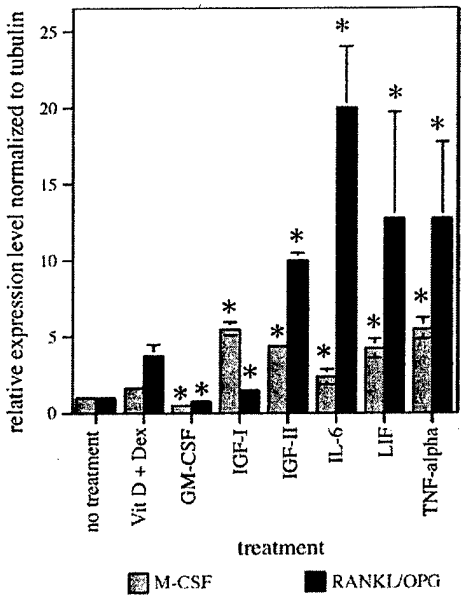

Fig. 2. Effects of growth factors on stromal cell RANKL/OPG ratio and M-CSF expression detected by Real Time PCR analysis. All samples were normalized to tubulin to ensure consistent loading of total RNA. Data are presented as treated/control (no treatment) ratios of the mean of at least three experiments. Vit.D + Dex = Vitamin D_3 plus dexamethizone. *$P < 0.05$, significantly different from vitamin D and dexamethazone-treated cells.

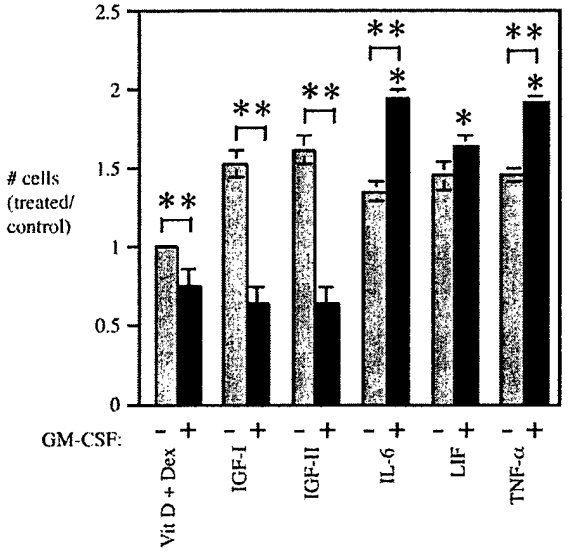

Fig. 3. The impact of stimulatory growth factors on GM-CSF-induced repression of osteoclast differentiation. Mouse osteoclast-like cells were differentiated as described in the presence of IGF-I, IGF-II, IL-6, LIF, or TNF-α, each at their ED_{50} (see Materials and methods) in either the absence (−) or presence (+) of 1.5 pg/ml GM-CSF. Cells were TRAP stained after 11 days in culture and multinucleated cells were counted by light microscopy. The ratio of treated to control (Vit.D + Dex) cells was calculated. *Significantly different from GM-CSF only-treated cells, $P < 0.05$. The mean control osteoclast count was 152 ± 37. **Significantly different from each other. $P < 0.05$.

6 treated cultures, addition of GM-CSF resulted in decreased RANKL expression while OPG expression was essentially unchanged. Examination of the effects of GM-CSF on either LIF or TNF-α responses showed that RANKL expression decreased while OPG expression increased with GM-CSF treatment. Comparisons of GM-CSF treatment alone (10.4, Table 1) to the addition of another growth factor (Table 2) showed that IGF-I, IL-6, and TNF-α decreased whereas IGF-II and LIF increased RANKL expression. OPG expression comparisons between GM-CSF alone (13.0, Table 1) and with addition of another growth factor showed decreased OPG with IGF-I, IL-6, LIF, and TNF-α co-treatment whereas expression increased with IGF-II. Examination of the ratio of RANKL to OPG

Table 2
Effect of GM-CSF on growth factor impacts on RANKL and OPG expression

Treatment	−	Vit.D + Dex	IGF-I		IGF-II		IL-6		LIF		TNF-α	
GM-CSF	−	+	−	+	−	+	−	+	−	+	−	+
RANKL	1.0	2.7	10.4	24.0	3.7	1.0	41.2	2.0	0.1	42.4	16.1	15.4	5.5
OPG	1.0	0.7	13.0	16.0	6.1	0.1	29.4	0.1	0.1	3.3	7.0	1.2	7.8

Real Time PCR analysis of RANKL and OPG m-RNA levels. All samples were normalized to tubulin to ensure consistent loading of total RNA. Data are presented as treated/control (−) ratios of the mean of at least three experiments.

(Fig. 4A) reveals that GM-CSF addition consistently decreased the RANKL/OPG ratio for all growth factor treatments when compared to growth factor without GM-CSF. Comparing GM-CSF responses alone (0.8, Fig. 2) to GM-CSF combined with another growth factor, the RANKL/OPG ratio was decreased for IGF-I treatment (0.6), remained relatively constant with TNF-α treatment (0.7), and was elevated with the addition of IGF-II (1.4), IL-6 (1.0), or LIF (2.3) to the GM-CSF treatment. A more complex pattern was observed for M-CSF expression (Fig. 4B). In both IGF-I and IGF-II treatments, addition of GM-CSF significantly decreased M-CSF expression whereas no

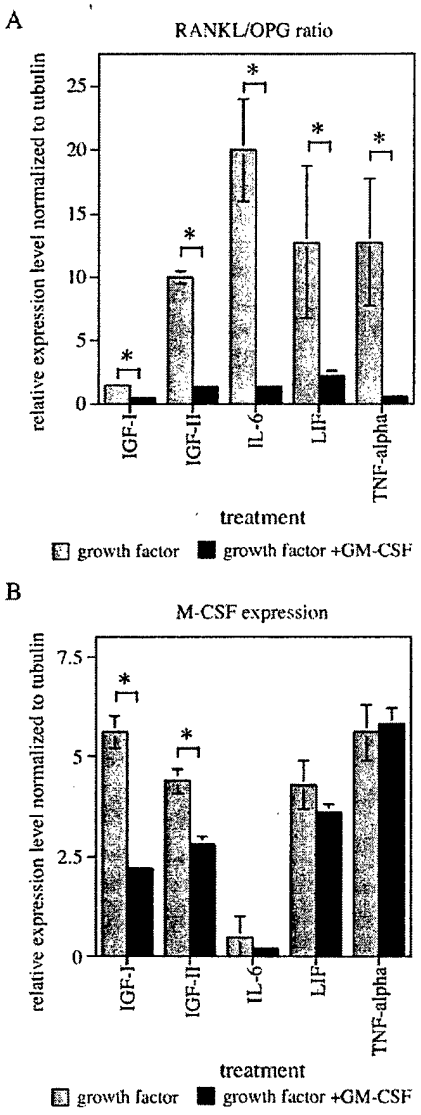

Fig. 4. Effects of GM-CSF on growth factors treatment of stromal cells. Real Time PCR analysis of RANKL/OPG ratios and M-CSF mRNA levels. All samples were normalized to tubulin to ensure consistent loading of total RNA. Data are presented as treated/control (no treatment) ratios of the mean of at least three experiments. *Significantly different from each other, $P < 0.05$.

significant change was observed in IL-6, LIF, and TNF-α treated cultures when GM-CSF was added to the cultures. Comparing GM-CSF treatment alone (0.5, Fig. 2) to co-treatment, M-CSF expression increased with addition of IGF-I (2.2), IGF-II (2.8), LIF (3.6), and TNF-α 5.8) to GM-CSF while IL-6 addition decreased M-CSF gene expression (0.2).

GM-CSF receptor expression

We next examined whether IL-6, LIF, or TNF-α repressed expression of the GM-CSF receptor to block the impact of GM-CSF on osteoclast differentiation (Table 3). RPA analysis of the alpha subunit of the GM-CSF receptor (GM-CSFRα) expression by support cells and osteoclast co-cultures showed that GM-CSFRα was expressed by osteoclast co-cultures and not support cells alone. GM-CSFRα expression was slightly decreased following IL-6, LIF, or TNF-α treatment. In GM-CSF-treated co-cultures, there was no GMCSFRα detected, consistent with the absence of osteoclasts in these cultures. The signaling component of the GM-CSF receptor, Beta C (βc), was highly expressed by both osteoclast co-cultures and support cells alone. As with GMCSFRα, it appears that βc receptor expression is only slightly depressed with all growth factor treatments.

Overcoming GM-CSF inhibition with growth factor combinations

Since the milieu in which osteoclasts differentiate includes multiple cytokines and other growth factors, we examined the impact of combinations of IL-6, LIF, and TNF-α on differentiation and overcoming GM-CSF-mediated inhibition of osteoclast differentiation (Fig. 5). As expected, addition of different combinations of growth factors that individually blocked GM-CSF repression of differentiation successfully blocked GM-CSF-mediated inhibition. Surprisingly, the combination of TNF-α and IL-6 with GM-CSF significantly stimulate differentiation compared to TNF-α and IL-6 without GM-CSF. However,

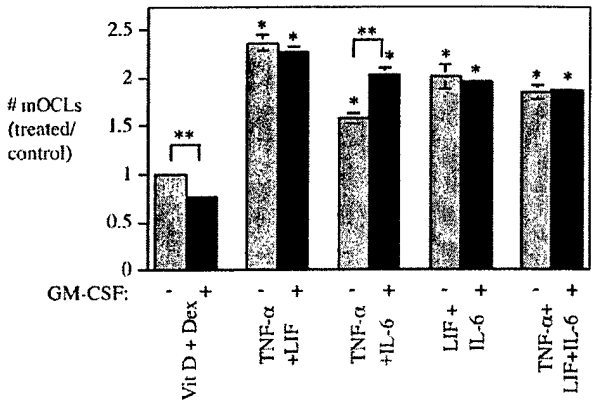

Fig. 5. Combinations of TNF-α, LIF, and IL-6 with GM-CSF influences on osteoclast differentiation. Mouse osteoclast-like cells were differentiated as described in the absence (−) or presence (+) of 1.5 pg/ml GM-CSF and various combinations of TNF-α, LIF, and IL-6 as indicated. Cells were TRAP stained after 11 days in culture and multinucleated cells were counted by light microscopy. The ratio of treated to control cells was calculated. *Significantly different from control (untreated) cells, $P < 0.05$. The mean control osteoclast count was 172 ± 34. **Significantly different from each other, $P < 0.01$.

addition of LIF to the TNF-α and IL-6 treatment resulted in abrogation of the GM-CSF-induced augmentation in osteoclast numbers. Examination of RANKL and OPG expression following stromal cell treatment with these combinations reveals that RANKL and OPG expression increased in all cases with the addition of GM-CSF (Table 4). The ratio of RANKL to OPG (Fig. 6A) significantly increased in the TNF-α plus IL-6 cultures with GM-CSF addition. A similar response was seen with the combination of TNF-α plus IL-6 plus LIF, although the magnitude of the response was less. A comparable pattern was observed in M-CSF expression (Fig. 6B).

RANK and c-fms expression

We examined the impacts of IGF-I, IGF-II, IL-6, LIF, TNF-α alone and in combinations on expression of the receptors for M-CSF (c-fms) and RANKL (RANK) in spleen cultures to determine if it was likely that these growth factors impact c-fms and RANK expression in

Table 3
Expression of GM-CSF receptor mRNA is not altered by TNF-α, LIF, or IL-6 treatment

Cell type	ST2	OC	ST2	OC	ST2	OC	ST2	OC	ST2	OC
Treatment	none		GM-CSF		IL-6		LIF		TNF-α	
GM-CSFRα	0.00	1.27	0.00	0.00	0.00	0.75	0.00	0.90	0.00	0.87
βc	1.30	1.44	0.70	0.86	0.93	0.72	0.77	0.97	0.84	0.84

Steady-state levels of GM-CSF receptor subunits in ST2 stromal support cells (ST2) and mouse osteoclast-like cell/ST2 cocultures (OC) treated with the indicated growth factor at their respective ED_{50S} were analyzed by RPA. Quantitation was carried out by densitometry using NIH Image 1.61. All samples were normalized to the housekeeping gene GAPDH to ensure consistent loading of total RNA. Data are presented as treated/control ratios of relative optical densities.

Table 4
Effect of GM-CSF on RANKL and OPG expression following treatment with growth factor combinations

Treatment	LIF + TNF-α		IL-6 + TNF-α		LIF + IL-6		LIF + TNF-α + IL-6	
GM-CSF	–	+	–	+	–	+	–	+
RANKL	0.2	29.3	0.6	52.7	22.0	52.4	22.6	118.3
OPG	0.2	43.4	0.7	9.5	18.4	30.7	11.2	35.1

Real Time PCR analysis of RANKL and OPG mRNA levels. All samples were normalized to tubulin to ensure consistent loading of total RNA. Data are presented as treated/control (−) ratios of the mean of at least three experiments.

osteoclast precursors (Table 5). We have selected spleen cultures as this model responds similarly to marrow precursors when treated with these growth factors (data not shown) and the tissue is less diverse in cells likely to express c-fms and RANK compared to marrow cultures. Most of the growth factors, alone and in combinations, did not significantly impact expression. However, expression of c-fms was somewhat elevated by IL-6, LIF, and GM-CSF treatment whereas RANK expression was elevated by GM-CSF alone and in combination with IL-6. In contrast, there was reduced RANK expression following TNF-α treatment.

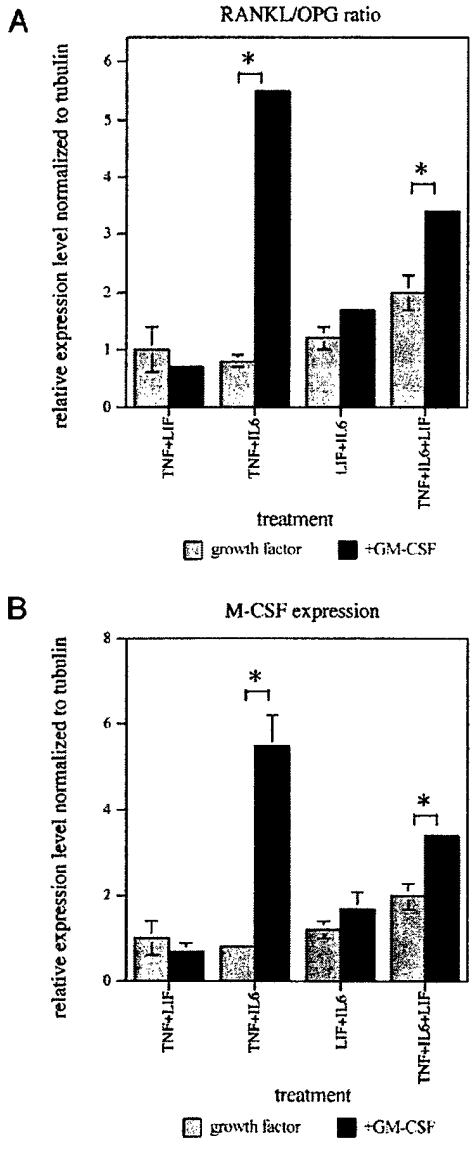

Fig. 6. Effects of GM-CSF on stromal cells treated with combinations of growth factors. Real Time PCR analysis of RANKL/OPG ratios and M-CSF mRNA levels. All samples were normalized to tubulin to ensure consistent loading of total RNA. Data are presented as treated/control (no treatment) ratios of the mean of at least three experiments. *Significantly different from each other, $P < 0.05$.

Table 5
Effect of growth factors on c-fms and RANK expression in spleen cultures containing osteoclast precursors

Treatment	c-fms	RANK
M-CSF + RANKL	1 ± 0	1 ± 0
M-CSF + IGF-I	0.75 ± 0.35	1.32 ± 0.41
M-CSF + IGF-II	1.01 ± 0.77	0.93 ± 0.17
M-CSF + IL-6	1.96 ± 0.38*	1.21 ± 0.38
M-CSF + LIF	2.44 ± 0.49*	1.02 ± 0.21
M-CSF + TNF-α	0.90 ± 0.06	0.54 ± 0.47
M-CSF + GM-CSF	1.23 ± 0.14*	1.68 ± 0.20*
M-CSF + GM-CSF + IGF-I	0.85 ± 0.09	0.82 ± 0.28
M-CSF + GM-CSF + IGF-II	0.99 ± 0.21	0.91 ± 0.42
M-CSF + GM-CSF + IL-6	1.38 ± 0.48	1.44 ± 0.18*
M-CSF + GM-CSF + LIF	1.06 ± 0.10	0.99 ± 0.01
M-CSF + GM-CSF + TNF-α	0.72 ± 0.28	1.05 ± 0.12
M-CSF + GM-CSF + IL-6 + TNF-α	0.93 ± 0.21	0.9 ± 0.19

Real-time PCR analysis of c-fms and RANK mRNA levels. All samples were normalized to tubulin to ensure consistent loading of total RNA. Data are presented as treated/control (M-CSF + RANKL treatment) ratios of the mean of two experiments.
* $P < 0.05$ compared to M-CSF + RANKL treatment.

Discussion

This initial phase of our studies of the impact of growth factor interactions on osteoclast differentiation focused on examining our culture system for consistency with published data [9,24,33,36–38]. As expected, IGF-I, IGF-II, IL-6, LIF, and TNF-α each individually stimulated osteoclast differentiation in our cultures. Comparisons between our gene expression results and published data reveal that many of our studies of the individual growth factor effects mirror what has already been published [2–12,39,40]. There are, however, some interesting differences. Specifically, we observed an increase in OPG following IGF-I treatment while Rubin et al. [41] documented a decrease. Since both sets of studies involved the ST2 stromal cell line, it must be concluded that the plasticity in these cells through continual passage in culture has lead to these differences in IGF-I responses. In both cases, however, the ratio of RANKL to OPG was increased with treatment. Nakashima et al. [42] found that IL-6 increased RANKL, and TNF-α decreased OPG expression in primary calvarial cells. In contrast, we were unable to detect an impact of IL-6 on RANKL and saw an increase in OPG following TNF-α treatment. These differences are likely due to differences in the model systems being studied, perhaps reflecting the heterogeneity of the calvarial culture model. Evaluation of articular cartilage and chondrocyte monolayers revealed no impact of IL-6 or LIF on M-CSF expression whereas GM-CSF treatment increased M-CSF expression [43]. Our studies showed that, in ST2 cells, IL-6 and LIF increased M-CSF expression and GM-CSF decreased M-CSF expression.

Again, these differences are likely due to the differences in the phenotypes of these cells.

Previous studies have shown that GM-CSF has opposing effects on osteoclast formation, appearing to depend on the state of differentiation of the target cell. GM-CSF stimulates proliferation of early pluripotential osteoclast precursors, but potently inhibits later stages of osteoclast differentiation by directing the pluripotential cells along alternate pathways [13–17]. The data presented here show that GM-CSF potently inhibits osteoclast formation from marrow precursors. Since GM-CSF is often produced in large quantities during pathological bone loss, we wanted to understand how osteoclasts are formed in the presence of this potent inhibitor. GM-CSF effects were abolished by the presence of IL-6, LIF, or TNF-α. Similar to GM-CSF, TNF-α, LIF, and IL-6 affect relatively early stages of osteoclast differentiation [44–46]. This overlap may allow these factors to overcome inhibition by GM-CSF. Indeed, differentiation induced by LIF, IL-6, or TNF-α was further enhanced by GM-CSF, indicating an additive or synergistic interaction between these factors. We examined GM-CSF impacts on M-CSF, RANKL, and OPG expression levels following IGF-I, IGF-II, LIF, IL-6, or TNF-α co-treatments and found that there was no consistent pattern of responses. RANKL increased when GM-CSF was combined with IGF-II yet decreased when combined with IGF-I, IL-6, or TNF-α. Likewise, OPG responses were similarly mixed with increased OPG following IGF-II, LIF, or TNF-α co-treatment, decreased OPG expression with IGF-II co-treatment, and no impact with IL-6 co-treatment. In all cases, the ratio of RANKL to OPG was repressed with GM-CSF co-treatment regardless of whether the growth factor was able to overcome GM-CSF-mediated repression of osteoclast differentiation. However, examination of GM-CSF impacts on the M-CSF showed repression of expression when the growth factor was unable to overcome GM-CSF-mediated repression of osteoclast differentiation (either IGF-I or IGF-II) and an inability of GM-CSF to repress M-CSF expression when the growth factor was able to overcome GM-CSF effects (IL-6, LIF, or TNF-α). Thus, it appears that blocking GM-CSF-mediated repression of M-CSF enables LIF, IL-6, or TNF-α to overcome GM-CSF inhibition of osteoclast differentiation. In contrast with our studies, Miyamoto et al. [13] documented that GM-CSF inhibited osteoclast differentiation following treatment with either RANKL plus M-CSF or TNF-α in the absence of M-CSF. Moreover, Servet-Delprat et al. [47] found that GM-CSF plus TNF-α directs macrophage precursors to dendritic cells. These discrepancies may be due to differences in model systems studied since our responses are to the combined effects of stromal cell-derived M-CSF and RANKL plus the growth factor under study. Since IL-6, LIF, or TNF-α seemed to render cells unresponsive to GM-CSF, we examined expression of the GM-CSF receptor in co-cultures stimulated by these factors. Our data support that the inability of GM-CSF to repress osteoclast formation in the presence of IL-6, LIF, or TNF-α is not due to downregulation of GM-CSF receptor transcription. Examination of expression of c-fms and RANK also did not provide consistent insights into mechanisms of action. Although there were some statistically significant impacts on expression, the lack of magnitude of these responses supports that regulation of expression of the receptors for M-CSF and/or RANKL is not likely to be the principle mechanism by which these growth factors impact osteoclast differentiation. The TNF-α-induced reduction in RANK expression may reflect the observations that TNF-α-mediated stimulation of osteoclastogenesis is independent of RANK stimulation. The observation that GM-CSF slightly elevated expression of c-fms and RANK supports that it is unlikely that GM-CSF-mediated repression of osteoclast differentiation is due to repression of the receptors for M-CSF or RANKL, at least within 3 days of treatment.

Given our data, it was not surprising that combinations of growth factors that individually could overcome GM-CSF-mediated repression of osteoclast differentiation also blocked this repression when combined together. What was surprising was that the addition of GM-CSF to the TNF-α plus IL-6 treatment enhanced osteoclast differentiation compared to the absence of GM-CSF. Gene expression studies revealed a synergistic increase in both the ratio of RANKL to OPG and M-CSF expression with GM-CSF addition. Curiously, adding LIF to the combined IL-6 and TNF-α did not result in increased osteoclast numbers with GM-CSF addition. Although the combination of TNF-α plus IL-6 plus LIF also showed gene expression pattern similar to cultures lacking LIF addition, the magnitude of this enhancement was much less when LIF was added. These data support that the additive response observed in osteoclast differentiation results from the magnitude of the increase in the RANKL/OPG ratio and M-CSF expression.

The data here presented show that the combined effects of growth factors secreted during pathological bone loss enhance osteoclast differentiation beyond that of individual growth factors when GM-CSF was added to the TNF-α plus IL-6 co-cultures. The data also suggest that GM-CSF may also contribute to elevated osteoclast differentiation in a variety of conditions where IL-6, LIF, and TNF-α are present together. Therefore, the variety of growth factors secreted during pathological bone loss may provide an effective means for generating large quantities of osteoclasts, overcoming the presence of growth factors that individually repress osteoclast differentiation. We conclude from these studies that plans to target individual growth factors for controlling osteoclast numbers must consider the entire milieu in which pathological bone loss proceeds to design effective therapies.

Acknowledgments

We would like to acknowledge Drs. David Monroe and Thomas Spelsberg for assistance with the Real Time

Polymerase Chain Reaction assays. This work was generously supported by a grant from the Department of Defense #DAMD17-00-1-0346, the Whiteside Institute for Clinical Research, National Institutes of Health grant #DE14680.

References

[1] D.G. Walker, Osteopetrosis cured by temporary parabiosis, Science 180 (1973) 875.
[2] T. Suda, N. Takahashi, T.J. Martin, Modulation of osteoclast differentiation, Endocr. Rev. 13 (1992) 66–80.
[3] T. Suda, K. Kobayashi, E. Jimi, N. Udagawa, N. Takahashi, The molecular basis of osteoclast differentiation and activation, Novartis Found. Symp. 232 (2001) 235–247 (discussion 247–50).
[4] S. Reddy, G.D. Roodman, Control of osteoclast differentiation, Crit. Rev. Eukaryot. Gene Expr. 8 (1998) 1–17.
[5] T. Martin, E. Romas, M. Gillespie, Interleukins in the control of osteoclast differentiation, Crit. Rev. Eukaryot. Gene Expr. 8 (1998) 107–123.
[6] K. Chihara, T. Sugimoto, The action of GH/IGF-I/IGFBP in osteoblasts and osteoclasts, Horm. Res. 48 (1997) 45–49.
[7] H. Kaji, T. Sugimoto, M. Kanatani, K. Nishiyama, M. Nasu, K. Chihara, Insulin-like growth factor-I mediates osteoclast-like cell formation stimulated by parathyroid hormone, J. Cell. Physiol. 172 (1997) 55–62.
[8] G. Fiorelli, L. Formigli, S. Zecchi Orldini, F. Gori, A. Falchetti, A. Morelli, A. Tanini, S. Benvenuti, M.L. Brandi, Characterization and function of the receptor for IGF-I in human preosteoclastic cells, Bone 18 (1996) 269–276.
[9] P. Hill, J. Reynolds, M. Meikle, Osteoblasts mediate insulin-like growth factor-I and -II stimulation of osteoclast formation and function, Endocrinology 136 (1995) 124–131.
[10] D.J. Baylink, R.D. Finkelman, S. Mohan, Growth factors to stimulate bone formation, J. Bone Miner. Res. 8 (Suppl. 2) (1993) S565–S572.
[11] H. Mochizuki, Y. Hakeda, N. Wakatsuki, N. Usui, S. Akashi, T. Sato, K. Tanaka, M. Kumegawa, Insulin-like growth factor-I supports formation and activation of osteoclasts, Endocrinology 131 (1992) 1075.
[12] M. Slootweg, W. Most, E. van Beek, L. Schot, S. Papapoulos, C. Lowik, Osteoclast formation together with interleukin-6 production in mouse long bones is increased by insulin-like growth factor-I, J. Endocrinol. 132 (1992) 433–438.
[13] T. Miyamoto, O. Ohneda, F. Arai, K. Iwamoto, S. Okada, K. Takagi, D.M. Anderson, T. Suda, Bifurcation of osteoclasts and dendritic cells from common progenitors, Blood 98 (2001) 2544–2554.
[14] G. Hattersley, T. Chambers, Effects of interleukin 3 and of granulocyte-macrophage and macrophage colony stimulating factors on osteoclast differentiation from mouse hemopoietic tissue, J. Cell. Physiol. 142 (1990) 201–209.
[15] Y. Fujikawa, A. Sabokbar, S.D. Neale, I. Itonaga, T. Torisu, N.A. Athanasou, The effect of macrophage-colony stimulating factor and other humoral factors (interleukin-1, -3, -6, and -11, tumor necrosis factor-alpha, and granulocyte macrophage-colony stimulating factor) on human osteoclast formation from circulating cells, Bone 28 (2001) 261–267.
[16] H. Yamazaki, T. Kunisada, T. Yamane, S.I. Hayashi, Presence of osteoclast precursors in colonies cloned in the presence of hematopoietic colony-stimulating factors, Exp. Hematol. 29 (2001) 68–76.
[17] W.J. Liggett, N. Shevde, P. Anklesaria, S. Sohoni, J. Greenberger, J. Glowacki, Effects of macrophage colony stimulating factor and granulocyte-macrophage colony stimulating factor on osteoclastic differentiation of hematopoietic progenitor cells, Stem Cells 11 (1993) 398–411.
[18] S.H. Wiebe, M. Hafezi, H.S. Sandhu, S.M. Sims, S.J. Dixon, Osteoclast activation in inflammatory periodontal diseases, Oral Dis. 2 (1996) 167–180.
[19] S.D. Neale, A. Sabokbar, D.W. Howie, D.W. Murray, N.A. Athanasou, Macrophage colony-stimulating factor and interleukin-6 release by periprosthetic cells stimulates osteoclast formation and bone resorption, J. Orthop. Res. 17 (1999) 686–694.
[20] J.W. Xu, Y.T. Konttinen, J. Lassus, S. Natah, A. Ceponis, S. Solovieva, P. Aspenberg, S. Santavirta, Tumor necrosis factor-alpha (TNF-alpha) in loosening of total hip replacement (THR), Clin. Exp. Rheumatol. 14 (1996) 643–648.
[21] L. Pederson, B. Winding, N. Foged, T. Spelsberg, M. Oursler, Identification of breast cancer cell line-derived paracrine factors that stimulate osteoclast activity, Cancer Res. 59 (1999) 5849–5855.
[22] D.R. Clohisy, D. Palkert, M.L. Ramnaraine, I. Pekurovsky, M.J. Oursler, Human breast cancer induces osteoclast activation and increases the number of osteoclasts at sites of tumor osteolysis, J. Orthop. Res. 14 (1996) 396–402.
[23] T. Suda, I. Nakamura, E. Jimi, N. Takahashi, Regulation of osteoclast function, J. Bone Miner. Res. 12 (1997) 869–879.
[24] G.D. Roodman, Advances in bone biology: the osteoclast, Endocr. Rev. 17 (1996) 308–332.
[25] S. Khosla, Minireview: the OPG/RANKL/RANK system, Endocrinology 142 (2001) 5050–5055.
[26] G.J. Atkins, D.R. Haynes, S.M. Geary, M. Loric, T.N. Crotti, D.M. Findlay, Coordinated cytokine expression by stromal and hematopoietic cells during human osteoclast formation, Bone 26 (2000) 653–661.
[27] G.J. Atkins, D.R. Haynes, S.E. Graves, A. Evdokiou, S. Hay, S. Bouralexis, D.M. Findlay, Expression of osteoclast differentiation signals by stromal elements of giant cell tumors, J. Bone Miner. Res. 15 (2000) 640–649.
[28] A.T. Mancino, V.S. Klimberg, M. Yamamoto, S.C. Manolagas, E. Abe, Breast cancer increases osteoclastogenesis by secreting M-CSF and upregulating RANKL in stromal cells, J. Surg. Res. 100 (2001) 18–24.
[29] H.M. Massey, J. Scopes, M.A. Horton, A.M. Flanagan, Transforming growth factor-beta1 (TGF-beta) stimulates the osteoclast-forming potential of peripheral blood hematopoietic precursors in a lymphocyte-rich microenvironment, Bone 28 (2001) 577–582.
[30] J.M. Quinn, K. Itoh, N. Udagawa, K. Hausler, H. Yasuda, N. Shima, A. Mizuno, K. Higashio, N. Takahashi, T. Suda, T.J. Martin, M.T. Gillespie, Transforming growth factor beta affects osteoclast differentiation via direct and indirect actions, J. Bone Miner. Res. 16 (2001) 1787–1794.
[31] N. Udagawa, N. Takahashi, E. Jimi, K. Matsuzaki, T. Tsurukai, K. Itoh, N. Nakagawa, H. Yasuda, M. Goto, E. Tsuda, K. Higashio, M.T. Gillespie, T.J. Martin, T. Suda, Osteoblasts/stromal cells stimulate osteoclast activation through expression of osteoclast differentiation factor/RANKL but not macrophage colony-stimulating factor: receptor activator of NF-kappa B ligand, Bone 25 (1999) 517–523.
[32] S. Wei, M.W. Wang, S.L. Teitelbaum, F.P. Ross, Interleukin-4 reversibly inhibits osteoclastogenesis via inhibition of NF-kappa B and mitogen-activated protein kinase signaling, J. Biol. Chem. 277 (2002) 6622–6630.
[33] A.A. Ragab, J.L. Nalepka, Y. Bi, E.M. Greenfield, Cytokines synergistically induce osteoclast differentiation: support by immortalized or normal calvarial cells, Am. J. Physiol., Cell Physiol. 283 (2002) C679–C687.
[34] A. Gingery, E. Bradley, A. Shaw, M.J. Oursler, Phosphatidylinositol 3-kinase coordinately activates the MEK/ERK and AKT/NFkappaB pathways to maintain osteoclast survival, J. Cell. Biochem. 89 (2003) 165–179.
[35] P. Chomczynski, N. Sacchi, Single-step method of RNA isolation by acid guanidinium thiocyanate–phenol–chloroform extraction, Anal. Biochem. 162 (1987) 156–159.
[36] G.D. Roodman, Cell biology of the osteoclast, Exp. Hematol. 27 (1999) 1229–1241.

[37] T. Suda, N. Udagawa, I. Nakamura, C. Miyaura, N. Takahashi, Modulation of osteoclast differentiation by local factors, Bone 17 (1995) 87S–91S.
[38] C.D. Richards, C. Langdon, P. Deschamps, D. Pennica, S.G. Shaughnessy, Stimulation of osteoclast differentiation in vitro by mouse oncostatin M, leukaemia inhibitory factor, cardiotrophin-1 and interleukin 6: synergy with dexamethasone, Cytokine 12 (2000) 613–621.
[39] P. Palmqvist, E. Persson, H.H. Conaway, U.H. Lerner, IL-6, leukemia inhibitory factor, and oncostatin M stimulate bone resorption and regulate the expression of receptor activator of NF-kappa B ligand, osteoprotegerin, and receptor activator of NF-kappa B in mouse calvariae, J. Immunol. 169 (2002) 3353–3362.
[40] B.A. Scheven, J.S. Milne, S.P. Robins, A novel culture system to generate osteoclasts and bone resorption using porcine bone marrow cells: role of M-CSF, Biochem. Biophys. Res. Commun. 231 (1997) 231–235.
[41] J. Rubin, C.L. Ackert-Bicknell, L. Zhu, X. Fan, T.C. Murphy, M.S. Nanes, R. Marcus, L. Holloway, W.G. Beamer, C.J. Rosen, IGF-I regulates osteoprotegerin (OPG) and receptor activator of nuclear factor-kappaB ligand in vitro and OPG in vivo, J. Clin. Endocrinol. Metab. 87 (2002) 4273–4279.
[42] T. Nakashima, Y. Kobayashi, S. Yamasaki, A. Kawakami, K. Eguchi, H. Sasaki, H. Sakai, Protein expression and functional difference of membrane-bound and soluble receptor activator of NF-kappaB ligand: modulation of the expression by osteotropic factors and cytokines, Biochem. Biophys. Res. Commun. 275 (2000) 768–775.
[43] I.K. Campbell, U. Novak, J. Cebon, J.E. Layton, J.A. Hamilton, Human articular cartilage and chondrocytes produce hemopoietic colony-stimulating factors in culture in response to IL-1, J. Immunol. 147 (1991) 1238–1246.
[44] C.W. Lowik, G. van der Pluijm, H. Bloys, K. Hoekman, O.L. Bijvoet, L.A. Aarden, S.E. Papapoulos, Parathyroid hormone (PTH) and PTH-like protein (PLP) stimulate interleukin-6 production by osteogenic cells: a possible role of interleukin-6 in osteoclastogenesis, Biochem. Biophys. Res. Commun. 162 (1989) 1546–1552.
[45] R. Kurzrock, Z. Estrov, M. Wetzler, J.U. Gutterman, M. Talpaz, LIF: not just a leukemia inhibitory factor, Endocr. Rev. 12 (1991) 208–217.
[46] G. van der Pluijm, W. Most, L. van der Wee-Pals, H. de Groot, S. Papapoulos, C. Lowik, Two distinct effects of recombinant human tumor necrosis factor-alpha on osteoclast development and subsequent resorption of mineralized matrix, Endocrinology 129 (1991) 1596–1604.
[47] C. Servet-Delprat, S. Arnaud, P. Jurdic, S. Nataf, M.F. Grasset, C. Soulas, C. Domenget, O. Destaing, A. Rivollier, M. Perret, C. Dumontel, D. Hanau, G.L. Gilmore, M.F. Belin, C. Rabourdin-Combe, G. Mouchiroud, Flt3+ macrophage precursors commit sequentially to osteoclasts, dendritic cells and microglia, BMC Immunol. 3 (2002) 15.

JOURNAL OF CELLULAR PHYSIOLOGY 200:99–106 (2004)

Roles of Stromal Cell RANKL, OPG, and M-CSF Expression in Biphasic TGF-β Regulation of Osteoclast Differentiation

MARY KARST,[1] GENEVIEVE GORNY,[1] RACHELLE J. SELLS GALVIN,[2] AND MERRY JO OURSLER[1,3]*

[1]Department of Biology, University of Minnesota, Duluth, Minnesota
[2]Lilly Research Labs, Eli Lilly and Company, Indianapolis, Indiana
[3]Endocrine Research Unit,
Mayo Clinic and Foundation Rochester, Minnesota

To better understand the complex roles of transforming growth factor-beta (TGF-β) in bone metabolism, we examined the impact of a range of TGF-β concentrations on osteoclast differentiation. In co-cultures of support cells and spleen or marrow osteoclast precursors, low TGF-β concentrations stimulated while high concentrations inhibited differentiation. We investigated the influences of TGF-β on macrophage colony stimulating factor (M-CSF), receptor activator of NF-κB ligand (RANKL), and osteoprotegerin (OPG) expression and found a dose dependent inhibition of M-CSF expression. RANKL expression was elevated at low TGF-β concentrations with a less dramatic increase in OPG. Addition of OPG blocked differentiation at the stimulatory TGF-β dose. Thus, low TGF-β concentrations elevated the RANKL/OPG ratio while high concentrations did not, supporting that, at low TGF-β concentrations, there is sufficient M-CSF and a high RANKL/OPG ratio to stimulate differentiation. At high TGF-β concentrations, the RANKL/OPG ratio and M-CSF expression were both repressed and there was no differentiation. We examined whether TGF-β-mediated repression of osteoclasts differentiation is due to these changes by adding M-CSF and/or RANKL and did not observe any impact on differentiation repression. We studied direct TGF-β impacts on osteoclast precursors by culturing spleen or marrow cells with M-CSF and RANKL. TGF-β treatment dose-dependently stimulated osteoclast differentiation. These data indicate that low TGF-β levels stimulate osteoclast differentiation by impacting the RANKL/OPG ratio while high TGF-β levels repress osteoclast differentiation by multiple avenues including mechanisms independent of the RANKL/OPG ratio or M-CSF expression regulation. J. Cell. Physiol. 200: 99–106, 2004.

Transforming growth factor-beta (TGF-β) is a ubiquitous multifunctional cytokine that has a spectrum of influences. The variety of reported responses to TGF-β depends, at least in part, on experimental conditions as well as the cell type under study. Within the bone environment, TGF-β is a key regulator of bone metabolism. Although all TGF-β isoforms bind to the same receptor complex, there have been some reports of different cellular responses to the different isoforms (Jennings et al., 1988; Segarini et al., 1988; ten Dijke et al., 1990; Lyons et al., 1991; Liu et al., 2000). In the presence of stromal support cells, TGF-β1 has a biphasic effect on osteoclast differentiation from marrow precursors, in that TGF-β1 stimulates differentiation at a low dose while inhibiting differentiation at a higher dose (Shinar and Rodan, 1990; Mundy, 1991; Yamaguchi and Kishi, 1995). Spleen cells, as well as marrow cells, contain osteoclast precursors and the possibility of a biphasic effect of TGF-β on spleen cell precursor differentiation has not yet been studied.

A great deal of information on osteoclast differentiation has been investigated using a co-culture system of osteoclast precursors from either spleen or marrow combined with a support cell line, such as osteoblasts or stromal cells (Udagawa et al., 1990; Takahashi et al., 1995). From these studies, it has been demonstrated

Contract grant sponsor: Department of the Army (DOD); Contract grant number: DAMD17-00-1-0346; Contract grant sponsor: Minnesota Medical Foundation; Contract grant sponsor: Lilly Center for Women's Health; Contract grant sponsor: National Institutes of Health (NIH); Contract grant number: DE14680.

*Correspondence to: Merry Jo Oursler, Department of Biochemistry and Molecular Biology, Mayo Foundation, 200 First Street SW, Rochester, MN 55905. E-mail: moursler@d.umn.edu

Received 6 October 2003; Accepted 14 November 2003

DOI: 10.1002/jcp.20036

that many factors influence osteoclast differentiation through effects on support cells (Khosla, 2001; Suda et al., 2001). It has been well-documented that macrophage colony stimulating factor (M-CSF) is required for osteoclast differentiation (Yoshida et al., 1990; Kodama et al., 1991; Takahashi et al., 1991; Suda et al., 1993). Although it has been documented that TGF-β influences M-CSF stimulated osteoclast differentiation, the impact of TGF-β on M-CSF expression has not been investigated during osteoclastogenesis (Sells Galvin et al., 1999; Fox et al., 2003). It is a goal of the research described here to address this question. There is also overwhelming evidence that interaction with support cell-derived receptor activator of NF-κB ligand (RANKL) induces osteoclast differentiation (Simonet et al., 1997; Suda et al., 2001). Osteoprotegerin (OPG) is a secreted stromal cell-derived decoy receptor that specifically binds RANKL and inhibits osteoclast differentiation (Simonet et al., 1997; Suda et al., 2001). The balance of RANKL relative to OPG expression modulates the rate of osteoclast differentiation and many factors that influence osteoclast differentiation do so by regulating OPG and RANKL expression in stromal support cells (Khosla, 2001; Theill et al., 2002). TGF-β1 treatment of stromal cells at relatively high doses (levels that inhibit osteoclast differentiation in co-cultures of marrow precursors with stromal cells) induces OPG and inhibits RANKL expression (Takai et al., 1998; Sells Galvin et al., 1999; Thirunavukkarasu et al., 2001; Quinn et al., 2001). It is, therefore, hypothesized that this modulation is responsible for TGF-β-mediated repression of osteoclast differentiation, but this has not yet been tested. It is a goal of the research described here to address this question.

The above observations have led us to examine the responses of osteoclast precursors resident in both marrow and spleen to a broad range of TGF-β1 and TGF-β2 concentrations, the impact of stimulatory and inhibitory TGF-β1 doses on M-CSF, RANKL, and OPG expression, and how these changes influence osteoclast differentiation. We have used as our model system the co-culture of osteoclast precursors from mouse spleen and marrow with ST2 stromal cells.

MATERIALS AND METHODS

Material

Unless otherwise noted, all chemicals were from Sigma Chemical Co., St. Louis, MO.

In vitro osteoclast differentiation with stromal support cells

Mouse marrow and spleen containing osteoclast precursors were obtained from female BalB/c mice (Taconic, Germantown, NY). Four to six-week-old mice were sacrificed and long bones of the hind limbs and spleen were aseptically removed. The distal ends of bones were clipped and the marrow flushed out by injecting sterile Mosconas buffer (8% NaCl, 0.2% KCl, 0.06% $NaH_2PO_4 + H_2O$, 2% glucose, 0.02% bicarbonate) into the marrow cavity with a 27-gauge needle. Marrow cells were counted and stored at 2.4×10^6 cells/tube in liquid nitrogen until used. Freezing media consisted of 12% dimethylsulfoxide (DMSO) in FBS as has been previously reported (Wesolowski et al., 1995). To generate marrow-derived osteoclasts, precursors were cultured with ST2 stromal cells (Riken Cell Bank, Tsukuba, Japan) during differentiation. ST2 cells (passage 10–13) were plated (4×10^4 cells/well) in a 48-well plate (Fisher, Pittsburgh, PA) 24 h prior to the addition of osteoclast precursors (1.5×10^6 marrow mononuclear cells or 4.8×10^7 spleen cells per plate) as previously reported (Gingery et al., 2003). Recombinant human TGF-β1 or TGF-β2 (R&D Systems, Minneapolis, MN) were added to four replicate wells for each dose. In some experiments, 1 ng/ml OPG, 25 ng/ml M-CSF (R&D), or 60 ng/ml RANKL (Calbiochem, La Jolla, CA) were added as indicated in the figure legends. The media was changed every 3 days. On day 6 for spleen cultures and either day 9 or 10 for marrow cultures, the cell co-cultures were washed three-times with phosphate buffered saline (1× PBS : 1.7 mM KH_2PO_4, 5 mM Na_2HPO_4, 150 mM NaCl, pH to 7.4) and fixed with 1% paraformaldehyde in PBS. After incubating for 30 min in the fixative, the cells were rinsed with water three-times and stored in water at 4°C until they were evaluated for differentiation.

Determination of differentiation

Tartrate resistant acid phosphatase (TRAP) staining was used to visualize differentiated cells according to manufacturer's directions (Sigma Chemical Co.). The number of multinucleated TRAP positive cells was counted using an Olympus Takyo inverted microscope at 200× magnification.

ST2 cell treatment, RNA isolation, real time polymerase chain reaction

ST2 cells were plated in 100 mM dishes and maintained until confluent. One plate was harvested as a time zero. The remaining cultures were maintained in base medium or base medium supplemented with 7×10^{-3} M ascorbic acid, 1×10^{-7} M dexamethasone, and 1×10^{-5} M vitamin D_3 as above and treated with either vehicle or a range of TGF-β1 concentrations for 3 days. RNA was isolated using Trizol Reagent according to manufacturer's directions (Gibco BRL, Grand Island, NY). The RNA was stored at −70°C until analyzed. Following LiCl precipitation to remove DNA, cDNA was synthesized by standard protocol: 4 μg total RNA was heat denatured at 68°C for 15 min in reverse transcription reaction buffer (50 mM Tris-HCl, 75 mM KCl, 3 mM $MgCl_2$, 50 mM DTT, 1 μM dNTPs, 500 ng oligo-dT primer). Following heat denaturation, 1 U of MMLV-RT (Invitrogen, Carlsbad, CA) was added and the mixture incubated at 37°C for 45 min followed by a 68°C incubation for an additional 15 min. The resultant cDNA was diluted 10-fold prior to analysis and 2 μl used for each reaction as follows: PCR buffer (20 mM Tris-HCl, 50 mM KCl, 3 mM $MgCl_2$, 300 nM of both the upstream and downstream primers (see Table below), and 1 U of Taq Polymerase (Promega, Madison, WI)). As control, tubulin was amplified simultaneously in separate reactions. Message levels are examined using the BioRad iCycler according to the specifics recommended by the manufacturer. The amount of target cDNA in the sample, relative to tubulin, was calculated using the formula $2^{-\Delta\Delta Ct}$, where ΔΔCt is the difference between the target and tubulin levels. The results were graphed

as relative quantification of the target gene compared to a control (vehicle) treatment. The Table below was the primer sequences used for amplification. All results were standardized to a corresponding tubulin reaction that is carried out simultaneously.

Target mRNA	5′ Primer	3′ Primer
M-CSF	CTCTGGCTGGCTTGG-CTTGG	GCAGAAGGATGAGGT-TGTG
OPG	ACGGACAGCTGGCAC-ACCAG	CTCACACACTCGGTTG-TGGG
RANKL	CCAGTGAAGCAGCAG-CCAGC	CCCTCTCATCAGCCCT-GTCC
Tubulin	CTGCTCATCAGCAAGAT-CAGAG	GCATTATAGGGXTCCA-CCACAG

Spleen and marrow precursors cultured without support cells

Marrow and spleen cells were harvested as outlined above and plated at 1×10^6 marrow cells per well and 2×10^6 spleen cells per well in a 48-well plate as we have detailed (Sells Galvin et al., 1999). Base medium was supplemented with 7×10^{-3} M ascorbic acid prior to plating the cells and cultures were supplemented with 30 ng/ml of RANKL and 25 ng/ml M-CSF with either vehicle, 2×10^{-4} ng/ml or 1 ng/ml TGF-β1. The culture media was changed every 3 days and cells were fixed in 1% paraformaldehyde in PBS to terminate culture. The cells were TRAP stained and evaluated as outlined above.

Statistical analysis

The effects of treatment are compared with the control values by one-way analysis of variance (ANOVA). Significant treatment effects are further evaluated by the Student's *t*-test. All analyses are performed with JMP version 4.04.

RESULTS

TGF-β dose responses

Dose response studies were performed to establish the impact of a broad range of TGF-β concentrations on osteoclast differentiation from both spleen and marrow precursors. Both TGF-β1 (Fig. 1A,B) and TGF-β2 (Fig. 1C,D) had biphasic effects on differentiation that were nearly indistinguishable. TGF-β stimulation of osteoclast differentiation at 2×10^{-4} ng/ml was significant and, at higher concentrations, the number of osteoclasts significantly decreased below control levels, with complete inhibition of osteoclast differentiation occurred at a dose of 2 ng/ml TGF-β. We focused additional studies on the low dose stimulation of differentiation and observed significant stimulation at both 1×10^{-4} and 2×10^{-4} ng/ml TGF-β1with higher, but not statistically significant levels at 3×10^{-4} ng/ml (Fig. 1E).

Roles of M-CSF, OPG, and RANKL expression

As shown in Figure 1, TGF-β stimulated differentiation at a low dose while inhibiting differentiation at higher doses. To study this, we examined the impact of these TGF-β concentrations on expression of M-CSF, OPG, and RANKL by real time reverse transcriptase polymerase chain reaction (Fig. 2). We document here that there was a dose dependent inhibition of M-CSF expression such that the levels are repressed although some expression is observed at low TGF-β concentrations (Fig. 2A). Interestingly, RANKL expression was elevated at low TGF-β concentrations only while there is a less dramatic increase in OPG (Fig. 2B,C). The RANKL/OPG ratio is the determining factor in whether there is sufficient RANKL to interact with its signaling receptor in the presence of OPG and our data support that low TGF-β concentrations elevate the RANKL/OPG ratio while high concentrations repressed the ratio (Fig. 2D). Thus, at low TGF-β concentrations, there is sufficient M-CSF and a high RANKL/OPG ratio and differentiation is elevated. We, therefore, added OPG to cultures to determine if reducing the RANKL/OPG ratio would block the low dose stimulation of osteoclast differentiation (Fig. 3). OPG blocked differentiation stimulation in the presence of either 1×10^{-4} or 2×10^{-4} ng/ml TGF-β. As documented above, at high TGF-β concentrations, the RANKL/OPG ratio and M-CSF expression are both repressed and there is no differentiation. These data suggested that the loss of M-CSF and/or the reduction in the ratio of RANKL to OPG was causing the high dose differentiation repression. We, therefore, examined differentiation in the presence of added M-CSF and/or RANKL in the presence of 2 ng/ml TGF-β (Fig. 4). Surprisingly, restoring M-CSF and/or elevating the RANKL/OPG ratio by adding RANKL had no impact on TGF-β-mediated repression of osteoclast differentiation at this suppressive dose. M-CSF addition in the absence of TGF-β stimulated differentiation while RANKL alone or in combination with M-CSF repressed differentiation compared to control levels in the absence of TGF-β. Given reports that high RANKL levels stimulate INF-β production to repress osteoclast differentiation, these latter finding are not surprising (Hayashi et al., 2002).

Spleen and marrow precursors cultured without stromal support cells

The above data supported that high TGF-β doses may have direct impacts on osteoclast precursors that could not be overcome by stromal cell-derived M-CSF and/or RANKL. To examine direct TGF-β influences on osteoclast differentiation, we used mouse model systems where osteoclasts are generated from marrow or spleen precursors from 8–10-week-old mice supplemented with RANKL and M-CSF (Fig. 5). In marrow precursor cultures, there was a dose-dependent increase in osteoclast differentiation with increasing TGF-β concentrations. Spleen cell precursor differentiation was only detected at the higher TGF-β concentration with no TRAP-positive cells present either in the absence of TGF-β or at the lower concentration.

DISCUSSION

As noted above, it has been established that TGF-β has a biphasic effect on osteoclast differentiation when osteoclast precursors originate from the marrow environment and are cultured in the presence of stromal

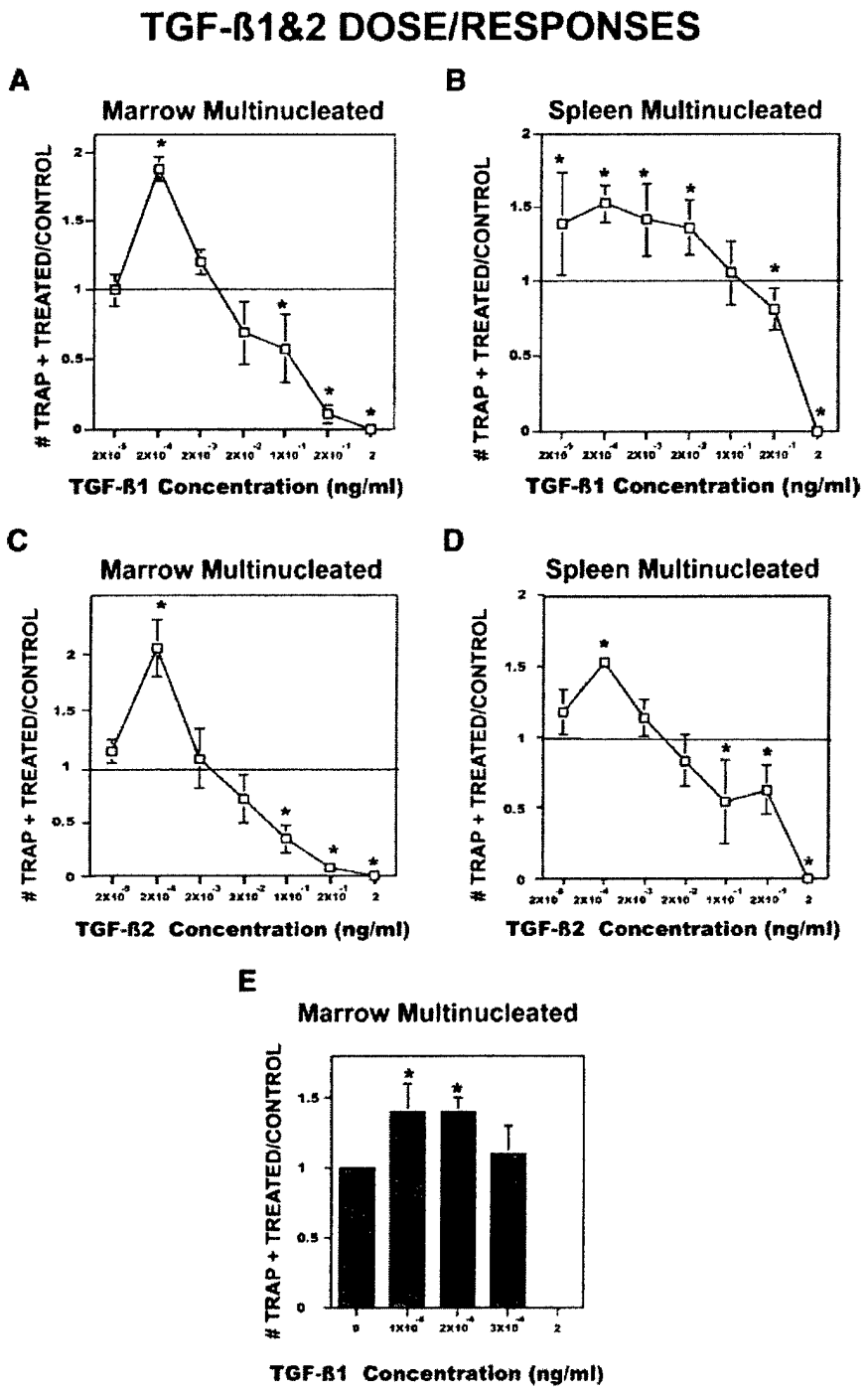

Fig. 1. Transforming growth factor-beta 1 (TGF-β1) and TGF-β2 influences on osteoclast differentiation in the presence of stromal support cells. Differentiation of osteoclasts from marrow (**A**, **C**, **E**) and spleen (**B**, **D**) were assessed as detailed in the absence (control) or presence of the indicated TGF-β1 (A, B, E) or TGF-β2 (C, D) concentration. Tartrate resistant acid phosphatase (TRAP) positive multinucleated cells were counted and reported as treated/control. The values are an average of 3–6 replicate experiments with at least four wells per dose in each experiment. $^*P < 0.05$ compared to control.

support cells (Shinar and Rodan, 1990; Mundy, 1991; Yamaguchi and Kishi, 1995). Here we document that precursors from both spleen and marrow tissues respond similarly to TGF-β in a biphasic pattern under these conditions. Given that TGF-β2 has different influences on some cell types compared with TGF-β1 (Jennings et al., 1988; Segarini et al., 1988; ten Dijke et al., 1990; Lyons et al., 1991; Liu et al., 2000), we

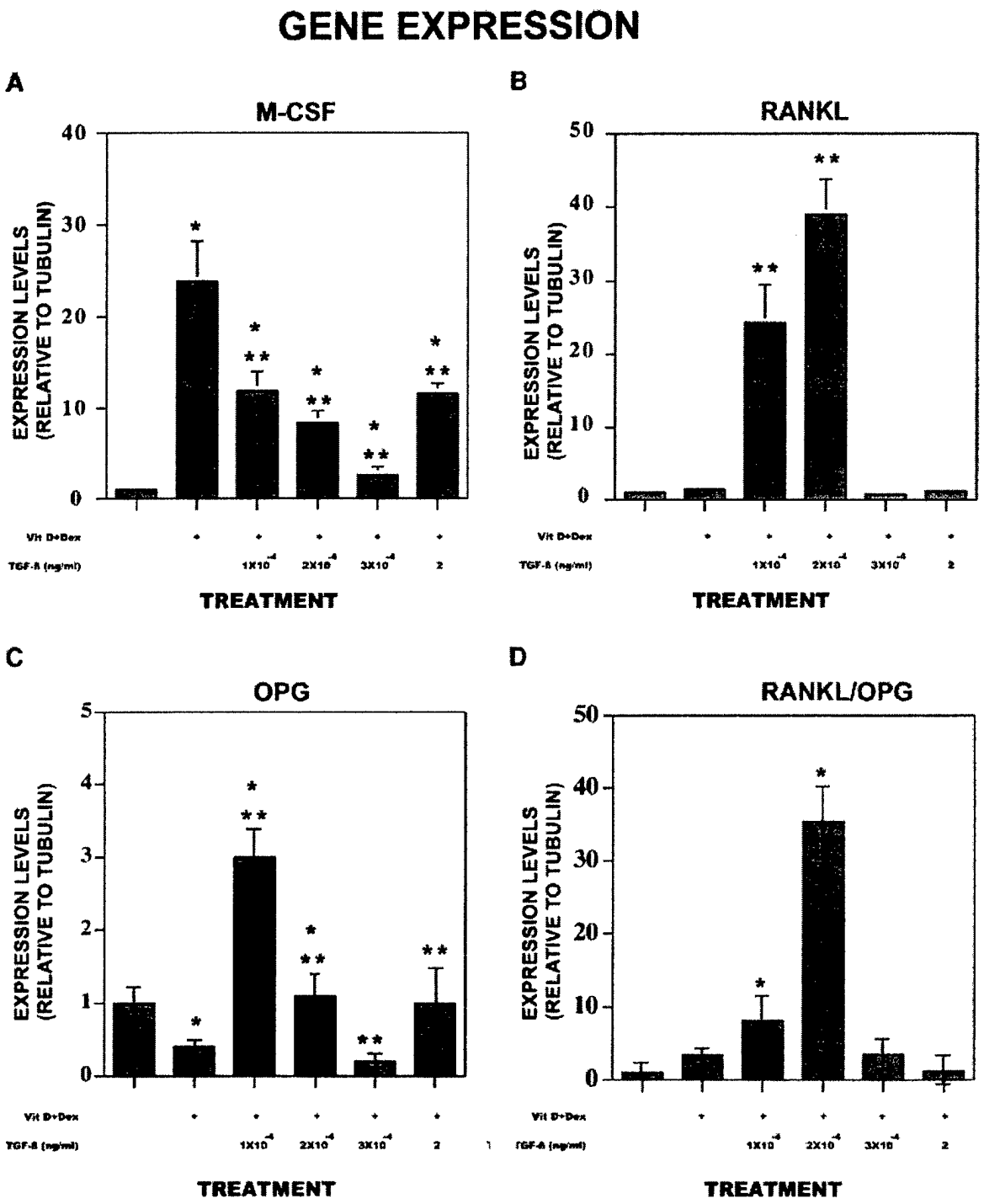

Fig. 2. TGF-β1 regulation of macrophage colony stimulating factor (M-CSF), receptor activator of NF-κB ligand (RANKL), and osteoprotegerin (OPG) mRNAs. ST2 cells were untreated (NONE) or treated with 10^{-5} M vitamin D and 10^{-7} M Dexamethazone (vit D + Dex), with or without the indicated TGF-β1 concentration for 3 days and RNA was isolated and analyzed as described. The values are representative of two replicate experiments. *$P < 0.05$ compared to no treatment (NONE); **$P < 0.05$ compared to vit D + Dex.

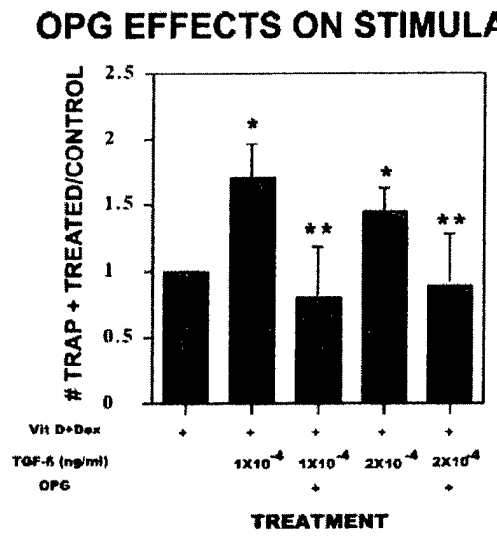

Fig. 3. OPG effects on differentiation stimulation. Osteoclasts were differentiated in co-cultures of bone marrow and ST2 cells with the addition of the indicated TGF-β1 concentration with or without 1 ng/ml OPG as indicated. TRAP positive multinucleated cells were counted and reported as treated/control. The values are an average of three replicate experiments with four wells per treatment in each experiment. $^{*}P < 0.05$ compared to no TGF-β; $^{**}P < 0.05$ compared to TGF-β treatment in the absence of OPG.

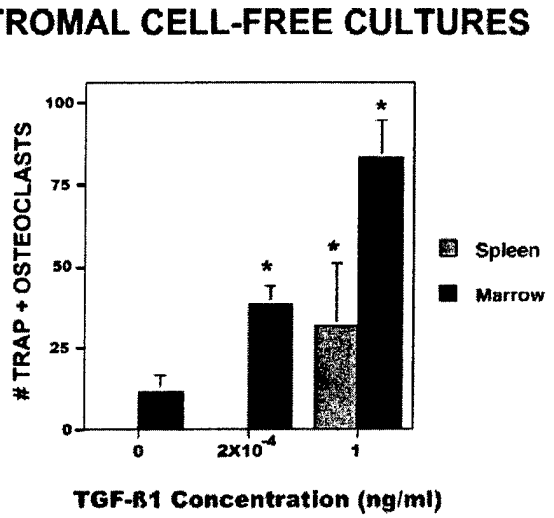

Fig. 5. Differentiation in the absence of stromal support cells. Precursors from marrow and spleen were cultured with M-CSF (25 ng/ml) and RANKL (30 ng/ml) in the presence or absence of TGF-β1 as described for 9 days and TRAP stained. Differentiation of cells from spleen and marrow were assessed as detailed. TRAP positive multinucleated cells were counted as outlined. The values are an average of three replicate experiments with at least four wells per dose in each experiment. $^{*}P < 0.05$ compared to no TGF-β treatment.

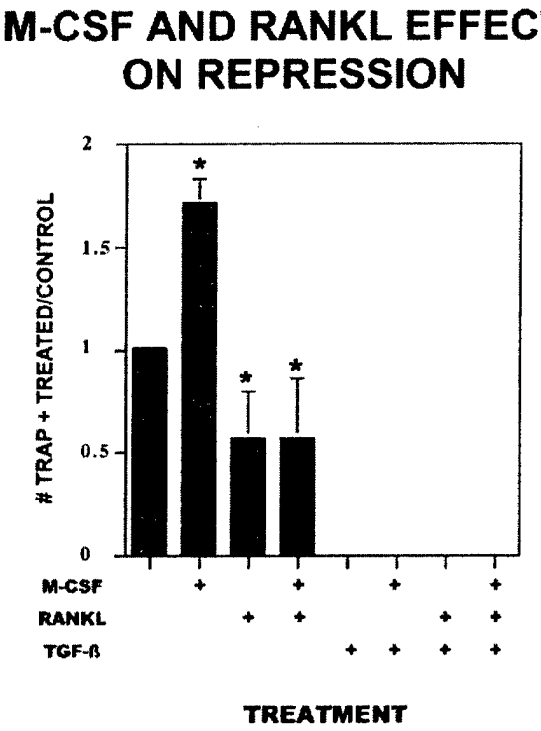

Fig. 4. M-CSF and RANKL effects on differentiation repression. Osteoclasts were differentiated in co-cultures of bone marrow and ST2 cells in the absence or presence of 2 ng/ml TGF-β1 with or without 25 ng/ml M-CSF and/or 60 ng/ml RANKL as indicated. TRAP positive multinucleated cells were counted and reported as treated/control. The values are an average of two replicate experiments with three wells per treatment in each experiment. $^{*}P < 0.05$ compared to no treatment.

explored whether there were differences between these isoforms in influencing either stimulation or repression of osteoclast differentiation. We document that both isoforms have similar impacts on stimulation and repression of osteoclast differentiation.

Our observations raised the question of the mechanism by which low TGF-β doses stimulate differentiation. We explored this by examining the impact of a range of TGF-β concentrations on M-CSF, OPG, and RANKL expression and document that low TGF-β doses elevated the RANKL/OPG ratio while not completely repressing M-CSF expression in stromal support cells. To examine whether the increased ratio of RANKL to OPG was responsible for increased differentiation, we added OPG during differentiation and found that suppression of the RANKL/OPG ratio in this manner repressed differentiation. Thus, the low dose TGF-β stimulation of spleen and marrow precursors cultured with stromal support cells may be accounted for by regulation of the RANKL/OPG expression ratio in the stromal cells. To our knowledge, this is the first study that TGF-β is capable of stimulating RANKL expression at any concentration. This interesting observation supports the cumulative observations that the TGF-β effects on stromal support cells are complex and may have multiple implications on the roles of TGF-β in bone metabolism.

Studies of inhibitory TGF-β doses were more complex, with repression of the RANKL/OPG ratio and some repression of M-CSF expression. These impacts seems likely to be the cause of repressed differentiation, yet adding M-CSF and/or RANKL to the cultures during differentiation did not alleviate the repression. These data support a here-to-fore undocumented TGF-β impact on osteoclast differentiation independent of these key stimulators of differentiation. Since one possible

explanation for differentiation repression independent of stromal cell M-CSF and RANKL expression would be direct repression of precursors, we examined this using a stromal cell-independent culture system. We found that marrow cells cultured in the absence of support cells responded to TGF-β treatment with a dose-dependent stimulation of differentiation. Thus, at a dose that inhibited osteoclast differentiation in co-cultures of stromal cells and precursor cells, there was a marked stimulation of differentiation of the precursor cells cultured without support cells. These data support that the TGF-β-mediated repression observed in the co-cultures is by regulating stromal cell expression of factor(s) in addition to M-CSF, RANKL, or OPG. Thus, our data support that TGF-β targets both support cells and osteoclast precursors during differentiation by influencing multiple targets in osteoclast precursors and support cells. When spleen precursors were evaluated in the absence of support cells, only the higher dose of TGF-β stimulated differentiation. This was an unexpected observation since the lower TGF-β concentration stimulated differentiation in the presence of support cells. This is in conflict with reports using spleen cells from younger mice including our study (Sells Galvin et al., 1999). Whether this is due to the age of the mouse from which the spleens were harvested is currently under investigation.

We have documented that mature osteoclasts secrete and activate TGF-β (Oursler, 1994). Moreover, there is evidence including the studies presented here that osteoclast precursors and mature cells respond directly to TGF-β (Fiorelli et al., 1994; Zheng et al., 1994). Thus, direct TGF-β effects on osteoclast precursors appear to be complex, including dose-dependent stimulation of osteoclast differentiation of precursors from both marrow and spleen tissues. These observations are consistent with TGF-β influences on other cell types in that TGF-β has been reported to either promote or repress either proliferation or differentiation in many cell systems (Massague, 1987; Roberts et al., 1990; Laiho and Keski-Oja, 1992). Taken together, our observations support the concept that multifunctional TGF-β has complex influences on osteoclast differentiation. In conjunction with reports that TGF-β regulates osteoclast activity and survival, it appears that TGF-β impacts on bone resorption are multifaceted and a complete understanding of TGF-β roles in bone metabolism require integration of all of the components of these impacts (Hughes et al., 1994; Pederson et al., 1999).

ACKNOWLEDGMENTS

We thank Dr. David Monroe and Dr. Thomas Spelsberg for their assistance in the mRNA expression studies.

LITERATURE CITED

Fiorelli G, Ballock RT, Wakefield LM, Sporn MB, Gori F, Masi L, Frediani U, Tanini A, Bernabei PA, Brandi ML. 1994. Role for autocrine TGF-beta 1 in regulating differentiation of a human leukemic cell line toward osteoclast-like cells. J Cell Physiol 160(3): 482–490.

Fox SW, Haque SJ, Lovibond AC, Chambers TJ. 2003. The possible role of TGF-beta-induced suppressors of cytokine signaling expression in osteoclast/macrophage lineage commitment in vitro. J Immunol 170(7):3679–3687.

Gingery A, Bradley E, Shaw A, Oursler MJ. 2003. Phosphatidylinositol 3-kinase coordinately activates the MEK/ERK and AKT/NFkappaB pathways to maintain osteoclast survival. J Cell Biochem 89(1):165–179.

Hayashi T, Kaneda T, Toyama Y, Kumegawa M, Hakeda Y. 2002. Regulation of receptor activator of NF-kappa B ligand-induced osteoclastogenesis by endogenous interferon-beta (INF-beta) and suppressors of cytokine signaling (SOCS). The possible counteracting role of SOCSs in IFN-beta-inhibited osteoclast formation. J Biol Chem 277(31):27880–27886.

Hughes DE, Wright KR, Mundy GR, Boyce BF. 1994. TGFB1 induces osteoclast apoptosis in vitro. J Bone Miner Res 9(Suppl):S138.

Jennings J, Mohan S, Linkhart T, Widstrom R, Baylink D. 1988. Comparison of the biological actions of TGF-beta-1 and TGF-beta-2: Differential activity of endothelial cells. J Cell Physiol 137:167–172.

Khosla S. 2001. Minireview: The OPG/RANKL/RANK system. Endocrinology 142(12):5050–5055.

Kodama H, Yamasaki A, Nose M, Niida S, Ohgame Y, Abe M, Kumegawa M, Suda T. 1991. Congenital osteoclast deficiency in osteopetrotic (op/op) mice is cured by injections of macrophage colony-stimulating factor. J Exp Med 173(1):269–272.

Laiho M, Keski-Oja J. 1992. Transforming growth factors-beta as regulators of cellular growth and phenotype. Crit Rev Oncog 3(1–2):1–26.

Liu J, Tseu I, Wang J, Tanswell K, Post M. 2000. Transforming growth factor beta2, but not beta1 and beta3, is critical for early rat lung branching. Dev Dyn 217(4):343–360.

Lyons R, Miller D, Graycar J, Moses H, CDerynck R. 1991. Differential binding of transforming growth factor-ß1, -ß2, -ß3 by fibroblasts and epithelial cells measured by affinity cross-linking of cell surface receptors. Mol Endocrinol 5:1887–1896.

Massague J. 1987. The TGF-beta family of growth and differentiation factors. Cell 49(4):437–438.

Mundy GR. 1991. The effects of TGF-beta on bone. Ciba Found Symp 157:137–143.

Oursler MJ. 1994. Osteoclast synthesis and secretion and activation of latent transforming growth factor beta. J Bone Miner Res 9(4):443–452.

Pederson L, Winding B, Foged N, Spelsberg T, Oursler M. 1999. Identification of breast cancer cell line-derived paracrine factors that stimulate osteoclast activity. Cancer Res 59(22):5849–5855.

Quinn JM, Itoh K, Udagawa N, Hausler K, Yasuda H, Shima N, Mizuno A, Higashio K, Takahashi N, Suda T, Martin TJ, Gillespie MT. 2001. Transforming growth factor beta affects osteoclast differentiation via direct and indirect actions. J Bone Miner Res 16(10):1787–1794.

Roberts AB, Flanders KC, Heine UI, Jakowlew S, Kondaiah P, Kim SJ, Sporn MB. 1990. Transforming growth factor-beta: Multifunctional regulator of differentiation and development. Philos Trans R Soc Lond B Biol Sci 327(1239):145–154.

Segarini P, Roberts A, rosen D, Seyedin S. 1988. Membrane binding characteristics of two forms of transforming growth factor-ß. J Biol Chem 262:14655–14662.

Sells Galvin RJ, Gatlin CL, Horn JW, Fuson TR. 1999. TGF-beta enhances osteoclast differentiation in hematopoietic cell cultures stimulated with RANKL and M-CSF. Biochem Biophys Res Commun 265(1):233–239.

Shinar CM, Rodan GA. 1990. Biphasic effects of transforming growth factor-B on the production of osteoclast-like cells in mouse bone marrow cultures: The role of prostaglandins in the generation of these cells. Endocrinology 126:3153–3158.

Simonet WS, Lacey DL, Dunstan CR, Kelley M, Chang MS, Luthy R, Nguyen HQ, Wooden S, Bennett L, Boone T, Shimamoto G, DeRose M, Elliott R, Colombero A, Tan HL, Trail G, Sullivan J, Davy E, Bucay N, Renshaw-Gegg L, Hughes TM, Hill D, Pattison W, Campbell P, Boyle WJ, et al. 1997. Osteoprotegerin: A novel secreted protein involved in the regulation of bone density [see comments]. Cell 89(2):309–319.

Suda T, Tanaka S, Takahashi N. 1993. Macrophage colon-stimulating factor (M-CSF) is essential for differentiation rather than proliferation of osteoclast progenitors. Osteoporos Int 3(Suppl 1):111–113.

Suda T, Kobayashi K, Jimi E, Udagawa N, Takahashi N. 2001. The molecular basis of osteoclast differentiation and activation. Novartis Found Symp 232:235–247; Discussion 247–250.

Takahashi N, Udagawa N, Akatsu T, Tanaka H, Isogai Y, Suda T. 1991. Deficiency of osteoclasts in osteopetrotic mice is due to a defect in the local microenvironment provided by osteoblastic cells. Endocrinology 128(4):1792–1796.

Takahashi S, Reddy SV, Dallas M, Devlin R, Chou JY, Roodman GD. 1995. Development and characterization of a human marrow

stromal cell line that enhances osteoclast-like cell formation. Endocrinology 136:1441–1449.
Takai H, Kanematsu M, Yano K, Tsuda E, Higashio K, Ikeda K, Watanabe K, Yamada Y. 1998. Transforming growth factor-beta stimulates the production of osteoprotegerin/osteoclastogenesis inhibitory factor by bone marrow stromal cells. J Biol Chem 273(42):27091–27096.
ten Dijke p, Iwata K, Goddard C, Pieler D, Canalis E, McCarthy T. 1990. Recombinant transforming growth factor type ß3: Biological activities and receptor-binding properties in isolated bone cells. Mol Cell Biol 10:4473–4479.
Theill LE, Boyle WJ, Penninger JM. 2002. RANK-L and RANK: T cells, bone loss, and mammalian evolution. Annu Rev Immunol 20:795–823.
Thirunavukkarasu K, Miles RR, Halladay DL, Yang X, Galvin RJ, Chandrasekhar S, Martin TJ, Onyia JE. 2001. Stimulation of osteoprotegerin (*OPG*) gene expression by transforming growth factor-beta (TGF-beta). Mapping of the OPG promoter region that mediates TGF-beta effects. J Biol Chem 276(39):36241–36250.
Udagawa N, Takahashi N, Akatsu T, Tanaka H, Sasaki T, Nishihara T, Koga T, Martin TJ, Suda T. 1990. Origin of osteoclasts: Mature monocytes and macrophages are capable of differentiating into osteoclasts under a suitable microenvironment prepared by bone-marrow-derived stromal cells. Proc Natl Acad Sci USA 87(18):7260–7264.
Wesolowski G, Duong LT, Lakkakorpu PT, Nagy RM, Tezuka K-I, Tanaka H, Rodan GA, Rodan SB. 1995. Isolation and characterization of highly enriched, prefusion mouse osteoclastic cells. Experimental Cell Res 219:679–686.
Yamaguchi M, Kishi S. 1995. Differential effects of transforming growth factor-beta on osteoclast-like cell formation in mouse marrow culture: Relation to the effect of zinc-chelating dipeptides. Peptides 16:1483–1488.
Yoshida H, Hayashi S, Kunisada T, Ogawa M, Nishikawa S, Okamura H, Sudo T, Shultz LD. 1990. The murine mutation osteopetrosis is in the coding region of the macrophage colony stimulating factor gene. Nature 345(6274):442–444.
Zheng MH, Fan Y, Wysocki SJ, Lau AT, Robertson T, Beilharz M, Wood DJ, Papadimitriou JM. 1994. Gene expression of transforming growth factor-beta 1 and its type II receptor in giant cell tumors of bone. Possible involvement in osteoclast-like cell migration. Am J Pathol 145(5):1095–1104.

Osteolytic Enzymes of Osteoclasts

Merry Jo Oursler

Endocrine Research Unit, Mayo Clinic and Foundation, Rochester, MN 55905

Introduction

Ninety percent of the protein in bone is Type I collagen that is in the form of a cross-linked triple helical structure, making it more resistant to proteolysis and enzymatic cleavage. The stability that this structure confers means that specific proteases are required for effective degradation [112, 113]. Bone also contains minerals in the form of hydroxyapatite crystals. Thus, for bone resorption to occur both the mineral and the protein components of this matrix must be removed. Osteoclasts are unique in that they create an external acidic hemivacuole adjacent to the bone surface as an early step in bone resorption [4]. This compartment is created when osteoclasts attach to bone. After attachment osteoclasts transport lysosomes to the portion of the plasma membrane that is juxtaposed to the area of the bone that is to be resorbed. The vesicles fuse with the plasma membrane and thereby, increase the plasma membrane surface area in this restricted region. Lysosome membranes also contain membrane tartrate resistant acid phosphatase (TRAP) and high levels of a hydrogen pump. Both of these enzymes are retained in the plasma membrane after fusion. Lysosome contents are discharged into this compartment as the vesicles fuse with the plasma membrane and this is followed by hydrogen pump-mediated acidification of the hemivacuole. The combined action of enzymes from the lysosomes (such as TRAP and cathepsins), the matrix metalloproteases

(MMPs), and the reduction in pH together cause bone to be resorbed. It has therefore been of great interest to discover the identity and nature of the enzymes that execute bone resorption in the hope of targeting these enzymes to regulate rates of bone loss. The osteolytic roles of TRAP, cathepsins, and MMPs are discussed in the remainder of this chapter.

Tartrate Resistant Acid Phosphatase (TRAP)

TRAP, expressed mainly in osteoclasts and related monohistiocytic cells, has the capacity to hydrolyze phosphoproteins, ATP and other nucleotide triphosphates, and arylphosphates [73]. Although it has been known for many years that osteoclasts express this membrane enzyme, its role in osteoclast activity has remained elusive. The porcine homolog, uteroferrin, may have as its function the delivery of iron that is secreted by the endometrium *in utero*[29]. However there is no indication that the enzyme fills this potential role in osteoclasts. Although there is only limited sequence similarity between the kidney bean purple acid phosphatase and TRAP, the fact that the conformation of what is thought to be the active site of TRAP resembles that of the known catalytic domain of the bean phosphatase strengthens the inference that the presumed site in TRAP is in fact the active site [111]. The crystal structure of TRAP also revealed a protease sensitive surface loop near the active site [111]. This explains the need for proteolytic activation of the enzyme.

Targeted TRAP disruption in mice resulted in altered epiphyseal growth plate development [55]. This is consistent with a disruption in chondro/osteoclast activity. In these animals, moreover, early onset osteopetrosis was observed. Since osteoclast differentiation levels seemed normal, the osteopetrosis probably resulted from reduced osteoclast activity. Given that osteoclasts in these mice contain high numbers of cytoplasmic vesicles near the ruffled border, the question arose whether TRAP in the lysosomal vesicle membrane was involved in transport to or fusion with the plasma membrane. Osteoclasts from these mice secreted normal levels of cathepsin K, leading to the conclusion that the accumulating vesicles were not lysosomal vesicles that fail to merge with the plasma membrane [55]. MITF and PU.1 are two transcription factors that synergistically activate TRAP gene expression [79]. Mice that are heterozygous for mutant MITF and a PU.1 null allele exhibit early onset osteopetrosis with osteoclasts of normal size and number [79]. The above studies support the concept that TRAP is involved in osteoclast activity, but its precise role has remained unresolved. Recent data documented that cathepsin K is a physiological activator of TRAP and that TRAP can dephosphorylate osteopontin [3]. Osteopontin is involved in stimulating osteoclast activity by promoting adhesion, migration, and resorption [13, 14, 30, 39, 57, 59, 82, 93, 96]. Razzouk et al [93] have investigated the importance of osteopontin phosphorylation in these roles and their data support that osteopontin phosphorylation may be involved in promoting resorption, but not attachment or actin ring formation. Thus, TRAP-mediated osteopontin dephosphorylation would repress bone resorption.

TRAP is expressed in osteoclasts, some tissue macrophages, dendritic cells, parenchymal liver cells, glomerular mesangial kidney cells, and pancreatic acinar cells [115]. In many cases, there are different RNAs expressed by these different cell types as the 5' untranslated regions of the mRNAs differ due to altered first exons. Walsh et al [115] have identified an osteoclast-specific transcription initiation site and further documented that there are four different promoter regions that are restricted in a tissue- and cell-specific manner. Since TRAP has long been considered a pivotal marker for osteoclasts, attempts have been made to correlate serum TRAP levels with resorption rates *in vivo*. This has met with little success. Attempts have recently been made to measure type 5b TRAP, whose expression is though to be restricted osteoclasts [60].

Cathepsins

Many studies have linked these lysosomal cysteine proteases to osteoclast-mediated bone resorption. Much of the evidence indicates that cystein protease inhibition can block bone resorption *in vitro* and *in vivo* [17, 19, 20, 22, 36, 46, 47, 53, 69, 72, 87, 90, 95, 99]. This includes studies where the activities of cathepsin B and cathepsin L were inhibited and resorption was slowed or stopped [22, 46, 47, 69, 87, 90, 95, 99]. In some studies, however, inhibition of either protease had only a modest or no effect on resorption [52, 64, 95, 110, 111, 118]. This has led to a search for alternate proteases responsible for osteoclast-mediated bone resorption. Cathepsin K (also referred to as O or X) was first identified by differential screening of a rabbit osteoclast cDNA library and both human

and mouse homologs have subsequently been cloned [61, 92, 109]. Mice with cathepsin K knocked out exhibited osteopetrosis, abnormal joint morphology, increased bone volume, greater trabecular thickness, and more trabeculae [48]. Differentiated osteoclasts were found in association with demineralized bone. This suggests that osteoclasts deficient in cathepsin K can demineralize the matrix but cannot degrade it. In other studies of cathepsin K knock out mice, osteopetrosis was observed even though the osteoclast numbers were normal, suggesting impaired osteoclast activity [97, 98]. In addition, the resorption surface was broadly demineralized, but there was undigested collagen present. The absence of cathepsin K and the presence of undigested collagen suggest that cathepsin K is involved in collagen degradation. Cultured osteoclasts from these mice also had impaired resorption activity [98]. Studies of human cathepsin K using Giant Cell Tumors of the Bone and bone tissues show that cathepsin K was highly expressed in osteoclasts, with no detectable cathepsin B or L expression [28]. From these studies it appears that other tissues do not express cathepsin K. However the failure to detect cathepsins B and L may simply be due to an insufficiently sensitive assay, in as much as in other reports these enzymes are detected in osteoclasts [22, 46, 47, 69, 87, 90, 95, 99]. Indeed, although the above study suggested that cathepsin K might be exclusively expressed by osteoclasts, it is clear from other data that cathepsin K expression is not restricted to osteoclasts [10-12, 15, 25, 26, 49-51, 68, 74, 78, 83, 84, 91, 92, 107].

The human disease pycnodysostosis is a lysosome disease that manifests itself as an inherited sclerosing skeletal dysplasia. Gelb et al [44] have shown that patients with this

disease have nonsense, missense, or stop codon mutations in their cathepsin K genes. Similar to mouse models lacking cathepsin K, pycnodysostotic osteoclasts can demineralize bone matrix but cannot degrade the matrix. These data support that cathepsin K is involved in human osteoclast-mediated bone resorption. In mice, Rantakokko et al [92] observed cathepsin K in both osteoclasts and hypertrophic chondrocytes. This observation adds support to the hypothesis that cathepsin K plays a role in matrix degradation as well.

An interesting study by Dodds et al [27] has examined the patterns of inactive and active cathepsin K protein in osteoclasts. In osteoclasts that are not involved in bone resorption, most of the cathepsin K was present as an inactive zymogen. In osteoclasts that were located closer to the bone matrix, active cathepsin K appeared restricted to the osteoclast area closest to the bone. When osteoclasts were actively resorbing bone, they contained only active cathepsin K that was localized at the bone surface in the ruffled membrane. Thus, local factors present in the immediate vicinity of the bone seem to be important in stimulating cathepsin K activation.

Early studies of the ability of cathepsin K to degrade bone proteins suggested that it was not very effective against collage or fibronectin, but readily degraded osteonectin [9]. It has since been documented that optimal cathepsin K activity toward collagen requires a complex of the cathepsin molecule and soluble glycosamino glycans [58]. Intriguingly, Hou et al [58] have shown that cathepsin K cleaved aggrecan aggregates at two specific sites, thereby generating the soluble glycosamino glycans required for formation of the

active complex themselves. Most cathepsins typically target collagen nonhelical regions or the destabilized helical region once collagenase has cleaved the structure [94]. Unlike other cathepsins, cathepsin K cleaves both helical and telopeptide regions of collagen [43]. Thus, typical of cathepsins, cathepsin K can cleave outside of the helical region. In addition, it can also act inside the helical region, i.e. the region that is usually attacked by the MMPs and neutral elasase [2, 6, 65, 75, 76, 88]. This dual ability to target both collagen regions is unique among the mammalian collagenases and is reminiscent of bacterial collagenase. A confirmation of the critical role played by cathepsin K in collagen digestion in humans comes from a study in which fibroblasts in pycnodysostotic embryos accumulate undigested collagen in lysosomal vacuoles [37]. Thus, cathepsin K can degrade the stable collagen triple helical structure and is therefore likely to be a reasonable target for pharmacologic intervention to block bone resorption (reviewed in [117]). As noted above, another role for cathepsin K in bone resorption may be to activate TRAP, causing osteopontin dephosphorylation and thereby negatively regulating bone resorption.

Cathepsin K inhibition by antisense or small molecules has been used to assess its role in osteoclast-mediated bone resorption. Pharmacological inhibitors of cathepsin K that span the active site inhibit resorption both *in vivo* and *in vitro* [71, 106, 110]. Blocking cathepsin K with antisense repressed bone resorption as well [62]. In an *in vivo* study using SB-357114 to block bone resorption, the inhibitor blocked both cathepsin K and cathepsin L activity [106]. Since these osteoclasts expressed much more cathepsin K than cathepsin L, cathepsin K may be the likely inhibition target, but this has not been

directly tested. Independent of the molecular target of this inhibitor, resorption was blocked, raising hope that targeted disruption of cathepsins may become an effective anti-resorptive therapy.

This returns us to the issue of the conflicting data of the potential roles of different cathepsins in osteoclast-mediated bone resorption. An interesting study by Furuyama et al [42] may help resolve this issue. Using calvarial organ cultures, they were able to detect trace levels of cathepsin L in untreated osteoclasts. When the cultures were treated with vitamin D, PTH, IL-1α, IL-6, or TNF- α - all known to stimulate born loss – the cathepsin L levels increased. In contrast, cathepsin K was abund under basal conditions and its concentration was unchanged following treatment with these stimulatory agents. Under basal conditions, resorption was blocked when cathepsin K was inhibited, but not when cathepsin L was inhibited. However, when the calvaria were treated with stimulatory factors, inhibition of either cathepsin K or cathepsin L partially inhibited resorption, with inhibition becoming additive when both inhibitors were used. These findings demonstrate that cathepsin K is important in basal bone resorption. Cathepsin L, on the other hand, may be involved bone loss under pathological conditions when its expression is elevated.

Matrix Metalloproteases (MMPs)

Studies of patients with pycnodysostosis have shown that, for the typical bone phenotype to become evident, there must be complete loss of cathepsin K activity [44]. However, even in cases with complete loss, whether in patients or mice, the calvaria appear normal. It would therefore seem that some bone resorption is taking place [16]. The collagenolytic mechanisms in these cases remain unknown, but may involve overexpression of other cathepsins, perhaps in conjunction with MMPs.

Individual MMPs are known by a variety of names and their substrates are as varied as their names. We will discuss MMP1, 3, 9, 12, 13, and 14 and their potential roles in osteoclast-mediated bone resorption. MMP1 is also known as collagenase-I. Its matrix substrates include intact collagen types I, II, III, VII, VIII, X [104]. MMP3 is also known as stromelysin and its substrates include osteopontin [1], decorin, proteoglycan, fibronectin, laminin, and type IV collagen, but not interstitial type I collagen [116]. MMP9 is also known as gelatinase B and its substrates include aggrecans, denatured type I collagen [40], and collagens IV, V, VIII, X, and XIV [104]. MMP12 is also known as macrophage metalloelastase. Its substrate is elastin and it has no collagen substrates [104]. MMP13 is also known as collagenase-3 and MMP14 is also known as MTI-MMP. Their substrates include type I collagen, other collagens, and additional extracellular matrix proteins [104]. Other non-matrix targets also exist for each MMP [104].

In bone, osteoblasts are a major source of MMP production. However MMP13 in bone is produced by osteocytes or mononuclear cells located near osteoclasts [23, 41, 102, 103]. Osteoclasts also produce some MMPs. Lin et al [77] found that rat osteoclasts expressed

MMP1 mRNA. Further, rabbit osteoclasts express MMP9 mRNA and MMPs1 and 9 mRNAs were present in human neonatal rib osteoclasts [7, 108]. Intriguingly, MMP1 and MMP9 mRNAs were also seen in a subset of osteoclasts situated at resorption sites and MMP9 mRNA was expressed in human giant cell tumors with the degree of expression correlating with the severity of the osteolysis [8, 70]. Moreover, osteoclast MMP1 and 9 production is regulated by IL-1, a cytokine that promotes bone resorption *in vivo* [54]. These data suggest a role for MMPs 1 and 9 in osteoclast-mediated bone degradation.

All MMPs require zinc for activity and, compared to MMP1, MMP3 has a deeper S_1' specificity pocket, which is distinctly different from the active site of MMP1 [24]. This could explain why it has proven possible to develop specific inhibitors that differentiate between these two enzymes. X-ray structure comparisons of MMPs 1 and 3 indicate there are two clusters of regions of differences between these two MMPs in regions that form the entrances to the active sites [24]. Differences in substrate specificity may be attributed to these structural differences [24].

Given that MMPs can destroy tissues, their enzymatic activity must be tightly regulated [104]. MMP activity can be controlled by modulating the gene expression level, by stimulating or inhibiting proenzyme activation, or with the aid of inhibitory molecules such as the tissue inhibitors of metalloproteinases (TIMPs) [105]. Expression stimulators include the membrane-anchored cysteine-rich protein RECK and alpha2-macroglobulin [81, 85, 86]. MMPs are synthesized with a pro-domain that blocks activity by means of

an unpaired cysteine in the carboxy terminus. X-ray analysis has shown that, by inserting the pro-domains of MMP3 and 9 into their respective clefts, activity is blocked [5, 31]. The unpaired cysteine acts as a fourth inactivating ligand for the zinc atom that is present in the active site. Activation can be by either proteolysis, so as to remove the pro-domain, or by a conformational change that releases the zinc atom from the cysteine. In that situation, the thiol group is replaced by water and the enzyme is thus enabled to remove the pro-domain. In most cases, MMP activation takes place outside of the cell. Given that MMPs reside in bone as latent enzymes, family members not synthesized by osteoclasts can be activated by osteoclastic activity and participate in bone degradation. Inactivation mechanisms include expression of TIMPs, which interact with the active site of MMPs and thus block activity [45]. In normal human bone, TIMP1 is highly expressed in osteoclasts derived from neonatal bone, but was absent in osteoclasts from pathological tissues (osteophytic and heterotopic bone – both having poorly organized bone formation) [7]. TIMP1 expression may therefore be important in the regulation of normal bone remodeling in the course of development.

Selective MMP inhibition studies have shown that the functional importance of a given MMP varies with the type of bone [38]. The presence of inflammatory cytokines may moreover alter MMP levels. Hill et al [54] have documented that MMP9 inhibition did not inhibit basal osteoclast activity *in vitro*, but did inhibit IL-1 stimulated calvarial explant bone resorption. Consequently, MMP9 may play a role in inflammatory cytokine-stimulated bone loss. Thus the specific function of MMPs in bone resorption seems to depend on the bone and/or the type of resorption stimulus.

Inhibition of either cathepsin or MMP decreased bone resorption, but inhibiting both was not additive [34, 36]. Even though cathepsins and MMPs thus appear to have similar functions and may be able to substitute for each other, MMPs act later in the resorption process than cathepsins do [38]. In view of the fact that these two enzyme classes act on different resorption steps, their actions may not be additive.

MMP13, synthesized by osteocytes but not by osteoclasts, has been detected in the resorption pit of cathepsin K knock out mice [35]. This observation raises the possibility that osteocytes may participate in osteoclast-mediated bone resorption by synthesizing and secreting MMP13. Everts et al [35] have proposed that the role of MMP13 is to "mop up" after cathepsin K-mediated bone resorption is completed.

Studies of mice lacking a given MMP provide insight into specific functions of the various family members. Bone resorption rates were normal in mice lacking MMP9, MMP12, and MMP14 [16]. However, mice lacking MMP13 had reduced bone resorption rates. This finding again supports a role for MMP13 in bone resorption. Although there was no apparent impact of MMP9 knock out on bone resorption, the bones from these mice had lengthened growth plates [114]. Since introduction of normal marrow restored development to normal, it was apparent that the defect was in the chondroclasts [114]. MMP9 knock out mice exhibited delayed osteoclast recruitment [32]. In patients with vanishing bone syndrome, there is severe bone degradation, mainly in the hands and the feet; this is due to the loss of the MMP2 gene [80]. The reasons why

loss of an MMP causes bone destruction are unknown, but possibilities include a compensatory over-production of other MMPs or a loss of coupling between osteoclasts and osteoblasts. Mice lacking MMP2 do not exhibit the same phenotype. This is another indication why reliance on mouse genetics may mislead in understanding of human disease.

MMPs also facilitate other aspects of osteoclast function. Inhibition of MMPs blocked osteoclast migration through collagen gel in an *in vitro* assay [16]. Osteoclasts deficient in MMPs 9, 12 and 14 have been examined for their migratory patterns [16]. MMP12 deficient osteoclasts migrated at normal rates whereas osteoclasts deficient in MMP9 or MMP14 had slower migration patterns. The MMPs can be found in podosomes, the osteoclast-bone attachment structure, and at the leading edges of normal migrating osteoclasts [63, 100]. Further supporting a MMP role in migration, MMP inhibition increased the lifespan of a podosome; this in turn will decrease migration[100]. Another function of MMPs may be to stimulate osteoclast recruitment [16].

One hypothesis is that MMP13-generated collagen fragments initiate bone resorption by activating osteoclasts [56]. In addition, MMP9 activity released TGF-ß from bone matrix, where TGF-ß is stored in significant amounts [66]. TGF-ß causes cell retraction thus leading to greater bone surface exposure, increasing osteoclast precursors attraction to the bone surface [66]. MMP14 causes membrane RANKL release, thereby perhaps influencing osteoclast differentiation and/or activation [67, 101]. Thus, MMPs most

likely coordinate matrix degradation and recruitment and differentiation of osteoclasts and chondroclasts and may be an important component of bone metabolism [89].

Conclusions

In light of the above information, cooperation among proteases is likely to be important in osteoclast-mediated bone resorption [18, 19, 21, 33, 36, 112, 113]. Although much more is now known about the enzymatic mechanisms by which bone is resorbed, it is equally clear that many gaps in our knowledge remain. The role of TRAP in bone resorption remains unresolved, as do the respective roles of cathepsins and MMPs. Furthermore, the mechanisms by which is resorbed in the course of bone development are likely to differ from those involved in bone turnover in the process of pathological bone loss. Changes in bone mass such as those that occur during menopause or as a result of anti-inflammatory therapies may involve a different set of enzymes. Similarly, bone loss induced by inflammatory cytokines may involve mechanisms that differ from those in other conditions of bone is resorption. It seems reasonable to hope that future studies of osteolytic enzymes will improve our knowledge of this important aspect of bone metabolism.

Acknowledgements

Dr. Oursler is supported by the Department of the Army Grant DAMD17-00-1-0346 and the National Institutes of Health Grant DE14680.

References

1. Agnihotri R, Crawford HC, Haro H, Matrisian LM, Havrda MC, Liaw L (2001) Osteopontin, a novel substrate for matrix metalloproteinase-3 (stromelysin-1) and matrix metalloproteinase-7 (matrilysin). J Biol Chem. 276:28261-7.
2. Aimes RT, Quigley JP (1995) Matrix metalloproteinase-2 is an interstitial collagenase. Inhibitor-free enzyme catalyzes the cleavage of collagen fibrils and soluble native type I collagen generating the specific 3/4- and 1/4-length fragments. J Biol Chem. 270:5872-6.
3. Andersson G, Ek-Rylander B, Hollberg K, Ljusberg-Sjolander J, Lang P, Norgard M, et al. (2003) TRACP as an osteopontin phosphatase. J Bone Miner Res. 18:1912-5.
4. Baron R, Neff L, Louvard D, Courtoy PJ (1985) Cell-mediated extracellular acidification and bone resorption: Evidence for a low pH in resorbing lacunae and localization of a 100-kDa lysosomal membrane protein at the osteoclast ruffled border. J. Cell Biol. 101:2210-2222.
5. Becker JW, Marcy AI, Rokosz LL, Axel MG, Burbaum JJ, Fitzgerald PM, et al. (1995) Stromelysin-1: three-dimensional structure of the inhibited catalytic domain and of the C-truncated proenzyme. Protein Sci. 4:1966-76.
6. Birkedal-Hansen H, Moore WG, Bodden MK, Windsor LJ, Birkedal-Hansen B, DeCarlo A, et al. (1993) Matrix metalloproteinases: a review. Crit Rev Oral Biol Med. 4:197-250.
7. Bord S, Horner A, Beeton CA, Hembry RM, Compston JE (1999) Tissue inhibitor of matrix metalloproteinase-1 (TIMP-1) distribution in normal and pathological human bone. Bone. 24:229-35.
8. Bord S, Horner A, Hembry RM, Reynolds JJ, Compston JE (1997) Distribution of matrix metalloproteinases and their inhibitor, TIMP-1, in developing human osteophytic bone. J Anat. 191 (Pt 1):39-48.
9. Bossard MJ, Tomaszek TA, Thompson SK, Amegadzie BY, Hanning CR, Jones C, et al. (1996) Proteolytic activity of human osteoclast cathepsin K. Expression, purification, activation, and substrate identification. J Biol Chem. 271:12517-24.
10. Brubaker KD, Vessella RL, True LD, Thomas R, Corey E (2003) Cathepsin K mRNA and protein expression in prostate cancer progression. J Bone Miner Res. 18:222-30.
11. Buhling F, Reisenauer A, Gerber A, Kruger S, Weber E, Bromme D, et al. (2001) Cathepsin K--a marker of macrophage differentiation? J Pathol. 195:375-82.
12. Buhling F, Waldburg N, Gerber A, Hackel C, Kruger S, Reinhold D, et al. (2000) Cathepsin K expression in human lung. Adv Exp Med Biol. 477:281-6.
13. Chellaiah MA, Hruska KA (2003) The integrin alpha(v)beta(3) and CD44 regulate the actions of osteopontin on osteoclast motility. Calcif Tissue Int. 72:197-205.
14. Chellaiah MA, Kizer N, Biswas R, Alvarez U, Strauss-Schoenberger J, Rifas L, et al. (2003) Osteopontin deficiency produces osteoclast dysfunction due to reduced CD44 surface expression. Mol Biol Cell. 14:173-89.

15. Chiellini C, Costa M, Novelli SE, Amri EZ, Benzi L, Bertacca A, et al. (2003) Identification of cathepsin K as a novel marker of adiposity in white adipose tissue. J Cell Physiol. 195:309-21.
16. Delaisse JM, Andersen TL, Engsig MT, Henriksen K, Troen T, Blavier L (2003) Matrix metalloproteinases (MMP) and cathepsin K contribute differently to osteoclastic activities. Microsc Res Tech. 61:504-13.
17. Delaisse JM, Boyde A, Maconnachie E, Ali NN, Sear CH, Eeckhout Y, et al. (1987) The effects of inhibitors of cysteine-proteinases and collagenase on the resorptive activity of isolated osteoclasts. Bone. 8:305-13.
18. Delaisse JM, Eeckhout Y, Sear C, Galloway A, McCullagh K, Vaes G (1985) A new synthetic inhibitor of mammalian tissue collagenase inhibits bone resorption in culture. Biochem Biophys Res Commun. 133:483-90.
19. Delaisse JM, Eeckhout Y, Vaes G (1980) Inhibition of bone resorption in culture by inhibitors of thiol proteinases. Biochem J. 192:365-8.
20. Delaisse JM, Eeckhout Y, Vaes G (1984) In vivo and in vitro evidence for the involvement of cysteine proteinases in bone resorption. Biochem Biophys Res Commun. 125:441-7.
21. Delaisse JM, Eeckhout Y, Vaes G (1985) Bisphosphonates and bone resorption: effects on collagenase and lysosomal enzyme excretion. Life Sci. 37:2291-6.
22. Delaisse JM, Ledent P, Vaes G (1991) Collagenolytic cysteine proteinases of bone tissue. Cathepsin B, (pro)cathepsin L and a cathepsin L-like 70 kDa proteinase. Biochem J. 279 (Pt 1):167-74.
23. Dew G, Murphy G, Stanton H, Vallon R, Angel P, Reynolds JJ, et al. (2000) Localisation of matrix metalloproteinases and TIMP-2 in resorbing mouse bone. Cell Tissue Res. 299:385-94.
24. Dhanaraj V, Ye QZ, Johnson LL, Hupe DJ, Ortwine DF, Dunbar JB, Jr., et al. (1996) X-ray structure of a hydroxamate inhibitor complex of stromelysin catalytic domain and its comparison with members of the zinc metalloproteinase superfamily. Structure. 4:375-86.
25. Diaz A, Willis AC, Sim RB (2000) Expression of the proteinase specialized in bone resorption, cathepsin K, in granulomatous inflammation. Mol Med. 6:648-59.
26. Diaz A, Willis AC, Sim RB (2002) Cathepsin K expression in epithelioid and multinucleated giant cells. J Pathol. 197:690; author reply 691.
27. Dodds RA, James IE, Rieman D, Ahern R, Hwang SM, Connor JR, et al. (2001) Human osteoclast cathepsin K is processed intracellularly prior to attachment and bone resorption. J Bone Miner Res. 16:478-86.
28. Drake FH, Dodds RA, James IE, Connor JR, Debouck C, Richardson S, et al. (1996) Cathepsin K, but not cathepsins B, L, or S is abundantly expressed in human osteoclasts. Journal of Biological Chemistry. 271:12511-12516.
29. Ducsay CA, Buhi WC, Bazer FW, Roberts RM, Combs GE (1984) Role of uteroferrin in placental iron transport: effect of maternal iron treatment on fetal iron and uteroferrin content and neonatal hemoglobin. J Anim Sci. 59:1303-8.
30. Ek-Rylander B, Flores M, Wendel M, Heinegard D, Andersson G (1994) Dephosphorylation of osteopontin and bone sialoprotein by osteoclastic tartrate-

resistant acid phosphatase. Modulation of osteoclast adhesion in vitro. J Biol Chem. 269:14853-6.

31. Elkins PA, Ho YS, Smith WW, Janson CA, D'Alessio KJ, McQueney MS, et al. (2002) Structure of the C-terminally truncated human ProMMP9, a gelatin-binding matrix metalloproteinase. Acta Crystallogr D Biol Crystallogr. 58:1182-92.
32. Engsig MT, Chen QJ, Vu TH, Pedersen AC, Therkidsen B, Lund LR, et al. (2000) Matrix metalloproteinase 9 and vascular endothelial growth factor are essential for osteoclast recruitment into developing long bones. J Cell Biol. 151:879-89.
33. Etherington DJ, Birkedahl-Hansen H (1987) The influence of dissolved calcium salts on the degradation of hard-tissue collagens by lysosomal cathepsins. Coll Relat Res. 7:185-99.
34. Everts V, Delaisse JM, Korper W, Beertsen W (1998) Cysteine proteinases and matrix metalloproteinases play distinct roles in the subosteoclastic resorption zone. J Bone Miner Res. 13:1420-30.
35. Everts V, Delaisse JM, Korper W, Jansen DC, Tigchelaar-Gutter W, Saftig P, et al. (2002) The bone lining cell: its role in cleaning Howship's lacunae and initiating bone formation. J Bone Miner Res. 17:77-90.
36. Everts V, Delaisse JM, Korper W, Niehof A, Vaes G, Beertsen W (1992) Degradation of collagen in the bone-resorbing compartment underlying the osteoclast involves both cysteine-proteinases and matrix metalloproteinases. J Cell Physiol. 150:221-31.
37. Everts V, Hou WS, Rialland X, Tigchelaar W, Saftig P, Bromme D, et al. (2003) Cathepsin K Deficiency in Pycnodysostosis Results in Accumulation of Non-Digested Phagocytosed Collagen in Fibroblasts. Calcif Tissue Int.
38. Everts V, Korper W, Jansen DC, Steinfort J, Lammerse I, Heera S, et al. (1999) Functional heterogeneity of osteoclasts: matrix metalloproteinases participate in osteoclastic resorption of calvarial bone but not in resorption of long bone. Faseb J. 13:1219-30.
39. Faccio R, Grano M, Colucci S, Zallone AZ, Quaranta V, Pelletier AJ (1998) Activation of alphav beta3 integrin on human osteoclast-like cells stimulates adhesion and migration in response to osteopontin. Biochem Biophys Res Commun. 249:522-5.
40. Fosang AJ, Last K, Knauper V, Neame PJ, Murphy G, Hardingham TE, et al. (1993) Fibroblast and neutrophil collagenases cleave at two sites in the cartilage aggrecan interglobular domain. Biochem J. 295 (Pt 1):273-6.
41. Fuller K, Chambers TJ (1995) Localisation of mRNA for collagenase in osteocytic, bone surface and chondrocytic cells but not osteoclasts. J Cell Sci. 108 (Pt 6):2221-30.
42. Furuyama N, Fujisawa Y (2000) Distinct roles of cathepsin K and cathepsin L in osteoclastic bone resorption. Endocr Res. 26:189-204.
43. Garnero P, Borel O, Byrjalsen I, Ferreras M, Drake FH, McQueney MS, et al. (1998) The collagenolytic activity of cathepsin K is unique among mammalian proteinases. J Biol Chem. 273:32347-52.
44. Gelb BD, Shi GP, Chapman HA, Desnick RJ (1996) Pycnodysostosis, a lysosomal disease caused by cathepsin K deficiency. Science. 273:1236-8.

45. Gomis-Ruth FX, Maskos K, Betz M, Bergner A, Huber R, Suzuki K, et al. (1997) Mechanism of inhibition of the human matrix metalloproteinase stromelysin-1 by TIMP-1. Nature. 389:77-81.
46. Goto T, Kiyoshima T, Moroi R, Tsukuba T, Nishimura Y, Himeno M, et al. (1994) Localization of cathepsins B, D, and L in the rat osteoclast by immuno-light and -electron microscopy. Histochemistry. 101:33-40.
47. Goto T, Tsukuba T, Ayasaka N, Yamamoto K, Tanaka T (1992) Immunocytochemical localization of cathepsin D in the rat osteoclast. Histochemistry. 97:13-8.
48. Gowen M, Lazner F, Dodds R, Kapadia R, Feild J, Tavaria M, et al. (1999) Cathepsin K knockout mice develop osteopetrosis due to a deficit in matrix degradation but not demineralization. J Bone Miner Res. 14:1654-63.
49. Haeckel C, Krueger S, Buehling F, Broemme D, Franke K, Schuetze A, et al. (1999) Expression of cathepsin K in the human embryo and fetus. Dev Dyn. 216:89-95.
50. Haeckel C, Krueger S, Kuester D, Ostertag H, Samii M, Buehling F, et al. (2000) Expression of cathepsin K in chordoma. Hum Pathol. 31:834-40.
51. Hansen T, Unger RE, Gaumann A, Hundorf I, Maurer J, Kirkpatrick CJ, et al. (2001) Expression of matrix-degrading cysteine proteinase cathepsin K in cholesteatoma. Mod Pathol. 14:1226-31.
52. Hayman AR, Cox TM (1994) Purple acid phosphatase of the human macrophage and osteoclast. Characterization, molecular properties, and crystallization of the recombinant di-iron-oxo protein secreted by baculovirus-infected insect cells. J Biol Chem. 269:1294-300.
53. Hill PA, Buttle DJ, Jones SJ, Boyde A, Murata M, Reynolds JJ, et al. (1994) Inhibition of bone resorption by selective inactivators of cysteine proteinases. J Cell Biochem. 56:118-30.
54. Hill PA, Murphy G, Docherty AJ, Hembry RM, Millican TA, Reynolds JJ, et al. (1994) The effects of selective inhibitors of matrix metalloproteinases (MMPs) on bone resorption and the identification of MMPs and TIMP-1 in isolated osteoclasts. J Cell Sci. 107 (Pt 11):3055-64.
55. Hollberg K, Hultenby K, Hayman A, Cox T, Andersson G (2002) Osteoclasts from mice deficient in tartrate-resistant acid phosphatase have altered ruffled borders and disturbed intracellular vesicular transport. Exp Cell Res. 279:227-38.
56. Holliday LS, Welgus HG, Fliszar CJ, Veith GM, Jeffrey JJ, Gluck SL (1997) Initiation of osteoclast bone resorption by interstitial collagenase. J Biol Chem. 272:22053-8.
57. Horton MA, Nesbit MA, Helfrich MH (1995) Interaction of osteopontin with osteoclast integrins. Ann N Y Acad Sci. 760:190-200.
58. Hou WS, Li Z, Buttner FH, Bartnik E, Bromme D (2003) Cleavage site specificity of cathepsin K toward cartilage proteoglycans and protease complex formation. Biol Chem. 384:891-7.
59. Hultenby K, Reinholt FP, Heinegard D, Andersson G, Marks SC, Jr. (1995) Osteopontin: a ligand for the alpha v beta 3 integrin of the osteoclast clear zone in osteopetrotic (ia/ia) rats. Ann N Y Acad Sci. 760:315-8.

60. Igarashi Y, Lee MY, Matsuzaki S (2002) Acid phosphatases as markers of bone metabolism. J Chromatogr B Analyt Technol Biomed Life Sci. 781:345-58.
61. Inaoka T, Bilbe G, Ishibashi O, Tezuka K, Kumegawa M, Kokubo T (1995) Molecular cloning of human cDNA for cathepsin K: novel cysteine proteinase predominantly expressed in bone. Biochem Biophys Res Commun. 206:89-96.
62. Inui T, Ishibashi O, Inaoka T, Origane Y, Kumegawa M, Kokubo T, et al. (1997) Cathepsin K antisense oligodeoxynucleotide inhibits osteoclastic bone resorption. J Biol Chem. 272:8109-12.
63. Irie K, Tsuruga E, Sakakura Y, Muto T, Yajima T (2001) Immunohistochemical localization of membrane type 1-matrix metalloproteinase (MT1-MMP) in osteoclasts in vivo. Tissue Cell. 33:478-82.
64. James IE, Marquis RW, Blake SM, Hwang SM, Gress CJ, Ru Y, et al. (2001) Potent and selective cathepsin L inhibitors do not inhibit human osteoclast resorption in vitro. J Biol Chem. 276:11507-11.
65. Kafienah W, Buttle DJ, Burnett D, Hollander AP (1998) Cleavage of native type I collagen by human neutrophil elastase. Biochem J. 330 (Pt 2):897-902.
66. Karsdal MA, Fjording MS, Foged NT, Delaisse JM, Lochter A (2001) Transforming growth factor-beta-induced osteoblast elongation regulates osteoclastic bone resorption through a p38 mitogen-activated protein kinase- and matrix metalloproteinase-dependent pathway. J Biol Chem. 276:39350-8.
67. Khosla S (2001) Minireview: the OPG/RANKL/RANK system. Endocrinology. 142:5050-5.
68. Konttinen YT, Mandelin J, Li TF, Salo J, Lassus J, Liljestrom M, et al. (2002) Acidic cysteine endoproteinase cathepsin K in the degeneration of the superficial articular hyaline cartilage in osteoarthritis. Arthritis Rheum. 46:953-60.
69. Kremer M, Judd J, Rifkin B, Auszmann J, Oursler MJ (1994) Estrogen Modulation of Osteoclast Lysosomal Enzyme Secretion. Journal of Cellular Biochemistry. 58:1-9.
70. Kumta SM, Huang L, Cheng YY, Chow LT, Lee KM, Zheng MH (2003) Expression of VEGF and MMP-9 in giant cell tumor of bone and other osteolytic lesions. Life Sci. 73:1427-36.
71. Lark MW, Stroup GB, James IE, Dodds RA, Hwang SM, Blake SM, et al. (2002) A potent small molecule, nonpeptide inhibitor of cathepsin K (SB 331750) prevents bone matrix resorption in the ovariectomized rat. Bone. 30:746-53.
72. Lerner UH, Grubb A (1992) Human cystatin C, a cysteine proteinase inhibitor, inhibits bone resorption in vitro stimulated by parathyroid hormone and parathyroid hormone-related peptide of malignancy. J Bone Miner Res. 7:433-40.
73. Li CY, Yam LT, Lam KW (1970) Acid phosphatase isoenzyme in human leukocytes in normal and pathologic conditions. J Histochem Cytochem. 18:473-81.
74. Li YP, Chen W (1999) Characterization of mouse cathepsin K gene, the gene promoter, and the gene expression. J Bone Miner Res. 14:487-99.
75. Li Z, Hou WS, Bromme D (2000) Collagenolytic activity of cathepsin K is specifically modulated by cartilage-resident chondroitin sulfates. Biochemistry. 39:529-36.

76. Li Z, Hou WS, Escalante-Torres CR, Gelb BD, Bromme D (2002) Collagenase activity of cathepsin K depends on complex formation with chondroitin sulfate. J Biol Chem. 277:28669-76.
77. Lin SK, Kok SH, Kuo MY, Wang TJ, Wang JT, Yeh FT, et al. (2002) Sequential expressions of MMP-1, TIMP-1, IL-6, and COX-2 genes in induced periapical lesions in rats. Eur J Oral Sci. 110:246-53.
78. Littlewood-Evans AJ, Bilbe G, Bowler WB, Farley D, Wlodarski B, Kokubo T, et al. (1997) The osteoclast-associated protease cathepsin K is expressed in human breast carcinoma. Cancer Res. 57:5386-90.
79. Luchin A, Suchting S, Merson T, Rosol TJ, Hume DA, Cassady AI, et al. (2001) Genetic and physical interactions between Microphthalmia transcription factor and PU.1 are necessary for osteoclast gene expression and differentiation. J Biol Chem. 276:36703-10.
80. Martignetti JA, Aqeel AA, Sewairi WA, Boumah CE, Kambouris M, Mayouf SA, et al. (2001) Mutation of the matrix metalloproteinase 2 gene (MMP2) causes a multicentric osteolysis and arthritis syndrome. Nat Genet. 28:261-5.
81. Migita K, Eguchi K, Tominaga M, Origuchi T, Kawabe Y, Nagataki S (1997) Beta 2-microglobulin induces stromelysin production by human synovial fibroblasts. Biochem Biophys Res Commun. 239:621-5.
82. Miyauchi A, Alvarez J, Greenfield EM, Teti A, Grano M, Colucci S, et al. (1993) Binding of osteopontin to the osteoclast integrin alpha v beta 3. Osteoporos Int. 3 Suppl 1:132-5.
83. Muir P, Hayashi K, Manley PA, Colopy SA, Hao Z (2002) Evaluation of tartrate-resistant acid phosphatase and cathepsin K in ruptured cranial cruciate ligaments in dogs. Am J Vet Res. 63:1279-84.
84. Nakase T, Takeuchi E, Sugamoto K, Kaneko M, Tomita T, Myoui A, et al. (2000) Involvement of multinucleated giant cells synthesizing cathepsin K in calcified tendinitis of the rotator cuff tendons. Rheumatology (Oxford). 39:1074-7.
85. Noda M, Oh J, Takahashi R, Kondo S, Kitayama H, Takahashi C (2003) RECK: a novel suppressor of malignancy linking oncogenic signaling to extracellular matrix remodeling. Cancer Metastasis Rev. 22:167-75.
86. Oh J, Takahashi R, Kondo S, Mizoguchi A, Adachi E, Sasahara RM, et al. (2001) The membrane-anchored MMP inhibitor RECK is a key regulator of extracellular matrix integrity and angiogenesis. Cell. 107:789-800.
87. Ohsawa Y, Nitatori T, Higuchi S, Kominami E, Uchiyama Y (1993) Lysosomal cysteine and aspartic proteinases, acid phosphatase, and an endogenous cysteine proteinase inhibitor, cystatin-beta, in rat osteoclasts. J Histochem Cytochem. 41:1075-83.
88. Ohuchi E, Imai K, Fujii Y, Sato H, Seiki M, Okada Y (1997) Membrane type 1 matrix metalloproteinase digests interstitial collagens and other extracellular matrix macromolecules. J Biol Chem. 272:2446-51.
89. Ortega N, Behonick D, Stickens D, Werb Z (2003) How proteases regulate bone morphogenesis. Ann N Y Acad Sci. 995:109-16.
90. Page AE, Warburton MJ, Chambers TJ, Pringle JA, Hayman AR (1992) Human osteoclastomas contain multiple forms of cathepsin B. Biochim Biophys Acta. 1116:57-66.

91. Punturieri A, Filippov S, Allen E, Caras I, Murray R, Reddy V, et al. (2000) Regulation of elastinolytic cysteine proteinase activity in normal and cathepsin K-deficient human macrophages. J Exp Med. 192:789-99.
92. Rantakokko J, Aro HT, Savontaus M, Vuorio E (1996) Mouse cathepsin K: cDNA cloning and predominant expression of the gene in osteoclasts, and in some hypertrophying chondrocytes during mouse development. FEBS Lett. 393:307-13.
93. Razzouk S, Brunn JC, Qin C, Tye CE, Goldberg HA, Butler WT (2002) Osteopontin posttranslational modifications, possibly phosphorylation, are required for in vitro bone resorption but not osteoclast adhesion. Bone. 30:40-7.
94. Reynolds JJ (1970) Degradation processes in bone and cartilage. Calcif Tissue Res. Suppl:52-6.
95. Rifkin BR, Vernillo AT, Kleckner AP, Auszmann JM, Rosenberg LR, Zimmerman M (1991) Cathepsin B and L activities in isolated osteoclasts. Biochem Biophys Res Commun. 179:63-9.
96. Ross FP, Chappel J, Alvarez JI, Sander D, Butler WT, Farach-Carson MC, et al. (1993) Interactions between the bone matrix proteins osteopontin and bone sialoprotein and the osteoclast integrin alpha v beta 3 potentiate bone resorption. J Biol Chem. 268:9901-7.
97. Saftig P, Hunziker E, Everts V, Jones S, Boyde A, Wehmeyer O, et al. (2000) Functions of cathepsin K in bone resorption. Lessons from cathepsin K deficient mice. Adv Exp Med Biol. 477:293-303.
98. Saftig P, Hunziker E, Wehmeyer O, Jones S, Boyde A, Rommerskirch W, et al. (1998) Impaired osteoclastic bone resorption leads to osteopetrosis in cathepsin-K-deficient mice. Proc Natl Acad Sci U S A. 95:13453-8.
99. Sasaki T, Ueno-Matsuda E (1993) Cysteine-proteinase localization in osteoclasts: an immunocytochemical study. Cell Tissue Res. 271:177-9.
100. Sato T, del Carmen Ovejero M, Hou P, Heegaard AM, Kumegawa M, Foged NT, et al. (1997) Identification of the membrane-type matrix metalloproteinase MT1-MMP in osteoclasts. J Cell Sci. 110 (Pt 5):589-96.
101. Schlondorff J, Lum L, Blobel CP (2001) Biochemical and pharmacological criteria define two shedding activities for TRANCE/OPGL that are distinct from the tumor necrosis factor alpha convertase. J Biol Chem. 276:14665-74.
102. Shimizu H, Sakamoto M, Sakamoto S (1990) Bone resorption by isolated osteoclasts in living versus devitalized bone: differences in mode and extent and the effects of human recombinant tissue inhibitor of metalloproteinases. J Bone Miner Res. 5:411-8.
103. Sodek J, Overall CM (1992) Matrix metalloproteinases in periodontal tissue remodelling. Matrix Suppl. 1:352-62.
104. Somerville RP, Oblander SA, Apte SS (2003) Matrix metalloproteinases: old dogs with new tricks. Genome Biol. 4:216.
105. Stamenkovic I (2003) Extracellular matrix remodelling: the role of matrix metalloproteinases. J Pathol. 200:448-64.
106. Stroup GB, Lark MW, Veber DF, Bhattacharyya A, Blake S, Dare LC, et al. (2001) Potent and selective inhibition of human cathepsin K leads to inhibition of bone resorption in vivo in a nonhuman primate. J Bone Miner Res. 16:1739-46.

107. Tepel C, Bromme D, Herzog V, Brix K (2000) Cathepsin K in thyroid epithelial cells: sequence, localization and possible function in extracellular proteolysis of thyroglobulin. J Cell Sci. 113 Pt 24:4487-98.
108. Tezuka K, Nemoto K, Tezuka Y, Sato T, Ikeda Y, Kobori M, et al. (1994) Identification of matrix metalloproteinase 9 in rabbit osteoclasts. J Biol Chem. 269:15006-9.
109. Tezuka K, Tezuka Y, Maejima A, Sato T, Nemoto K, Kamioka H, et al. (1994) Molecular cloning of a possible cysteine proteinase predominantly expressed in osteoclasts. J Biol Chem. 269:1106-9.
110. Thompson SK, Halbert SM, Bossard MJ, Tomaszek TA, Levy MA, Zhao B, et al. (1997) Design of potent and selective human cathepsin K inhibitors that span the active site. Proc Natl Acad Sci U S A. 94:14249-54.
111. Uppenberg J, Lindqvist F, Svensson C, Ek-Rylander B, Andersson G (1999) Crystal structure of a mammalian purple acid phosphatase. J Mol Biol. 290:201-11.
112. Vaes G (1988) Cellular biology and biochemical mechanism of bone resorption. A review of recent developments on the formation, activation, and mode of action of osteoclasts. Clin Orthop. 239-71.
113. Vaes G, Delaisse JM, Eeckhout Y (1992) Relative roles of collagenase and lysosomal cysteine-proteinases in bone resorption. Matrix Suppl. 1:383-8.
114. Vu TH, Shipley JM, Bergers G, Berger JE, Helms JA, Hanahan D, et al. (1998) MMP-9/gelatinase B is a key regulator of growth plate angiogenesis and apoptosis of hypertrophic chondrocytes. Cell. 93:411-22.
115. Walsh NC, Cahill M, Carninci P, Kawai J, Okazaki Y, Hayashizaki Y, et al. (2003) Multiple tissue-specific promoters control expression of the murine tartrate-resistant acid phosphatase gene. Gene. 307:111-23.
116. Wilhelm SM, Collier IE, Kronberger A, Eisen AZ, Marmer BL, Grant GA, et al. (1987) Human skin fibroblast stromelysin: structure, glycosylation, substrate specificity, and differential expression in normal and tumorigenic cells. Proc Natl Acad Sci U S A. 84:6725-9.
117. Yamashita DS, Dodds RA (2000) Cathepsin K and the design of inhibitors of cathepsin K. Curr Pharm Des. 6:1-24.
118. Zaidi M, Troen B, Moonga BS, Abe E (2001) Cathepsin K, osteoclastic resorption, and osteoporosis therapy. J Bone Miner Res. 16:1747-9.